17665

NATIONAL LIBRARY
OTTAWA

BIBLIOTHÈQUE NATIONALE
OTTAWA

CANADA

NAME OF AUTHOR...COLIN ROBERT RAMSAY

TITLE OF THESIS...METAMORPHISM AND GOLD MINERALISATION OF ARCHAEAN META-SEDIMENTS NEAR YELLOWKNIFE, N.W.T. CANADA

UNIVERSITY...OF ALBERTA

DEGREE FOR WHICH THESIS WAS PRESENTED...Ph.D.

YEAR THIS DEGREE GRANTED...1973

Permission is hereby granted to THE NATIONAL LIBRARY OF CANADA to microfilm this thesis and to lend or sell copies of the film.

The author reserves other publication rights, and neither the thesis nor extensive extracts from it may be printed or otherwise reproduced without the author's written permission.

(Signed)...CRRamsay

PERMANENT ADDRESS:

School of Mines
University of Zambia
Lusaka, Zambia.

DATED...19th July...1973

NL-91 (10-68)

THE UNIVERSITY OF ALBERTA

METAMORPHISM AND GOLD MINERALISATION OF ARCHAEAN META-SEDIMENTS NEAR YELLOWKNIFE, N. W. T., CANADA

by

© COLIN ROBERT RAMSAY

A THESIS

SUBMITTED TO THE FACULTY OF GRADUATE STUDIES AND
RESEARCH IN PARTIAL FULFILLMENT OF THE REQUIREMENTS
FOR THE DEGREE OF DOCTOR OF PHILOSOPHY

DEPARTMENT OF GEOLOGY

EDMONTON, ALBERTA
FALL, 1973

THE UNIVERSITY OF ALBERTA

FACULTY OF GRADUATE STUDIES AND RESEARCH

The undersigned certify that they have read, and recommend to the Faculty of Graduate Studies and Research for acceptance, a thesis entitled 'Metamorphism and gold mineralisation of Archaean metasediments near Yellowknife, N. W. T., Canada' submitted by Colin Robert Ramsay in partial fulfillment of the requirements for the degree of Doctor of Philosophy.

R St J Lambert
Supervisor

H. Baadsgaard

Smith

E. R. Kanasewich

Edward D Ghent
External Examiner

Date 16th July 1973

For wives, like Lyn, who suffer many
of the tribulations of our science but
reap few of its rewards.

ABSTRACT

Some 150 sq. kms. of Archaean meta-sediments east of Yellowknife Bay (N. W. T., Canada) have been mapped and sampled. Structural analysis at a reconnaissance level indicates that the area is structurally inhomogeneous and divisible into domains on the basis of structural style. Many of the structural features are best explained as results of intrusion and inflation of the granitic batholiths. An evolutionary model is suggested in which the area evolved from oceanic crust in a single tectonic cycle in which batholith emplacement was the principal causative factor.

A broad metamorphic aureole approximating an Abukuma facies series surrounds the late, potassic Prosperous Lake pluton. The biotite zone of this aureole is examined in detail using micro-probe analyses of 14 rocks, 59 sheet silicates, 10 oxides and numerous plagioclases. Silicate compositions were controlled by complex interaction of physical and chemical controls whose relative importance varied in different rock types and for different mineral groups. The analytical, modal and textural data indicate that biotite originated by the reaction

$$\text{Chlorite} + \text{Muscovite(1)} + \text{Ilmenite} \longrightarrow \text{Biotite} + \text{Muscovite(2)} + H_2O + [\text{Rutile, Quartz, K-feldspar}]$$

in which muscovite became depleted in K and (Fe+Mg+Mn) but gained

a little Ti.

The cordierite isograd is discussed in some detail and analyses of 17 silicates and 12 oxides are given. The cordierite originated by the reaction

$$\text{Chlorite} + \text{Muscovite}(1) + \text{Quartz} + \text{Biotite}(1) \longrightarrow$$
$$\text{Cordierite} + \text{Biotite}(2) + H_2O + [\text{Ilmenite, Chlorite, Muscovite}(2)]$$

in which pre-existing biotite donated Si, Mg and K but no texturally distinct new biotite was formed.

Garnet is commonly present in some areas close to the pluton and shows signs of instability in some rocks. Incipient sillimanite, corroded staurolite and Ca-poor amphiboles occur at the highest grades and andalusite is present sporadically.

Metamorphism occurred in a single cycle involving the development and decay of a thermal dome accompanied by continuous pressure decrease. An initial phase of this cycle (300° C. @ 3 kb. to 700° C. @ 5 kb.) yielded the zonal succession chlorite -- biotite -- garnet -- staurolite which was immediately over-printed by the zonal series biotite -- cordierite -- andalusite -- sillimanite (350° C. @ 2.5 kb. to 700° C. @ 3.0-3.5 kb.).

Gold-quartz veins in this aureole have been examined via structural considerations and a fluid inclusion survey. They were deposited during the relaxation stage of deformation when dilatant structures permitted the passage of metamorphic fluid bearing gold, probably as sulphide complexes. This fluid was an immiscible mixture of a brine of moderate salinity and a CO_2-rich fluid. The initial stages of vein formation occurred at about 250° C. but the gold was only precipitated by the later fluids at about 150° C.

ACKNOWLEDGEMENTS

Dr. R. St. J. Lambert suggested this project to me and has been principal advisor throughout. I am most grateful to him and to Drs. R. D. Morton and H. Baadsgaard who advised on aspects of the study. Dr. H. A. K. Charlesworth introduced me to the structural programmes and read an early draft of the structural section. Dr. D. G. W. Smith spent many hours teaching me the use of the micro-probe and its correction programmes and Dr. Thomas Frisch lent me standards, advice and assistance on many occasions. Mr. D. A. Tomlinson and Mrs. Rene Bliss assisted in the micro-probe laboratory. Dr. G. J. Dickie and Miss Ann Bartlett-Page built the data storage file for me. Dr. C. M. Scarfe and Messers. K. Schimann, S. R. Winzer and P. A. Nielsen read various sections of the text and suggested improvements. I have had numerous helpful discussions with Mr. J. P. N. Badham and discussed structural problems with Dr. S. A. Drury. Dr. R. E. Folinsbee introduced me to the use of the heating stage and Dr. S. B. Woods (Dept. of Physics) assisted with the calibration of the Pt-resistance thermometer. Messers. P. Longdon, M. Kis and J. Gould assisted ably in the field and Mr. Frank Dimitrov and my wife drafted many of the diagrams. Mr. Robert Hornal of the Dept. of Indian Affairs and Northern Development in Yellowknife lent me equipment for use in the field and assisted generously with air transport. Mr. Z. Nikic of the Con Mine and Mr. R. W. Spence of Giant Yellowknife Mines Ltd. kindly

permitted me to see various company reports on the Ptarmigan, Tom and Tin properties and gave me permission to examine the Ptarmigan and Tom veins.

I had direct financial support from the Boreal Institute of the University of Alberta, from teaching assistantships in the Dept. of Geology and from an International Nickel Co. of Canada Ltd. research fellowship. Indirect support derived mainly from National Research Council of Canada grants to staff members in the Dept. of Geology, notably support of the micro-probe laboratory by grants to Dr. D. G. W. Smith.

For advice, guidance and support from all these sources I am most grateful. All errors are my own.

TABLE OF CONTENTS

Page

ABSTRACT v

ACKNOWLEDGEMENTS viii

PART I : INTRODUCTION

THE NATURE OF THE SLAVE CRATON 1
- Definition of the Slave Craton 3
- Lithology 3
- Structure 7
- Metamorphism 8
- Economic Mineralisation 10

THE YELLOWKNIFE AREA AS A SAMPLE OF THE CRATON 11

PART II : STRUCTURE AND EVOLUTION

PREVIOUS WORK 17

SCOPE OF THE PRESENT STUDY 19
- Structural Domains 20

HAY LAKE DOMAIN 20
- The Obvious Folds 20
- Cleavage 22
- The Early Isocline Problem 25
- Some Deviations 28
- Nature of the Hay Lake Domain 29

YELLOWKNIFE BRIDGE DOMAIN 29
- Folds 30
- Cleavage 30
- Nature of the Yellowknife Bridge Domain 32

DUCK LAKE DOMAIN 33
- Folds 33
- Cleavage 33
- Aplite Dykes 36
- The South-Eastern Granodiorite and its Contacts 37
- Interaction of Duck Lake and Hay Lake Structures . . . 39
- Nature of the Duck Lake Domain 41

STUART LAKE DOMAIN. 41
- Folds 41
- Cleavage 43
- Nature of the Stuart Lake Domain 43

Page

ISLAND LAKE DOMAIN 43
  Folds 43
  Cleavage 45
  Micro-folds 46
  Nature of the Island Lake Domain 46

FAULTS 46

SYNTHESIS : TECTONIC HISTORY 49

AN EVOLUTIONARY MODEL 51

PART III : PETROLOGY

NATURE OF THE SEDIMENTS 54
  Sedimentary Petrology of the Burwash Fm. 54
  Sedimentary Petrology of the Walsh Fm. 59
  Relation of Bulk Composition to Metamorphic Grade . . 59

THE PROSPEROUS LAKE AUREOLE 60
  Chlorite Zone 60
  Biotite Zone 61
  Cordierite Zone 62
  Cordierite-Garnet 'Zone' 63
  Sillimanite-Staurolite 'Zone' 63
  The Facies Series 63
  Assignment of Metamorphic Grade 64

THE SAMPLE SERIES 65
  Sedimentological Criteria 65
  Other Criteria 67
  The Sample Series 67
  Analytical Methods 69

BIOTITE ZONE MINERAL CHEMISTRY 69
  Biotite 69
  Muscovite 78
  Chlorite 84
  Plagioclase 90
  Potassium Feldspar 96
  Oxides and Sulphides 96

CONTROLLING ROLE OF METAMORPHIC GRADE 99

CONTROLLING ROLE OF ROCK COMPOSITION 101
  The Rock Compositions 101
  Influence on Mineral Compositions 101
  Influence on Pro-grade Maturation of Minerals 103
  Conclusions 103

CONTROLLING ROLE OF PRESSURE 105

Page

CONTROLLING ROLE OF FLUID COMPOSITION 106

THE CONTROLS OF MINERAL COMPOSITION 107
  Permissive Controls 107
  Modifying Controls 108

THE ORIGIN OF BIOTITE 109
  The Problem 110
  The Data 113
  The Participant Phases 113
  The Reaction 124
  Discussion 125
  Comparison with Previous Studies 127
  Conclusion 129

THE ORIGIN OF CORDIERITE 131
  The Problem 131
  The Isograd 133
  The Role of Biotite 135
  Cordierite Poikiloblasts 138
  Mineral Compositions 144
  Cordierite-forming Reaction 146
  Controls of the Appearance of Cordierite 148
  Minor Reaction Products 150
  Relation to Experimental Work 150

THE CORDIERITE ZONE 153
  Rocks of the Cordierite Zone 155
  Mineralogy 156
  Mineral Assemblages 157
  Origin of Andalusite 159
  Conclusion 162

THE CORDIERITE-GARNET 'ZONE' 162
  Areal Distribution of Garnet 164
  Mineralogy and Textural Relations 164
  Mineral Assemblages 167
  Evolution of the Cordierite-Garnet 'Zone' 169

THE SILLIMANITE-STAUROLITE 'ZONE' 171
  The Assemblages 172
  Paragenesis 172

METAMORPHIC HISTORY 172

PART IV : GOLD MINERALISATION

INTRODUCTION 180
  Nature of the Deposits 181
  Genetic Theories 183
  Scope of the Present Investigation 184

Page

THE GOLD DEPOSITS 185
  Ptarmigan Mine 185
  Tom Veins 187
  The Rich Deposit 190
  The Tin Deposit 192

STRUCTURAL RELATIONS 193

IRREGULAR QUARTZ BODIES 197

TEMPERATURE RELATIONS : FLUID INCLUSIONS 198
  Scope of the Fluid Inclusion Study 199
  Petrological Constraints 199
  Fluid Inclusions in Irregular Veins 200
  Fluid Inclusions in Gold-Quartz Veins 222

GOLD IN THE COUNTRY ROCKS 232

ORIGIN OF THE GOLD DEPOSITS 232

PART V : SUMMARY AND CONCLUSIONS

LOCAL APPLICABILITY 239
  Structure 239
  The Prosperous Lake Aureole 240
  Biotite Zone Mineralogy 241
  Controls of Biotite Zone Mineralogy 242
  The Origin of Biotite 243
  The Origin of Cordierite 244
  The Origin of the Gold Deposits 245

GENERAL 246
  Evolution of Cratons 246
  Controls of Mineral Composition 246
  The Biotite Isograd 247
  Stoichiometry of Reactions 247
  Hydrothermal Transport of Gold 248

APPENDIX : METHODOLOGY

Mapping and Sampling 263
Structural Methods 264
Petrographic Methods 265
Rock Analyses 270
Mineral Analyses 276
Fluid Inclusion Methods 284

MAP (In back pocket)

LIST OF TABLES

Table		Page
1	Proposed tectonic history of the Yellowknife Bay - Prosperous Lake area.	47
2	Analyses of 14 rocks from Prosperous Lake.	56
3	Micro-probe analyses of biotites from the biotite zone.	70
4	Structural formulae of the biotites in Table 3.	71
5	Miscellaneous analytical data on biotites, muscovites and chlorites from the biotite zone.	77
6	Micro-probe analyses of muscovites from the biotite zone.	79
7	Structural formulae of the muscovites in Table 6.	80
8	Micro-probe analyses of chlorites from the biotite zone.	85
9	Structural formulae of the chlorites in Table 8.	86
10	Partial micro-probe analyses of plagioclases from the biotite zone.	91
11	Micro-probe analyses of rutiles and ilmenites.	97
12	Modal analyses of meta-pelites and meta-greywackes.	114
13	Frequency of mineral assemblages above and below the cordierite isograd.	134
14	Micro-probe analyses and structural formulae of minerals in cordierite-free rocks and the groundmasses of cordierite-bearing rocks from the vicinity of the cordierite isograd.	140
15	Micro-probe analyses and structural formulae of cordierites, minerals included in cordierite and a pinite from the vicinity of the cordierite isograd.	142
16	Mineral assemblages of rocks from the cordierite isograd in which minerals have been analysed.	143
17	Mineral assemblages of the cordierite zone.	158
18	Mineral assemblages of the cordierite-garnet zone.	168

Table		Page
19	Type and abundance of fluid inclusions in irregular quartz veins.	212
20	Salinity data for fluid inclusions in irregular quartz veins.	217
21	Phases recorded in previous studies of inclusions in metamorphic quartz veins.	221
22	Descriptions of gold-quartz vein samples.	223
23	Type and abundance of fluid inclusions in gold-quartz veins.	225
24	Salinity data for fluid inclusions in gold-quartz veins.	229
25	Phases recorded in previous studies of gold-quartz veins.	231
26	Data on the gold contents of rocks of Archaean greenstone belts in Canada.	233
A1	Precision estimates for the rock analyses.	275
A2	Standards used in the micro-probe analyses.	277
A3	Data on the principal standards used in the microprobe analyses.	280
A4	Replicate analyses of minerals.	282

LIST OF FIGURES

Figure		Page
1	Locality diagram.	2
2	Generalised geology of the Slave Craton.	4
3	Table of formations.	12
4	General geology and structural domains.	18
5	Orientation of structures in the Hay Lake domain.	21
6	Areal distribution of micro-folds in the Hay Lake domain.	26
7	Orientation of structures in the Yellowknife Bridge and Duck Lake domains.	31
8	North-western margin of the South-Eastern Granodiorite.	38
9	Refolded isoclines north-west of Duck Lake.	40
10	Orientation of structures in the Stuart Lake domain.	42
11	Orientation of structures in the Island Lake domain.	44
12	An evolutionary model.	50
13	Diagram depicting the rock compositions.	57
14	Sedimentological parameters and arbitrary definition of rock fields.	66
15	Locations of biotite zone samples.	68
16	SAF diagram depicting minerals from the biotite zone.	72
17	AKF diagram depicting minerals from the biotite zone.	73
18	AFM diagram depicting minerals from the biotite zone.	74
19	Relation of biotite composition to metamorphic grade.	76
20	Relation of muscovite composition to metamorphic grade.	82
21	Chlorite classification diagram.	87
22	Relation of chlorite composition to metamorphic grade.	89

Figure		Page
23	Relation of plagioclase composition to metamorphic grade and petrographic type.	95
24	Relation of biotite composition to biotite modal concentration.	118
25	Relation of chlorite and muscovite modal percentages to biotite modal percentage.	119
26	Relation of muscovite composition to biotite modal concentration.	121
27	Relation of ilmenite and rutile modal percentages to biotite modal percentages.	123
28	Simplistic diagram for the transfer of components during the formation of biotite.	126
29	Relation of biotite and chlorite modal percentages to metamorphic grade.	128
30	The cordierite isograd.	132
31	Modal percentage of biotite across the cordierite isograd.	139
32	Compositions of biotites from the cordierite isograd related to pro-grade trends in composition.	145
33	AKF diagram depicting rocks and minerals from the vicinity of the cordierite isograd.	147
34	Thompson AFM projection of rocks and minerals from the vicinity of the cordierite isograd.	149
35	Sketch of a thin-section in which cordierite poikiloblasts have different characters.	151
36	The high-grade zones of the aureole.	154
37	Metamorphic evolution of the Prosperous Lake aureole.	174
38	Ptarmigan Mine geological sketch.	186
39	Tom No. 3 vein geological sketch.	188
40	Rich deposit geological sketch.	191
41	Gold-bearing structures in the Yellowknife area.	195

Figure		Page
42	Locations of quartz vein samples used in the fluid inclusion study.	202
43	Types of fluid inclusions observed.	208
44	Homogenisation behaviour of fluid inclusions in irregular quartz veins.	214
45	Cumulative frequency plot for homogenisation temperatures in irregular quartz veins.	215
46	Relation of minimum homogenisation temperature to metamorphic grade index.	219
47	Homogenisation behaviour of fluid inclusions in gold-bearing veins.	227
A1	Specimen petrographic data sheet.	266
A2	Specimen SAFRAS output table of petrographic data.	268
A3	Calibration curves used in the whole-rock analyses.	272

LIST OF PLATES

Plate		Page
1	Structural features of the Hay Lake, Island Lake and Yellowknife Bridge structural domains.	24
2	Structural features of the Duck Lake structural domain.	35
3	Photomicrographs of biotite zone rocks.	116
4	The cordierite, cordierite-garnet and sillimanite-staurolite zones.	137
5	Quartz veins and fluid inclusions.	206

PART I : INTRODUCTION

The Prosperous Lake area is a portion of the typical Archaean greywacke-greenstone-granodiorite terrain which constitutes the Slave Craton. It is located near Yellowknife, N.W.T. (Fig. 1). The meta-sediments in this area have been studied with the principal objectives of elucidating their metamorphic evolution and relating their gold-quartz mineralisation to their metamorphic history.

To these ends field-work was carried out in the summers of 1970 (two weeks), 1971 (eight weeks) and 1972 (two weeks). During this time the metamorphic aureole of the Prosperous Lake granite was systematically sampled, structural data were collected and the gold-bearing veins were examined and sampled. The structural data are used to give some idea of tectonic history and the petrography of the Prosperous Lake aureole is described. The biotite zone and the cordierite isograd are considered in detail. The study concludes with consideration of the nature of the gold-quartz veins.

THE NATURE OF THE SLAVE CRATON

There is a plethora of recent reviews on the Slave Craton and only the essence of pertinent facets will be given here. The reviews by Green and Baadsgaard (1971; representing the University of Alberta school of thought) and McGlynn and Henderson (1970 and 1972; representing the Geological Survey of Canada school) are

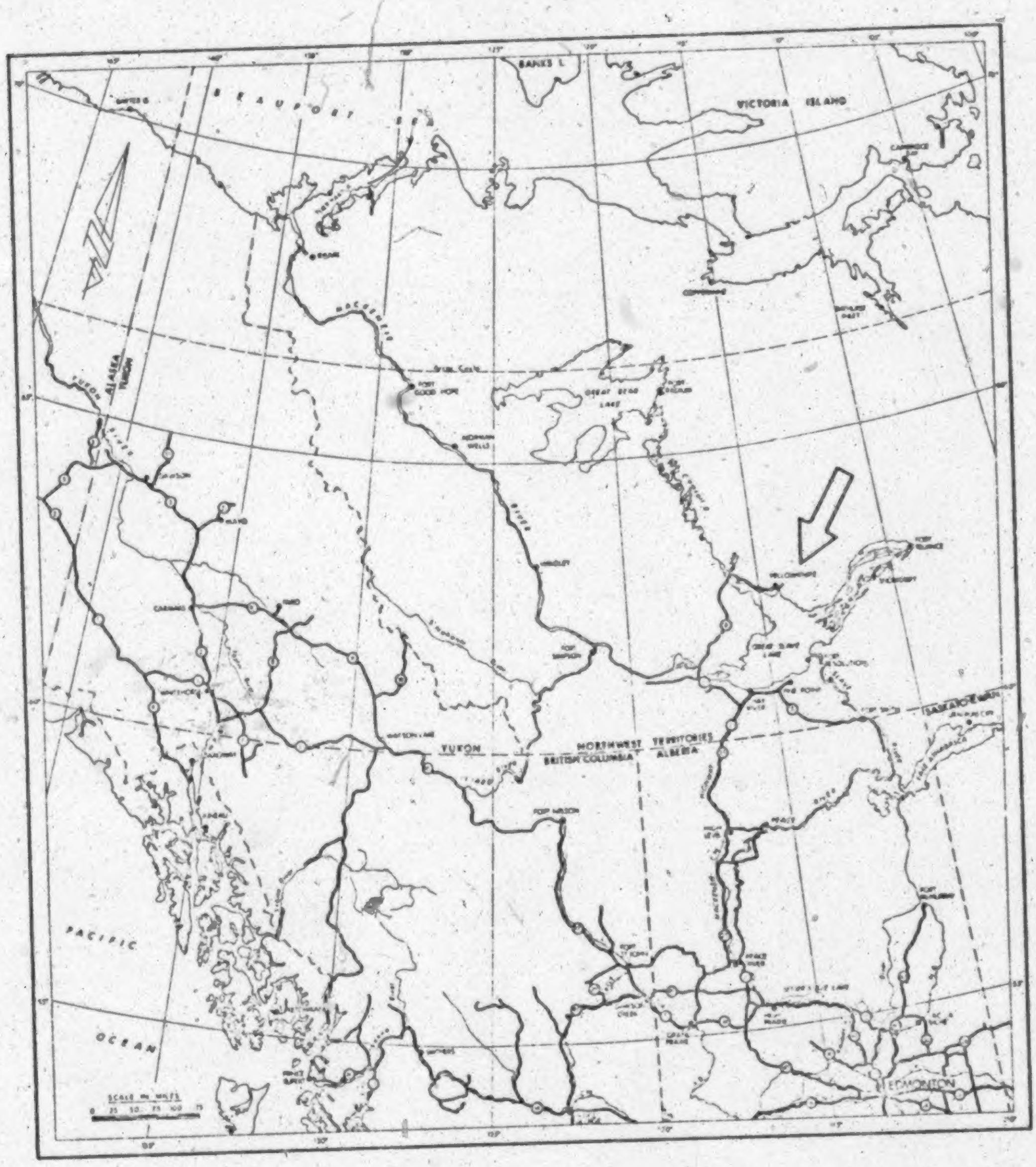
BANKS I.
BEAUFORT SEA
VICTORIA ISLAND
ALASKA
YUKON
GREAT BEAR LAKE
YELLOWKNIFE
GREAT SLAVE LAKE
YUKON
NORTHWEST TERRITORIES
BRITISH COLUMBIA
ALBERTA
SASKATCHEWAN
PACIFIC
OCEAN
EDMONTON
SCALE IN MILES

FIGURE 1 : Yellowknife area - location and access.

perhaps the most important, but others include Stockwell et al. (1970), Hoffman and Henderson (1972), Green (1968) and Boyle (1961).

Definition of the Slave Craton

This region was originally defined as the "Yellowknife Sub-province" on the basis of its "rock types, major faults and mineral occurrences" by Jolliffe (1948). The lavas overlain by greywacke and argillite, the characteristic metamorphism to cordierite-bearing nodular rocks and the granitic intrusions were considered lithologically characteristic. The major faults trend north-west to north, are left-lateral and generally lack quartz breccias and stockworks. Gold-quartz veins are very numerous and pegmatites associated with the younger granites characteristically contain Ta, Li, Be or Sn.

Jolliffe's definition has been entirely substantiated by more recent work (mainly extended map coverage and radiometric dating) but the region is now called the Slave Structural Province in Geological Survey literature. Since the region conforms entirely to the definition of a craton (Anhaeusser et al., 1969) it is herein called the Slave Craton. It is areally defined by the features summarised below.

Lithology

The craton consists predominantly of the greywacke-greenstone-granodiorite trinity so typical of the Archaean cratons. Figure 2 shows the distribution of these lithologies, to which should be added migmatites, pegmatites, acid and basic dykes, alkaline plutons and ultrabasic rocks in smaller amounts.

The basement problem. There have been several

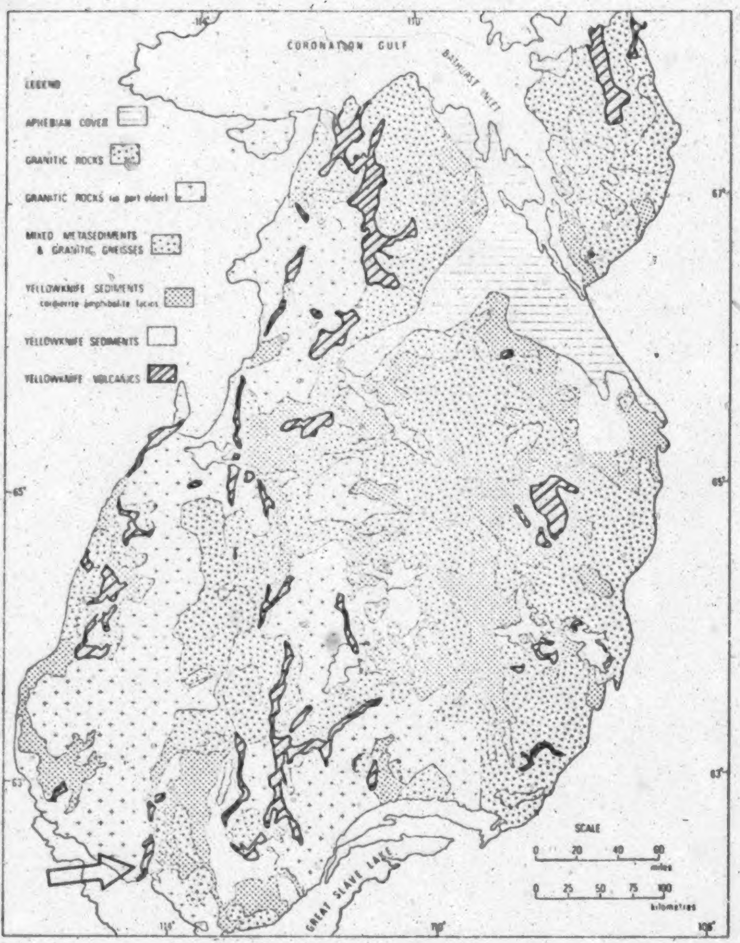
114°
110°
CORONATION GULF
BATHURST INLET
LEGEND
APHEBIAN COVER
GRANITIC ROCKS
GRANITIC ROCKS (in part older)
MIXED METASEDIMENTS & GRANITIC GNEISSES
YELLOWKNIFE SEDIMENTS cordierite amphibolite facies
YELLOWKNIFE SEDIMENTS
YELLOWKNIFE VOLCANICS
67°
65°
63°
SCALE
0 20 40 60
miles
0 25 50 75 100
kilometres
GREAT SLAVE LAKE
114°
110°
106°

FIGURE 2 : Simplified geology of the Slave Craton (after McGlynn and Henderson, 1972). The arrow indicates the approximate area of Fig. 4.

reports of rocks which might constitute basement to the Kenoran supracrustal sequence (Baragar, 1966; Heywood and Davidson, 1969; Stockwell, 1933). These rocks generally exhibit structural or stratigraphic relations suggesting that they comprise pre-Kenoran basement but are of very limited extent and, where radiometrically dated, have yielded Kenoran ages (Wanless and Loveridge, 1972). The presence of granitic cobbles in conglomerates overlying the greenstones has frequently been cited as evidence for the existence of pre-Kenoran continental basement, but these cobbles have also yielded Kenoran ages (Green and Baadsgaard, 1971). In view of these radiometric ages and the apparently uncontaminated mantle origin of the major plutons (Green and Baadsgaard, op. cit.) the evidence for pre-Kenoran basement is inconclusive.

The greenstones. The oldest exposed rocks are therefore probably the greenstones, dated as 2650 m.y. by Green and Baadsgaard. These typically occur in narrow belts between the major plutons and the overlying meta-sediments (Fig. 2) and comprise thicknesses up to 9000 m. or about 15 per cent of the area (McGlynn and Henderson, 1972) -- rather less than is typical for cratons. These rocks are metamorphosed submarine lavas of basaltic to andesitic composition with minor acidic and pyroclastic material. There are typically numerous dykes of about the same age as the flows (Henderson and Brown, 1966). The greenstones probably dip monoclinally basinwards under the meta-sediments.

Conglomerates and sandstones. Overlying the greenstones there is commonly a discontinuous conglomerate horizon of local provenance consisting of fragments of volcanic rocks, greywacke, shale, quartz and chert (Henderson, 1970). Granitic boulders (quartz diorite, according to Green and Baadsgaard) occur locally. These rocks indicate an erosional period of short duration and in some places are overlain by sediments indicative of shallow water deposition.

The meta-sediments. Great thicknesses of metamorphosed greywackes and mudstones fill the basins in the craton (Fig. 2). These have been shown by Henderson (1972) to be turbidites which flowed off topographic highs located roughly where the granodiorite batholiths now outcrop. These meta-sediments are the main topic of this thesis.

The granitic rocks. It has long been recognised that granitic batholiths of two general ages are present. Henderson (1943) recorded "an older granodiorite and quartz diorite which is cut by a younger granite" and representatives of these categories have been dated by Green and Baadsgaard as 2590-2610 m.y. and 2575 m.y., respectively. In addition there are the gneisses and migmatites shown in Fig. 2 and thought by McGlynn and Henderson to be derived from sedimentary strata. These three types of granitic rock conform to the categories typical of cratons (Anhaeusser et al., 1969) i.e.: (1) A complex array of migmatites and banded gneisses with more homogeneous granitic phases. (2) Circular or elliptical diapiric granodiorite bodies which may be gradational with the gneisses and migmatites and are thought by Anhaeusser et al. to have been emplaced by "slow upwelling and forceful emplacement of discrete and largely plastic granitic masses." (3) Potash-rich, coarse-grained granites which intrude and cross-cut all earlier structures. There are, in the Slave Craton, areas where detailed mapping has revealed rather more complexity than implied by this simple model (e.g. Davidson, 1972; Heywood and Davidson, 1969) but in general it seems applicable.

Other intrusive rocks. All the supracrustal rocks have been intruded by numerous quartz veins and there are many diabase dykes and sills in discrete sets dated at 2300-2400 m.y., 2000-2100 m.y., 1400-1500 m.y., 1200 m.y. and 600-700 m.y. (McGlynn and Henderson, 1972). Pegmatites are commonly associated with the late potassic plutons and in some areas constitute a considerable proportion of the exposure. They have been studied by Jolliffe (1944), Rowe (1952), Hutchinson (1955) and Kretz (1968 and 1970). In addition to these common intrusions there are a few ultrabasic rocks and alkaline intrusive complexes. The locations and references to these are given by McGlynn and Henderson (1972).

Structure

Perhaps less is known of the structure than of any other geological facet of the Slave Craton and, although the faults and shear zones are well mapped, the ubiquitous fold structures are not. The general model is one of unfolded greenstones dipping monoclinally under the sedimentary basins and containing no known mesoscopic folds while the sediments in the basins are intensely and complexly folded. Early work (e.g. Riley, 1938; Henderson and Jolliffe, 1939; Henderson, 1943; Jolliffe, 1942 and 1946; Campbell, 1947) indicated that the sediments had first been isoclinally folded on gently plunging axes and then deformed on 'cross-folds'. The orientation of the structures varies in such a fashion that both Henderson and Campbell believed the granitic plutons to have been the main deforming agents. More recent and detailed work has either been confined to margins of the craton which have been involved in Hudsonian events (e.g. Ross, 1966) or has considered mainly the structures of the greenstone belts (e.g. Henderson and Brown, 1966). The last known deformational event involved dissection by numerous faults and diabases (e.g. Wilson, 1941).

Structurally, therefore, the craton is poorly understood but appears to be entirely typical of such terrains (Anhaeusser _et al._, 1968; Anhaeusser _et al._, 1969). It should be emphasised that most of the structures in such areas are best ascribed to vertical tectonic movements and the influence of plutonic emplacement rather than to regional compressive forces.

Metamorphism

Anhaeusser _et al._ (1969, p. 2189) have described the typical metamorphism of the cratons as follows. "There is an intimate relationship between metamorphism and deformation, and the sequence is usually of two or more periods of mineral development and deformation, followed by widespread post-tectonic recrystallisation and late-stage retrogression . . . ." Although imperfectly understood, the metamorphic history of the Slave Craton conforms closely to this scheme. Previous petrological work (e.g. Denton, 1940; Folinsbee, 1940, 1941, 1942; Henderson, 1943) showed that all supracrustal rocks in the area have been metamorphosed to at least the lower greenschist facies and many belong to higher grades, primarily in aureoles round plutons. Broad aureoles of porphyroblastic rocks surround the late potassic granites (Henderson and Jolliffe, 1941; Fortier, 1946). Denton, Folinsbee and Henderson all agreed that the metamorphic history of the area involved (1) a phase of regional metamorphism under moderate confining pressure with (2) superimposed aureoles of a more static, thermal nature. In addition, Folinsbee suggested (3) a late phase of hydrothermal retrogression. This general model has been substantiated by all more recent work (e.g. Tremblay, 1952; Boyle, 1961; Ross, 1966; Davidson, 1967; Kretz, 1968; Heywood and Davidson, 1969) but the rocks formed in the two main phases cannot readily be distinguished.

Very little is known of the metamorphic zonation round the syn-tectonic granodiorites, but according to Folinsbee (1942) these aureoles are characterised by the zonation chlorite-biotite-andalusite-staurolite-garnet in meta-sediments. Boyle (1961) mapped greenschist, epidote amphibolite and amphibolite facies in meta-volcanic rocks near the Western Granodiorite.

In contrast, several studies have been made on the extensive thermal aureoles surrounding the late potassic granites which are characterized by abundance of cordierite in meta-sediments (Davidson, 1967; Kretz, 1968; Heywood and Davidson, 1969; Kamineni and Wong, 1973). The metamorphic progression in meta-sediments in these aureoles is rather consistent. At lowest grades the chlorite-muscovite schists of regional extent are not always to be seen but give way to large areas of biotite zone rocks. This biotite zone is terminated abruptly by the cordierite isograd, above which cordierite is abundant in a large proportion of the rocks. Andalusite occurs sporadically in this zone. Garnet is sometimes present and cummingtonite is a characteristic phase in some rock compositions. Sillimanite occurs at the highest grades, which are not achieved in all aureoles. Little is known of the metamorphic zonation in meta-basic rocks in these aureoles (but see Heywood and Davidson, 1969).

The generalised metamorphic history evolving from the early studies and all work since (including the present study) is therefore of a moderate-pressure ubiquitous metamorphism which merges into superimposed aureoles round plutons. This sequence is thought not to have occurred in discrete events (as suggested by Folinsbee, 1942) but by a gradual change in thermal conditions with heat flow increasingly dominated by the plutons as pressure decreased. Such a model was first suggested by Denton (1940).

Economic Mineralisation

The Slave Craton lacks the ultrabasic rocks so productive in other cratons (e.g. Rhodesia, Western Australia) and its economic geology is therefore dominated entirely by gold. There is, in addition, a wide variety of economic minerals of the quartz vein and pegmatite associations, notably spodumene in pegmatites. Reviews of the economic geology of the craton have been given by Jolliffe (1944), Lord (1951), Rowe (1952) and Lang *et al.* (1970).

There is abundant literature on the gold deposits, dating from the first review by Jolliffe in 1937 to the detailed geochemical study of Boyle (1961). This last source gives a review and a comprehensive list of references. Gold-quartz veins occur in both the metavolcanic and meta-sedimentary rocks though the only operating mines are now in the former. The gold-bearing veins are in all cases structurally controlled. Those in the meta-volcanic rocks occur in shear zones; those in meta-sediments are variably controlled, most commonly being "introduced along zones of structural weakness which, in most places, are clearly dependent on folding." (Henderson and Jolliffe, 1939, p. 324).

THE YELLOWKNIFE AREA AS A SAMPLE OF THE SLAVE CRATON

Because of its ready accessibility, the area round Yellowknife is becoming the type area for the Slave Craton and numerous detailed studies have been made there. The following table lists the definitive work on each of the main topics and a brief synopsis will then be given.

Topic	Author
Maps	Jolliffe (1942, 1946)
Geochronology	Green and Baadsgaard (1971)
Stratigraphy	Henderson (1970)
Sedimentology	Henderson (1972)
Meta-volcanic rocks	Baragar (1966); Henderson and Brown (1966)
Plutons	Boyle (1961); Green and Baadsgaard (1971). No detailed study.
Structure	Campbell (1947); Henderson and Brown (1966). No detailed study.
Metamorphism	Boyle (1961); Kretz (1968); Folinsbee (1942).
Pegmatites	Jolliffe (1944); Hutchinson (1955); Kretz (1968, 1970)
Gold mineralisation	Boyle (1961), Coleman (1957)

The general geology of the area is shown in Fig. 4. The supracrustal rocks comprise the normal upward succession (Fig. 3) from volcanic rocks, through shallow-water sediments to deep-water turbidites. Of the basal volcanic rocks the Duck Fm. (flows of

TABLE OF FORMATIONS

		WEST SIDE OF YELLOWKNIFE BAY			EAST SIDE OF YELLOWKNIFE BAY		
ERA	SUPERGROUP	GROUP	FORMATION	LITHOLOGY	LITHOLOGY	FORMATION	GROUP
Cenozoic				Pleistocene glacial deposits.	Pleistocene glacial deposits.		
				Profound	Unconformity		
Proterozoic				Diabase gabbro.	Diabase gabbro.		
				Intrusive	Contact		
Archean				Western granodiorite. Quartz-feldspar porphyry. Gabbro diorite.	Prosperous Lake granite. Southeastern granodiorite. Quartz-feldspar porphyry. Gabbro diorite.		
				Intrusive	Contact		
	Yellowknife	Duncan Lake	Jackson Lake	Volcanic lithic sandstone conglomerate.	Slate with interbedded siltstone and greywacke	Walsh	Duncan Lake
			Unconformity		Felsic volcanics, agglomerate and tuff.	Banting	
				Diorite gabbro.			
			Intrusive contact		Greywacke with thin slate interbeds	Burwash	
		Beaulieu	Kam	Pillowed and massive basalt, andesite and dacite flows.	Intermediate volcanics	Duck	Beaulieu

FIGURE 3 : Table of formations in the Yellowknife area (from Henderson, 1970).

intermediate composition) has not been studied in detail, but the Kam Fm. is well known. It consists of about 9000 m. of pillowed basaltic to andesitic flows with minor tuff, agglomerate and breccia and very numerous penecontemporaneous gabbro dykes and sills. These are now amphibole and chlorite schists with marked metamorphic zonation round the Western Granodiorite (Boyle, 1961). The lavas were thought by Green and Baadsgaard (1971) to have been extruded, without contamination, onto thin oceanic crust.

The Kam Fm. is unconformably overlain by conglomerates and sandstones of the Jackson Lake Fm., but the rest of the succession on the West side of Yellowknife Bay is not visible as a consequence of faulting and alluvial or water cover. On the East side the Duck Fm. is conformably overlain by the Burwash Fm. This formation is a thick sequence (4500 m.) of graded and interbedded greywackes and mudstones deposited by turbidity currents derived from the West (Henderson, 1972).

The Burwash Fm. is conformably overlain by the Banting Fm. which is composed of mixed volcanic rocks. It is overlain in turn by the turbidites of the Walsh Fm. which resemble the Burwash Fm. rocks but are more fine-grained, more thinly-bedded and contain a higher proportion of siltstone.

The structural history of the Yellowknife area is not well understood. The meta-volcanic rocks and the shallow-water sediments appear unfolded (except perhaps on a very large scale) while the turbidites of the Walsh and Burwash Fms. have been thrown into numerous folds, basins and domes on a mesoscopic scale. All rocks have been extensively dissected by major faults, most of which strike

N.N.W. and some of which carry diabase dykes.

The supracrustal rocks have been intruded by three major granitic plutons which typify plutons elsewhere in the craton and also have typical metamorphic aureoles. The South-Eastern Granodiorite was, according to Green and Baadsgaard, emplaced at the onset of the Kenoran orogeny (2620-2640 m.y. ago). It is a biotite granodiorite (in part quartz diorite) with a lobate outline and sub-concordant contacts suggestive of diapiric emplacement. It has a narrow metamorphic aureole (Jolliffe, 1942; Folinsbee, 1942). The Western Granodiorite is a more massive, homogeneous pluton of quartz diorite to adamellite composition. It shows definite cross-cutting relationships to the country rocks and has a marked metamorphic aureole extending approximately to the west shore of Yellowknife Bay. According to Green and Baadsgaard the Western Granodiorite was emplaced slightly later than the South-Eastern Granodiorite (2595-2610 m.y.), but this has been disputed by Thorpe (1971) who recalculated Green's (1968) data to derive ages of 2610 m.y. for the South-Eastern pluton and 2699 m.y. for the Western. (The author's opinion of this problem is given below.) There is, however, no doubt that the Prosperous Lake intrusion is the youngest major pluton in the area (2572 m.y.). It is a biotite-muscovite adamellite containing, and surrounded by, numerous pegmatites. It has cross-cutting relationships and sharp intrusive contacts with the country rocks and has a very broad metamorphic aureole approximating an Abukuma facies series. The pluton and its aureole typify the late potassic granites which outcrop throughout the craton.

Hence the Yellowknife area is not only readily accessible, but has had much of its geology unravelled and also constitutes a good sample of the lithologies and structures of the Slave Craton.

PART II : STRUCTURE AND EVOLUTION

As noted above, there has been no detailed analysis of folding history in the Prosperous Lake meta-sediments, though the overall style may be inferred from studies elsewhere in the craton (Riley, 1938; Henderson and Jolliffe, 1939; Henderson, 1943; Fortier, 1946; Tremblay, 1952; Ross and McGlynn, 1965; Ross, 1966; Heywood and Davidson, 1969; Henderson *et al.* 1972). These have unanimously concluded that the general history is of sub-horizontal isoclinal folds, later deformed by "cross-folds". While the latter are readily apparent, the early isoclines usually can only be deduced from the alternation of way-up criteria in traverses across strike. They have also been revealed by detailed stereographic analysis (Ross and McGlynn, 1965) and fabric studies (Fyson, pers. comm., 1973). Isoclinal fold crests are reported to be rare and this is usually ascribed to shearing and rupturing in the hinge zones. Several problems therefore emerge:

1. Evidence for this two-phase deformation is rarely observed in the field in the Prosperous Lake area. Are the early isoclines present?
2. What is the nature of the cross-folding?
3. Existing maps of the Prosperous Lake area (Jolliffe, 1942 and 1946) suggest that structural style (e.g. fold orientation) varies within this restricted area. Is this so and what is the reason for it?
4. What are the temporal relations between metamorphism,

intrusion and folding?

5. Previous work in this craton (above) and others (Goodwin, 1972; Anhaeusser et al., 1969) suggests that there is commonly a causative relationship between intrusion and deformation in cratons. Is this so in the Prosperous Lake area?

PREVIOUS WORK

Jolliffe (1942 and 1946) suggested that the meta-sediments occur in an asymmetrical, north-easterly plunging syncline whose axis strikes up Yellowknife Bay (Fig. 4) and that the south-eastern limb comprised the large area of complexly cross-folded sediments of the Prosperous Lake area. This syncline (the Yellowknife Bay Syncline) was modified by the presence of a minor anticline (the Duck Lake Anticline; see Fig. 4) on the south-eastern limb and by numerous cross-folds. Jolliffe held that the north-easterly syncline was related to emplacement of the Western Granodiorite and(or) the South-Eastern Granodiorite, while cross-folding was related to the emplacement of the Prosperous Lake granite. Similar views have been propagated by Campbell (1947) and Henderson (1971 and pers. comm., 1972).

Evidence for the existence of the Yellowknife Bay Syncline is substantial and includes the occurrence of the Banting Fm. on both limbs near Walsh Lake and way-up criteria in the same area (Henderson, pers. comm., 1972). However, to consider this the principal structural element of the area, as both Jolliffe and Campbell did, involves several major assumptions: (1) That there is a lateral facies

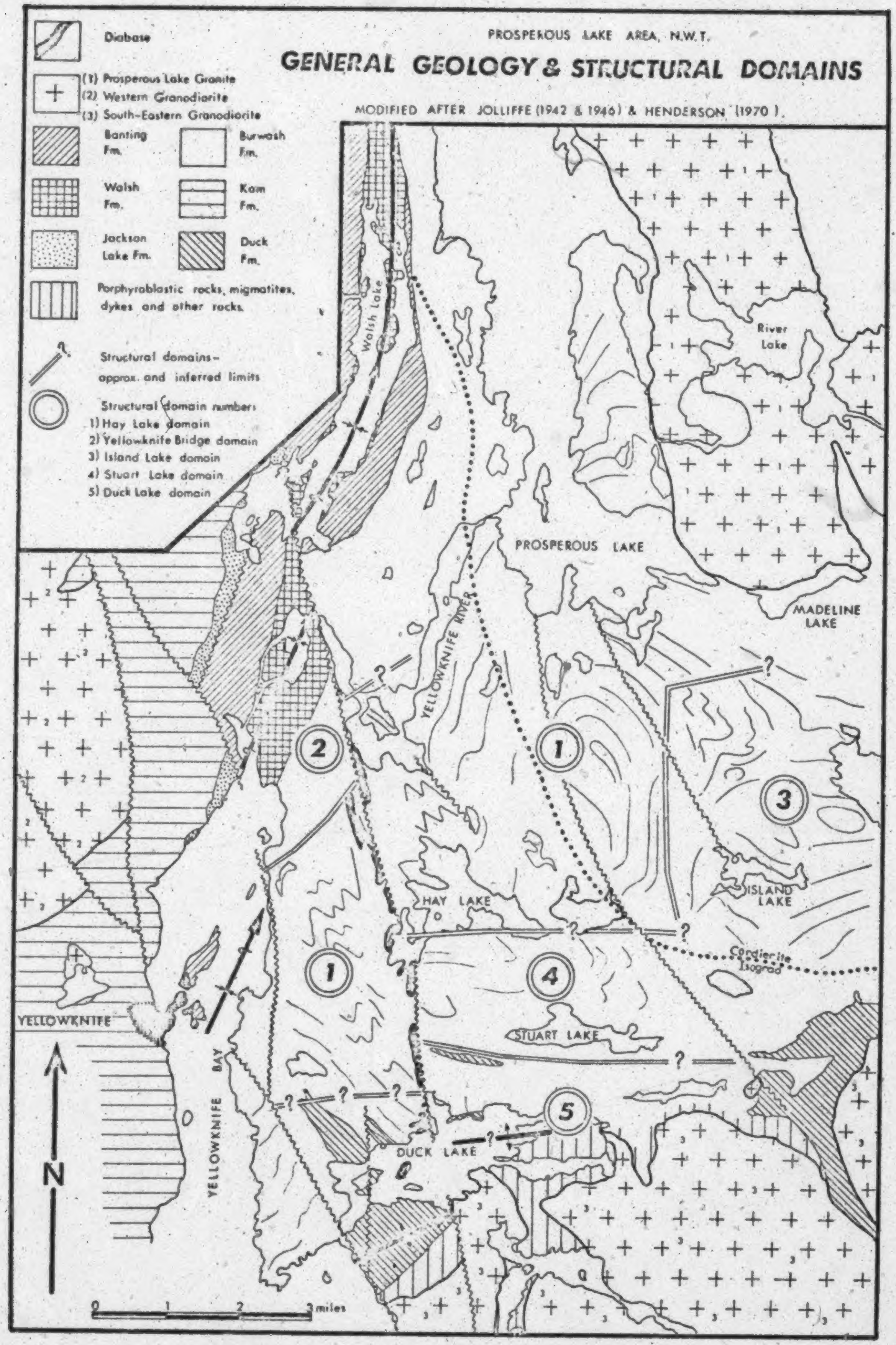
PROSPEROUS LAKE AREA, N.W.T.
GENERAL GEOLOGY & STRUCTURAL DOMAINS
MODIFIED AFTER JOLLIFFE (1942 & 1946) & HENDERSON (1970).
Diabase
(1) Prosperous Lake Granite
(2) Western Granodiorite
(3) South-Eastern Granodiorite
Banting Fm.
Burwash Fm.
Walsh Fm.
Kam Fm.
Jackson Lake Fm.
Duck Fm.
Porphyroblastic rocks, migmatites, dykes and other rocks.
Structural domains - approx. and inferred limits
Structural domain numbers
1) Hay Lake domain
2) Yellowknife Bridge domain
3) Island Lake domain
4) Stuart Lake domain
5) Duck Lake domain
Walsh Lake
River Lake
PROSPEROUS LAKE
MADELINE LAKE
YELLOWKNIFE RIVER
HAY LAKE
ISLAND LAKE
Cordierite Isograd
STUART LAKE
DUCK LAKE
YELLOWKNIFE
YELLOWKNIFE BAY
N
0 1 2 3 miles

FIGURE 4

variation from meta-volcanics and conglomeratic sandstones on the north-western limb to turbidites on the south-eastern; (2) That faulting parallel to the syncline axis has negligible influence on this interpretation though it is probably of regional extent (Henderson and Brown, 1966) and (3) That way-up determinations in the Burwash Fm. are representative of the major structure despite the later deformation. The present author has no new evidence but suggests that the Yellowknife Bay Syncline may be a smaller structure than previously suggested, perhaps being simply a peripheral syncline of the Western Granodiorite.

The existence of Duck Lake Anticline is less certain. It is suggested by way-up and dip determinations on Horseshoe Island (Jolliffe, 1942; Henderson, pers. comm., 1972) but its north-easterly extension into the Duck Lake area is dubious. The structure there is very complex (see below) and not readily interpreted in terms of a simple anticline. These doubts were apparently shared by Fortier (1946) who showed the fold axis in this area as striking north-westerly, a more reasonable explanation in view of the outcrop configuration of the Duck Fm. (Fig. 4).

SCOPE OF THE PRESENT STUDY

This structural analysis was carried out on a reconnaissance level to form a basis for the petrological study. It is ancillary to the petrological work and field coverage was less detailed than is usual in a structural study.

Aerial photograph interpretation and published maps supply abundant information on bedding orientation, including way-up determinations. Field-work was therefore designed primarily to collect data on minor structures and cleavages. Overall traverse density is about 0.8 km. per square km. of mapped area. Details of mapping and data-processing methods are given in the Appendix below and the raw data is compiled on the appended map.

Structural Domains

The area has been found to be structurally inhomogeneous and has been divided into five 'structural domains' whose areal extents are shown in Fig. 4. These domains are defined and delimited on the basis of the following criteria:

1. Fold orientation.
2. Fold style.
3. Orientation and nature of cleavage.
4. Presence of aplite dykes.

HAY LAKE DOMAIN

This large domain has been faulted (Fig. 4) but is otherwise not fault-bounded, grading into other domains at all known margins. The rocks belong almost entirely to the Burwash Fm.

The Obvious Folds

The domain contains numerous mesoscopic and macroscopic folds (Plate 1A; Jolliffe, 1942 and 1946) whose axial traces strike almost exclusively to the north- west (Fig. 5A). Figure 5B indicates that the axes plunge southwards. (The computed mean fold axis for this distribution plunges 57° on 187°, but the scatter is considerable and only a general conclusion should be drawn.)

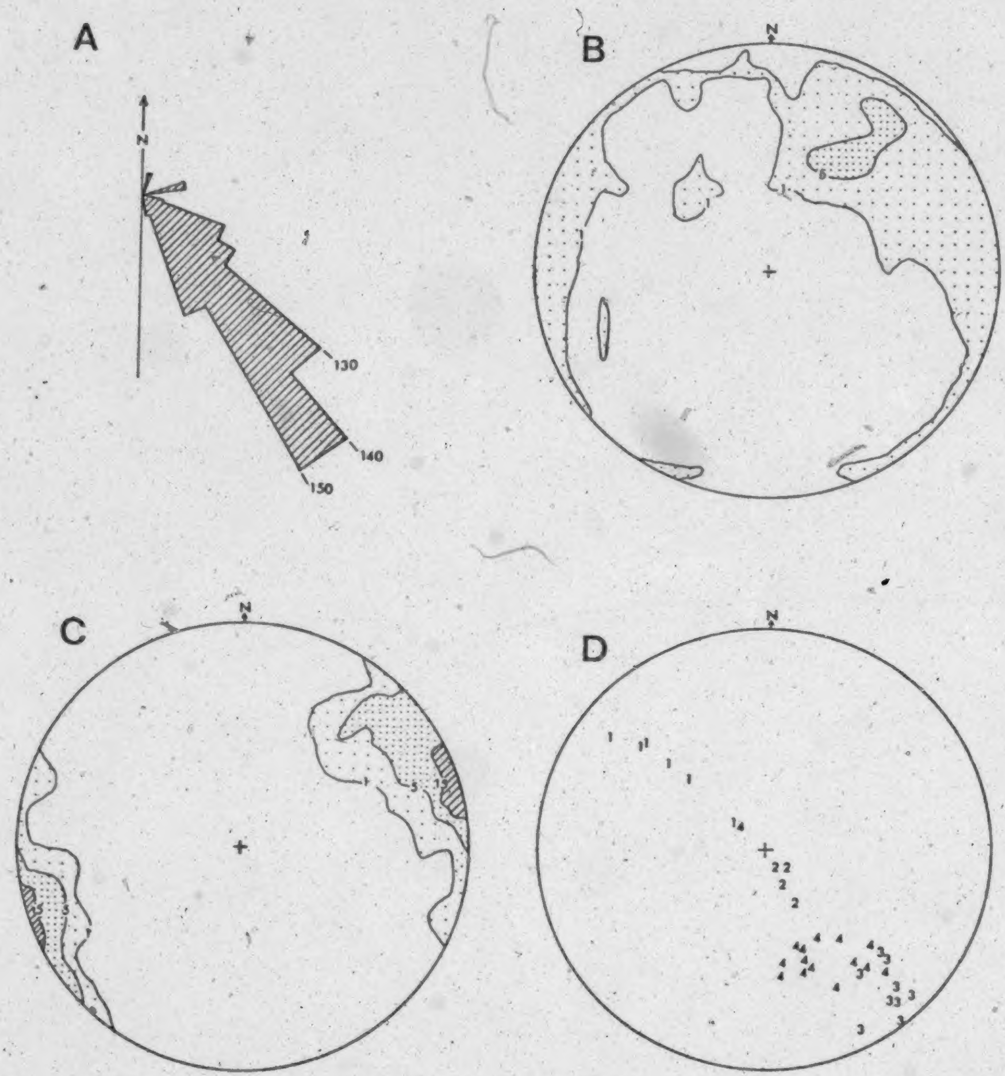

FIGURE 5 : Orientation of structures in the HAY LAKE STRUCTURAL DOMAIN. (A) Major and minor fold axial trace orientations; seven minor folds and 31 major folds are plotted. (B) Poles to bedding; percentage of 199 points per 1% area. (C) Poles to cleavages; percentage of 127 points per 1% area. (D) Axes of the micro-folds shown in Fig. 6; the numbers apply to Fig. 6.

Combining this plunge with the axial trace indicated by Fig. 5A shows that the axial surface dips steeply (~65°) to the south-west. Chevron-shaped folds are characteristic of the western part of the domain, usually being tight folds with about 45° between limb outcrops and having closely-spaced parallel axial planes. In the south-western (Cliff Lake) portion of the domain, the folds tend to be more open, more rounded and more widely spaced. The Cinnamon Island fault separates the western portion from the eastern in which chevron folds are uncommon. Here the strata tend to be very openly folded and in some areas appear unfolded, while still retaining the axial planar and cleavage orientations characteristic of the domain.

Cleavage

Cleavage in the domain is a weak schistosity defined by lepidoblastic orientation of micaceous minerals. Cordierite porphyroblasts are commonly slightly flattened in the plane of cleavage (Plate 1D) though the degree of flatness varies even at one locality. Figure 5C shows that the cleavage orientation deviates little from its mean north-westerly strike and steep south-westerly dip. (The computed mean dip is 84° on 244°.) This strike is parallel to that of the fold axial planes. The dip is not exactly the same as that of the axial planes but, considering the uncertainties of measuring weak cleavages on glaciated outcrops, it may be assumed that the cleavage is axial planar to the folds. This is also observable in the field (e.g. Plate 1C).

Time of deformation. The axial planar cleavage of the dominant folds is defined by alignment of micas and flattened cordierite

PLATE 1

Structures in the Hay Lake, Yellowknife Bridge and Island Lake domains.

A. Closure of a typical Hay Lake domain fold near the southern shore of Prosperous Lake.

B. Micro-folds in a thin quartzite bed near the south-western shore of Prosperous Lake (Hay Lake domain).

C. Detail of the fold in A (above) showing weak axial planar alignment of cordierite porphyroblasts.

D. Cordierite porphyroblasts with weakly preferred orientation on the south-eastern shore of Prosperous Lake (Hay Lake domain).

E. Example of small, sub-vertical folds in the Duck Fm. north-east of the Yellowknife River bridge (Yellowknife Bridge domain).

F. Example of cleavage(B) passing through cordierite porphyroblasts in the Island Lake domain near Island Lake. Note that the porphyroblasts have a preferred orientation parallel to cleavage(B).

G. Weakly developed cleavage(B) at a high angle to aligned cordierites representing the common schistosity. Near Island Lake in the Island Lake domain.

H. Strongly developed cleavage(B) in one bed but absent from the adjacent bed. Near Island Lake in the Island Lake domain.

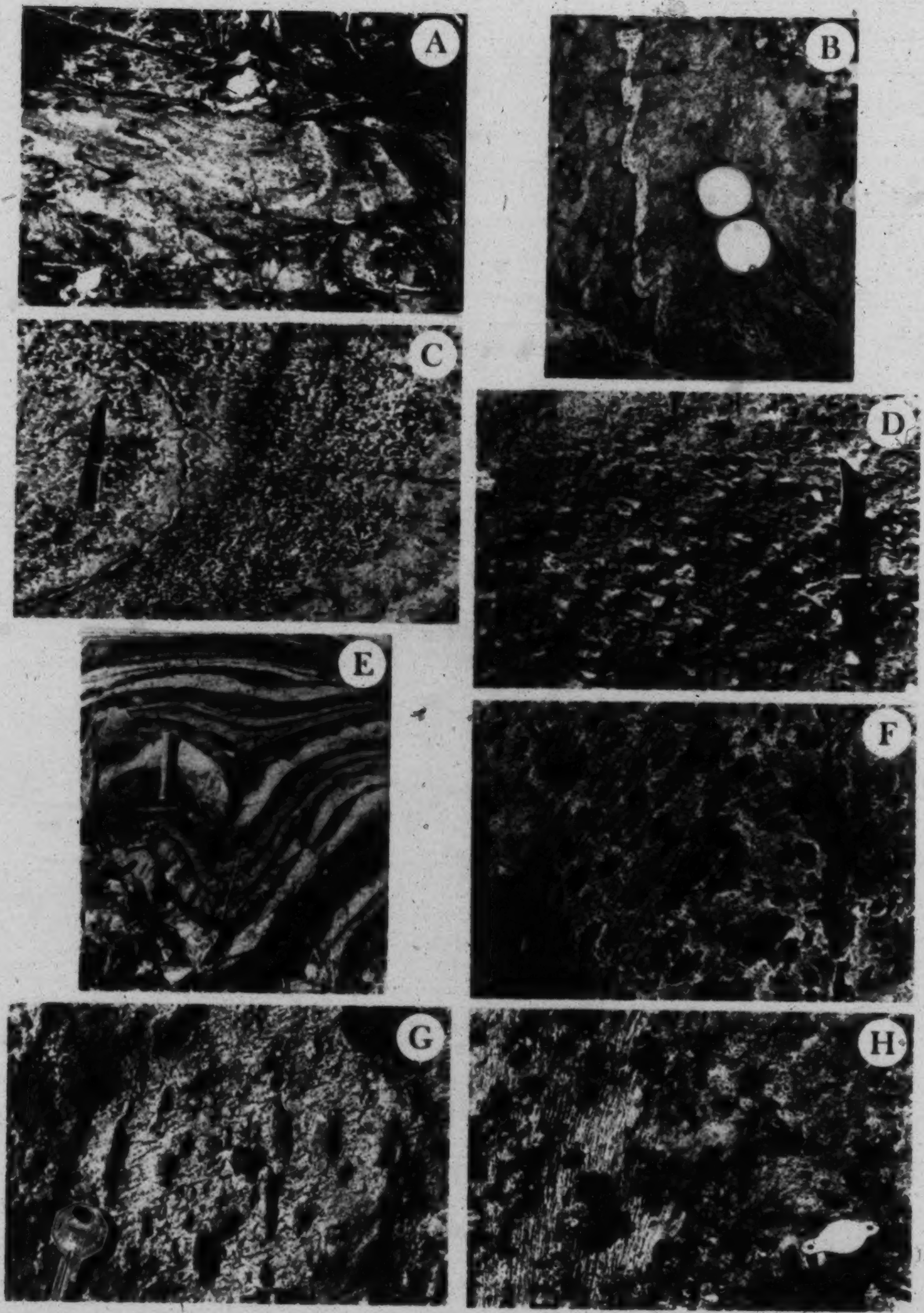

PLATE 1

porphyroblasts (Plate 1D). The areal distribution of cordierite clearly relates its formation to intrusion of the Prosperous Lake granite. Therefore the deformation, metamorphism and intrusion were synchronous and hence probably causally related. Similar conclusions were reached by Fortier (1946).

The Early Isocline Problem

Only one isoclinal fold has been observed in the Hay Lake domain (on a small outcrop north-west of Cliff Lake) and the domain is devoid of interference structures on both macroscopic and mesoscopic scales. There is, therefore, little direct evidence for the existence of the early isoclinal folding phase so common elsewhere. The numerous (>4000) way-up determinations recorded by Jolliffe (1942 and 1946) do not solve this problem either. In a few areas, e.g. between Madeline and Prosperous Lakes, there is evidence that a traverse across strike yields alternating right-way-up and inverted sections, but this does not apply to the whole domain.

Numerous micro-folds (Plate 1B) occur in the Hay Lake domain, both in thin quartzite beds and in quartz veinlets. The latter have been ignored because their initial orientation is unknown but the axes (often rodded) of the former have marked preferred orientation (Fig. 5D). Three problems arise from this. (1) On a simple model of cylindrical folding, this girdle implies re-folding on a sub-horizontal axis trending north-east. No evidence for such an event has been observed anywhere in the domain. (2) The girdle is parallel to the axial plane of the folds in the domain and the micro-folds are not parallel to the average fold axis for the domain. This may indicate

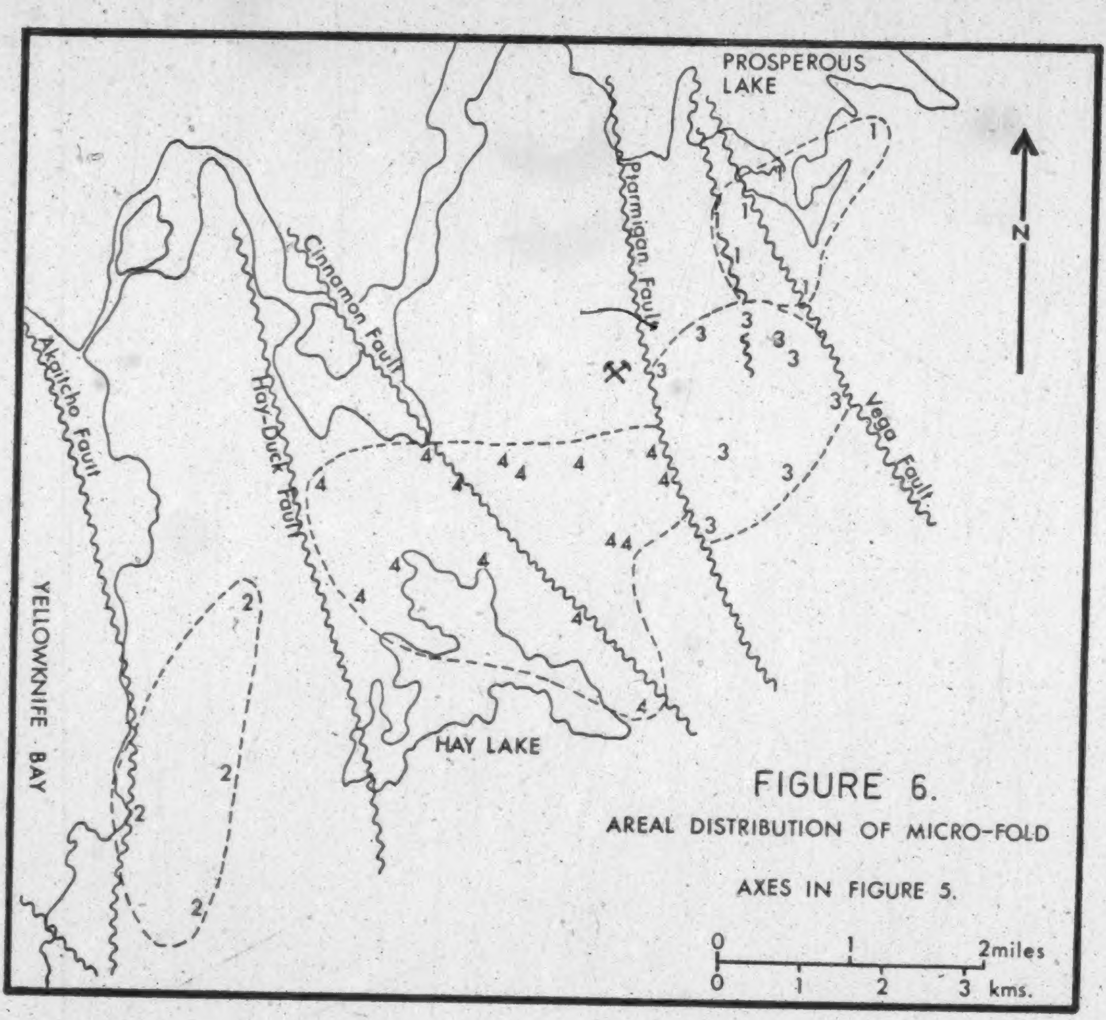
PROSPEROUS LAKE
N
Ptarmigan Fault
Vega Fault
Cinnamon Fault
Hay-Duck Fault
Akaitcho Fault
HAY LAKE
YELLOWKNIFE BAY
1
1
1
1
3
3
3
3
3
3
3
3
3
3
4
4
4
4
4
4
4
4
4
4
4
4
4
4
4
2
2
2
2
0
1
2miles
0
1
2
3
kms.

FIGURE 6.
AREAL DISTRIBUTION OF MICRO-FOLD AXES IN FIGURE 5.

that folding was non-cylindrical (Turner and Weiss, 1963) but it is uncertain whether this is a result of superimposed folds or a single folding event. (3) The micro-folds from restricted areas plot in clusters on the stereogram and there is some indication that these areas are fault-bounded (Fig. 6). This possibly implies a rotational component in the late faulting, but it seems improbable in view of the known nature and extent of the faults which preclude more than very minor rotation. Thus the micro-folds are of undetermined origin. There are several possible explanations for their observed distribution but re-folding is not necessarily implied.

Fabric. Rocks from the western portions of the domain, at low metamorphic grades, have a very fine-grained lepidoblastic or phyllitic foliation defined by muscovite and chlorite. Biotite porphyroblasts cut across this (Plate 3B) or, in a few instances, are parallel to it. Towards the east in the domain the schistosity is increasingly defined by biotite and cordierite as the chlorite and muscovite are metamorphically consumed. These textural relations suggest that an early episode of recrystallisation (the early isocline formation?) was succeeded by another (metamorphism by the Prosperous Lake pluton) which imposed a new schistosity on the old.

Conclusion. The data at hand fail to prove or disprove the existence of early isoclines in this domain. The fabric relations are compatible with their presence and the variable orientation of the micro-fold axes suggests some deformation since micro-fold formation. However, the spatial distribution of the micro-folds indicates that such re-orientation did not occur during formation of the 'obvious' folds. Further, isoclinal closures are extremely rare and interference structures are absent. This author concludes tentatively that there was no early isoclinal folding in the Hay Lake domain, but more detailed work is required to clarify the problem.

Some Deviations

Although the overall pattern of cleavage orientation in the domain is simple (above) several localised deviations from it have been noted:

1. In general terms the strike of cleavage becomes more meridional from the east to the west within the domain (ca. 315° near Prosperous Lake; ca. 345° near Yellowknife Bay). The reason is not known, but this is the cause of much of the circumferential scatter in Fig. 5C.
2. West of the Hay-Duck fault, and particularly in the northern half of that area, a subordinate N. N. E.'ly cleavage is common. Typically a large fold has axial planar cleavage typical of the Hay Lake domain in most of its outcrop but in some areas has a cleavage striking N. N. E. This is usually seen in pelitic beds and is parallel to the cleavage in the Yellowknife Bridge domain (below). It is thought to represent relics of that cleavage incompletely overprinted by the later schistosity.
3. Cleavage is draped round irregular quartz veins at many localities.
4. Between Hay Lake, Cinnamon Island and the Ptarmigan Mine pelitic rocks are strongly lineated and commonly

have two fissility planes. Though somewhat variable, these strike 355-005° and 320-335°, both dipping steeply east. They may be due to the same effect as in 2. above, but no detailed study of their origin has been attempted.

The lineation comprises fine crinkles or striae on cleavage planes, plunging 5-40° on 340°, and cannot be due to the intersection of the two fissilities. Thin-sections perpendicular to the lineation reveal marked kinking of the schistosity and kinks are commonly observed in the field. The lineation therefore probably represents the intersection of kink planes and cleavage.

Nature of the Hay Lake Domain

Glossing over these complexities, the structure of the domain appears fairly simple. There was apparently an early phase of recrystallisation (perhaps accompanied by isoclinal folding) to produce a chlorite-muscovite (-?biotite) schistosity. These rocks were deformed into numerous folds with axial planar cleavage striking northwest and dipping steeply south. The early cleavage was increasingly overprinted by the metamorphic recrystallisation accompanying the deformation so that relics may be seen in the low-grade rocks in the west but not in the east. The north-westerly folding phase was synchronous with intrusion of the Prosperous Lake pluton and its attendant metamorphism.

THE YELLOWKNIFE BRIDGE DOMAIN

The mapped area of this domain is small but it may extend to the S.S.W. and N.N.E. (see Fig. 41). The rocks belong to the Burwash Fm. and the Walsh Fm., whose thin-bedded, incompetent nature has produced a characteristic fold style (Plate 1E).

Folds

There are numerous mesoscopic and macroscopic folds, most of which have very steep plunges and axial traces striking N. N. E. (Plate 1E; Fig. 7A). Gentle warps in the bedding are common, but a typical fold in the Walsh Fm. ranges from 3 to 30 m. in wavelength and amplitude, has about 60-80° between limb outcrops and plunges very steeply southwards. In the more massive rocks of the Burwash Fm. the folds are less common, rather larger and more open but have the same orientation. A few folds have been observed to have axial traces striking north-west, the characteristic orientation for the Hay Lake domain.

Cleavage

Cleavage is defined by phyllitic orientation of very fine-grained muscovite and chlorite. The relationship of biotite to this foliation is unknown. In outcrop the cleavage is seen to be axial planar to many folds (though its strike varies by up to 20° at any one locality), and this is confirmed by Fig. 7B. There is considerable circumferential spread in this stereogram, overlapping with Hay Lake domain cleavage orientations.

In addition to this axial planar cleavage there is sometimes a weak fissility parallel to bedding, particularly in Walsh Fm. slates. This was at first thought to represent an early schistosity, but thin-sections show no sign of metamorphic foliation parallel to this fissility and no evidence to support the idea has been found. Probably

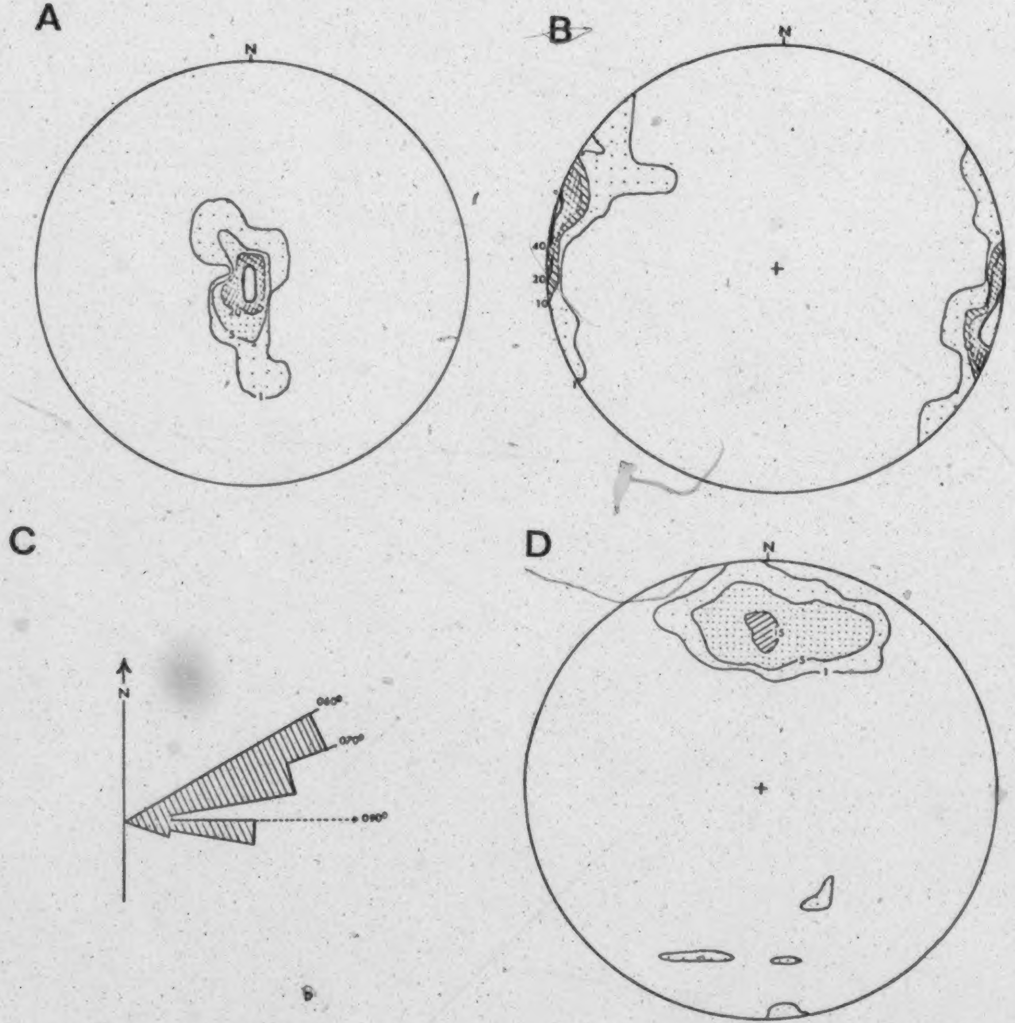

FIGURE 7 : Orientation of structures in the YELLOWKNIFE BRIDGE and DUCK LAKE STRUCTURAL DOMAINS. (A) Minor fold axes in the Yellowknife Bridge domain; percentage of 27 points per 1% area. (B) Poles to cleavages in the Yellowknife Bridge domain; percentage of 49 points per 1% area. (C) Axial traces of 14 major and minor folds in the Duck Lake domain. (D) Poles to rational cleavages (see text) in the Duck Lake domain; percentage of 53 points per 1% area.

it is simply due to sedimentary lamination.

In the more massive Burwash Fm. rocks the cleavage is weaker and commonly refracted in graded beds, which confuses the measurement of cleavage orientation. Diamond-shaped pencils occur in some slatey beds, testifying to the presence of two fissility planes. One of these is always parallel to bedding and is therefore thought to be of primary origin; the other is most commonly the dominant N.N.E.'ly cleavage, occasionally the north-westerly Hay Lake direction.

Nature of the Yellowknife Bridge Domain

The domain is bounded in the east by a fault but is thought to merge southwards into the adjacent domain. It is also thought to extend westwards beyond the Yellowknife River. The structure is dominated by N.N.E.'ly trends. No signs of poly-phase deformation have been observed though the folds plunge very steeply. The occasional occurrence of folds and cleavages with the north-westerly Hay Lake trend may indicate weak effects of the Hay Lake deformation within the domain. Because of this, and because the mineralogy of the Yellowknife Bridge rocks is paragenetically earlier than that associated with Hay Lake domain structures, the Yellowknife Bridge structures are thought to be earlier than the Hay Lake structures. There is no definite genetic connection between the Yellowknife Bridge structures and the Western Granodiorite but the domain is geographically adjacent to the pluton and its structures are roughly parallel to the contacts. As such the deformation may have been caused by inflation of the pluton (e.g. Clifford, 1972).

THE DUCK LAKE DOMAIN

This domain is markedly different from the others, containing highly complex structures and distinctive lithologies. It has only been defined east of the Hay-Duck fault but presumably there is an equivalent to the west (Fig. 4).

Folds

The folds are isoclinal. Several large isoclines and a few minor ones have been found (Plate 2A and map). Axial planes of these folds strike east to north-east (Fig. 7C) and the axes plunge gently (20 to 45°), in some instances to the east, in others to the west. Axial planes and beds dip steeply (65 to 80°) southwards, towards the pluton. Only at two locations, very close to the pluton contact, was bedding observed to dip away from the contact.

Cleavage

The nature of the cleavage is very complex and largely unresolved. Its character varies from location to location. Commonly two distinct schistosities are present, one being irregular as though deformed (Plate 2B and C). The latter cleavages have not been measured but the coherent, rational cleavage of the dominant orientation dips steeply to the south (Fig. 7D) and is axial planar to the isoclinal folds. If this stereogram is taken to represent the simplified pattern of cleavage, two principal deviations from it may be recognized:

1. North of Duck Lake the cleavage in meta-greywackes is weak and rational. Meta-pelites, however, commonly contain irregular cleavage, though coherent folds in this cleavage are rare. Some of this

PLATE 2

Structures in the Duck Lake domain.

A. Minor isoclinal fold on the north shore of Duck Lake. The fold has a sub-horizontal axis and steeply dipping limbs.

B. Small folds in schistosity east of Duck Lake. Photograph taken looking down the axes of the folds, whose crests form a strong lineation parallel to the axis of a major isocline.

C. Complex (deformed?) schistosity at the closure of a major isocline east of Duck Lake. Representative schistosity planes are marked in black. See text for discussion.

D. Typical aplite dykes transecting bedding in the Duck Lake area.

E. Typical outcrop appearance of the aplite dykes in the Duck Lake domain.

F. Migmatite in the contact zone of the South-Eastern Granodiorite. The light-coloured rock is a slightly porphyritic feldspathic rock and the dark is biotitic meta-sediment.

G. Minor fold near the north shore of Duck Lake displaying two distinct cleavages. One is folded, the other is axial planar to the fold and oriented parallel to typical Hay Lake domain cleavage.

H. Complexly (probably multiply) deformed quartz-rich bed or veinlet. The more open fold has an axial planar cleavage dipping steeply on 070°, i.e. parallel to Hay Lake domain structures. There are also traces of an earlier foliation which has been deformed.

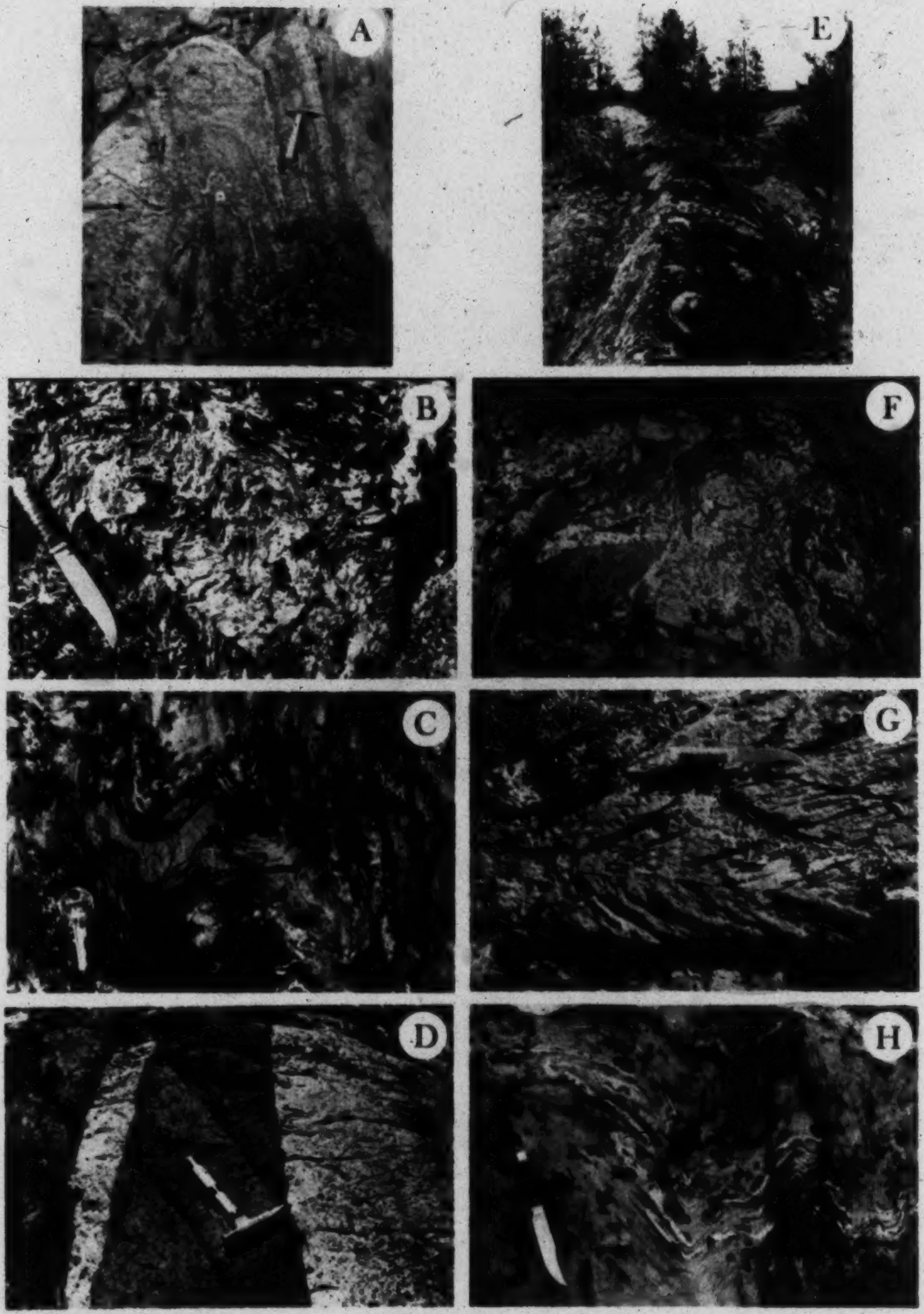

PLATE 2

irregularity is attributable to quartz segregations but much is not. No consistent orientation or style for this irregularity has been recognised. As metamorphic grade increases southwards, the irregularity gradually vanishes.

2. East of Duck Lake, often near the closures of major isoclines, a different problem is encountered. Commonly an undulating cleavage blends into an axial planar cleavage (Plate 2C). In some instances the hinges of these folds(?) form strong lineations parallel to the major fold axes. Thin-sections show this cleavage to be a micro-folded schistosity defined by aligned chlorite, muscovite and biotite.

Aplite Dykes

Numerous porphyritic biotite aplite dykes outcrop in the Duck Lake domain (Plate 2D and E). These are somewhat variable but are light-coloured, slightly porphyritic rocks with a moderately strong foliation defined by aligned micas. They consist of fine-grained granular quartz, sodic plagioclase and aligned biotite, with subhedral phenocrysts of sodic plagioclase and occasionally quartz or corroded muscovite.

The dykes are about 1/2-3 m. thick, strike approximately east-west and dip steeply southwards towards the granodiorite. They cross-cut bedding and are not folded by the major isoclines. Some are slightly boudinaged but otherwise are long, straight and undeformed. Their number increases towards the pluton margin and in some areas they constitute a large proportion of the outcrop.

The dykes are clearly related to the intrusion of the South-Eastern Granodiorite. They are sub-parallel to the margin of the pluton but are at a high angle to local apophyses. They have not been observed cutting the granodiorite and are therefore thought to have been emplaced before it. Probably they are ring-dykes intruded in advance of the batholith.

The South-Eastern Granodiorite and Its Contacts

In the Duck Lake area the pluton consists of unfoliated, structureless, medium-grained granodiorite containing about 15 per cent biotite. Its outline is highly irregular and bulbous (Fig. 4; Fig. 8) and migmatites, gneisses, dykes, etc. are commonly found in the re-entrants. The nature of the contact is variable with all gradations between the following types:

1. The simplest contact zone involves only a progressive increase in the number of aplite dykes followed by a sharp, unsheared contact between meta-sediments and massive granodiorite. A few biotitic screens of meta-sediment may occur in the granodiorite.
2. In other areas aplite dykes become more numerous until there are about equal amounts of dyke and meta-sediment. This grades to a zone of migmatites (Plate 2F) in which porphyritic feldspathic rocks are present, thoroughly infolded with the meta-sediment. This in turn grades to massive granodiorite. The width of such a contact zone is 100-200 m.

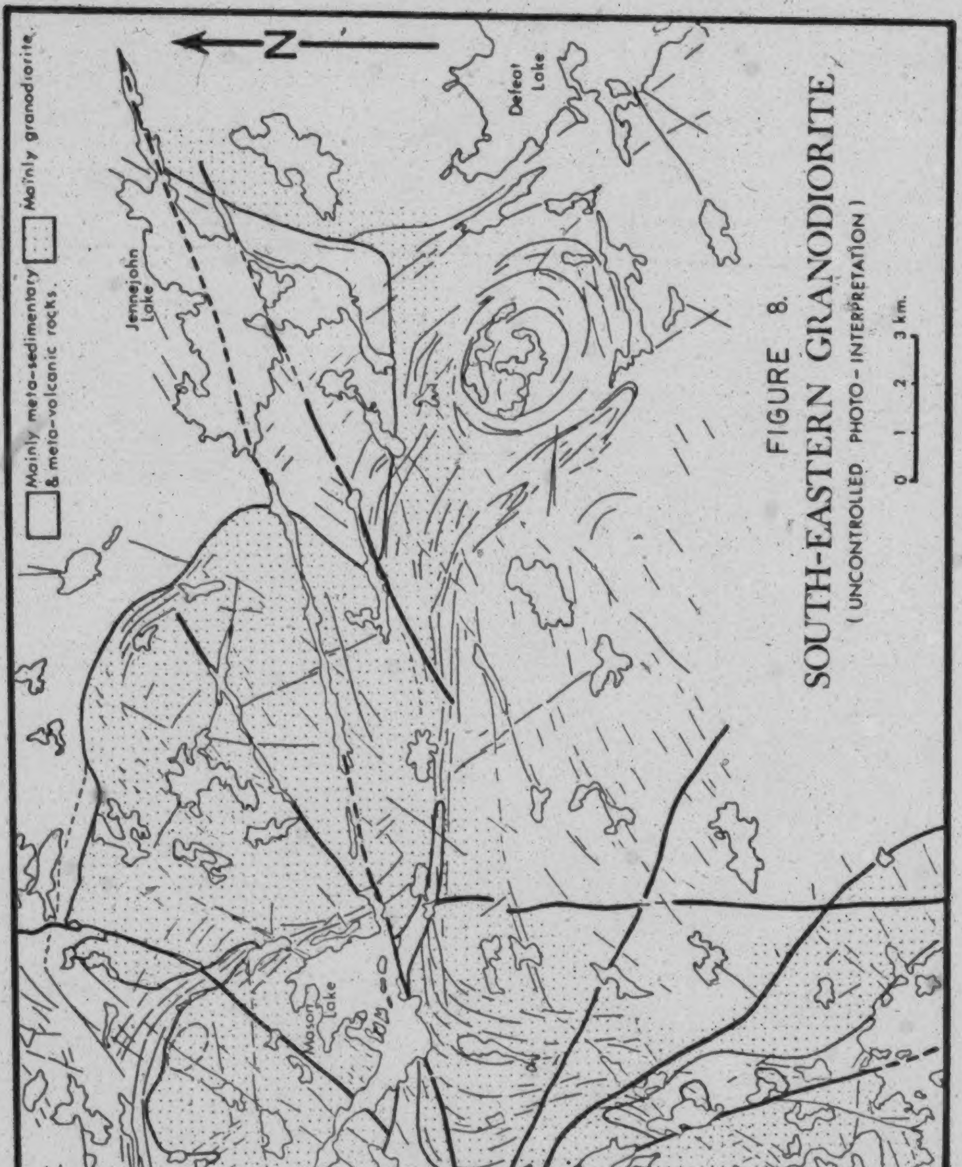
N
Mainly meta-sedimentary & meta-volcanic rocks.
Mainly granodiorite.
Defeat Lake
Jennejohn Lake
Mason Lake
Willow Lake
Duck Lake
YELLOWKNIFE BAY
0 1 2 3 km.

FIGURE 8.
SOUTH-EASTERN GRANODIORITE
(UNCONTROLLED PHOTO-INTERPRETATION)

3. A more chaotic assemblage of mixed rocks occurs in the re-entrant screen of meta-sediment between Duck and Mason Lakes. Many rock types have been observed: biotitic schists (± porphyroblasts); aplite dykes; feldspar porphyries; hornblende diorites (oligoclase phenocrysts in a fine mass of aligned hornblende and biotite); quartz veins; migmatites.

These contact relations and the structural setting leave little doubt that the exposed granodiorite represents the upper-most levels of a diapirically emplaced pluton. It was composed of several diapiric bulbs and apparently advanced by both digestion and deformation of country rocks.

Interaction of Duck Lake and Hay Lake Structures

East of the Hay-Duck fault the Stuart Lake domain (below) is thought to represent the interaction of these two structural styles. West of the fault there is a much smaller area of interaction exposed, but one locality is of particular interest as refolded isoclines may be readily observed there (Fig. 9). (This locality is near the shore of Duck Lake about 800 m. west of the Hay-Duck fault.) Most of the minor folds and cleavages trend north-westerly and resemble typical Hay Lake domain structures, suggesting that they were formed during that deformational event. Similar suggestions of multiple deformation may be observed on a small scale, e.g. folded cleavage and multiply deformed quartz veinlets (Plate 2G and H). The inference is that isoclines of the Duck Lake domain were re-folded in the Hay Lake style.

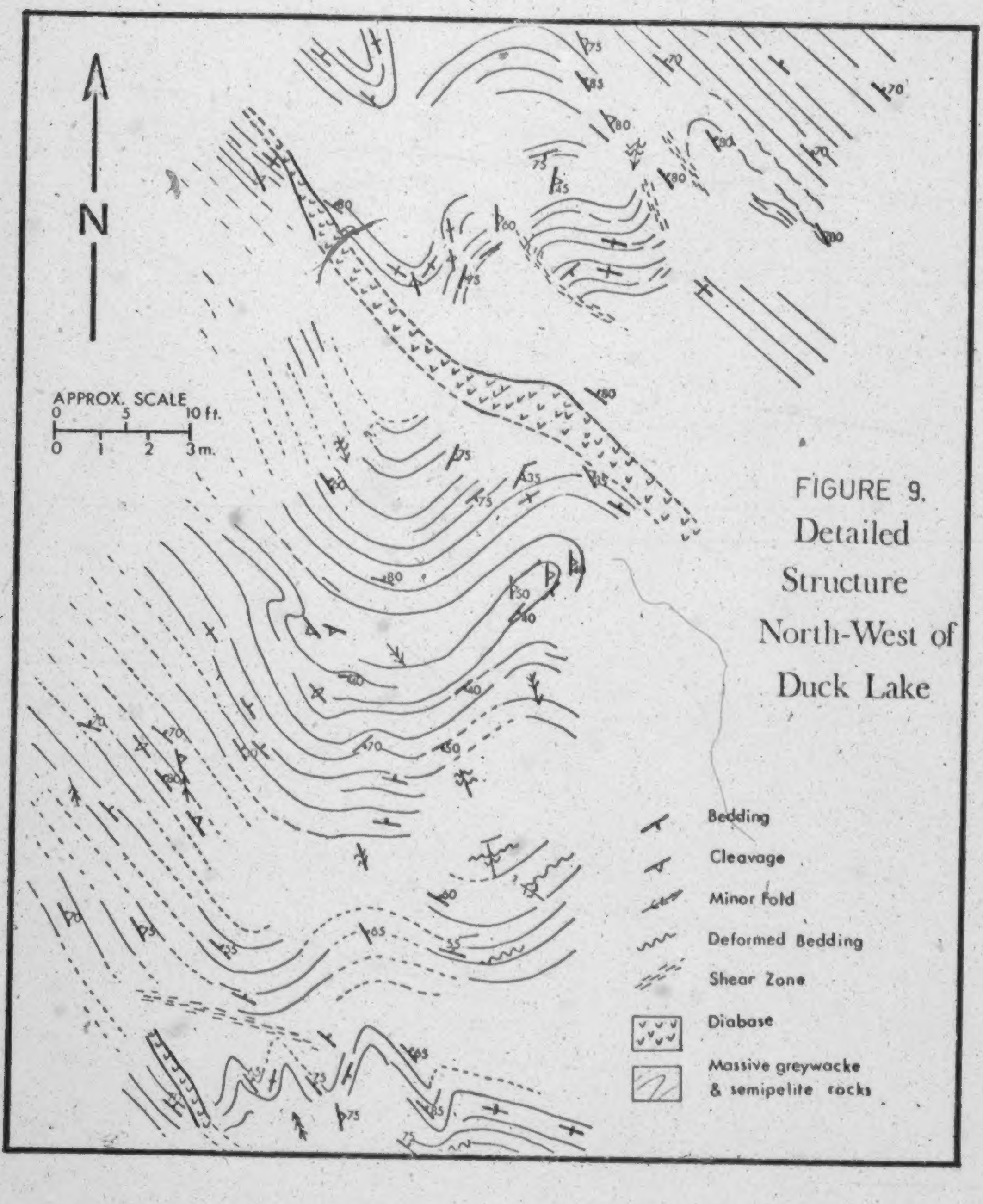
N
APPROX. SCALE
0 5 10 ft.
0 1 2 3 m.
Bedding
Cleavage
Minor Fold
Deformed Bedding
Shear Zone
Diabase
Massive greywacke & semipelite rocks

FIGURE 9.
Detailed Structure North-West of Duck Lake

Nature of the Duck Lake Domain

This domain is an area of complex lithologies and deformation intimately related to the intrusion of the South-Eastern Granodiorite. The characteristic fold style is one of shallowly plunging isoclines sub-parallel to the contacts of the pluton and dipping steeply into it. Deformed schistosity in the hinges of these folds may indicate that the rocks were deformed or recrystallized prior to the isoclinal folding. Alternatively it may have resulted from the isoclinal folding itself by some unknown mechanism (e.g. Roberts, 1971; Williams, 1972). The structural history probably began with isoclinal folding. These folded rocks were intruded by aplite ring-dykes and then by the main mass of granodiorite. Rocks in the extremities of the domain were later deformed by the Hay Lake deformational event.

THE STUART LAKE DOMAIN

This is a small area between the Hay Lake and Duck Lake domains and having features of both. The rocks all belong to the Burwash Fm. and are weakly cleaved semi-schists similar to those of the Hay Lake domain. The northern and southern boundaries are gradational.

Folds

The domain is characterised by open folds with axial planes striking east-west (Fig. 10A) and dipping to the south. The folds are overturned so that both limbs dip southwards (Fig. 10B).

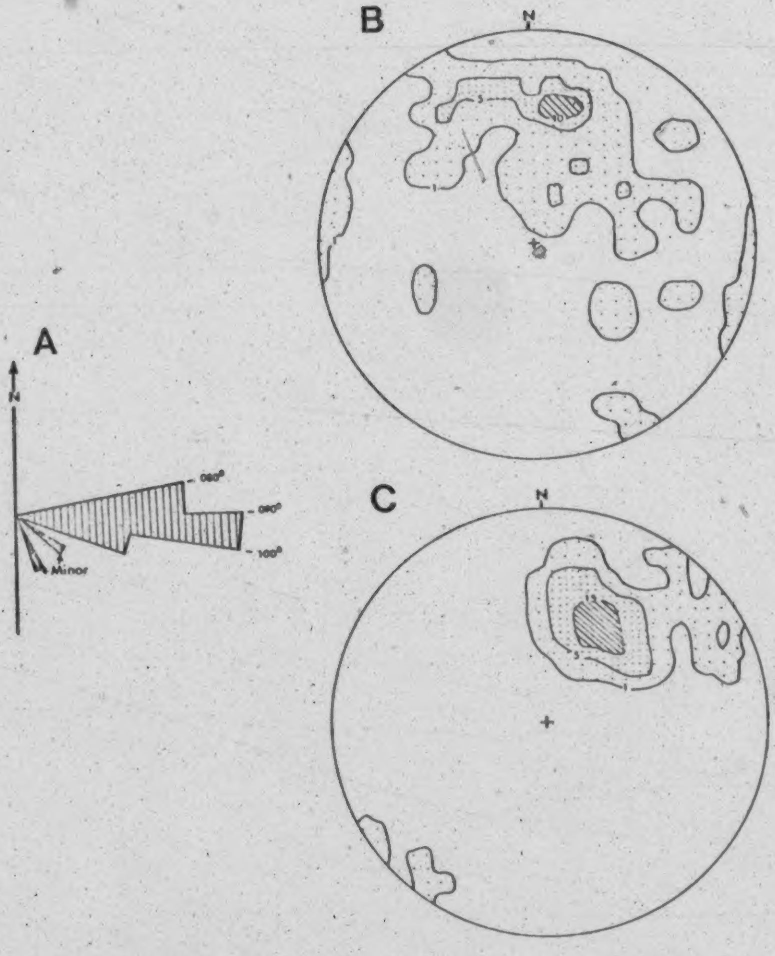
B
N
5
1
A
N
080°
090°
100°
Minor
C
N
13
5
1

FIGURE 10 : Orientation of structures in the STUART LAKE STRUCTURAL DOMAIN. (A) Fold axial traces; nine major folds and two minor folds are represented. (B) Poles to bedding; percentage of 44 points per 1% area. (C) Poles to cleavage; percentage of 43 points per 1% area.

Cleavage

The cleavage is defined by preferred orientation of chlorite, muscovite and biotite, as in the Hay Lake domain. It strikes to the north-west but dips rather more gently (ca. 50°) than in the Hay Lake domain. The reason for this is not known. This schistosity is axial planar to the two minor folds in Fig. 10A but not to the major folds. No indication of deformation of the cleavage been noted. In a few locations there are two cleavage orientations (strike 290-300°, dip moderately south; strike 320°, dip more steeply south) but they are similar and tentatively ascribed to refraction effects.

Nature of the Stuart Lake Domain

This domain has fold axial planes roughly parallel to those of the Duck Lake domain but has a more open fold style and a non-axial planar schistosity approximately parallel to that of the Hay Lake domain. Apparently the major folds were produced during formation of the Duck Lake isoclines as peripheral effects of that deformation. Later recrystallisation and minor deformation produced a few minor folds and schistosity oriented parallel to Hay Lake domain structures and probably were synchronous with them.

THE ISLAND LAKE DOMAIN

This domain comprises rocks of the Burwash Fm. displaying clearly visible interference structures and an unusual metamorphic foliation termed 'cleavage (B)'. The entire domain is situated above the cordierite isograd.

Folds

Most fold axial planes strike to the north-west as in the Hay Lake domain (Fig. 11A) but several strike to the north-east,

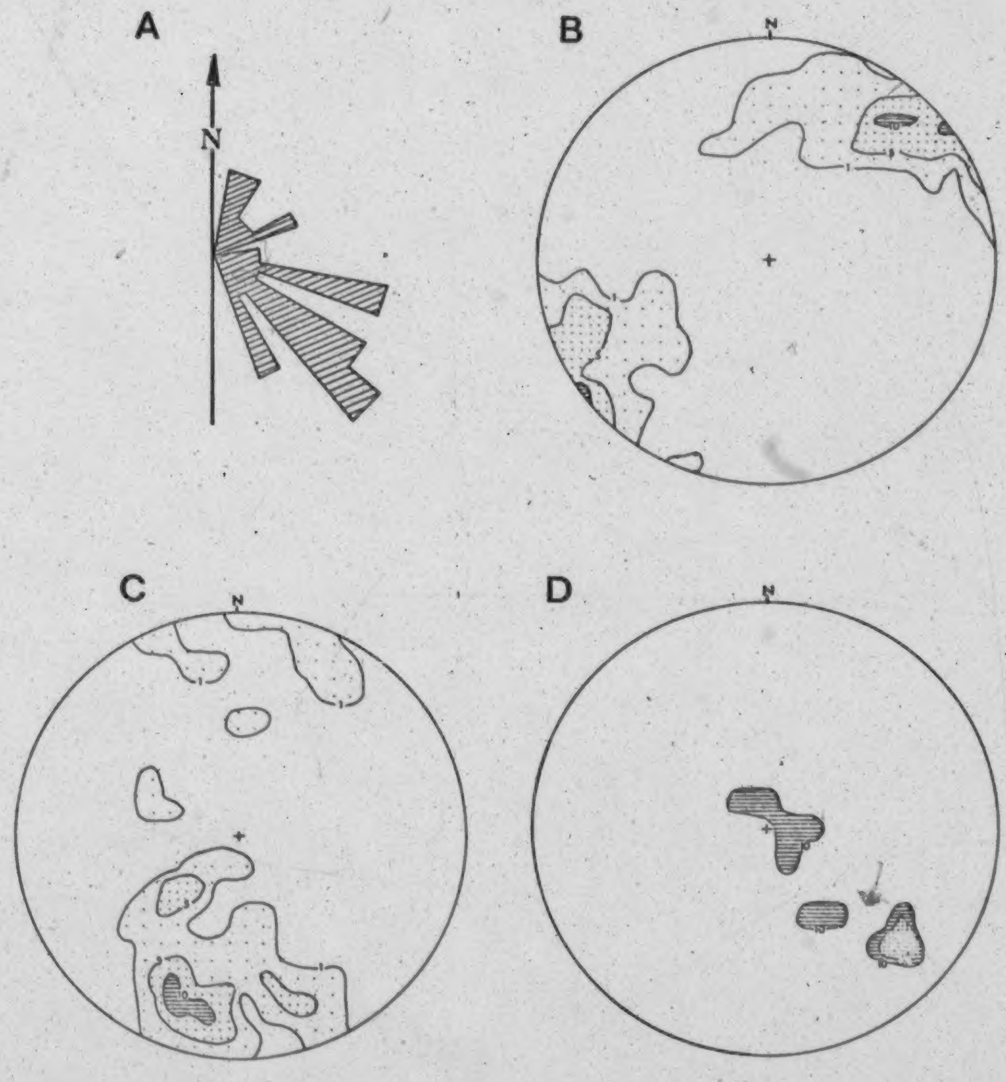

FIGURE 11 : Orientation of structures in the ISLAND LAKE STRUCTURAL DOMAIN. (A) Fold axial traces; 27 major folds and two minor folds are represented. (B) Poles to common cleavage; percentage of 88 points per 1% area. (C) Poles to cleavage(B) (see text); percentage of 43 points per 1% area. (D) Micro-fold axes; percentage of five points per 1% area.

an orientation observed nowhere else in the area. As a result there are domal and basinal structures indicative of folding on two roughly perpendicular axes.

South of Island Lake is a series of clearly exposed re-folded isoclines. The origin of these is uncertain, but their style and location suggest that they might be refolded folds of the Duck Lake domain type.

Cleavage

The dominant cleavage is the same as that of the Hay Lake domain in appearance. It is somewhat variable but is subvertical and strikes north-west, again as in the Hay Lake domain (Fig. 11B). This stereogram gives some suggestion that the cleavage has been folded on a south-easterly plunging axis which is roughly parallel to the micro-fold axes in the area (Fig. 11D). The general orientation is axial planar to the dominant fold trend and is apparently equivalent to the Hay Lake cleavage.

The presence of cleavage (B) characterises the domain. It consists of parallel biotitic streaks in the rock (Plate 1F, G and H) rather than a penetrative alignment of evenly spaced micas. It has sporadic occurrence and is commonly found only in the more quartzose beds (Plate 1H), though in some localities it is common enough to be the dominant metamorphic foliation. Beds exhibiting cleavage (B) often have traces of normal schistosity at high angles to it (Plate 1G). Cordierite porphyroblasts may be flattened parallel to either foliation. Cleavage (B) commonly passes through the porphyroblasts (Plate 1F).

It seems logical to link cleavage (B) and the north-easterly fold axes since neither occurs outside this domain. However, the orientation of cleavage(B) is variable (Fig. 11C), suggesting that the two should not be linked as the youngest event. Thus it seems possible that this cleavage is an earlier structure deformed during the Hay Lake deformation.

Micro-folds

These are rare in this domain. They resemble those of the Hay Lake domain (above) in appearance and in orientation (Fig. 11D) and so the problem of their origin is also the same. The fact that they have the same orientation as in the Hay Lake domain indicates that they have not been deformed since the Hay Lake deformational phase. Therefore the north-easterly folding in this domain pre-dated the Hay Lake event.

The Nature of the Island Lake Domain

Deformation in this area involved one more phase of deformation than recorded in the Hay Lake domain. Apparently there was very localised folding on north-easterly trending axes before the Hay Lake deformation was superimposed on it. These fold axes and cleavage (B) are tentatively ascribed to the influence of the Duck Lake deformation, overprinted by the Hay Lake structures.

FAULTS

The area has been dissected by numerous late faults, particularly near Yellowknife Bay. They belong to the system described in detail by Henderson and Brown (1966) and post-date both metamorphism and the fold structures, so no detailed description is necessary here. Several points should, however, be recorded.

TABLE I : Proposed tectonic history of the Yellowknife Bay-Prosperous Lake area. Dates are from Green and Baadsgaard (1971).

	Event	Date (m.y.)	Structural Effects	Metamorphic Effects	Comments
	Faulting, diabase intrusion.	?1140 (see comments)	Kinking possibly of this age.	Localised retrogressive alteration.	Anomalous reference isochron of Green (1968).
Prosperous Lake Cycle	Pegmatites				
	Gold-quartz veins				Fortier (1946).
	Prosperous Lake adamellite	2575±25	Widespread folding on axes trending North-West.	Extensive zoned metamorphism of an Abukuma facies series.	Deformation, intrusion and metamorphism causally related and synchronous.
	Hay Lake deformation				
	Yellowknife Bridge deformation		Steeply plunging folds trending E. N. E. May have formed by inflation of the Western Granodiorite.		Fold attitudes suggest that strata were inclined prior to folding.
	Western Granodiorite	2590-2610	May have caused the Yellowknife Bay syncline.	Contact metamorphism.	Relation of intrusion and deformation not definitely established
Duck Lake Cycle	South-Eastern Granodiorite	2620-2640		Contact metamorphism.	Pluton, dykes, folding and metamorphism intimately related.
	Aplitic dykes (? ring-dykes)				
	Duck Lake deformation		Steeply-dipping, isoclinal folds with sub-horizontal axes.		
	?		See comments.		Undulatory (? deformed) cleavage in the Duck Lake domain may indicate prior deformation.
	Sedimentation				May have continued during intrusion of granodiorites.
	Volcanism	2650-2625			
	Oceanic crust				

1. Hydrothermal alteration is a marked feature of these faults, though most have parts free of alteration. Typically they are narrow structures lacking quartz veins but they have caused chloritization of mafic minerals in the adjacent rocks and produced a faint hematitic colouration. Pyrite and carbonate usually are present in small amounts and micro-veinlets carrying K-feldspar are common. Shearing and brecciation (or incipient brecciation) is rare but does occur at some localities. Quartz mineralisation has been observed only on the Vega fault. Similar alteration is also associated with diabases.
2. Between the Hay-Duck fault and Yellowknife Bay this alteration has affected a large proportion of the rocks because faults are so numerous. This is thought to be the reason for the anomalous Rb-Sr isochron (reference isochron = 1140 m. y.) which Green (1968) obtained for meta-sediments collected in this area. If this is correct, it suggests that the faults were active and diabases were intruded at that time.
3. The lateral displacement on the faults usually cannot be determined accurately. The Hay-Duck fault has about 2 km. of horizontal movement. The displacement on the Cinnamon Island fault is unknown but there is considerable structural discontinuity across it (see above). The Ptarmigan and Vega faults

apparently have very little lateral displacement. Petrologically there is no mineralogical change across any of these faults in the aureole of the Prosperous Lake granite and no detectable discontinuity in trends of mineral composition. This is because the faults are tangential to the isograds so that limited lateral movement has not caused any change in metamorphic grade across the faults.

SYNTHESIS: TECTONIC HISTORY

This reconnaissance study has revealed rather more complexities than it has explained. While complete elucidation of the structural history must await detailed study, a tentative picture may be deduced by fitting the structural information (above) to the existing geochronological data. Table 1 summarises this suggested history.

It is uncertain whether the South-Eastern or the Western Granodiorite should be taken as the oldest pluton as geochronologists have disagreed on the interpretation of Green's (1968) data (Green and Baadsgaard, 1971; Thorpe, 1971) and no structural evidence has been found on this question. Here the sequence suggested by Green and Baadsgaard is followed because it is based on both Rb-Sr and U-Pb dating methods and they are in agreement.

Deformation of the sedimentary rocks occurred in very localised domains. Three of these are geographically and genetically related to the major batholiths and two of them resulted from superimposition of the structures of two domains. This relationship is in accord with those observed in other cratonic terrains (Anhaeusser et al., 1969; Goodwin, 1972) and is best explained by the batholith inflation

FIG. 12 : YELLOWKNIFE EVOLUTIONARY MODEL

(Modified after models of Glikson, 1972, and Badham, personal communication, 1972.)

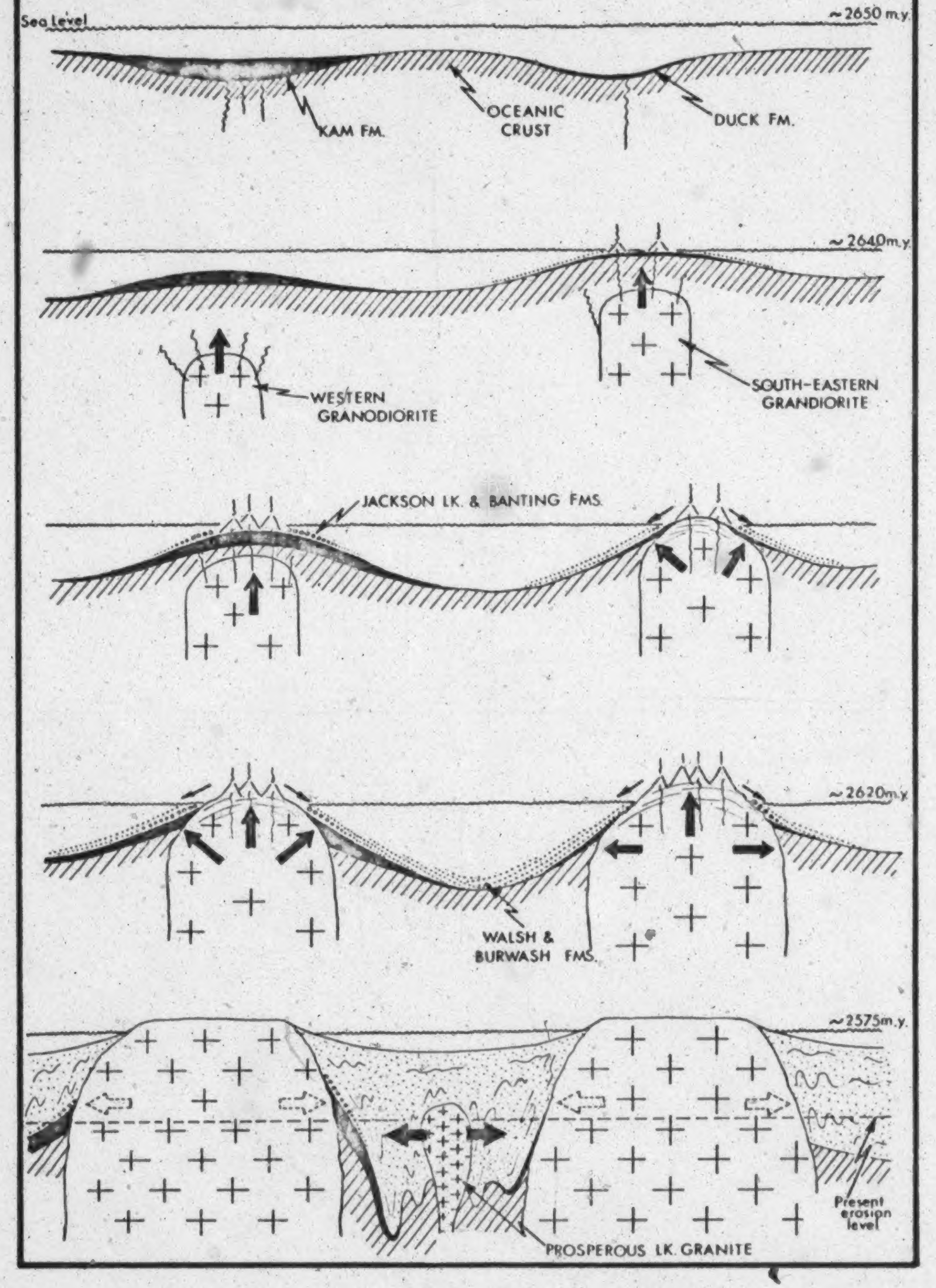
Sea Level
~2650 m.y.
KAM FM.
OCEANIC CRUST
DUCK FM.
~2640 m.y.
WESTERN GRANODIORITE
SOUTH-EASTERN GRANDIORITE
JACKSON LK. & BANTING FMS.
~2620 m.y.
WALSH & BURWASH FMS.
~2575 m.y.
Present erosion level
PROSPEROUS LK. GRANITE

model of Clifford (1972).

Where refolded folds have been observed they can usually be ascribed to the marginal overlap of two deformational domains and there is no conclusive evidence for ubiquitous early isoclinal folds.

AN EVOLUTIONARY MODEL

In view of the rarity and ambiguity of evidence for a granitic basement to the Kenoran succession, the author follows Glikson (1972) in believing the craton to have evolved on oceanic crust (also Green and Baadsgaard, 1971). Perhaps the localised areas of granitic 'basement' are explained by the existence of very small, very thin areas of differentiated sialic 'scum' on the surface of this basic crust. The distinction of this oceanic crust from the basal lavas may well be principally semantic so that the Kam Fm. might be considered to be oceanic crust unless a significant time difference can be demonstrated between these lavas and their basement.

The formative cycle in the Slave Craton (Fig. 12) began very late (2650 m.y.) compared to that of other cratons and probably represents the last occasion on which crustal conditions permitted craton formation. (Consequently the Slave Craton differs in some respects from the others, principally in that a rather shallower structural and stratigraphic level is exposed.) Broad linear downwarps in the oceanic crust occurred and were filled (2650 m.y.) by volcanic rocks (the Kam and Duck Fms.). As thermal processes continued, large volumes of granodiorite magma were generated and migrated diapirically upwards, up-doming the extruded lava piles. These batholiths were emplaced at slightly different times in the period 2640-2620 m.y.⁴ and in regions with variable thicknesses of volcanic rocks (compare the Western and South-Eastern Granodiorites.) They were preceded by ring-dykes, acid or intermediate lavas and pyroclastics which formed clusters of elongate volcanic islands. The erosion of these 'island clusters' led first to mature sediments and conglomerates (Jackson Lake and Banting Fms.) above the volcanic rocks. As up-doming continued, the troughs deepened and the sediment supply increased so that the basins became filled with turbidites. Throughout this process the batholiths continued to rise, intruding and tilting the lower supracrustal rocks. Inflation of these early batholiths then caused deformation, certainly close to their margins (the Duck Lake and Yellowknife Bridge domains) and possibly over more extensive areas. The temperature at this stage in the presently exposed rocks was sufficient to cause regional metamorphism to chlorite and perhaps biotite grade with localised grade increases adjacent to the plutons. About 2575 m.y. ago pressure decreased (possibly by cessation of batholith inflation combined with erosional unloading) and the thermal regime changed from one of widespread low temperatures to localised intense 'thermal domes' often located in the keels of the sedimentary troughs. These migrated upwards very slowly and there is some evidence (below) that they caused local grade increases to garnet and staurolite grades before superimposing extensive thermal aureoles characterised by cordierite. This upward migration of the isotherms was accompanied by anatectically-formed, hydrous, potassic magma whose intrusion and(or) inflation caused widespread deformation (the Hay Lake structural domain). This deformation impinged on but commonly did not re-fold rocks already deformed by the previous batholiths. Metamorphism continued until just after cessation of folding. At a much later stage the rocks were faulted, intruded by diabases, and hydrothermally retrogressed near the faults.

PART III : PETROLOGY

NATURE OF THE SEDIMENTS

The rocks examined in detail are metamorphosed turbidites of the Walsh and Burwash Fms. The sedimentary petrology of these rocks is well known and the mode of their deposition is agreed to be by turbidity currents (Ross, 1962; Henderson, 1970, 1972). The source area was a complex of intermediate to acid plutonic and volcanic rocks, but there is disagreement as to whether this complex was pre-Kenoran sialic basement or a penecontemporaneous intrusive complex. The Geological Survey of Canada school (e.g. McGlynn and Henderson, 1970) holds that a mobile sialic crust was uplifted and eroded, possibly (Henderson, 1972) in the manner suggested by Hamilton and Myers (1970). Writers in the University of Alberta have generally suggested that an island arc (or 'island cluster') model is applicable, beginning on Kenoran oceanic crust (Folinsbee et al., 1968; Green, 1968; Green and Baadsgaard, 1971; this thesis).

Sedimentary Petrology of the Burwash Fm.

The Burwash Fm. rocks are dominated by greywackes, with subordinate amounts of mudstone (as thin beds or at the tops of graded beds) and very minor calc-silicate beds or nodules.

Greywackes. The graded greywackes of the Burwash Fm. have been described in detail by Henderson (1972). They are extremely immature sediments with abundant (recrystallised) matrix and plainly visible clasts (Plate 3A). The matrix is typically 0.02 to 0.07 mm. in grain-size, increasing from 0.02-0.05 mm. in the lower biotite zone to 0.04-0.07 mm. at the cordierite isograd. The clastic fragments grade in size from these values to about 1.4 mm. and clasts larger than 2 mm. are very rare. Henderson's studies (1972 and pers. comm., 1972) have shown the clastic population to be as follows:

Clasts	Quartz > Rock Fragments > Plagioclase
Quartz	Monocrystalline > Polycrystalline
Rock Fragments . .	Igneous > Sedimentary >> Metamorphic Volcanic > Others Felsic Volcanic > Other Volcanic
Feldspar.	K-Feldspar Absent

In contrast, Ross (1962) reported that rock fragments were absent from equivalent rocks at Mesa Lake. In the rocks studied herein recognisable rock fragments are present but minor in amount. It is probable that the rock fragments have merged unrecognisably with the matrix and Henderson's data are accepted. Micro-probe analyses (below) have shown the plagioclase clasts to have a wide range in original composition (55-98% Ab). The absence of clastic K-feldspar is probably attributable to the complete metamorphic transformation of originally small amounts to muscovite.

In bulk composition the Burwash greywackes are typical of Archaean greywackes though having slightly lower CaO and CO_2 contents (see Table 2; Figs. 13, 33 and 34; Henderson, 1972; Boyle, 1961). Compared to greywackes in general the Burwash rocks have

TABLE 2 : Analyses of 14 rocks from Prosperous Lake.

Sample No.	Meta-pelites						Meta-greywackes							
	P-1	P-3	PW-11	P-12	P-13	P-14	G-1	G-2	G-3	G-5	G-7	G-11	GW-12	G-14
SiO_2	53.7	48.7	66.0	58.7	50.3	56.6	65.4	71.4	65.0	64.1	67.5	67.0	71.0	67.0
TiO_2	0.8	0.9	0.6	0.7	0.9	0.8	0.7	0.5	0.6	0.6	0.6	0.6	0.5	0.7
Al_2O_3	21.2	22.8	15.8	18.5	22.3	19.4	15.8	14.6	14.4	16.8	14.9	14.3	13.4	14.2
Fe_2O_3	1.3	1.1	1.4	1.7	2.5	0.6	1.6	0.9	0.4	1.6	1.0	0.5	0.7	1.1
FeO	8.0	7.7	5.2	6.0	7.4	8.0	4.9	3.0	5.5	4.4	5.0	4.2	5.0	5.2
MnO	0.1	0.1	0.1	0.1	0.1	0.1	0.1	0.1	0.1	0.1	0.1	0.1	0.1	0.1
MgO	4.3	4.6	2.9	4.3	4.6	3.9	3.2	1.6	2.9	2.9	2.7	2.5	2.6	2.7
CaO	1.5	1.9	0.2	1.1	1.9	1.5	1.4	1.7	2.0	1.7	1.3	1.5	0.3	1.3
Na_2O	2.6	3.9	3.0	2.6	2.7	2.2	2.5	2.8	2.6	2.9	2.6	2.8	2.5	3.3
K_2O	3.4	3.3	1.7	2.5	3.6	3.1	2.0	1.9	1.8	2.6	2.1	2.0	1.2	1.5
l. o. i. *	3.8	3.7	3.6	3.7	4.1	3.3	2.6	1.2	1.6	2.0	2.6	1.9	2.9	2.1
Total	100.7	98.7	100.5	99.9	100.4	99.5	100.2	99.7	96.9	99.7	100.4	97.4	100.2	99.2

Method of Gulson and Lovering (1968) - see Appendix.

*Loss on ignition.

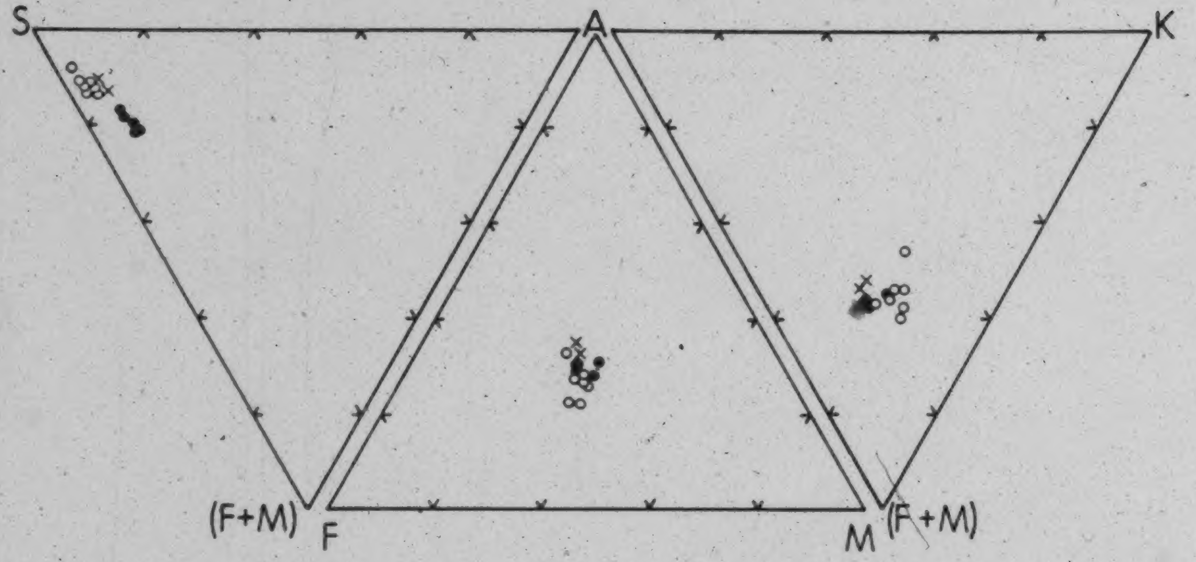

$'\mathbf{S}' = SiO_2$; $'\mathbf{A}' = Al_2O_3 - (K_2O + Na_2O + CaO)$; $'\mathbf{K}' = K_2O + Na_2O$; $'\mathbf{F}' = \sum FeO + MnO$;
$'\mathbf{M}' = MgO$

● Meta-pelite } Burwash Fm.
○ Meta-greywacke } Burwash Fm.
× .... Walsh Fm.

FIGURE 13 : Composite triangular diagram depicting the compositions of the 14 analysed rocks from the Walsh and Burwash Fms.

rather higher FeO : Fe_2O_3 and slightly higher MgO (e.g. see average of Pettijohn, 1957) but are otherwise very similar. In terms of the metamorphic petrology below, they are considered semi-pelitic.

Mudstones. These rocks are texturally and compositionally gradational with the greywackes. Ideally they lack recognisable clastic grains and have very fine grain-size, increasing from 0.02-0.05mm. in the lower biotite zone to 0.04-0.08 mm. at the cordierite isograd. Texturally and mineralogically they are entirely metamorphic.

The composition of the mudstones is illustrated by Table 2 and Figs. 13, 33 and 34. Further analyses are given by Henderson (1972) and Boyle (1961). Compared to Henderson's average of twenty Archaean 'slates', the Burwash rocks have rather higher Al_2O_3 : SiO_2 and FeO : Fe_2O_3, marginally higher MgO contents and consistently lower CaO. Relative to the average pelite (Shaw, 1956) Al_2O_3 : SiO_2, FeO : Fe_2O_3 and MgO are markedly higher and Na_2O content is slightly so. In metamorphic terms they are, however, definitely 'pelitic'.

Calc-silicates. These rocks occur as thin beds, typically ca. 5-10 cms. thick, or nodules throughout the Burwash Fm. Their character is now entirely metamorphic. Because of their commonly nodular and zoned appearance, these rocks have commonly been inferred to be concretionary in origin (e.g. Heywood and Davidson, 1969). However, the same rocks occur as definite beds and these are tectonically boudinaged in places. The 'concretions', therefore, are more likely simply to be well separated boudins. It is suggested that these rocks were originally tuff beds deposited between turbidity currents. The only available analysis (Tremblay, 1952) is consistent with this suggestion.

Their mineralogical response to metamorphism has been briefly described by Ross (1966) and Heywood and Davidson (1969). They are considered no further in the present report.

Sedimentary Petrology of the Walsh Fm.

These rocks are not known in great detail though they have been briefly described by Henderson (1970). They are generally similar to the Burwash Fm. equivalents but are more thinly and uniformly bedded. There is a much smaller proportion of sandstone and less differentiation into greywacke and mudstone, so that the dominant rock-type is siltstone.

Micro-probe analyses (below) have shown that the plagioclase clasts are all albite, a distinction from the Burwash Fm. which suggests a different sedimentary source.

Bulk analyses of two Walsh Fm. rocks are shown in Table 2 (see also Figs. 13, 33 and 34). The lack of sandstone-mudstone differentiation is illustrated by this table which shows that the Walsh meta-pelite and meta-greywacke are very similar though distinctly different from the Burwash rocks. They both resemble the Burwash greywackes in composition but are characterised by exceptionally low CaO contents.

Relation of Bulk Composition to Metamorphic Grade

Kretz (1968) gave analyses which suggested that the $Na_2O : K_2O$ ratio of meta-sediments in the Sparrow Lake area might decrease with increasing distance from the pluton. He suggested that rocks metamorphosed at progressively higher temperatures had experienced proportionate addition of Na and removal of K. These data were mainly for grades above the cordierite isograd but Table 2, giving analyses for the biotite zone, shows no such changes. Therefore the problem cannot be fully evaluated but Table 2 suggests that any systematic compositional changes are of negligible magnitude in the context of the following discussion.

THE PROSPEROUS LAKE AUREOLE

The metamorphic aureole of the Prosperous Lake adamellite is a small section of an extensive region of metamorphic rocks surrounding the Prosperous Lake, Duncan Lake and Sparrow Lake plutons (e.g. see Kretz, 1968, Fig. 1 or Fortier, 1946). The present study is confined to a wide traverse across this aureole (Figs. 4 and 15) typifying the pro-grade sequence. The same aureole has been studied on the other side of the plutonic complex by Kretz (1968) and Kamineni (Ph. D. thesis in preparation).

The Chlorite Zone

The lowest metamorphic grade sampled (Fig. 15) is immediately to the east of the Akaitcho fault. All Burwash Fm. samples thin-sectioned have contained biotite unless thoroughly hydrothermally retrogressed. Samples from the Walsh Fm. do not contain biotite, but this is shown below to be a result of compositional controls. Therefore, no chlorite zone has been sampled or studied. Commonly, however, biotite-free rocks are reported at the lowest grades elsewhere in the craton (e.g. Henderson, 1943; Ross, 1966) and Henderson (1972 and pers. comm., 1972) has found biotite-free meta-sediments between the Akaitcho fault and Yellowknife Bay. It seems that the biotite isograd was very close to the present shore of the bay but that the Akaitcho fault has placed chlorite zone rocks adjacent to biotite zone rocks.

Where they have been described, the chlorite zone meta-sediments are composed of very fine-grained chlorite and muscovite (with clasts of quartz and plagioclase in meta-greywackes) in a recrystallised matrix of quartzo-feldspathic material.

The Biotite Zone

This is a wide section (ca. 8 km.; see Fig. 15) of the aureole with its upper grade limit defined by the cordierite isograd. The biotite isograd is not exposed and within the biotite zone the Walsh Fm. rocks lack biotite (see below).

Meta-pelites. The pelitic rocks at lowest grade are very fine-grained semi-schists with a phyllitic or lepidoblastic arrangement of chlorite and muscovite in fine granoblastic quartz and feldspar. Large ragged porphyroblasts of biotite cross-cut this foliation (see Plate 3B) and are sometimes themselves weakly aligned. Rutile and ilmenite are ubiquitous in the Burwash Fm. and minor graphite, pyrrhotite, pyrite and chalcopyrite are present in some rocks. The modal amounts of chlorite, muscovite and biotite vary greatly (approximately from 0-30% modal). Potassium feldspar is present in small amounts in all of the eighteen meta-pelites stained.

Meta-greywackes. These are blastopsammitic rocks (Plate 3) entirely comparable in mineralogy to the meta-pelites. Foliation of the sheet silicates is commonly lacking or very weakly developed. The biotite is present as scattered anhedral flakes or in poly-crystalline clots or aggregates. The plagioclase clasts show evidence of variable degrees of recrystallisation.

The Walsh Fm. The difference between these rocks and the Burwash Fm. has already been noted. Mineralogically they are similar except in that they lack both biotite and ilmenite. Texturally they are less markedly blastopsammitic, lacking the coarse clastic fragments of the Burwash Fm.

The Cordierite Zone

As traditionally mapped in the Slave Craton, the metasediments are divided into two grades -- those above the cordierite isograd being obviously 'nodular' and those below it being free of these porphyroblasts. For present purposes the cordierite zone is taken to extend from the cordierite isograd to the line where garnet is first observed (Fig. 36).

In a very short pro-grade interval cordierite appears in a large proportion of the rocks (Plate 4; Fig. 30). There is no apparent control of its initial appearance by rock composition. Above the isograd cordierite occurs in many rocks to the highest grades observed and the original nature of the sediment (greywacks vs. mudstone) is increasingly difficult to discern. Fine-grained chlorite and muscovite are much less abundant than in the biotite zone but are present in some rocks. Biotite is ubiquitous and abundant and the cordierite is present as large, diffuse poikiloblasts. Andalusite occurs sporadically in the lower cordierite zone but more commonly in the upper cordierite zone where it is thought to be a stable member of the pro-grade sequence.

The Cordierite-Garnet 'Zone'

In the highest-grade parts of the aureole (Fig. 36), adjacent to the pluton margin, garnet is very common, occurring in a wide range of rock compositions and commonly co-existing with cordierite. The limits of the garnet-bearing rocks have been mapped by Jolliffe (1942 and 1946) and confirmed during the present study. Coarse subhedral to euhedral andalusite is present and gedrite occurs in rocks at the highest metamorphic grades. Cummingtonite is characteristic of narrow siliceous lenses.

The Sillimanite-Staurolite 'Zone'

Sillimanite has been observed at only two localities in this section of the aureole (Fig. 36) but it is commonly recorded as being characteristic of the highest grades attained elsewhere in the craton (e.g. Ross, 1966; Davidson, 1967; Heywood and Davidson, 1969; Kretz, 1968). At both of these locations the sillimanite is incipient and in complex parageneses involving staurolite.

The Facies Series

The zonal series described above closely approximates an Abukuma facies series (Winkler, 1967). The main differences are that andalusite is not common and apparently appears only after cordierite, and that garnet and staurolite are found at high grades. The latter problem is discussed below, but it is thought to indicate that metamorphism began at slightly higher pressures than represented by the principal facies series.

The aureole, therefore, is an excellent example of the equivalence of low-pressure regional metamorphism and relatively high-pressure contact metamorphism.

Conditions of metamorphism. This facies series suggests, in very approximate terms, that metamorphism operated at about 2.5 to 4.0 kb. (see below). Since the metamorphism is an aureole round a pluton there is thought to have been very little pressure change with increasing grade. The lowest biotite zone probably represents temperatures of the order of 300-400° C. (Turner, 1968), the cordierite isograd about 550° C. (Davidson, 1967; Seifert, 1970; Den Tex, 1971) and the granite contact (with its occasional sillimanite) about 650-700° C. (e.g. Den Tex, 1971; Davidson, 1967). There is little available evidence for the fluid composition except that graphite is present. This indicates that CO_2 was a major constituent of the metamorphic fluids and leaves the possibility that methane was also present (French, 1966).

Assignment of Metamorphic Grade

For many of the arguments developed below, a non-mineralogical index of metamorphic grade is required. The pluton outcrop is asymmetrically located within the isothermal surface represented by the cordierite isograd (Fig. 15) so that the grade index cannot simply be distance from the pluton contact, which is the commonly used parameter. Metamorphic grade in the aureole is therefore assigned on the basis of the perpendicular distance from the cordierite isograd. The general configuration of the aureole and sampling sites (Fig. 15) and the textural changes along this direction suggest that this is a reliable index of metamorphic grade. This contention is confirmed by the fact that use of this index yields compositional trends well established for pro-grade changes in muscovites (below).

THE SAMPLE SERIES

Several of the petrological arguments below depend on the selection of two isochemical sample series -- meta-greywackes and meta-pelites. The widespread distribution of turbidites of one formation guarantees that the same general range of compositions occurs at all grades in the aureole, but further discrimination into two consistent but distinct rock series was required.

Sedimentological Criteria

Samples were initially taken to represent, by field inspection, the meta-pelite and meta-greywacke rock-types. All the samples from the biotite zone (170 thin-sections) were petrographically examined and several sedimentological parameters systematically recorded. By plotting these parameters against one another (Fig. 14) and comparing the scatter of points to the field-names, it was possible to display the variability in these parameters and delimit restricted fields for the 'typical' meta-greywacke and meta-pelite. These limits are:

	Meta-pelites	Meta-greywackes
Max. clastic grain size (mm.)	0.25	0.2-1.3
Recognisable sand grains (%)	8	19-51
Total quartz and feldspar (%)	70	55-80

Samples for detailed study were then selected from within these fields.

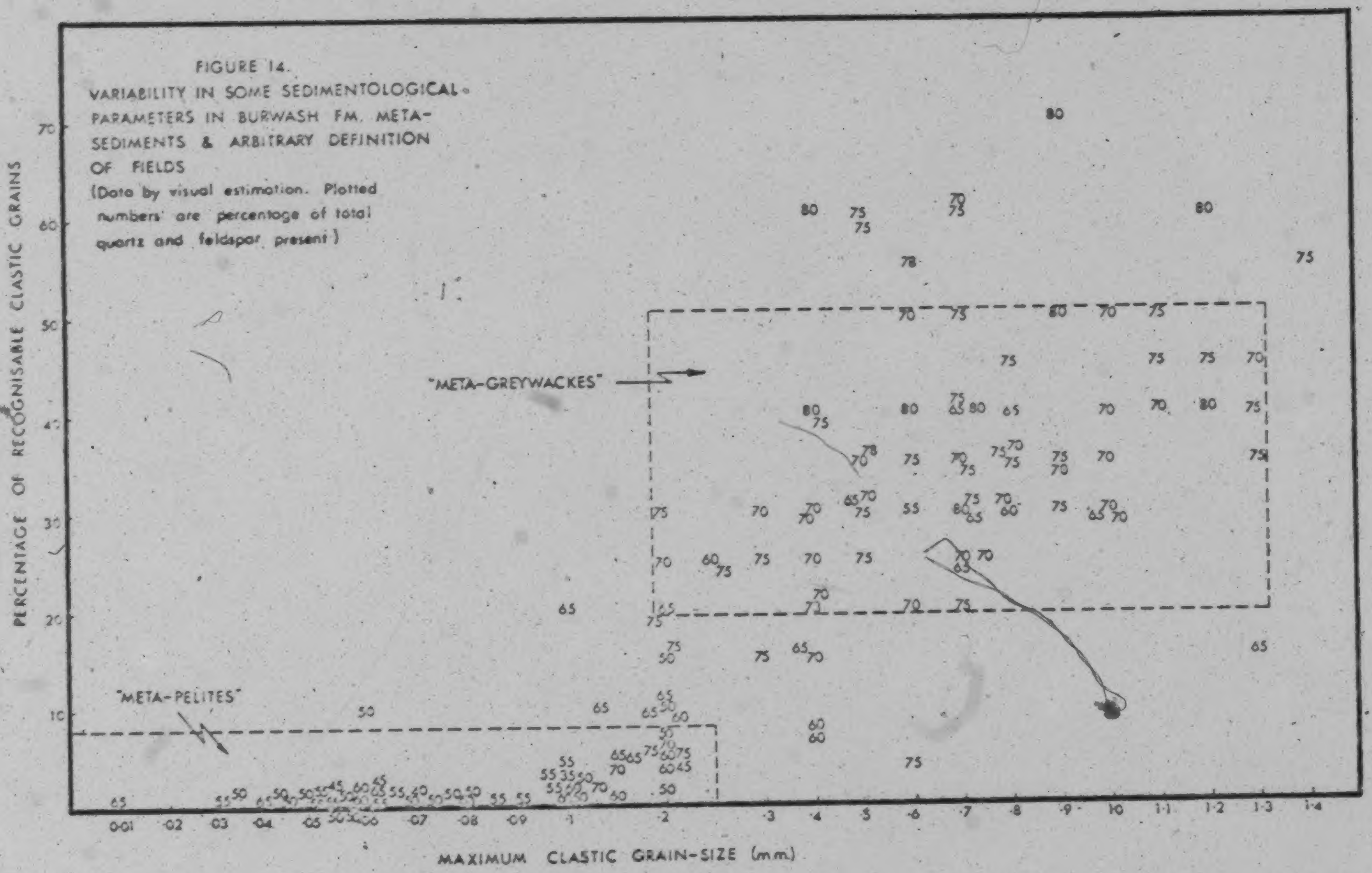

FIGURE 14.
VARIABILITY IN SOME SEDIMENTOLOGICAL PARAMETERS IN BURWASH FM. META-SEDIMENTS & ARBITRARY DEFINITION OF FIELDS
(Data by visual estimation. Plotted numbers are percentage of total quartz and feldspar present)

Other Criteria

Samples for detailed study were also required to conform to the following conditions:

1. They should comprise an evenly-spaced sample array in a pro-grade traverse across the aureole.
2. They should display minimal weathering or hydrothermal alteration. Some narrow chloritised veinlets were inevitably present in the selected samples as most rocks in this area have suffered this mode of alteration. The principal alteration is the retrogression of biotite to chlorite and K-feldspar and the altered areas are readily recognised and avoided in micro-probe analysis. In the whole-rock analyses the effects of the alteration would be a very small increase in SiO_2 content and occasionally K_2O, sulphide or carbonate.

The Sample Series

On the basis of these criteria two sample series have been selected. The extent to which these series are isochemical may be judged from Table 2 and Figs. 13, 33 and 34. The compositional fields are very restricted but commonly overlap slightly. Three Walsh Fm. samples have been included. These are compositionally similar to the Burwash meta-greywackes regardless of their petrographic designation as meta-pelites or meta-greywackes.

The locations of samples used in studying the biotite zone are shown in Fig. 15. The meta-pelite samples are numbered

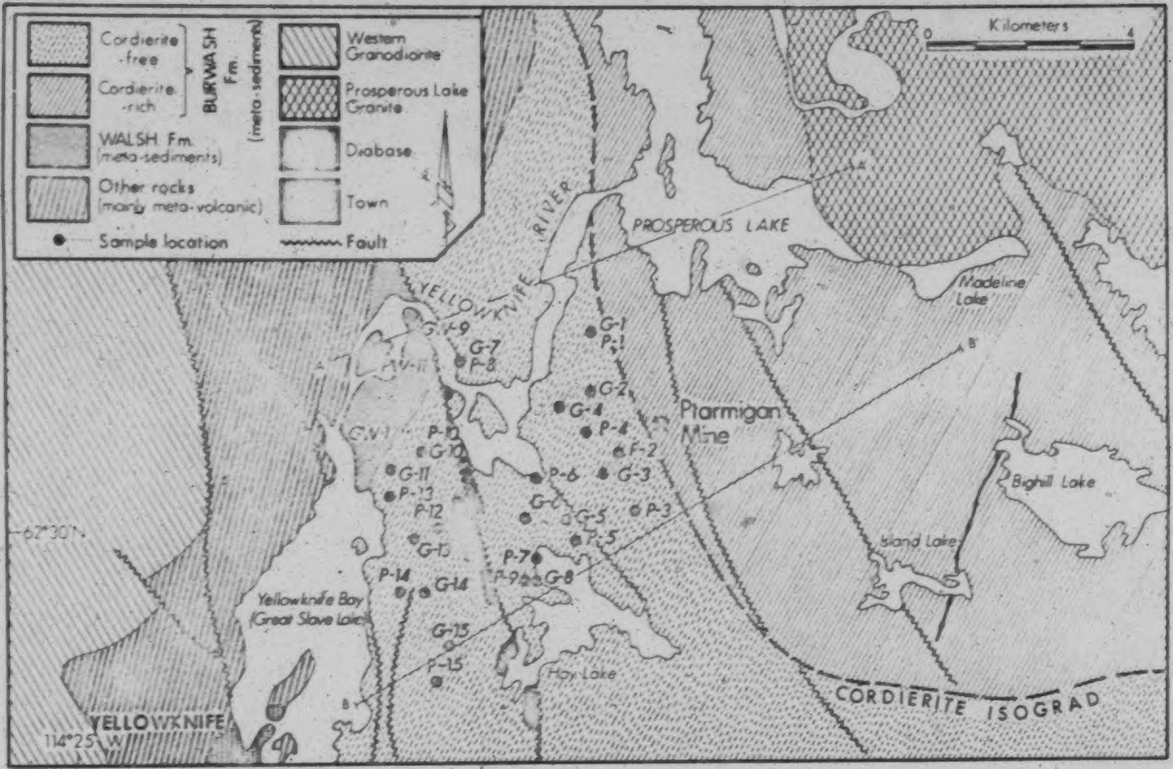
Cordierite -free
Cordierite -rich
BURWASH Fm. (meta-sediments)
WALSH Fm. (meta-sediments)
Other rocks (mainly meta-volcanic)
Sample location
Western Granodiorite
Prosperous Lake Granite
Diabase
Town
Fault
Kilometers
0
4
PROSPEROUS LAKE
YELLOWKNIFE RIVER
Madeline Lake
Ptarmigan Mine
Bighill Lake
Island Lake
Hay Lake
Yellowknife Bay (Great Slave Lake)
YELLOWKNIFE
CORDIERITE ISOGRAD
62°30'N
114°25' W
A
B
B'
G-1
P-1
G-2
G-4
P-4
F-2
G-3
P-6
P-3
G-5
P-5
P-7
P-9
G-8
G-7
P-8
G-9
G-10
P-10
G-11
P-13
P-12
G-13
P-14
G-14
G-15
P-15
G.V-1
G.V-11

FIGURE 15 : Geological sketch of the Prosperous Lake area (modified after Jolliffe, 1942 and 1946, and Henderson, 1970) showing locations of samples for detailed study of the biotite zone and approximate limits of the detailed study traverse across the aureole.

in order of decreasing metamorphic grade with the prefixes 'P' for Burwash Fm. samples and 'PW' for Walsh Fm. samples. The meta-greywackes are numbered on the same scheme but pre-fixed 'G' and 'GW' respectively. Samples from above the cordierite isograd are numbered in order of increasing metamorphic grade with prefixes as above. (This complexity is maintained to preserve the published sample numbers -- Ramsay, in press, 1973). The locations of samples from the cordierite isograd are shown in Fig. 30.

Analytical Methods

The reader is referred to the Appendix for all details of methodology, accuracy, etc.

BIOTITE ZONE MINERAL CHEMISTRY

(Note: This and the next four sections are an expanded version of work in press at present -- Ramsay, in press, 1973.)

Biotite

Analyses and structural formulae of twenty biotites from the biotite zone are given in Tables 3 and 4. As illustrated by Figs. 16, 17 and 18 the compositional variability is remarkably small, being confined to the ratios Fe/Mg (Fig. 18) and (Fe+Mg)/Al (Fig. 17).

Influence of metamorphic grade. Within this restricted compositional field there are several systematic trends related to metamorphic grade (see Fig. 19). The main points are:

1. Well-defined trends are apparent in the elements of the alkali site. In biotites from meta-greywackes Na/K increases and total X-site occupancy decreases

TABLE 1. Micro-probe analyses (weight %) of BIOTITES from the biotite zone of the Whetstone Lake metamorphic aureole

Sample Number	Meta-pelites									
	P-1	P-2	P-3	P-5	P-6	P-7	P-10	P-12	P-13	P-14
SiO_2	35.63	35.80	35.06	35.35	36.01	35.76	35.98	36.13	35.89	36.07
TiO_2	1.76	1.79	1.73	1.81	1.75	1.79	1.69	1.82	1.76	1.87
Al_2O_3	18.03	17.55	17.84	18.14	18.12	17.81	17.55	17.50	17.46	17.52
FeO*	19.15	18.38	18.46	18.59	18.00	18.34	19.15	18.48	19.57	19.10
MnO	0.14	0.14	0.15	0.17	0.19	0.16	0.16	0.14	0.15	0.13
MgO	9.88	9.78	10.26	10.04	10.67	10.66	10.84	11.05	9.95	10.16
CaO	n.p.	n.p.	n.p.	n.p.	n.p.	n.p.	n.p.	n.p.	Tr	n.p.
Na_2O	0.11	0.08	0.05	0.11	0.11	0.12	0.05	0.05	0.05	0.07
K_2O	9.63	9.85	9.62	9.73	9.70	9.74	9.34	9.72	9.74	9.86
Total	94.35	93.17	94.20	93.88	93.91	93.46	94.63	93.89	94.59	94.87

Sample Number	Meta-greywackes									
	G-1	G-2	G-3	G-5	G-6	G-7	G-10	G-11	G-13	G-14
SiO_2	35.73	35.77	36.50	35.89	36.20	36.35	36.06	36.57	35.97	35.74
TiO_2	1.85	1.50	1.55	1.69	1.71	1.53	1.94	1.86	1.76	1.85
Al_2O_3	18.05	18.75	16.83	18.00	17.47	17.53	17.64	17.16	18.01	17.76
FeO*	18.70	18.66	18.77	18.46	18.17	18.93	17.84	18.28	18.26	19.04
MnO	0.15	0.17	0.15	0.20	0.19	0.15	0.23	0.05	0.20	0.15
MgO	10.35	10.33	11.46	10.43	11.11	10.31	9.82	10.84	10.33	10.09
CaO	n.p.	n.p.	n.p.	n.p.	n.p.	n.p.	n.p.	n.p.	n.p.	n.p.
Na_2O	0.11	0.13	0.11	0.07	0.08	0.29	0.04	0.07	0.09	0.06
K_2O	9.33	9.32	9.40	9.63	9.67	9.66	9.68	9.77	9.85	9.68
Total	94.31	94.52	94.55	95.03	94.66	95.05	94.55	94.60	94.47	94.29

*Total Fe as FeO.

n.p. = not present. Tr = detected but less than 0.01%.

Additional data: FeO in P-3 = 17.41%, in G-3 = 17.96%.
Fe_2O_3 in P-3 = 1.03%, in G-3 = 0.86%.

TABLE 4 : Structural formulae (atomic proportions) of the BIOTITES whose analyses are given in Table 3. (Formulae based on 22 oxygen ions.)

Sample No.	P-1	P-3	P-4	P-5	P-6	P-7	P-10	P-12	P-13	P-14
Si	5.472	5.485	5.414	5.449	5.486	5.467	5.474	5.497	5.510	5.512
Al	2.528	2.515	2.586	2.551	2.514	2.533	2.526	2.503	2.490	2.488
Al	0.736	0.657	0.659	0.757	0.741	0.694	0.639	0.638	0.675	0.670
Ti	0.205	0.206	0.201	0.189	0.200	0.206	0.194	0.208	0.203	0.215
Fe^{2+}*	2.345	2.247	2.398	2.286	2.188	2.237	2.336	2.243	2.397	2.340
Fe^{3+}*	0.113	0.108	0.116	0.110	0.105	0.108	0.113	0.108	0.116	0.113
Mn	0.018	0.018	0.020	0.022	0.019	0.021	0.021	0.018	0.019	0.017
Mg	2.260	2.461	2.360	2.318	2.422	2.429	2.470	2.506	2.277	2.314
Ca	0.000	0.000	0.000	0.000	0.000	0.000	0.000	0.000	0.000	0.000
Na	0.033	0.018	0.015	0.033	0.032	0.036	0.015	0.015	0.015	0.021
K	1.886	1.929	1.894	1.914	1.885	1.900	1.832	1.888	1.908	1.923
ΣY-site	5.677	5.697	5.754	5.682	5.675	5.695	5.773	5.721	5.687	5.669
ΣX-site	1.919	1.947	1.909	1.947	1.917	1.936	1.847	1.903	1.923	1.944

Sample No.	G-1	G-2	G-3	G-5	G-6	G-7	G-10	G-11	G-13	G-14
Si	5.472	5.449	5.577	5.483	5.519	5.539	5.522	5.570	5.496	5.487
Al	2.528	2.551	2.423	2.517	2.481	2.461	2.478	2.430	2.504	2.513
Al	0.732	0.811	0.556	0.715	0.657	0.700	0.710	0.655	0.741	0.703
Ti	0.195	0.172	0.178	0.193	0.198	0.209	0.223	0.213	0.202	0.213
Fe^{2+}*	2.285	2.261	2.288	2.301	2.207	2.295	2.338	2.221	2.226	2.332
Fe^{3+}*	0.110	0.109	0.110	0.111	0.106	0.111	0.113	0.107	0.107	0.112
Mn	0.020	0.022	0.019	0.026	0.024	0.019	0.030	0.006	0.026	0.019
Mg	2.362	2.345	2.610	2.364	2.520	2.335	2.241	2.461	2.352	2.309
Ca	0.000	0.000	0.000	0.000	0.000	0.000	0.000	0.000	0.000	0.000
Na	0.033	0.038	0.033	0.021	0.021	0.027	0.012	0.021	0.027	0.018
K	1.862	1.813	1.849	1.869	1.878	1.873	1.891	1.899	1.921	1.881
ΣY-site	5.704	5.720	5.761	5.710	5.712	5.669	5.655	5.663	5.654	5.688
ΣX-site	1.895	1.851	1.882	1.890	1.902	1.900	1.903	1.921	1.948	1.899

*Based on the average of the two determined ferrous : ferric ratios throughout.

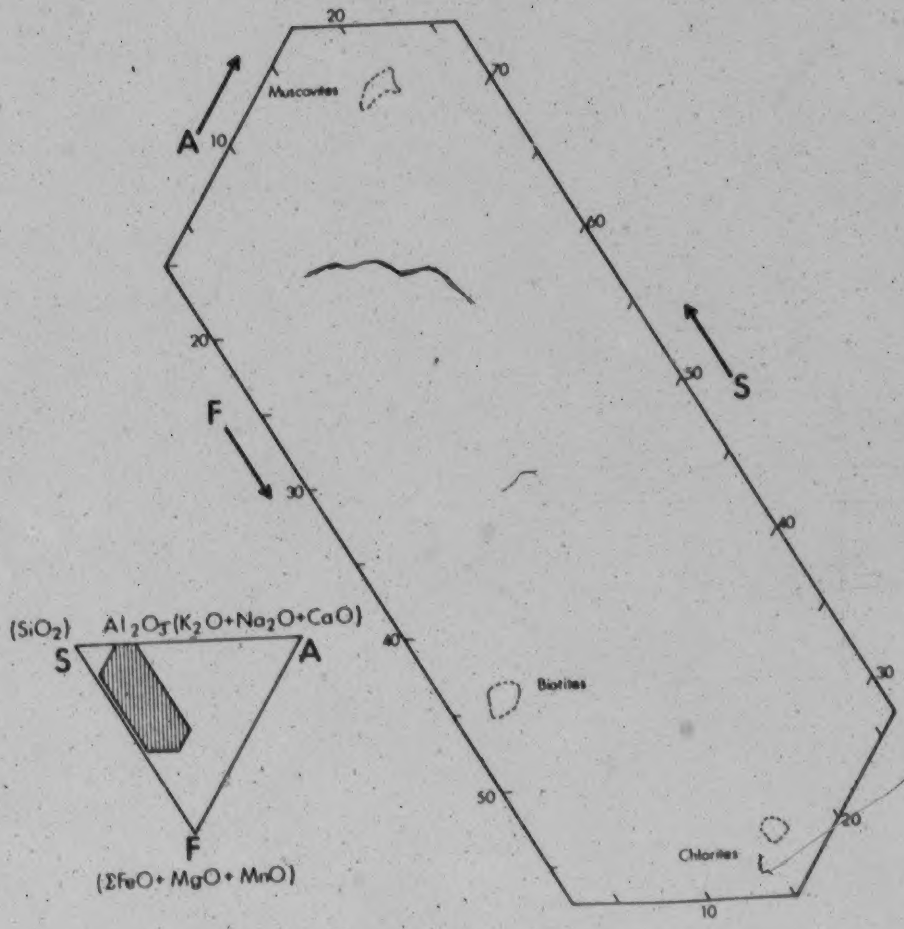

FIGURE 16 : SAF triangular diagram showing restricted compositional fields of the analysed biotites, chlorites and muscovites from the biotite zone.

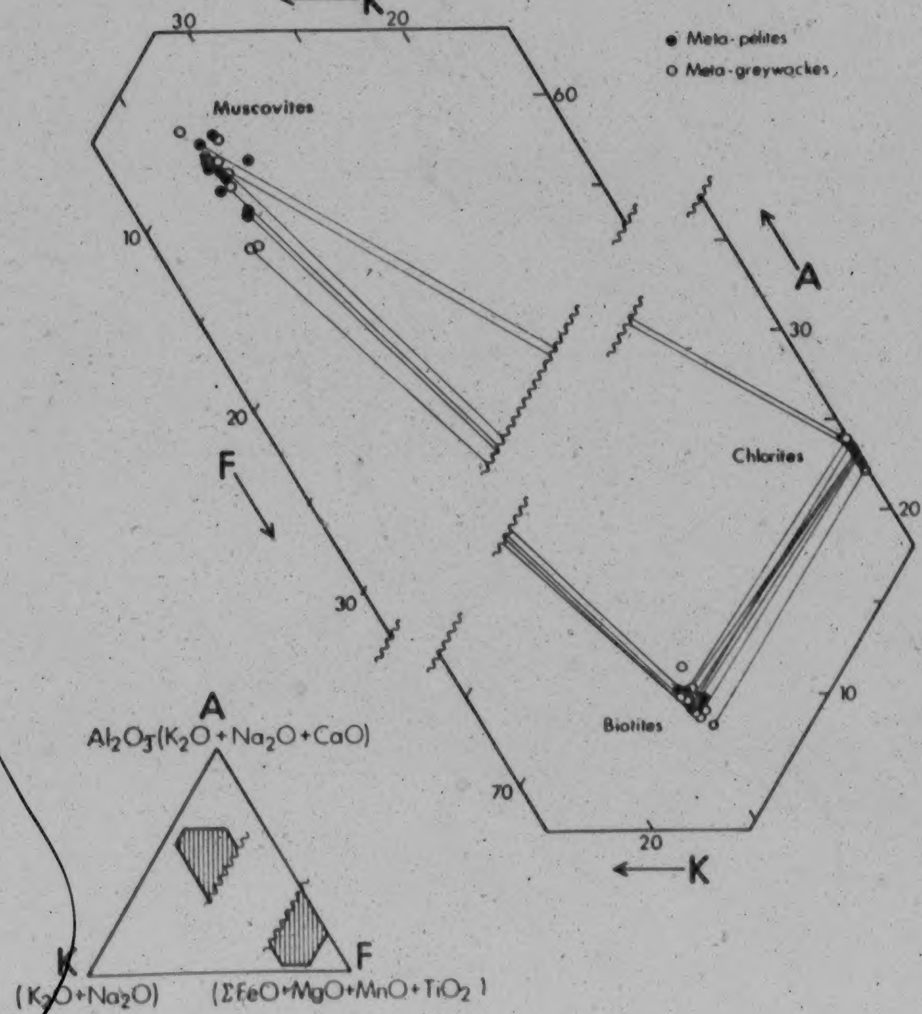

FIGURE 17 : Modified AKF triangular diagram, with some representative tie-lines, showing the compositional variability of the analysed biotites, chlorites and muscovites from the biotite zone.

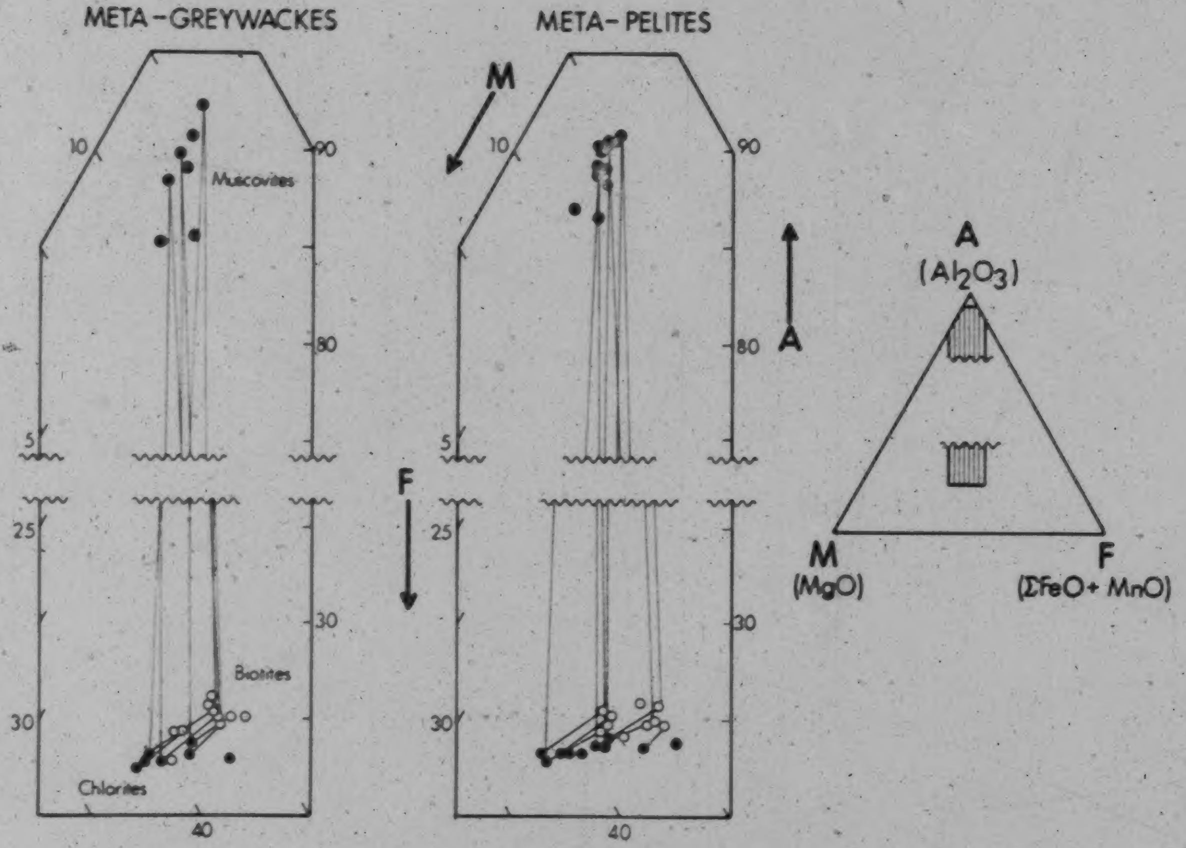

FIGURE 18 : AMF triangular diagram, with some representative tie-lines, illustrating the compositional variability of the analysed biotites, chlorites and muscovites from the biotite zone.

at higher metamorphic grades. Limited data on the Ba contents (Table 5) suggest that this is insufficient to compensate for the X-site deficiency. In meta-pelite biotites the Na and K contents and the X-site total are independent of metamorphic grade.

2. The trends are less striking in the elements of the Y-site. Al^{VI} is generally more abundant at higher grades. Ti and Mn contents (Table 3) are independent of grade. In meta-greywacke biotites Mg/Fe increases towards the cordierite isograd. In meta-pelite biotites there is no correlation between increased grade and Fe but the Mg content may decrease slightly. There is a pro-grade increase in Y-site occupancy in meta-greywackes but not in meta-pelites.
3. In the tetrahedral site the minimum Si content falls at higher grade and the meta-pelite biotites trend to lower Si/Al^{IV}. (Note that only one point prevents there being a strong, general pro-grade Si decrease. If this analysis is in error, Si decrease is the correct trend.)

The important features of Fig. 19 are the differing response of biotites in the two rock types to increased metamorphic grade and the marked compositional changes in the meta-greywacke biotites.

Comparative discussion. Abundant data on greenschist facies biotites are now available (e.g. Lambert, 1959; Brown, 1967;

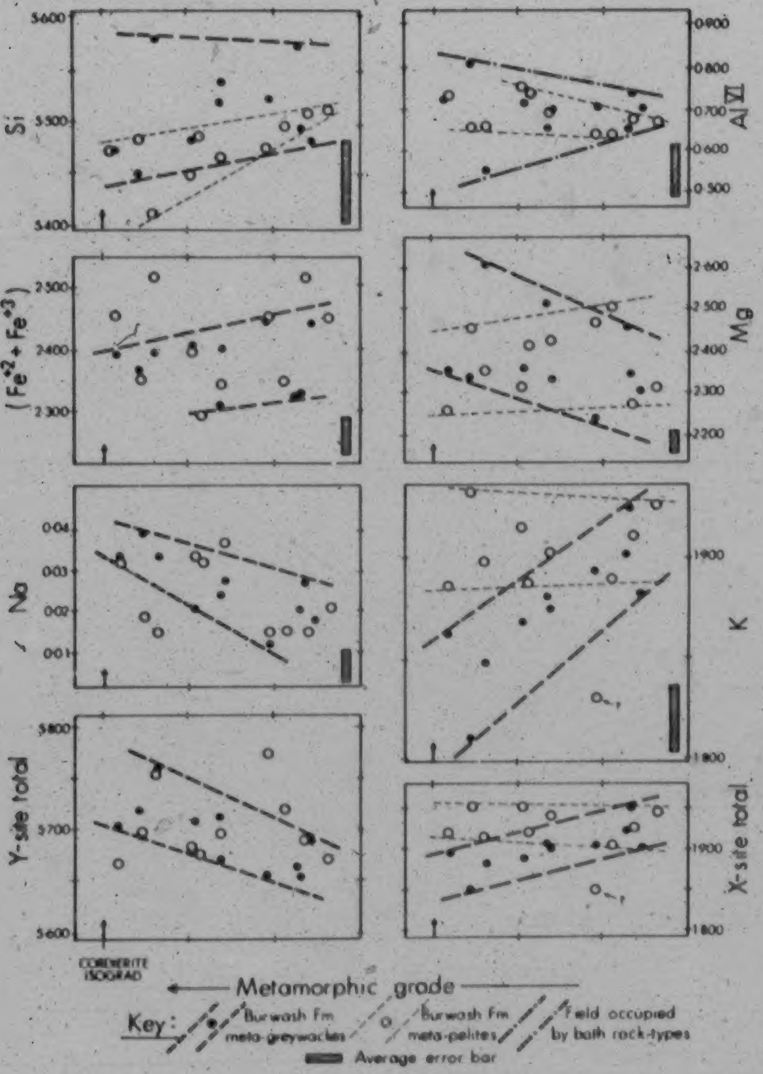

FIGURE 19 : Diagram illustrating the relationship of biotite composition (atomic proportions) to metamorphic grade. The point marked (?) apparently represents a chloritised biotite. Derivation of the 'average error bars' is explained in the appendix. For Si and Al^{VI} they represent maximum errors at 99% confidence; for other elements they reflect the ranges of replicate analyses. In both cases they were calculated for minerals of average composition.

TABLE 5 : Miscellaneous additional analytical data on biotites, muscovites and chlorites from the biotite zone of the Prosperous Lake metamorphic aureole.

Mineral	Element	Sample No. and Concentration(%)
Biotite	P	G-3 : Tr; P-6 : Tr; P-3 : Tr
	Cl	G-3 : Tr; P-6 : Tr; P-3 : 0.02
	F	G-3 : 0.18; P-6 : 0.18; P-3 : 0.27
	BaO	G-15 : 0.15; P-1 : 0.11
Muscovite	P	G-5 : 0.01
	Cl	G-5 : Tr
	F	G-5 : 0.01
Chlorite	BaO	P-7 : 0.02; G-5 : 0.03
	P	G-3 : Tr; P-4 : Tr; P-6 : Tr

Also: Sr - n.p. in 3 biotites, 2 chlorites and 6 muscovites.

Symbols as in Table 3.

Butler, 1967; Mather, 1970 and Pinsent, 1971). The Prosperous Lake biotites are compositionally similar to those analysed in the above studies, though rather more magnesian. Evidently there is a very restricted range of composition for biotites in such rocks.

Lambert (1959), Butler (1967) and Pinsent (1971) noted alkali deficiencies and low X-site totals are also apparent in the data of Brown (1967), Mather (1970) and particularly Cooper (1972). In the Prosperous Lake biotites the X-site deficiency and the Y-site total both increase towards the cordierite isograd which may indicate Fe or Mg in twelve-fold coordination (McNamara, 1965). Alternatively hydronium ions may complete the X-site complement.

Variation of biotite composition with metamorphic grade has been discussed by several authors (e.g. Lambert, 1959; Butler, 1967; Guidotti, 1969) but most data are for higher grades and higher pressure-gradients than those discussed here. Butler (1967) found that Al^{IV} increased at higher grade; Fig. 19 suggests a similar trend, at least in meta-pelites. The pro-grade increase of Mg/Fe demonstrated by Lambert (1959) occurs in the meta-greywacke biotites but not in the meta-pelite group. Al^{VI} may also increase slightly, in which case the trend is in agreement with that described by Butler (1967).

Muscovite

Tables 6 and 7 give analytical data on twenty biotite zone muscovites and their limited compositional variability is illustrated by Figs. 16, 17 and 18. They are slightly phengitic muscovites

TABLE 6 : Micro-probe analyses (weight %) of MUSCOVITES from the biotite zone of the Prosperous Lake metamorphic aureole.

Sample Number	In meta-pelites									
	P-1	P-3	P-4	P-5	P-6	P-7	P-8	P-9	P-10	PW-11
SiO_2	45.99	46.66	46.12	46.45	45.82	46.27	47.73	46.86	46.24	47.29
TiO_2	0.34	0.43	0.38	0.38	0.44	0.48	0.39	0.44	0.30	0.25
Al_2O_3	34.00	33.53	34.03	33.56	33.55	33.69	33.22	33.27	33.93	34.29
Fe_2O_3*	1.13	1.10	1.21	1.19	1.22	1.29	1.29	1.23	1.37	1.30
MnO	n. p.	n. p.	n. p.	Tr	0.02	0.02	0.01	n. p.	0.01	0.01
MgO	0.67	0.88	0.80	0.86	0.77	0.73	1.30	0.97	1.00	0.80
CaO	0.05	0.07	0.03	0.04	0.08	0.05	0.03	0.06	0.03	0.04
Na_2O	0.55	0.38	0.52	0.50	0.48	0.61	0.32	0.39	0.35	0.53
K_2O	10.34	10.70	10.55	10.49	10.37	10.34	10.88	10.78	10.84	10.28
BaO	0.45	0.34	0.33	0.32	0.86	0.74	0.17	0.40	0.32	0.11
Total	93.52	94.09	93.97	93.80	93.61	94.22	95.34	94.40	94.39	94.90

Sample Number	In meta-pelites			In meta-greywackes					
	P-12	P-13	P-14	G-1	G-5	G-7	G-11	GW-12	G-14	G-15
SiO_2	46.17	46.05	47.71	45.41	46.18	45.79	46.07	47.34	46.11	47.02
TiO_2	0.29	0.37	0.24	0.37	0.36	0.39	0.36	0.52	0.45	0.33
Al_2O_3	34.08	34.39	32.97	34.68	33.45	34.00	32.34	34.98	33.67	32.31
Fe_2O_3*	1.43	1.60	1.67	1.07	1.18	1.18	2.00	1.20	1.37	1.58
MnO	n. p.	0.02	0.01	0.01	0.02	0.02	0.01	0.01	0.01	0.02
MgO	0.93	0.98	1.18	0.59	1.10	0.91	1.11	0.76	0.91	1.37
CaO	0.02	0.04	0.06	0.04	0.03	0.02	0.02	0.03	0.02	0.07
Na_2O	0.35	0.28	0.33	0.64	0.39	0.48	0.40	0.81	0.36	0.28
K_2O	10.88	10.65	10.78	10.46	10.72	10.57	10.94	10.10	10.68	10.92
BaO	0.33	0.31	0.29	0.77	0.54	0.38	0.14	0.19	0.33	0.27
Total	94.48	94.69	95.24	94.04	93.97	93.74	93.39	95.94	93.91	94.17

*Total Fe as Fe_2O_3.

n. p. and Tr : as in Table 3.

TABLE 7 : Structural formulae (atomic proportions) of the MUSCOVITES whose analyses are given in Table 6. (Formulae based on 22 oxygen ions.)

Sample No.	P-1	P-3	P-4	P-5	P-6	P-7	P-8	P-9	P-10	P-12
Si	6.237	6.290	6.228	6.278	6.236	6.249	6.344	6.305	6.227	6.214
Al	1.763	1.710	1.772	1.722	1.764	1.751	1.656	1.695	1.773	1.786
Al	3.671	3.617	3.643	3.624	3.617	3.611	3.547	3.581	3.612	3.620
Ti	0.035	0.044	0.039	0.039	0.045	0.049	0.039	0.045	0.030	0.029
Fe*	0.115	0.112	0.123	0.121	0.125	0.131	0.129	0.125	0.139	0.145
Mn	0.000	0.000	0.000	0.001	0.002	0.002	0.001	0.000	0.001	0.000
Mg	0.135	0.177	0.161	0.173	0.156	0.147	0.258	0.195	0.201	0.187
Ba	0.024	0.018	0.018	0.017	0.046	0.039	0.009	0.021	0.017	0.017
Ca	0.007	0.010	0.004	0.006	0.012	0.007	0.004	[illegible]009	0.004	0.003
Na	0.145	0.099	0.136	0.131	0.127	0.160	0.082	0.102	0.091	0.091
K	1.789	1.840	1.817	1.809	1.800	1.781	1.845	1.850	1.862	1.868
ΣY-site	3.956	3.949	3.966	3.958	3.946	3.940	3.974	3.945	3.983	3.981
ΣX-site	1.965	1.967	1.975	1.962	1.985	1.988	1.940	1.982	1.975	1.980

Sample No.	PW-11	P-13	P-14	G-1	G-5	G-7	G-11	GW-12	G-14	G-15
Si	6.290	6.179	6.358	6.151	6.253	6.205	6.287	6.231	6.237	6.350
Al	1.710	1.821	1.642	1.849	1.747	1.795	1.713	1.769	1.763	1.650
Al	3.665	3.617	3.536	3.688	3.591	3.635	3.488	3.658	3.605	3.492
Ti	0.025	0.037	0.024	0.038	0.037	0.040	0.037	0.051	0.046	0.034
Fe*	0.130	0.162	0.167	0.109	0.120	0.120	0.205	0.119	0.139	0.161
Mn	0.001	0.002	0.001	0.001	0.002	0.002	0.001	0.001	0.001	0.002
Mg	0.159	0.196	0.234	0.119	0.222	0.184	0.226	0.149	0.183	0.276
Ba	0.006	0.016	0.015	0.041	0.029	0.020	0.008	0.010	0.018	0.014
Ca	0.006	0.006	0.009	0.006	0.004	0.003	0.003	0.004	0.003	0.010
Na	0.137	0.073	0.085	0.168	0.102	0.126	0.106	0.207	0.094	0.073
K	1.744	1.823	1.832	1.807	1.852	1.827	1.904	1.696	1.843	1.881
ΣY-site	3.980	4.014	3.963	3.955	3.972	3.981	3.957	3.979	3.975	3.964
ΣX-site	1.892	1.918	1.942	2.022	1.987	1.976	2.021	1.917	1.958	1.979

*Total Fe as Fe^{3+}.

intermediate in composition between ideal muscovites and those of Barrovian terrains (e.g. Mather, 1970). The spread of points in Figs. 16 and 17 suggests that Al/(Mg+Fe) variability is dominant with rather constant Si and (Na+K) contents. As so commonly recorded, many of these muscovites have X-site deficiencies.

Influence of metamorphic grade. Fig. 20 relates muscovite composition to metamorphic grade and the main features are as follows:

1. Well-defined trends are apparent in the X-site occupancy. The X-site total is nearly ideal but exhibits a slight pro-grade increase. Na/K increases at higher grades. Although Ba content is considerable, it is not grade-dependent (Tables 6 and 7).
2. Y-site occupancy is also dependent on grade, with the total decreasing from nearly ideal values at low grades and converging on deficient values at the cordierite isograd. Al^{VI} increases markedly at the expense of Mg and Fe and the ranges of Al^{VI}, Mg and Fe decrease. Ti and Mn contents are independent of grade (Tables 6 and 7).
3. The tetrahedral site exhibits pro-grade decrease in Si (increasing Al^{IV}/Si) in meta-greywacke muscovites. This trend is, however, dominated by one data point. It may be that the meta-greywacke points should simply conform to the narrowing Si range displayed by the meta-pelite muscovites.

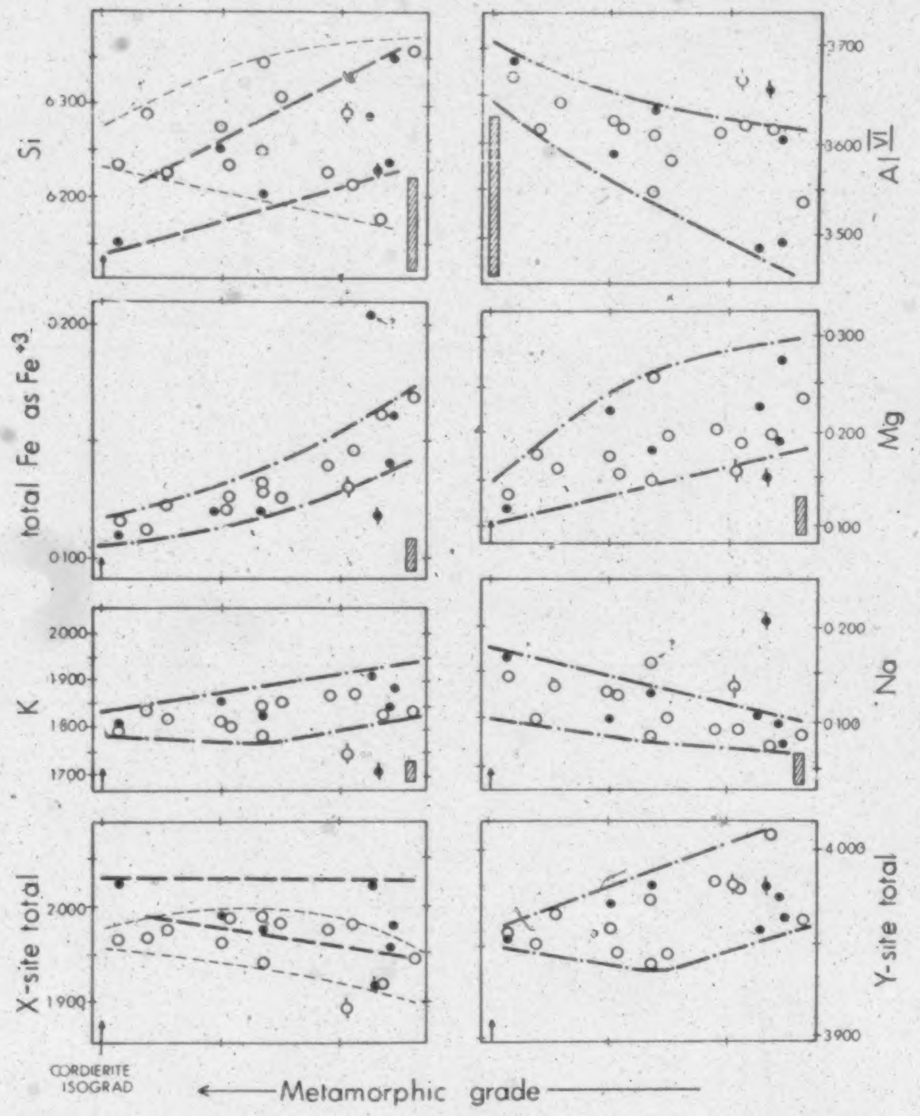

FIGURE 20 : Diagram illustrating the relationship of muscovite composition (atomic proportions) to metamorphic grade. Points marked (?) do not conform to otherwise well-defined trends. Walsh Fm. muscovites are not included in the delineated fields. Symbols as in Figs. 19 and 22.

Comparative discussion. The compositional variability of muscovite has been extensively studied (e.g. Lambert, 1959; Ernst, 1963; McNamara, 1965; Velde, 1965, 1967 and 1968; Brown, 1967 and 1968; Butler, 1967; Guidotti, 1969; Mather, 1970; Pinsent, 1971; Makanjuola and Howie, 1972; Hermes, 1973). It is impossible to discuss here all these papers or their present relevance, but a recent review by Cipriani et al. (1971) showed that the main variations are:

$$\mathrm{Si} + \mathrm{Mg}\ (\text{or } \mathrm{Fe}^{++}) \rightleftharpoons \mathrm{Al}^{IV} + \mathrm{Al}^{VI}$$

and

$$\mathrm{Si} + \square^{XII} \rightleftharpoons \mathrm{Al}^{IV} + \mathrm{K}\ (\text{or } \mathrm{Na}),$$

with increased celadonite content favoured by low temperature and high pressure. Fig. 20 reflects these substitutions with Fe and Mg contents decreasing at higher metamorphic grades while (Na + Ba + K), Al^{VI} and the maximum Al^{IV} contents all increase. There is also evidence for gradual pro-grade filling of the twelve-fold void site in that the X-site deficiency is generally larger at lower grades. However, the increasing deficiency of Y-site occupancy is not explained by these substitution reactions. Further, Fig. 18 indicates that substitution of Mg for Al predominates over that of Fe (see also Makanjuola and Howie, 1972). The pattern of Si contents is more complex than indicated by the above equations, at least in the meta-pelites.

The crux of the 'phengite problem' is whether phengite composition has been controlled by metamorphic grade or rock composition. Fig. 20 demonstrates clearly that, when rocks of similar bulk chemistry are selected, the compositions of the phengites in them are grade-dependent. There is a general pro-grade approach to ideal muscovite achieved by a narrowing of the compositional range as well as by a linear approach to ideality.

Chlorite

Chlorite of three petrographic types is present in these rocks. These types are not compositionally distinct and are therefore designated by suffixes. Chlorite (A) occurs as small flakes in rocks throughout the biotite zone (Plate 3A and B). Chlorite (B) is present in small amounts in the higher-grade half of the zone and is of medium grain-size and usually interleaved with biotite. Chlorite (B-X) is similar to chlorite (B), occurring as large, thin flakes in a few rocks in the upper biotite zone but it often cuts across biotite grains (Plate 3E).

Analyses of chlorites are given in Tables 8 and 9. There is a limited compositional range (Figs. 16, 17 and 18) and chlorites of the three petrographic types are entirely comparable in composition. Figure 21 shows that all the analysed chlorites are ripidolites. There is a limited range of Al/(Mg + Fe + Mn) ratios (Figs. 16 and 17) and a somewhat larger spread of Mg/(Fe+Mn) ratios (Figs. 18 and 21). The more Fe-rich chlorites contain slightly more Al (Fig. 18) but Si/Al does not vary significantly (Figs. 16 and 21).

Influence of metamorphic grade. Grade has much less influence on chlorite than on biotite or muscovite (Tables 8 and 9; Fig. 22) but the main features are as follows:

1. There is no divergence of trends for chlorites from different rock types of the Burwash Fm. but those from the Walsh Fm. are slightly distinct. Chlorites (B)

TABLE 8 : Micro-probe analyses (weight %) of CHLORITES from the biotite zone of the Prosperous Lake metamorphic aureole.

	In meta-pelites									
Sample No.	P-1	P-4	P-6	P-7	P-9	PW-11	P-12	[illegible]-13	P-2	P-3
Type**	A	A	A	A	A	A	A	A	B	B
SiO_2	24.07	24.34	24.75	24.77	24.68	24.76	24.91	24.22	24.64	24.44
TiO_2	0.06	0.08	0.08	0.07	0.07	0.05	0.07	0.07	0.09	0.08
Al_2O_3	22.59	22.40	22.35	21.72	22.08	22.07	22.11	22.33	22.05	21.67
FeO*	24.44	24.14	23.10	23.14	23.97	26.14	23.58	25.79	24.21	23.08
MnO	0.27	0.26	0.33	0.32	0.29	0.21	0.25	0.32	0.35	0.24
MgO	14.31	14.60	15.88	15.18	14.92	12.99	15.24	13.91	14.40	15.71
CaO	-	0.02	0.03	Tr	-	-	Tr	-	0.01	-
Na_2O	-	n. p.	0.02	n. p.	-	-	n. p.	-	Tr	-
K_2O	-	0.12	0.07	0.09	-	-	0.10	-	0.09	-
Total	85.74	85.96	86.61	85.29	86.01	86.22	86.26	86.64	85.84	85.22

	In meta-greywackes								
Sample No.	P-4	P-7	G-1	G-3	G-5	G-7	GW-9	G-11	G-14
Type**	B-X	B	A	A	A	A	A	A	A
SiO_2	24.87	24.62	24.88	24.96	24.45	24.23	24.66	25.56	24.51
TiO_2	0.08	0.09	0.09	0.09	0.10	0.08	0.08	0.08	0.08
Al_2O_3	22.26	22.54	22.35	21.35	21.09	22.29	21.36	21.40	21.78
FeO*	24.26	23.30	24.02	23.58	23.78	24.55	25.53	23.36	24.53
MnO	0.26	0.32	0.29	0.30	0.32	0.28	0.25	0.31	0.29
MgO	14.55	15.22	15.51	15.75	14.93	14.31	13.59	15.29	14.40
CaO	0.03	-	-	0.02	-	0.03	-	-	-
Na_2O	Tr	0.01	-	Tr	n. p.	0.01	-	-	-
K_2O	0.10	0.06	-	0.06	0.03	0.09	-	-	-
Total	86.41	86.16	87.14	86.11	84.70	85.87	85.47	86.00	85.59

*Total Fe as FeO

**See text for explanation of types.

n. p. and Tr : as in Table 3; dash = not analysed.

TABLE 9 : Structural formulae (atomic proportions) of the CHLORITES whose analyses are given in Table 8. (Formulae based on 14 oxygen ions.)

Sample No.	P-1	P-4	P-6	P-7	P-9	PW-11	P-12	P-13	P-2	P-3
Si	2.587	2.608	2.616	2.660	2.635	2.665	2.648	2.594	2.644	2.625
Al	1.413	1.392	1.384	1.340	1.365	1.335	1.352	1.406	1.356	1.375
Al	1.448	1.437	1.399	1.409	1.413	1.464	1.417	1.414	1.432	1.369
Ti	0.005	0.006	0.007	0.006	0.006	0.004	0.006	0.006	0.007	0.006
Fe*	2.197	2.163	2.041	2.078	2.140	2.353	2.096	2.310	2.173	2.074
Mn	0.025	0.023	0.029	0.029	0.026	0.019	0.022	0.029	0.032	0.022
Mg	2.292	2.332	2.500	2.430	2.375	2.083	2.413	2.222	2.303	2.516
Ca	-	0.002	0.003	0.001	-	-	0.001	-	0.001	-
Na	-	0.001	0.003	0.001	-	-	0.001	-	0.001	-
K	-	0.017	0.010	0.012	-	-	0.013	-	0.012	-
ΣY-site	5.967	5.981	5.992	5.966	5.960	5.923	5.969	5.981	5.961	5.987

Sample No.	P-4	P-7	G-1	G-3	G-5	G-7	GW-9	G-11	G-14
Si	2.647	2.616	2.620	2.661	2.657	2.605	2.674	2.717	2.640
Al	1.353	1.384	1.380	1.339	1.343	1.395	1.326	1.283	1.360
Al	1.441	1.439	1.393	1.344	1.358	1.430	1.403	1.397	1.406
Ti	0.006	0.007	0.007	0.007	0.008	0.006	0.006	0.007	0.006
Fe*	2.160	2.070	2.115	2.102	2.161	2.208	2.315	2.076	2.210
Mn	0.023	0.029	0.026	0.027	0.029	0.025	0.023	0.027	0.026
Mg	2.309	2.410	2.435	2.504	2.418	2.293	2.197	2.422	2.312
Ca	0.003	-	-	0.002	-	0.004	-	-	-
Na	0.001	0.002	-	0.001	0.000	0.002	-	-	-
K	0.014	0.008	-	0.008	0.004	0.012	-	-	-
ΣY-site	5.957	5.965	5.976	5.995	5.978	5.980	5.944	5.929	5.960

*Total Fe as Fe^{2+}.

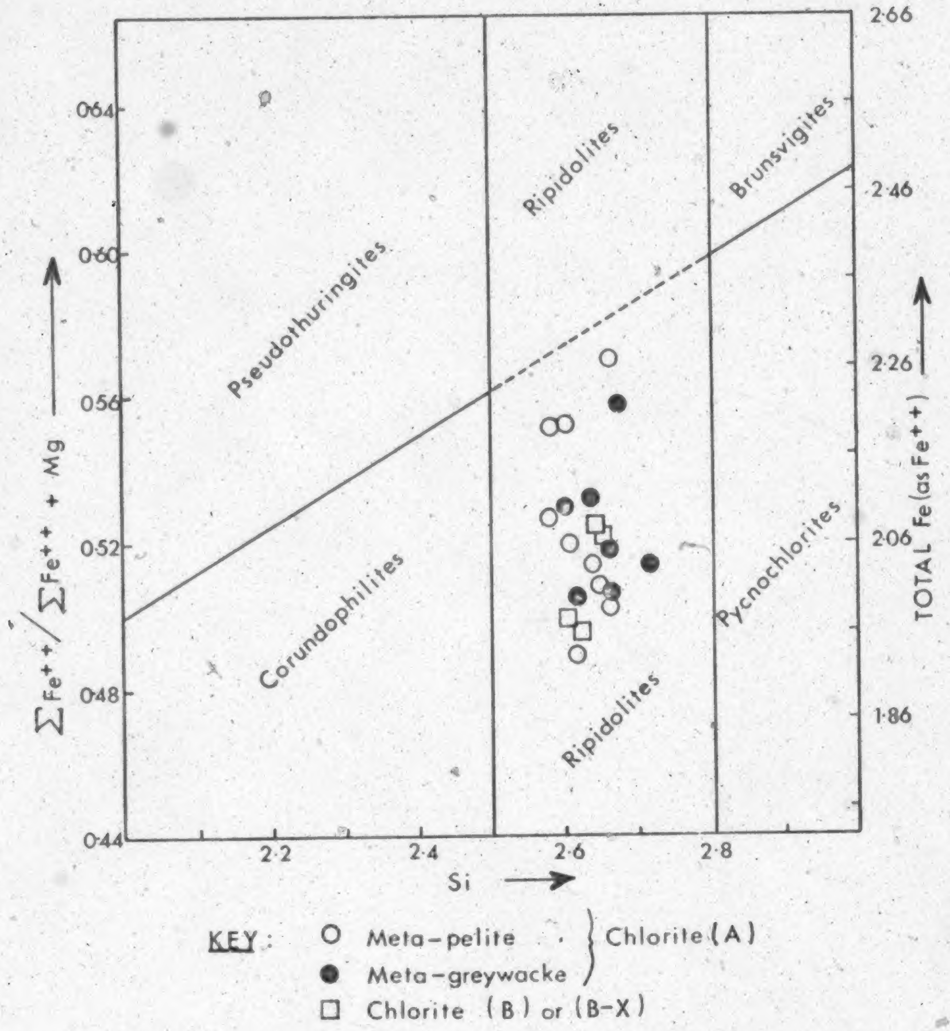

FIGURE 21 : Chlorite classification diagram (modified after Hey, 1954 and Deer et al., 1966) showing the chlorites from the biotite zone of the Prosperous Lake aureole.

and (B-X) are entirely similar in composition to chlorite (A).

2. The Mg/Fe ratio increases only marginally towards the cordierite isograd and its variability cannot be primarily due to grade. Ti and Mn contents are not affected by grade.
3. The observed range of Al^{VI} contents increases markedly towards the cordierite isograd and Si/Al^{IV} decreases very slightly, though having a wide range.
4. The presence of the medium-grained chlorites (B) and (B-X) is also a function of metamorphic grade. Chlorite (B) occurs only in the upper half of the biotite zone. Apparently the compositional maturation of the minerals necessitated the appearance of a new phase at this grade. As a result chlorite (B) crystallised with medium grain-size because of easy growth at elevated temperatures but with composition the same as chlorite (A) because they crystallised under the same controlling conditions. Chlorite (B-X) is first present just below the cordierite isograd but persists at all higher grades. Its suggested origin is given below.

Comparative discussion. The composition of these chlorites resembles that usually found in greenschist facies meta-greywackes and meta-pelites (e.g. McNamara, 1965; Brown, 1967; Mather, 1970; Pinsent, 1971) though they are more magnesian than is usual. Brown (1967) recorded similar compositional variability,

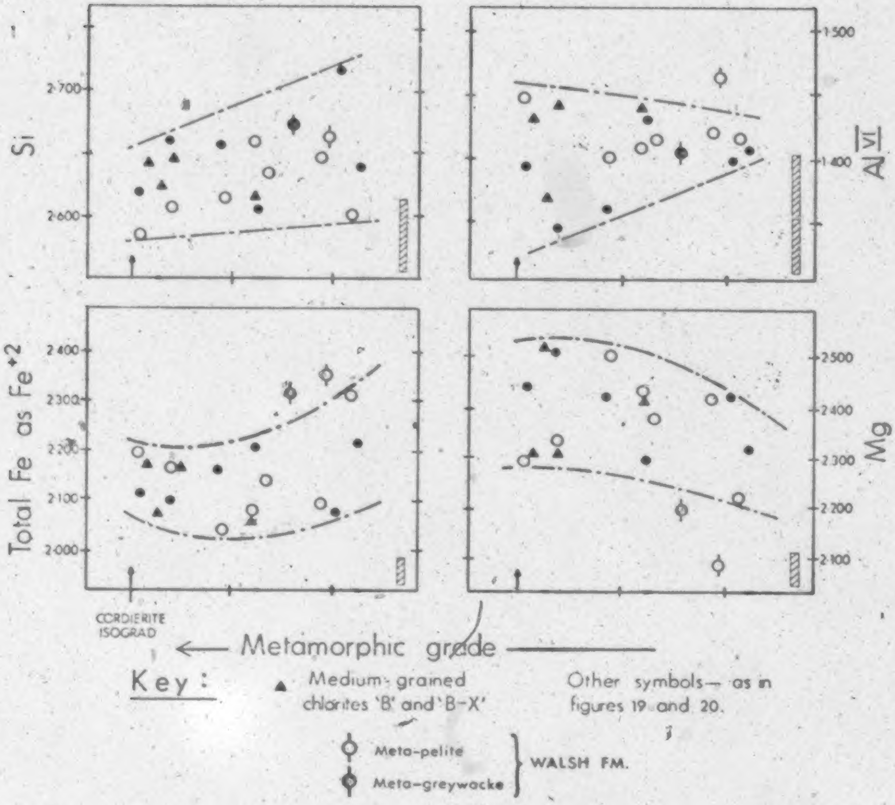

FIGURE 22 : Diagram illustrating the relationship of chlorite composition (atomic proportions) to metamorphic grade. Clearly grade has less influence on chlorite than on biotite (Fig. 19) or muscovite (Fig. 20).

dominantly in Mg/Fe. Cooper (1972) demonstrated a pro-grade increase of Mg/Fe more marked than that shown in Fig. 22 but recognised significant bulk compositional control. He also showed that the more Fe-rich chlorites contain more Al as implied by Fig. 18. In the Prosperous Lake chlorites the significant Mg/Fe variability (Fig. 18) can only partially be attributed to grade control (Fig. 22). The bulk compositional control was apparently dominant (see below).

Plagioclase

Feldspar and quartz comprise the fine-grained groundmasses of these rocks and occur as clastic relics in the metagreywackes (Plate 3G and H). The plagioclase clasts show variable development of marginal corrosion, shadowy extinction, inclusions and breakdown of twin lamellae, reflecting variable reactive response to metamorphism. On this basis clastic grains in several rocks have been petrographically designated as 'active clasts' (showing marked development of the above features; see Plate 3H), 'stable clasts' (free of these indicators of reactivity; Plate 3G) or 'matrix feldspar' (fine-grained groundmass) and analysed for Na, Ca and K (Table 10). Figure 23 relates their composition to petrographic type and metamorphic grade. Several conclusions (tentative in view of the small number of samples) may be drawn concerning the response of the clastic plagioclases to metamorphism:

1. Plagioclases in the Walsh Fm. rocks are sodic. This is in contrast to the Burwash Fm. rocks and reflects differing sedimentary sources.
2. In the Burwash Fm. there is a wide range of plagioclase compositions at low metamorphic grade but

TABLE 10 : Partial micro-probe analyses of plagioclases from the greenschist facies of the Prosperous Lake aureole.

Rock No.	Weight Percentages			Molecular Percentages			Petrographic* Type
	Na_2O	CaO	K_2O	Ab	An	Or	
G-1	8.67	5.53	1.56	73.3	25.8	0.9	"Active"
	8.42	5.71	0.05	72.1	27.0	0.8	"
	7.89	5.91	0.17	70.0	29.0	1.0	"Matrix"
	8.11	5.99	0.14	70.4	28.8	0.8	"
	8.33	5.65	0.16	72.1	27.0	0.9	"
	8.30	5.60	0.15	72.2	26.9	0.9	"
	8.28	5.57	0.12	72.4	26.9	0.7	"
G-5	8.35	6.58	0.13	72.5	26.8	0.7	"Active"
	8.13	6.06	0.13	70.3	29.9	0.8	"
	9.42	3.77	0.22	80.9	17.9	1.2	"Matrix"
	7.82	6.12	0.15	69.2	29.9	0.9	"
	8.21	5.83	0.18	71.1	27.9	1.0	"
	8.13	5.59	0.14	71.9	27.3	0.8	"
	8.11	6.06	0.15	70.2	29.0	0.8	"
GW-9	11.20	0.39	0.10	97.6	1.9	0.5	"Active"
	11.38	0.33	0.10	97.9	1.6	0.5	"
	11.04	0.45	0.11	97.2	2.2	0.6	"
	11.56	0.14	0.09	98.9	0.6	0.5	"
	11.21	0.47	0.10	97.2	2.3	0.5	"Stable"
	11.54	0.25	0.12	98.1	1.2	0.7	"
	11.48	0.37	0.12	97.6	1.7	0.7	"
	10.82	0.42	0.09	97.4	2.1	0.5	"
	10.89	0.36	0.11	97.6	1.8	0.6	"Matrix"
	10.64	0.26	0.12	98.0	1.3	0.7	"
	10.55	0.99	0.11	94.5	4.9	0.6	"
	10.71	0.57	0.12	96.5	2.8	0.7	"
	11.52	0.17	0.12	98.5	0.8	0.7	"
G-10	11.47	0.47	0.10	97.2	2.2	0.6	"Active"
	11.04	0.66	0.10	96.2	3.2	0.6	"
	7.14	8.53	0.16	59.7	39.4	0.9	"
	11.44	0.61	0.14	96.4	2.9	0.7	"
	11.66	0.51	0.11	97.0	2.4	0.6	"Stable"
	11.53	0.41	0.09	97.6	1.9	0.5	"
	[illegible].28	1.07	0.12	94.4	4.9	0.7	"
	8.84	5.12	0.16	75.1	24.0	0.9	"Matrix"
	7.68	6.61	0.18	67.1	31.9	1.0	"
	7.17	7.81	0.12	62.0	37.3	0.7	"

(Continued overleaf)

TABLE 10 : (continued)

G-10 (cont'd)	9.89	3.08	0.15	84.6	14.6	0.8	"Matrix"
	10.49	1.55	0.13	91.8	7.5	0.7	"
G-11	11.12	0.27	0.09	98.2	1.3	0.5	"Active"
	6.63	8.48	0.10	58.2	41.2	0.6	"
	6.76	8.26	0.11	59.3	40.0	0.7	"
	6.35	9.19	0.15	55.1	44.1	0.8	"
	6.23	8.95	0.13	55.3	44.0	0.7	"
	11.16	0.42	0.10	97.4	2.0	0.6	"
	11.08	0.45	0.10	97.2	2.2	0.6	"
	10.71	1.38	0.15	92.6	6.6	0.8	"Stable"
	11.53	0.42	0.15	97.2	2.0	0.8	"
	11.44	0.38	0.12	97.5	1.8	0.7	"
	6.62	8.46	0.13	58.2	41.1	0.8	"
	6.80	8.33	0.12	59.2	40.1	0.7	"
	10.80	0.28	0.11	98.0	1.4	0.6	"Matrix"
	10.99	0.43	0.13	97.2	2.1	0.7	"
	7.04	7.62	0.17	62.0	37.1	0.9	"
	6.70	8.22	0.23	58.8	39.9	1.3	"
	6.38	9.05	0.13	55.6	43.6	0.8	"
GW-12	11.09	0.50	0.10	97.0	2.4	0.6	"Active"
	10.68	0.75	0.09	95.7	3.7	0.5	"
	10.85	0.59	0.08	96.6	2.9	0.5	"
	11.11	0.75	0.09	95.9	3.6	0.5	"
	10.70	0.93	0.11	94.9	4.5	0.6	"
	11.10	0.48	0.08	97.2	2.3	0.5	"
	11.35	0.28	0.07	98.3	1.3	0.4	"Stable"
	11.17	0.32	0.07	98.0	1.6	0.4	"
	10.98	0.39	0.08	97.6	1.9	0.5	"
	10.70	0.24	0.08	98.3	1.2	0.5	"Matrix"
	10.80	0.67	0.08	96.2	3.3	0.5	"
	10.63	0.43	0.14	97.0	2.2	0.8	"
	10.63	0.26	0.07	98.2	1.3	0.5	"
	10.54	0.66	0.10	96.1	3.3	0.6	"
G-14	7.14	7.69	0.17	62.1	37.0	0.9	"Active"
	7.15	7.51	0.14	62.8	36.4	0.8	"
	11.14	0.91	0.09	95.2	4.3	0.5	"
	10.95	1.21	0.09	93.7	5.8	0.5	"
	10.78	1.67	0.14	91.4	7.8	0.8	"
	11.52	0.39	0.11	97.5	1.8	0.6	"
	10.63	0.47	0.28	96.0	2.4	1.7	"
	9.97	2.46	0.12	87.4	11.9	0.7	"Stable"
	10.93	0.59	0.10	96.5	2.9	0.6	"
	11.34	0.34	0.10	97.8	1.6	0.6	"

(Continued overleaf)

TABLE 10 : (continued)

G-14 (cont'd)	10.89	0.58	0.11	96.5	2.8	0.7	"Stable"
	11.11	0.63	0.10	96.4	3.0	0.6	"
	8.45	5.09	0.15	74.4	24.8	0.8	"Matrix"
	7.48	6.79	0.30	65.4	32.8	1.8	"
	8.80	4.96	0.15	75.6	23.5	0.9	"
	10.31	0.69	0.10	95.8	3.6	0.6	"
	8.13	5.84	0.15	71.0	28.2	0.8	"

*See text for explanation of types.

this narrows to only Ab_{69-74} at the cordierite isograd.

3. Although the allocation of petrographic types is subjective and subject to error, several points are noteworthy. The 'matrix' plagioclases at low grade have a wide range of composition but near the cordierite isograd the range is narrow, suggesting metamorphic equilibration of clastic grains. The 'active' grains are far removed from the convergence composition at low grades. In the higher-grade rocks the few remaining clasts are close to the convergence composition.

Apparently the Burwash Fm. initially contained varied plagioclases whose composition was controlled by the source of sediment. Homogenisation gradually occurred by breakdown of those grains furthest removed from the convergence composition.

Comparative discussion. There is no indication in Fig. 23 of control by a peristerite solvus, although Crawford (1966) and Cooper (1972) concluded that plagioclase compositions were determined by the peristerite solvus and interaction with other Ca-bearing phases. Such interaction is the usual control of plagioclase composition in rocks of this type and most pertinent studies have involved calcic phases (e.g. Lambert, 1959; Brown, 1967; Pinsent, 1971). The Prosperous Lake rocks lack such phases and all Ca must be accommodated in plagioclase. The result is gradual pro-grade homogenisation with the final plagioclase composition, determined by the amount of Ca in the rock (compare the plagioclases of the Walsh and Burwash Fms.).

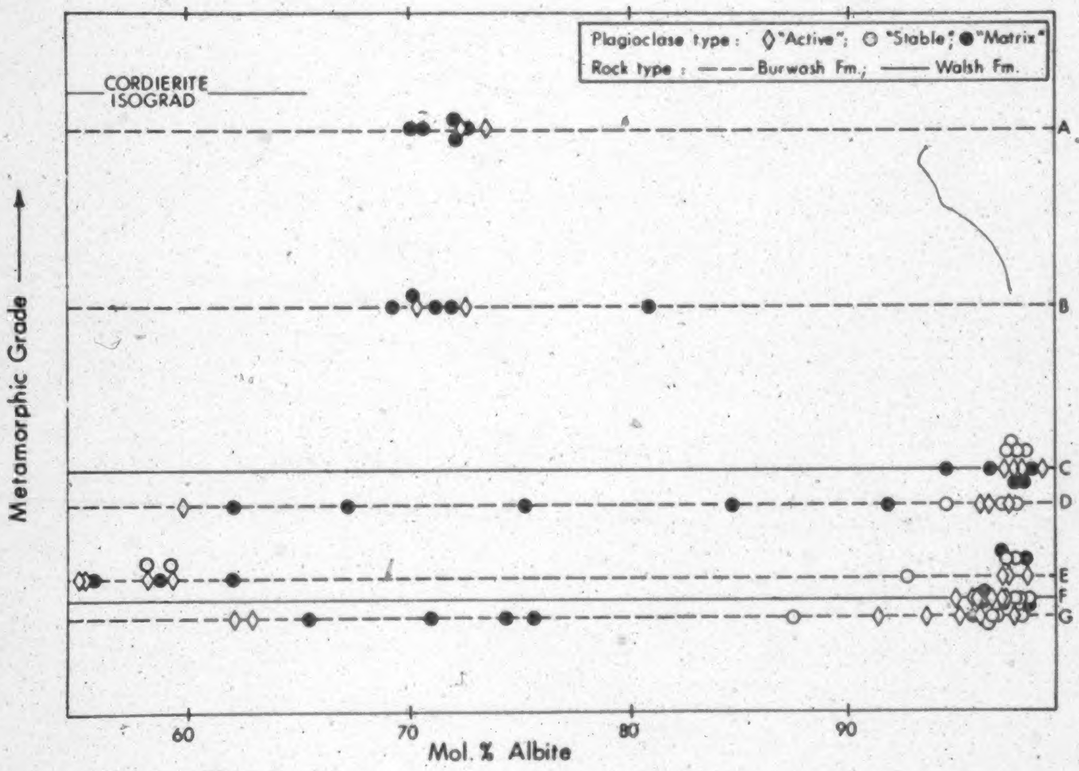

FIGURE 23 : Diagram illustrating the relationship between plagioclase composition, plagioclase petrographic type and metamorphic grade in some meta-greywackes from the biotite zone. Sample numbers : A = G-1; B = G-5; C = GW-9; D = G-10; E = G-11; F = GW-12; G = G-14.

Potassium Feldspar

There is no clastic K-feldspar in these rocks, presumably as a result of metamorphic degradation to muscovite. Minor, fine-grained K-feldspar is present in the matrix with an uneven and genetically significant distribution (discussed below). No systematic compositional investigation of this mineral has been attempted but micro-probe analysis of grains from sample P-4 has confirmed that K-feldspar is present. It is a pure potash microcline containing less than one per cent Na_2O (usually less than 0.25 per cent).

Oxides and Sulphides

Opaque minerals comprise up to about five per cent of the mode of these rocks. Rutile and ilmenite are the oxides present (see Plate 3C and D). Magnetite has not been observed. The Walsh Fm. samples lack ilmenite. Micro-probe analyses of these phases (including some from the vicinity of the cordierite isograd) are given in Table 11.

Rutile occurs in porphyroblastic aggregates (Plate 3C). It is very uniform in composition, containing very minor Si, Al and Fe and only traces of Mg and Mn. The ilmenites have more variable composition from one rock to another and commonly have marked grain-to-grain variation in Mn content. They display the high pyrophanite contents characteristic of metamorphic ilmenites (Rumble, 1971), containing about 6 mol. % $MnTiO_3$.

Influence of metamorphic grade. It seems possible that the amount of Si or Al substituting for the Ti of rutiles and ilmenites in rocks saturated in Si and Al might be temperature-dependent, though at higher pressures octahedral Si might be significant.

TABLE 11 : Micro-probe analyses of rutiles and ilmenites.

(a) RUTILES.

Oxide	Biotite Zone							Cordierite Isograd				
	P-1	P-4	P-12	P-13	G-2	G-11	G-14	P-16	P-17	P-18	P-19	G-17
SiO_2	0.20	0.19	0.25	0.24	0.23	0.27	0.24	0.19	0.24	0.22	n.a.	0.23
TiO_2	96.48	96.55	95.63	95.26	96.44	95.97	96.15	98.32	98.46	97.81	97.20	97.03
Al_2O_3	0.12	0.07	0.26	0.21	0.10	0.09	0.17	0.08	0.13	0.09	n.a.	0.08
ΣFeO	0.25	0.21	0.32	0.30	0.39	0.25	0.31	0.36	0.43	0.40	0.49	0.12
MnO	0.02	0.00	0.01	0.01	0.01	0.03	0.03	0.01	0.01	0.02	n.a.	0.01
MgO	0.02	0.02	0.03	0.05	0.03	0.03	0.02	0.04	0.03	0.01	0.03	0.02
Total	96.48	97.04	96.50	96.07	97.20	96.64	96.92	99.00	99.30	98.55	97.72	97.49

(b) ILMENITES

Oxide	Biotite Zone			Cordierite Isograd						
	P-12	G-2	G-11	P-16	P-17	P-17*	P-18	P-19	P-19*	G-17
SiO_2	0.20	0.13	0.24	0.17	0.25	0.23	0.21	0.14	0.18	0.22
TiO_2	50.39	51.30	51.40	52.28	52.18	52.44	51.51	51.86	51.20	51.48
Al_2O_3	0.12	0.05	0.08	0.07	0.09	0.07	0.08	0.08	0.09	0.07
ΣFeO	42.68	44.00	42.74	43.53	43.83	44.89	41.69	41.36	44.21	43.20
MnO**	3.17	2.77	2.77	3.23	2.21	1.84	5.20	3.54	2.23	3.30
MgO	0.04	0.04	0.17	0.06	0.12	0.13	0.05	0.05	0.08	0.10
Total	96.60	98.29	97.40	99.34	98.68	99.60	98.74	97.03	97.99	98.37

* Included in cordierite poikiloblast.

** Marked grain-to-grain variation.

n. a. Not analysed.

However, the only suggestion in Table 11 that this is so is that the Al_2O_3 content of low-grade rutiles is generally higher than those near the cordierite isograd. None of the other elements exhibit any grade-dependence.

Sulphides. Pyrrhotite is the dominant sulphide, though it is usually subordinate in amount to the titaniferous oxides. It is commonly closely associated with traces of chalcopyrite and sometimes pyrite. In three analyses of pyrrhotites and two of chalcopyrites the elements Si, Ti, Al, Mn and Mg were found in concentrations from 0.1-0.02 per cent.

Comparative discussion. This assemblage of oxides and sulphides is rare. Kanehira et al. (1964) demonstrated that the assemblage ilmenite + pyrrhotite + graphite was characteristic of low-grade meta-pelites in low-pressure facies series. The assemblage in the Prosperous Lake rocks is the same except in that rutile is also present. Ilmenite and rutile are recorded together by Evans and Guidotti (1966), Westra (1970) and Rumble (1971). Of these authors, only Westra reported paragenetic details, demonstrating that the rutile preceded the ilmenite-hematite minerals. The same explanation applies to the Prosperous Lake rocks. It is shown below that ilmenite was a reactant and rutile a product in the reaction which formed biotite. Thus the Burwash Fm. rocks originally contained the characteristic opaque mineral assemblage for their metamorphic style, but partial reaction of ilmenite to rutile later led to the unusual coexistence of these phases.

CONTROLLING ROLE OF METAMORPHIC GRADE

The figures and discussion above leave no doubt that metamorphic grade (primarily metamorphic temperature) was a principal control of mineral composition. It does, however, seem to have operated to different extents on different mineral groups. The observed compositional response to increased grade was a maturation process consisting of one or more of the following factors:

1. Typically there is a progressive change in elemental concentration towards higher grades (e.g. Fe in muscovite; Fig. 20).
2. There is commonly a pro-grade narrowing of the range of composition (e.g. Al^{VI} in muscovite).
3. In a few instances the range of composition seems to increase with grade (e.g. Al^{VI} in biotite, Fig. 19).

The first of these factors is readily explained in terms of the most stable composition at progressively increasing temperature. Thus the pro-grade approach to ideality exhibited by the muscovites simply reflects relative instability of phengitic muscovites at high temperatures (Velde, 1965).

The progressive narrowing of the compositional range is, however, more difficult to explain except in the special case of the plagioclases (see above). For the other minerals the following cause is suggested. At low grades host-rock composition was an important control but it was gradually superceded, at higher grades, by temperature. Thus slightly different host-rocks initially developed compositionally distinct metamorphic minerals, perhaps as a result of having different proportions of the reactant phases. This range of composition was tolerated at low temperature but increasingly restricted as temperature increased. For example, local variations in the proportions of muscovite-forming phases may initially have produced variably phengitic muscovites. As temperature increased the tolerable range of composition was restricted (Velde, 1965) so that the most phengitic muscovites became less so and the range gradually narrowed.

Control by metamorphic grade operated differently on different mineral groups. Thus meta-greywacke biotites exhibit primarily linear compositional changes (factor 1 above) with little sign of convergence (factor 2); meta-pelite biotites and chlorites were only slightly affected by increased grade; the muscovites display a combination of the linear and convergent trends. The reason for this is not clear but it seems probable that increased temperature would influence mineral composition if the following two conditions both applied:

1. A change in composition is energetically favourable.
2. Such a change is not prevented by other controlling factors. This is most likely to be a bulk compositional control.

It has been experimentally and empirically shown (e.g. Velde, 1965; Cipriani et al., 1971) that it is energetically favourable for muscovite to approach compositional ideality as temperature increases. The fact that this has demonstrably occurred in the Prosperous Lake rocks implies that no other control prevented the process. For example, Al must have been sufficiently available.

Since meta-greywacke biotites exhibit pro-grade compositional changes and meta-pelite biotites do not, it seems that the pro-grade maturation was energetically favourable but was prevented in the meta-pelites. The most likely cause of this prevention is the bulk composition and this aspect is investigated further below.

CONTROLLING ROLE OF ROCK COMPOSITION

The Rock Compositions

Analyses of composite samples from this area are to be found in Boyle (1961) and Henderson (1972). Folinsbee (1942) and Tremblay (1952) also made analyses of equivalent rocks from higher metamorphic grades. Table 2 presents new analyses of fourteen rocks and their compositions are graphically compared in Fig. 13. The meta-greywackes have a larger range of Al_2O_3 content and generally higher proportions of (Na_2O + K_2O) and SiO_2 than the meta-pelites but have similar MgO/(FeO + MnO). The two analysed rocks of the Walsh Fm. have SiO_2 contents comparable to the meta-greywackes but are similar to the meta-pelites in Al_2O_3 and K_2O components. They also are much poorer in CaO than the Burwash Fm. rocks. As pointed out by Henderson (1972) all these rocks display the high FeO/Fe_2O_3 and Na_2O/K_2O ratios characteristic of greywacke sequences and the meta-greywackes and meta-pelites differ in Na_2O/K_2O ratio (Table 2).

Influence on Mineral Composition

Although there are no gross differences between minerals from Burwash meta-pelites, Burwash meta-greywackes and Walsh Fm. rocks (Figs. 16, 17 and 18) there are subtle distinctions between them. The meta-greywacke chlorites have marginally lower

Al_2O_3 contents than the others, reflecting a lower availability of that element (Tables 8 and 2). The meta-greywacke biotites are more variable than those from meta-pelites (Fig. 17) and have generally higher Si/Al^{IV} (Fig. 19). The muscovites are more variable in the meta-greywackes particularly in Al/(Fe+Mg) (Fig. 17) and Al/Mg (Fig. 18), and the total X-site occupancy is lower in meta-pelite muscovites (Fig. 20; cf. Butler, 1967, p. 252). Muscovites in the Walsh Fm. are distinct by several parameters (Fig. 20), notably in having higher Al^{VI}/Mg, Al^{VI}/Fe and Na/K. These distinctions directly reflect the higher Al/(Fe+Mg) and Na/K ratios of the Walsh Fm. rocks (Fig. 13 and Table 2). There is, however, no apparent reason for the larger X-site deficiency which they also display (Fig. 20).

Host-rock composition was the dominant control for the plagioclases and probably for the chlorites (above). The controlling mechanism for the former has been deduced above and a comparable effect applies to the chlorites. These were paragenetically earlier than biotite (below) and when formed they were therefore the only abundant Mg-rich phase. While Fe might have been accommodated in oxides, effectively all the Mg had to be incorporated in chlorite. Thus the Mg/Fe ratio of the rock would be a very important control, suppressing any tendency for pro-grade increase of Mg/Fe.

Since the mineral assemblage is the same in all the Burwash rocks, the observed differences cannot be attributed to competition by other mineral species (Butler, 1965 and 1967), but this remains a possibility for the biotite-free Walsh Fm. samples.

Influence on Pro-grade Maturation of Minerals

In several instances minerals in meta-pelites and meta-greywackes exhibit different response to increased metamorphic grade (Figs. 19 and 20).

Biotites in the meta-pelites show less compositional maturation than those from meta-greywackes. The different trends for Na reflect the higher $Na_2O/(Na_2O + K_2O)$ ratios of the meta-greywackes, which apparently resulted in more Na being taken into the X-site. This implies that pro-grade increase of Na was the favoured trend but was prevented in the meta-pelites because of insufficient Na supply. The pro-grade decrease of K in meta-greywacke biotites is partly due to increased Na, but the X-site total also decreases so this is not the sole cause. Perhaps another element (e.g. Ba or Rb) was available only in meta-greywackes and increasingly occupies the X-site. The increase of Mg/Fe in the meta-greywacke biotites is probably the favoured trend (Lambert, 1959), but it is not clear why the same is not observed in the meta-pelites.

Conclusions

The controlling role of bulk composition in rocks of this type is not agreed. Butler (1967) found it necessary to subdivide his analysed micas into those which coexisted with epidote and those which did not, but otherwise believed bulk composition to have had negligible effect. Guidotti (1969), however, reconsidered Butler's data and concluded that bulk composition would have a significant effect on phengite composition in certain mineral assemblages. Velde (1965) and Brown (1968) indicated that phengite composition was strongly controlled by bulk composition but Velde (1967 and 1968) suggested that the Si content of phengites was largely independent of this control. Makanjuola and Howie (1972) have maintained that there is a controlling influence on a variety of minerals by rock composition. This conclusion is, however, based on positive correlations between compositional parameters in minerals and rocks and should therefore be treated with suspicion.

There is no doubt that the bulk composition has influenced the compositions of the minerals at Prosperous Lake. The observed effects (above) exemplify general circumstances under which such control may operate:

1. Large differences in mineral composition may be expected when bulk compositions differ sufficiently to develop distinct mineralogies. Mineral compositions may then differ as a result of formation by different reactions or competition with different mineral assemblages (e.g. chlorites and muscovites in the Walsh and Burwash Fms.; Cooper, 1972, Fig. 2; Brown, 1967, Fig. 11; Hermes, 1973, Figs. 6 and 7).
2. Within a suite of rocks of one mineral assemblage subtleties of bulk composition are not only reflected in varying modes but also in mineral composition (e.g. muscovite X-site occupancy is generally higher in meta-greywackes than meta-pelites; see Fig. 20).
3. Subtleties of bulk composition in a rock suite of one assemblage can alter or prevent the pro-grade

compositional maturation of the minerals (e.g. the different maturation trends of meta-pelite and meta-greywacke biotites; see Fig. 19).

4. If only one mineral rich in a particular element is present (and has a variable composition) its composition must be influenced by the abundance of that element in the rock (e.g. Ca and the different plagioclases of the Walsh and Burwash Fms.; Mg and the variability of the chlorites).

CONTROLLING ROLE OF PRESSURE

The influence of pressure can only be evaluated by comparison with other metamorphic terrains. The Prosperous Lake muscovites have compositions typical of high thermal gradient terrains (see Cipriani et al., 1971, p. 27) with low celadonite contents. The similarity of biotite compositions from different pressure regimes (compare Table 2 with Butler, 1967, and Brown, 1967) indicates that pressure is not an important control of biotite composition. However, two features of these biotites may be consequent on the pressure conditions because they are not normally found under higher pressure gradients: (1) the grade-dependence of the X-site deficiency and (2) the pro-grade increase of Na in meta-greywacke biotites. The compositions of the chlorites are independent of the pressure regime (compare Table 4 with data in Mather, 1970, and Brown, 1967). The opaque mineral assemblage is that characteristic of low-pressure greenschist facies in Japan (Kanehira et al., 1964) except that rutile is also present.

CONTROLLING ROLE OF FLUID COMPOSITION

It is impossible to examine this problem directly but it seems likely that the composition of the fluid medium influenced the composition of the minerals crystallising in it. It is therefore critically important whether there was a progressive change in fluid composition across the aureole, i.e. whether fluid composition within restricted systems was determined internally (closed system behaviour) or externally (open system behaviour). For example, the emplacement of the central pluton may have caused a radial flow of fluid whose composition would have been progressively modified by interaction with the host rocks. This would lead to changes in mineral composition only apparently related to metamorphic grade. There is, however, considerable evidence against this possibility. For instance, the pro-grade changes in muscovite are similar to those observed in regional metamorphic terrains where no central pluton was present to induce fluid migration. The same applies to several of the changes in biotite composition. Further, the small volume of fluid relative to solid in these non-porous rocks suggests to this author that fluid composition would probably be locally buffered by the bulk rock composition. Thus the CO_2 content would be buffered by the presence of graphite and the redox properties by the ferrous : ferric ratio of the rock. Even if these buffered fluid compositions depended secondarily on temperature they would be locally, rather than externally determined.

It seems probable, therefore, that externally controlled changes in fluid composition were not important in determining mineral compositions in this particular rock suite. No doubt the presence of fluid was critically important in determining rates and volumes of reaction, but its composition was determined by mineralogy, rock composition, pressure and temperature, which were therefore the ultimate controls of mineral composition.

THE CONTROLS OF MINERAL COMPOSITION

Considering metamorphic rocks in general the controls of mineral composition may be divided into two types: (1) those which permit the existence of the mineral and (2) those which modify its composition.

Permissive Controls

These are well known through the evolution of the facies concept. They are:

1. Energetic controls. The appearance of a mineral is absolutely dependent on the physical conditions being within its field of stability. The obvious factors are P and T but the partial pressures of the various gases, the pH of the system, etc., may be equally important.
2. Crystallographic controls. If the energetic controls permit appearance of the phase, it is then essential that adequate supplies of the required elements be available. What constitutes an 'adequate supply' is crystallographically controlled in that elements must be available in approximately the correct proportions. (Availability is not simply a function of bulk composition but also of metasomatic activity, reaction relationships, etc.) The crystallographic control is therefore approximately equivalent to a control by suitability of rock type (though not compositional subtleties within

that rock type) and to the 'bulk compositional control' commonly cited with reference to ACF and AKF diagrams.

Modifying Controls

For minerals of fixed composition, the above controls are sufficient to determine their presence or absence. When mineral composition is variable the permissive controls (above) determine the appearance of a mineral but not its exact composition. There are several important modifying controls, often acting simultaneously. The extent to which each operates on a particular mineral group is very variable and it is probable that the controlling factors operate to different extents in different physical environments. In other words, the relative priorities of these factors are different for different minerals in the same metamorphic terrain and probably for the same minerals in different terrains. The main modifying controls are:

3. Partition. In rocks of similar type but different mineral assemblage mineral compositions are determined by different 'networks' of partition equilibria and may differ as a result.
4. Crystal chemistry. The demands of electrical neutrality must sometimes result in modification of the mineral compositions. If, for instance, increased temperature requires the substitution of Al^{3+} for Mg^{2+} in muscovites, the crystallo-chemical control necessitates simultaneous changes in other elements.
5. Metamorphic grade. Within the stability fields of

the minerals metamorphic T and P commonly impose a gradual compositional maturation.

6. Bulk composition. Within a given bulk compositional field subtleties of bulk composition can exert marked control.
7. Modal proportions. It is shown in the following section that the modal proportion of minerals in rocks of very similar bulk chemistry may influence mineral chemistry. This may be a consequence of partition relationships or simply a reflection of the reaction control (8, below).
8. Reaction relationships. It also appears from the next section (Fig. 26) that the composition of a mineral participating in a reaction may change progressively with the extent of that reaction.
9. Others. It is probable that other controls also operate (e.g. externally buffered fluids).

It is suggested that all of these factors may operate together, in similar or opposite sense. In particular circumstances one may be dominant and modify or even prevent the operation of another, but this is no guarantee that the same priorities apply in other circumstances.

THE ORIGIN OF BIOTITE

As noted above, the biotite isograd is not visible in the area mapped. Therefore the nature of the biotite-forming reaction must be deduced indirectly using data on mineral chemistry, modal proportions and textural relations.

The Problem

Despite the zonal significance and ubiquitous occurrence of biotite, its origin in the greenschist facies has never been fully resolved. It is generally accepted that the reaction involves the addition of elements (mainly K, Si and Ti) to chlorite but the following major problems persist. (1) What is the source of these elements and are they derived from a single reacting phase? (2) Do the reactant phases change in composition during the reaction or are they simply consumed? (3) Are there any subordinate reaction products and, if so, what are they?

C. E. Tilley initiated the controversy in 1926 when he concluded that biotite was formed by the reaction

$$\text{K-rich Muscovite} + \text{Chlorite} + \text{Quartz} \longrightarrow$$
$$\text{Biotite} + \text{less K-rich Muscovite} + H_2O$$

Then, until about 1965, petrologists swung to the opinion that chlorite changed composition during the reaction. This was suggested by numerous workers including Turner (1948), Ramberg (1952), Fyfe, Turner and Verhoogen (1958), Turner and Verhoogen (1951 and 1960), Barth (1962) and Winkler (1965). The suggested reactions generally conformed to that suggested by Winkler (1965):

$$\text{Muscovite} + \text{(Mg, Fe)-rich Chlorite} \longrightarrow$$
$$\text{Biotite} + \text{Al-rich Chlorite} + \text{Quartz} + H_2O$$

Recently, however, abundant compositional data on greenschist facies minerals have become available and it is apparent that chlorite composition does not, in fact, change during the reaction (e.g. Chinner, 1960, p. 212; Brown, 1967). With the formulation and clarification of the phengite problem (Lambert, 1959) attention has been re-focussed on the role of muscovite in the production of biotite. Yoder (1959) suggested that Si-rich sericite would react with chlorite to give biotite and muscovite. A comparable reaction was experimentally demonstrated by Winkler (1962) and the idea was developed further by Ernst (1963) and Mather (1970). There is, however, some contrary evidence suggesting that muscovite composition does not change during the reaction. For example, Brown (1967) concluded from numerous analyses that neither chlorite nor muscovite changed in composition.

There have also been suggestions that other phases are reactants. Thus it has been suggested that the required K and Si are derived from K-feldspar (Ernst, 1963; Winkler, 1965; Mather, 1970; Brown, 1971) and McNamara (1966) believed the K to be derived from aqueous KOH solution. There have also been suggestions that oxide phases are involved. Harker (1939, p. 214) listed magnetite and rutile as reactants and Deer, Howie and Zussman (1962, p. 71) mentioned 'iron ore' and rutile.

The definitive study at present is that by Mather (1970) who reviewed previously suggested reactions and showed them to be unsatisfactory. He then demonstrated two important facts:

1. Muscovite coexisting with biotite is less phengitic than that which is not.
2. The composition of the muscovite is critical in defining the range of rock compositions in which biotite may appear. As the muscovite becomes

less phengitic at higher grades the variety of rocks which may contain biotite increases.

It is not entirely clear what reaction Mather envisaged for the formation of the biotite and there appears to be some contradiction in what he has written:

p. 263 and 267 . . . The assemblage chlorite + phengitic muscovite + microcline breaks down to yield chlorite + biotite + less-phengitic muscovite. With increasing grade (and complete removal of microcline?) the stability field of the biotite-bearing assemblage is enlarged and biotite is produced by a new reaction between phengitic muscovite and chlorite yielding less-phengitic muscovite, chlorite and biotite.

p. 267 and 268 . . . The sequence of metamorphic zones is described as follows.

'Zone 1 : chlorite and microcline are . . . stable . . . .

Zone 2 : chlorite and microcline react . . . .

Zone 3 : chlorite and phengite react . . . .'

It is therefore unclear whether Mather believed the required elements to be derived from microcline alone until it was all removed and then from phengite, or whether microcline and phengite were simultaneous reactants. As Mather was obviously aware in setting up the zones, this point is critical in determining the reaction isograds. It also implies a fundamental difference between the biotite isograds of terrains where microcline is present and those where it is not.

It was with the above problems and disagreements in mind that the following investigation of the origin of biotite at Prosperous Lake was designed.

The Data

Modal analyses of the rocks are given in Table 12. The accuracy of these determinations is estimated as ±10-15 per cent (see Appendix). Data on the mineral chemistry of these rocks is given above.

Some use is made below of graphs correlating variables subject to the closure effect (Chayes, 1971). In view of the ranges of percentages in these graphs the correlations are believed to be significant but evidence from them is deliberately restricted to supportive rather than crucial roles in the argument.

The Participant Phases

Biotite. The habit of biotite is variable. In some rocks it occurs as subhedral plates with weakly preferred orientation; in others there are biotite-rich clots with minor chlorite or oxide minerals. In many rocks, particularly meta-pelites, it occurs as large, slightly poikiloblastic porphyroblasts commonly associated with rutile (Plate 3B). Some biotite flakes have quartzo-feldspathic peripheral zones deficient in chlorite and muscovite or are associated with unusually coarse quartz grains. In the extreme case this yields quartzose augen surrounded by biotite (Plate 3F). Biotite formation clearly post-dated that of chlorite and muscovite and the textures suggest that rutile and quartz were also involved in the reaction.

Biotites in meta-greywackes show systematic compositional changes with metamorphic grade but those in meta-pelites do not

TABLE 12 : Modal analyses of meta-pelites and meta-greywackes.

	Meta-greywackes														
Sample No.	G-1	G-2	G-3	G-4	G-5	G-6	G-7	G-8	GW-9	G-10	G-11	GW-12	G-13	G-14	G-15
Grade Index	1.5	4.0	5.4	6.7	10.2	13.4	13.5	14.5	16.5	19.0	22.7	23.2	23.2	24.3	24.4
Qtz + Plag	55	66	66	59	50	65	57	65	65	55	65	63	61	62	67
K-feldspar	2.0*	0.4	1.2*	Tr	2.0	1.0**	0.4*	2.3**	Tr	Tr*	2.0	0.7	Tr	0.3	0.7
Biotite	14 *	23	14 *	33	20 *	19 **	14	24 **	0.0	32	12	0.0	12	13 *	19
Muscovite	12	4.4	0.0	1.8	14	0.2	13	0.0	9.7	0.5	10	7.1	0.2	2.7	3.9
Chlorite	15	5.0	17	3.5	12	14	12	7.6	21	9.9	9.5	26	23	20	8.1
Chlorite B	(0.8)	(0.4)	(0.0)	(0.0)	(0.0)	(0.0)	(0.0)	(0.0)	(0.0)	(0.0)	(0.0)	(0.0)	(0.0)	(0.0)	(0.0)
Total Opaques	2.4	1.5	1.5	2.9	1.6	1.0	2.4	1.3	2.0	2.1	1.3	2.9	3.7	1.9	1.6
Rutile	(1.0)	(0.6)	(0.3)	(0.7)	(0.5)	(0.3)	(1.1)	(0.3)	(1.9)	(1.0)	(0.7)	(2.7)	(0.6)	(0.6)	(0.5)
Ilmenite	(1.3)	(0.9)	(0.9)	(0.3)	(0.9)	(0.6)	(0.8)	(0.6)	(0.0)	(1.0)	(0.3)	(0.0)	(1.8)	(0.7)	(0.7)
Pyrrhotite	(Tr)	(0.0)	(0.3)	(1.4)	(Tr)	(0.0)	(0.2)	(0.3)	(0.0)	(Tr)	(0.2)	(Tr)	(0.9)	(0.5)	(0.3)
Tourmaline	Tr	Tr	0.0	0.2	0.2	0.3	0.6	Tr	Tr	0.2	0.0	Tr	0.0	0.2	Tr
Others	0.0	0.0	Tr	Tr	0.3	0.2	Tr	Tr	Tr	Tr	0.0	0.0	Tr	Tr	0.2
Total	100.4	100.3	99.7	100.4	100.1	100.7	99.4	100.2	100.7	99.7	99.8	99.7	99.9	100.1	100.5
No. of points	1100	800	800	800	1300	800	800	800	800	1300	800	800	800	800	800

	Meta-pelites														
Sample No.	P-1	P-2	P-3	P-4	P-5	P-6	P-7	P-8	P-9	P-10	PW-11	P-12	P-13	P-14	P-15
Grade Index	1.5	3.1	4.0	5.6	10.2	11.0	13.5	13.5	15.0	19.0	20.5	20.8	23.5	26.2	26.4
Qtz + Plag	42	39	44	24	36	51	41	59	29	47	45	41	34	45	54
K-feldspar	1.2	2.1*	0.8	18	4.4	0.5*	3.8*	0.5*	3.5*	1.4*	Tr	1.3*	1.6	1.3*	0.2
Biotite	23	43	18	10 *	20	25	27	9.6*	34 **	0.9*	0.0	7.5*	15	12 *	23
Muscovite	17	6.0	11	30	23	1.4	13	15	23	19	29	25	25	16	3.7
Chlorite	14	2.7	24	17	15	21	15	12	10	30	24	22	22	24	17
Chlorite B	(0.4)	(1.6)	(2.2)	(2.6)	(0.2)	(Tr)	(1.6)	(0.0)	(Tr)	(0.0)	(0.0)	(0.0)	(0.0)	(0.0)	(0.0)
Total Opaques	2.2	0.8	2.1	0.9	1.6	0.9	1.0	3.3	0.9	2.8	2.4	3.9	2.2	1.8	1.8
Rutile	(1.8)	(0.5)	(1.5)	(0.8)	(1.0)	(0.3)	(0.7)	(2.0)	(0.6)	(2.1)	(2.3)	(3.0)	(1.4)	(0.6)	(0.9)
Ilmenite	(Tr)	(0.2)	(Tr)	(Tr)	(Tr)	(0.6)	(Tr)	(1.1)	(Tr)	(0.6)	(0.0)	(0.7)	(0.5)	(0.8)	(0.9)
Pyrrhotite	(0.2)	(Tr)	(0.4)	(Tr)	(0.2)	(Tr)	(Tr)	(0.2)	(0.3)	(Tr)	(0.0)	(Tr)	(Tr)	(0.3)	(Tr)
Tourmaline	Tr	6.8	0.5	0.4	Tr	0.6	Tr	0.3	Tr	0.2	0.0	0.5	Tr	Tr	0.2
Others	Tr	0.0	0.2	0.0	0.0	Tr	Tr	Tr	0.0	Tr	Tr	0.0	0.0	0.0	Tr
Total	98.4	100.4	100.6	100.3	100.0	100.4	100.8	99.7	100.4	101.3	100.4	100.2	99.8	100.1	99.9
No. of points	800	800	800	800	800	800	800	800	800	800	800	800	800	800	800

Tr = trace (<0.2%)

*Trace of secondary K-feldspar or chloritised biotite present.

**Appreciable secondary K-feldspar or chloritised biotite.

Grade Index: Arbitrary linear scale of distance from cordierite isograd.

PLATE 3

Photomicrographs of biotite zone rocks.

(KEY : bi = biotite; mu = muscovite; chl = chlorite; rut = rutile; ilm = ilmenite; co = cordierite; gt = garnet; st = staurolite.)

A. General view showing blastopsammitic texture of a typical biotite zone meta-greywacke. Sample G-14. Crossed nicols.

B. Biotite and rutile porphyroblasts and a fine-grained, lepidoblastic, (kinked) matrix of chlorite and muscovite in a typical biotite zone meta-pelite. Sample P-5. Plane polarised light.

C. Rutile porphyroblast in sample P-4. Biotite, quartz and K-feldspar are associated with the rutile. Note that the lepidoblastic matrix foliation has been deformed by the rutile. Plane polarised light.

D. (1) Ilmenite grain with embayed outline suggestive of corrosion. Sample P-14. Reflected light.
(2) Composite rutile porphyroblast. Sample P-1. Reflected light.

E. Chlorite(B-X) cutting across biotite grains in sample P-2. Plane polarised light.

F. Quartzose augen surrounded by biotite in a fine-grained groundmass. Note associated rutile. Meta-pelite. Plane polarised light.

G. Example of a 'stable' clastic plagioclase grain in a meta-greywacke (see text). Sample G-14. Crossed nicols.

H. Example of an 'active' clastic plagioclase grain in meta-greywacke G-14 (see text). Crossed nicols.

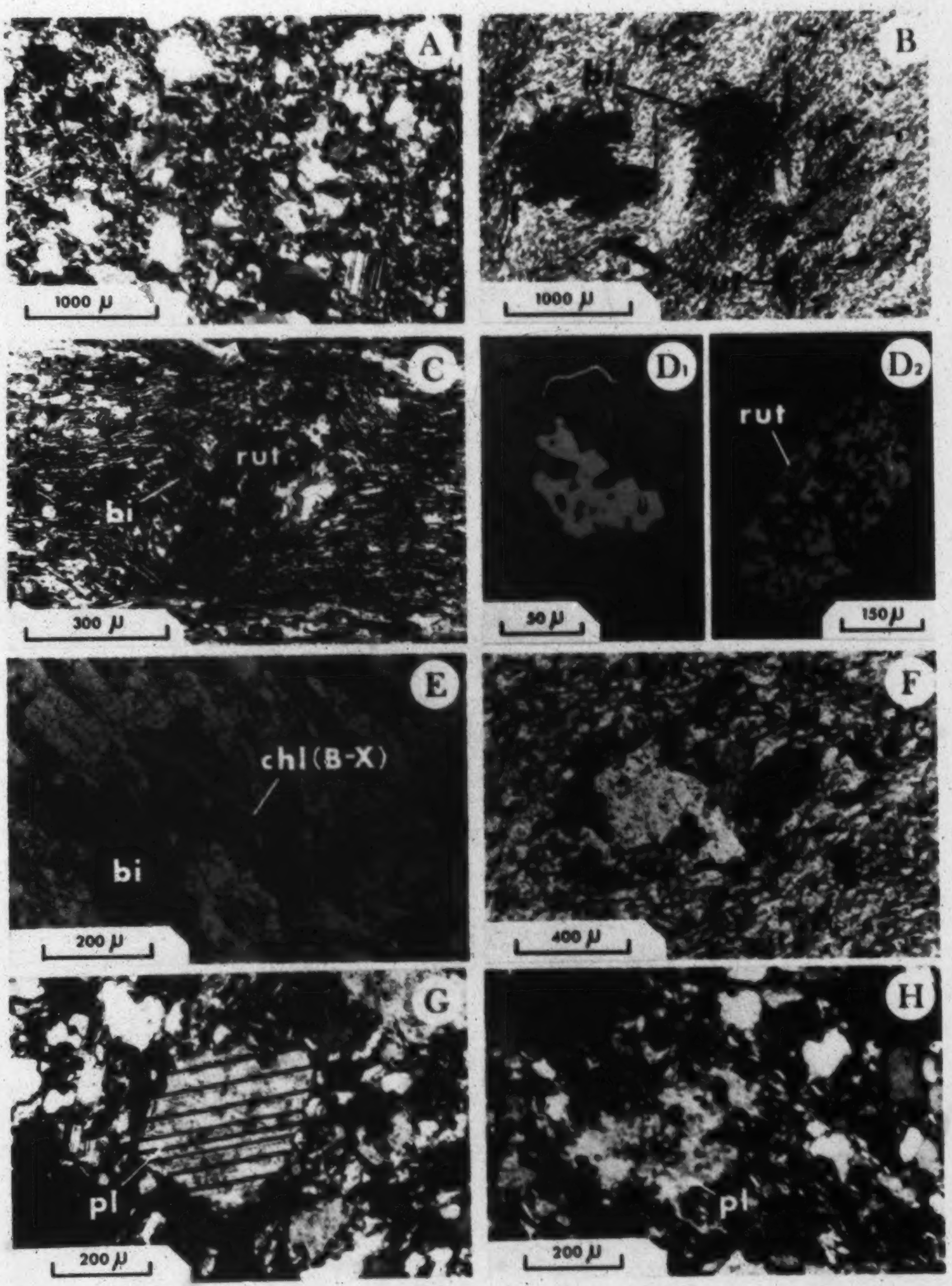
A
1000 μ
B
bi
1000 μ
C
rut
bi
300 μ
D1
50 μ
D2
rut
150μ
E
chl (B-X)
bi
200 μ
F
400 μ
G
pl
200 μ
H
pl
200 μ

PLATE 3

(Fig. 19). Figure 24 shows the corollary of this -- when biotite composition is plotted against biotite mode the meta-greywackes show no correlation but the meta-pelite biotites display increasing $Al^{VI}/(Fe + Mn + Mg)$ as biotite mode increases. This problem is discussed further below.

As the principal reaction product the amount of biotite present is a measure of the extent of reaction (e.g. Everett, 1959, p. 98) since the rocks were biotite-free before the reaction occurred. The modal percentage of biotite is therefore used below as an index of the extent to which the reaction proceeded.

Chlorite occurs as very small flakes in the groundmasses of both meta-pelites and meta-greywackes (Plate 3B and C). There is a slight tendency to lower chlorite modal percentages at higher grades (Fig. 29) but there is little compositional dependence on grade (above).

Fig. 25 implies consumption of chlorite in the biotite-forming reaction. Graphs (not shown) of chlorite composition against biotite modal percentage indicate that chlorite composition did not change as the reaction progressed. The possible exception is that the chlorites of the biotite-free Walsh Fm. rocks have higher Fe/Mg ratios than those in the biotite-bearing Burwash Fm. which might be attributable to different host-rock compositions.

Thus all the available information indicates that chlorite was a principal reactant phase but apparently did not change in composition during the reaction.

Muscovite. Small muscovite flakes (Plate 3B, C and F) are abundant in the meta-pelites but less so in the meta-greywackes

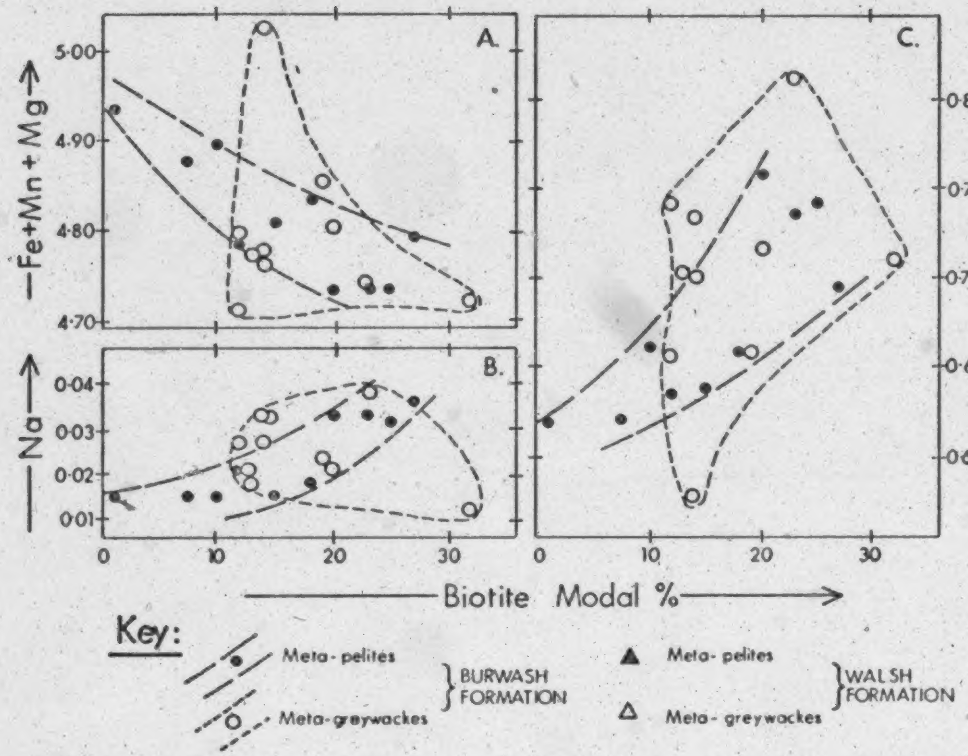

FIGURE 24 : Relationship of biotite composition to extent of reaction as represented by the modal percentage of biotite. The ordinate axis represents atomic proportions in the structural formulae. The key applies also to Figs. 25, 26, 27 and 28.

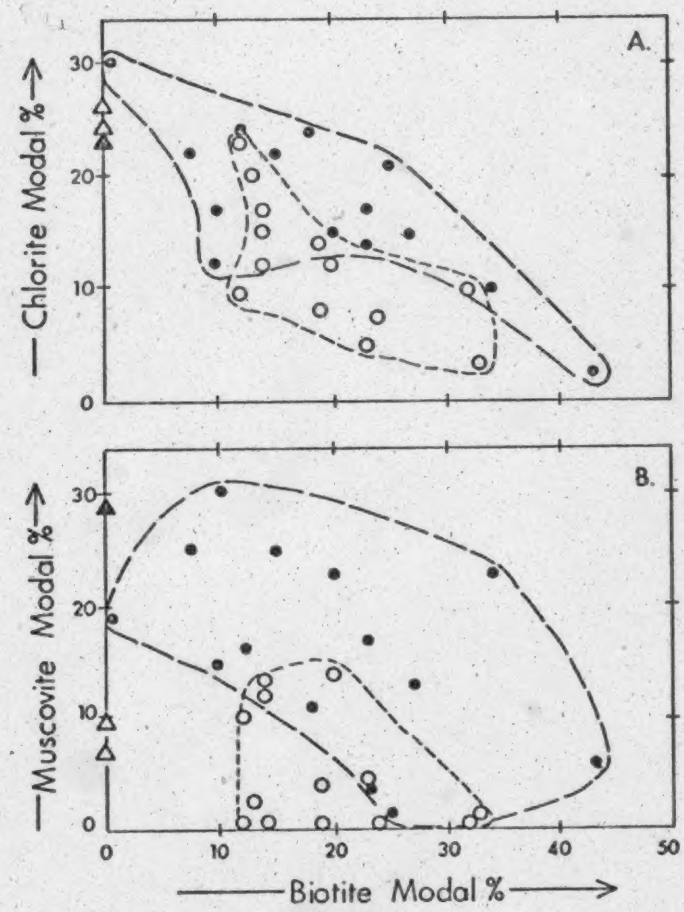

FIGURE 25 : Mutual relationships of chlorite and muscovite modal percentages to biotite modal percentage. Symbols as in Fig. 24.

(Table 12). Muscovite abundance is not related to metamorphic grade but there is a broad antipathetic relationship between muscovite and biotite modes in meta-pelites (Fig. 25). This is at least compatible with consumption of muscovite during formation of biotite.

Figure 26 shows that there are systematic relationships between the composition of muscovite and the amount of biotite present. (It might be argued that these trends are a result of both muscovite composition and biotite mode being related to metamorphic grade but the relative linearities of the trends in Figs. 26 and 28 and the fact that the Ti content of muscovite is not grade-dependent -- above -- suggest that this is not so). Figure 26 therefore implies changes in muscovite composition as the biotite-forming reaction progressed. These include the decrease of K suggested by Tilley (1926) and a decrease of (Fe + Mg + Mn) compatible with decreasing phengite content (Mather, 1970 and Ernst, 1963), but no change in Si or Al^{VI} contents is apparent. They also include increased Ti content and decreased total Y-site occupancy.

Titaniferous oxides. The ilmenite in these rocks characteristically occurs as anhedral grains with embayed outlines (Plate 3D) suggestive of corrosion. In some instances it forms subhedral plates aligned parallel to the groundmass foliation indicating paragenetic contemporaneity with it. Ilmenite has not been observed in Walsh Fm. rocks, but in the Burwash Fm. its modal amount is related to that of biotite as shown in Fig. 27 -- there is a marked decrease in the maximum ilmenite content as biotite mode increases. This is compatible with the textural indications that ilmenite was consumed in the reaction. However, the most substantial proof that ilmenite

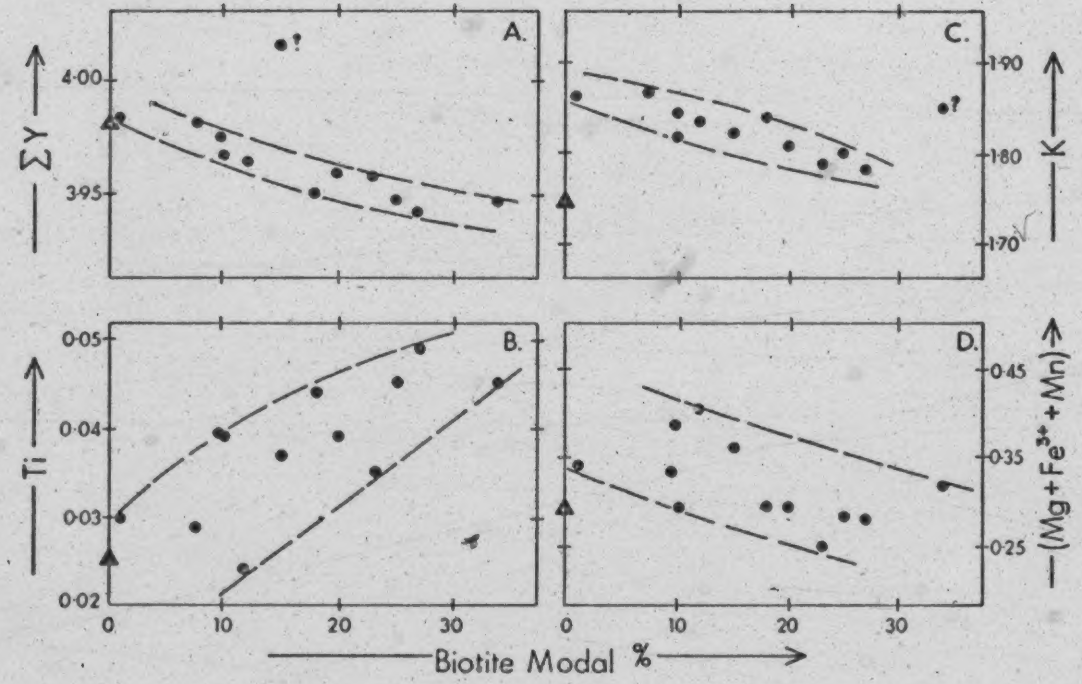

FIGURE 26 : Showing dependence of muscovite composition on the extent of reaction as represented by the modal percentage of biotite. Only meta-pelites are shown because data from meta-greywackes had too limited a range to reveal trends. Points marked (?) fall away from otherwise well-defined trends. Ordinate axis graduated in atomic proportions. Symbols as in Fig. 24.

participated is that rutile was co-genetic with biotite (below) and the Ti content of the biotite is higher than that of either the chlorite or the muscovite. A Ti-rich reactant is therefore mandatory and the nature of the rutile proves that it was a product not a reactant.

The rutile commonly occurs intergrown with the ilmenite or closely associated with it, but more typically is alone. It forms small anhedra (including flakes on biotite cleavages), short prisms, or the very characteristic composite porphyroblasts depicted in Plate 3C and D. These are typically associated with biotite porphyroblasts and, in some instances, deform the groundmass foliation (Plate 3C). In the Walsh Fm. the rutile occurs as tiny anhedra very distinct from those of the Burwash Fm. and none of the composite porphyroblasts have been observed. Thus there is very little doubt from the textural relations that rutile was co-genetic with biotite and it is therefore not immediately apparent why there is a marked negative correlation between the modal amounts of rutile and biotite (Fig. 27). This correlation might simply be due to the closure effect (Chayes, 1971) but alternatively might indicate that rutile was simply produced in whatever amounts were required to take up the Ti which could not be accommodated in biotite. Where biotite is abundant these excesses were small and little rutile was formed. This implies, of course, that the amount of ilmenite decomposing was not controlled by demand for Ti.

The above features clearly indicate that ilmenite was present before the appearance of biotite and was consumed in the reaction, while rutile was a secondary product co-genetic with biotite. The absence of biotite in the ilmenite-free Walsh Fm. rocks tends to confirm that ilmenite was essential to the reaction.

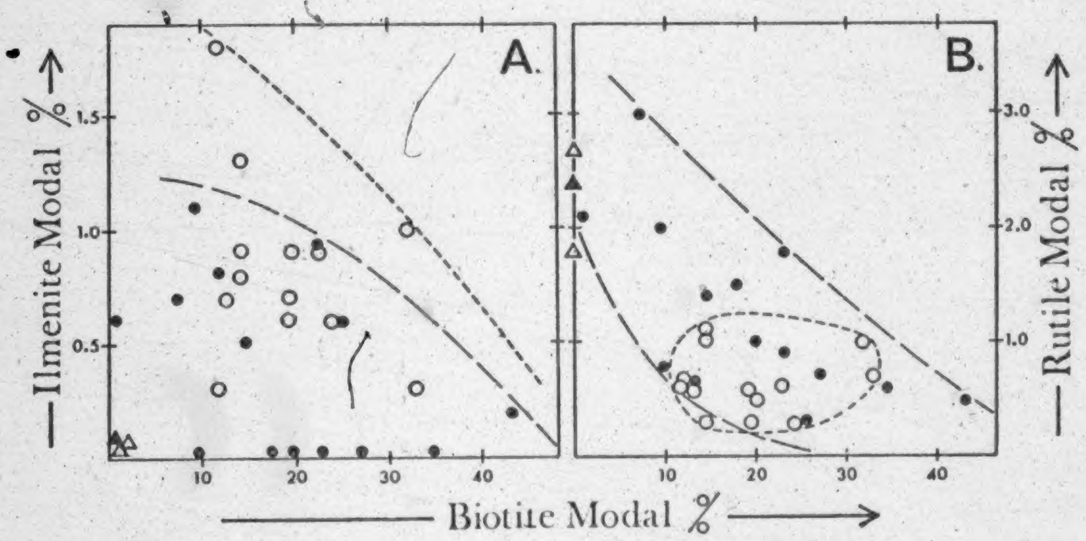

FIGURE 27 : Illustrating the relationship of ilmenite and rutile modal percentages to biotite modal percentage. Symbols as in Fig. 24.

Potassium feldspar. K-feldspar occurs in the fine-grained portions of these rocks but never as clastic relics. Secondary K-feldspar is also present in most of the rocks from this area in small amounts localised along veinlets or associated with chloritised biotite. (The secondary K-feldspar and the altered biotite do not hinder the study of these rocks because they are so readily recognised and avoided.) The primary K-feldspar exhibits several significant textural features. It is occasionally found interleaved with biotite or included in biotite poikiloblasts. It is very commonly associated with rutile porphyroblasts and occurs in some quartzose augen. These features suggest that K-feldspar was a by-product of the biotite-forming reaction.

Plagioclase and quartz. There is no evidence that plagioclase participated in the reaction but the abundance and diverse habit of that mineral might obliterate such evidence and its participation cannot be ruled out. Quartz, however, displays textures suggestive of being co-genetic with biotite, forming augen (Plate 3F) associated with biotite or occuring as quartzose rims round the biotite porphyroblasts.

The Reaction

The evidence above leads to the conclusion that the operative reaction at Yellowknife was a complex process approximated by:

$$\text{Chlorite} + \text{Muscovite}(1) + \text{Ilmenite} \longrightarrow$$
$$\text{Biotite} + \text{Muscovite}(2) + H_2O + \left[\text{Rutile, Quartz, K-feldspar}\right]$$

Chlorite did not change in composition but was simply consumed as the reaction progressed. Muscovite was consumed but that remaining suffered compositional changes. The composition of the biotite produced was dependent, at least in the meta-pelites, on the extent of reaction. Rutile and probably quartz and K-feldspar were produced only in amounts necessary to take up excesses of elements. The role of K-feldspar is uncertain except in that it was co-genetic with rutile and biotite.

Discussion

Mechanisms. The mechanism of a reaction in which a reactant is partially consumed and also altered in composition must be complex. Figure 28 is a simplistic model for the transfer of material in such a reaction, illustrating two discrete stages in the continuous process. Decomposition of muscovite (1) apparently liberated elements in proportions rather different from those required for the conversion of chlorite to biotite. The resultant excesses (and deficiencies) were accommodated either in muscovite (2) or in K-feldspar and quartz. Excess Ti liberated by ilmenite decomposition was similarly fixed as rutile, though Fig. 26 suggests that a little of it was taken up in muscovite (2). Muscovite (2) was then the reactant for the next step of the continuous process. This model fails to explain the dependence of biotite composition on the extent of reaction (Fig. 24). No entirely satisfactory explanation for this is apparent. Possibly in rocks where the extent of reaction was large the depletion of reactants (e.g. ilmenite) caused a paucity of elements (e.g. Fe) so that biotite composition deviated from the optimum to accommodate this shortage.

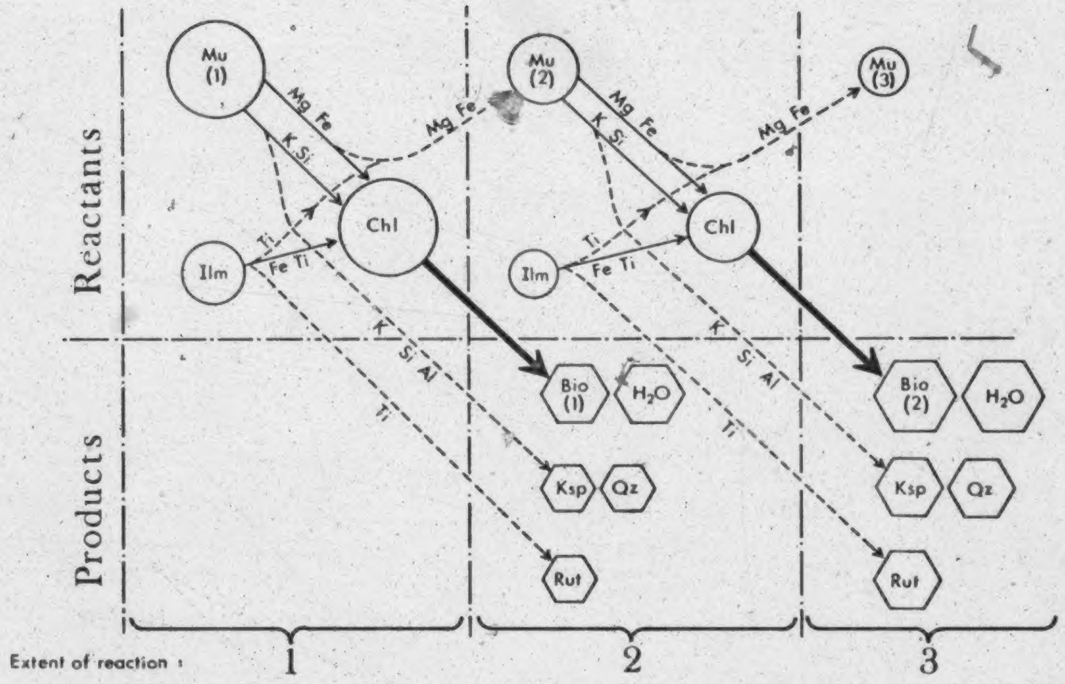
Reactants
Products
Mu (1)
Mu (2)
Mu (3)
Chl
Chl
Ilm
Ilm
Mg Fe
K Si
Ti
Fe Ti
Mg Fe
K Si Al
Ti
Bio (1)
H_2O
Ksp
Qz
Rut
Bio (2)
H_2O
Ksp
Qz
Rut
Extent of reaction :
1
2
3

FIGURE 28 : Simplistic diagram illustrating the suggested transfer of elements during the conversion of chlorite to biotite. It attempts to explain the features of Figs. 24 to 27 which suggest that the reaction involved both changes in amounts of the phases and (in some cases) compositional changes in them. Dashed lines indicate excesses of elements and the sizes of the circles indicate crudely the amounts of the phases present. Three stages in the continuous process are shown.

Termination of the reaction. Figure 29 shows that the extent of reaction varies widely at any particular metamorphic grade. The reaction was not, therefore, simply a continuous process whose balance shifted to the products at higher temperature, and some other control must have operated. The most likely cause of termination of the reaction is the removal of one reactant. However, only 53 per cent of these rocks effectively lack one reactant (i. e. contain less than 0.3 per cent modal). Only another 6 per cent have two reactants present in such small amounts that they might be isolated from one another (i. e. totalling less than 3 per cent modal). Clearly there are many rocks in which all three reactants are abundantly present. The following reason is suggested. When conditions of incompatibility were reached, there was rapid reaction of incompatible phases in effective physical contact. This ceased when two reactants became separated but increased temperature and duration of metamorphism permitted diffusion of components from increasing distances. In time one reactant would have been completely removed by this mechanism but the system was cooled before this was achieved. Thus the wide range of modal percentages in Fig. 29 and the coexistence of reactants in some rocks is due to effective isolation of reactants while the second-order pro-grade increase in biotite content is due to more complete reaction by diffusive processes.

Comparison with Previous Studies

None of the numerous proposed reactions which involve changing chlorite composition (e. g. Ramberg, 1952; Winkler, 1967; Turner, 1968) occurred in the Yellowknife rocks. There is, however,

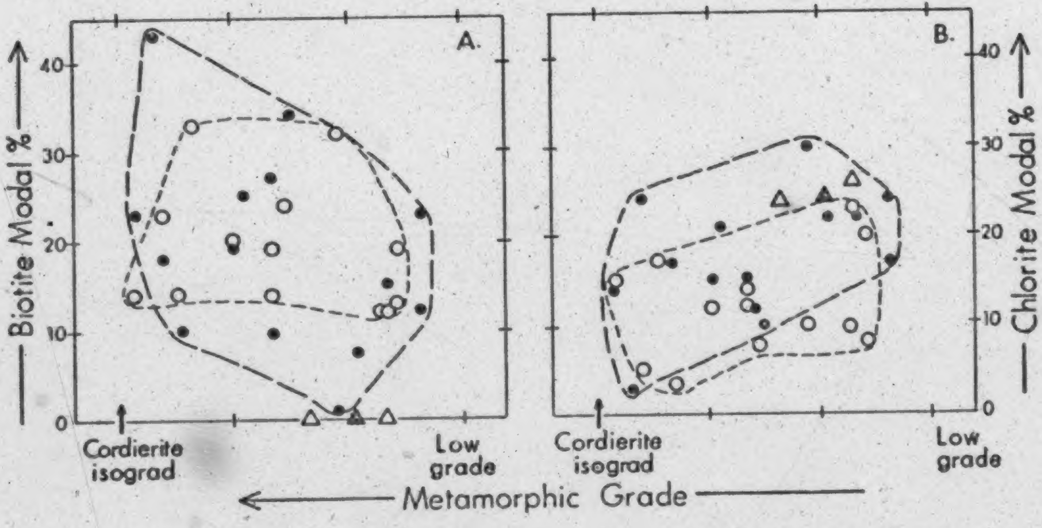

FIGURE 29 : Illustrating the relationship between metamorphic grade and the modal percentages of chlorite and biotite. Only very broad trends are apparent (see text). The modal percentage of muscovite shows no systematic relation to grade. Symbols as in Fig. 24.

little doubt that marked changes in muscovite composition occurred (cf. Brown, 1967).

Little pertinent information is available on the participation of titaniferous oxides in comparable silicate reactions. Evans and Guidotti (1966, p. 58) suggested that a reaction with ilmenite might account for increased Ti in biotites and Muller (1966) described the retrogression of biotite to chlorite, muscovite, ilmenite, rutile, sphene and hematite. This is similar to the pro-grade reaction suggested above and constitutes strong evidence for its feasibility.

The reaction differs from that suggested by Mather (1970) in three ways. (1) Detrital K-feldspar is entirely absent and there was no chance for the first of Mather's reactions to occur. (2) The phengite content of the Yellowknife muscovites is small (Table 6) so that muscovite composition did not influence the conditions of reaction and biotite was formed at similar metamorphic grades in all rocks which contained the essential reactants. This telescoping of the biotite isograds in different rock compositions may be expected in all low P/T facies series. (3) The titaniferous oxides at Yellowknife were involved in the reaction. Mather's Table 2 shows that his reaction cannot be balanced in terms of TiO_2 and some source of Ti is required. Mather gave no information on the oxides present and it seems possible that ilmenite was also involved in the Aberfoyle rocks. This point is, in fact, of general application and many biotite isograds may involve titaniferous oxides as essential reactants.

Conclusion

Biotite originated in the Burwash Fm. by the complex reaction described above. While the identity of the reactant and product phases is not surprising, it is the apparent complexities of the reaction which warrant much further work. In 1926 Tilley concluded a paper on rocks of this type by remarking that, "The mechanism of mineralogical transformations in crystalline schists is something much more complex than is explained away by the customary simple equations." This is clearly still true for biotite-forming reactions.

The most obvious unsolved complexities apparent from the above study are as follows: (1) Apparently a paucity of reactants where the extent of reaction was large caused the biotite composition to vary with the extent of reaction. Is this really the cause of the correlation between biotite mode and composition and is the effect of general applicability? (2) What mechanism accounts for both consumption and compositional modification of the reactant muscovite? (3) Why should muscovite be compositionally modified but not chlorite? (4) It has been suggested above that the minor reaction products were produced only in amounts sufficient to take up elemental excesses which could not be accommodated in the principal products. This implies that the stoichiometric coefficients vary from rock to rock for the 'same' reaction. Does the exact nature of mineral reactions depend on the relative amounts of the reactants present? (5) The formation of biotite at Yellowknife was dependent on the presence of ilmenite, as shown by the absence of biotite in the ilmenite-free Walsh Fm. Minor constituents, particularly opaque phases, have commonly been ignored in petrographic studies. Are they essential to many reactions and does their presence or absence commonly control the appearance of a new phase?

THE CORDIERITE ISOGRAD

The cordierite isograd has traditionally been used throughout the Slave Craton to separate two readily mappable metamorphic zones (the biotite and cordierite zones) and consequently has been extensively mapped (e.g. Henderson and Jolliffe, 1941; Jolliffe, 1942 and 1946). Kretz (1968) and Davidson (1967) have attributed the appearance of cordierite to the reaction of chlorite, muscovite and quartz to produce cordierite, biotite and water, but no detailed petrological study has been made and there has been no specific study of the Prosperous Lake area.

The Problem

There are numerous possible reactions to account for the appearance of cordierite in pelitic and semi-pelitic schists (Schreyer and Yoder, 1961). Perhaps the most commonly suggested and the most clearly understood one is

$$\text{Muscovite} + \text{Chlorite} + \text{Quartz} \longrightarrow \text{Cordierite} + \text{Biotite} + H_2O$$

(Tilley, 1924; Winkler and von Platen, 1958; Schreyer and Yoder, 1961; Hess, 1969; Seifert, 1970; Bird and Fawcett, 1971). There are, however, severe restrictions on the bulk compositions in which this simultaneous first appearance of cordierite and biotite will occur. Seifert (1970, p. 76) noted that it will only occur if the bulk composition lies in the muscovite-chlorite two-phase field in the AKF diagram. In more aluminous compositions cordierite will appear at lower temperatures; in less aluminous rocks biotite will appear first. As a

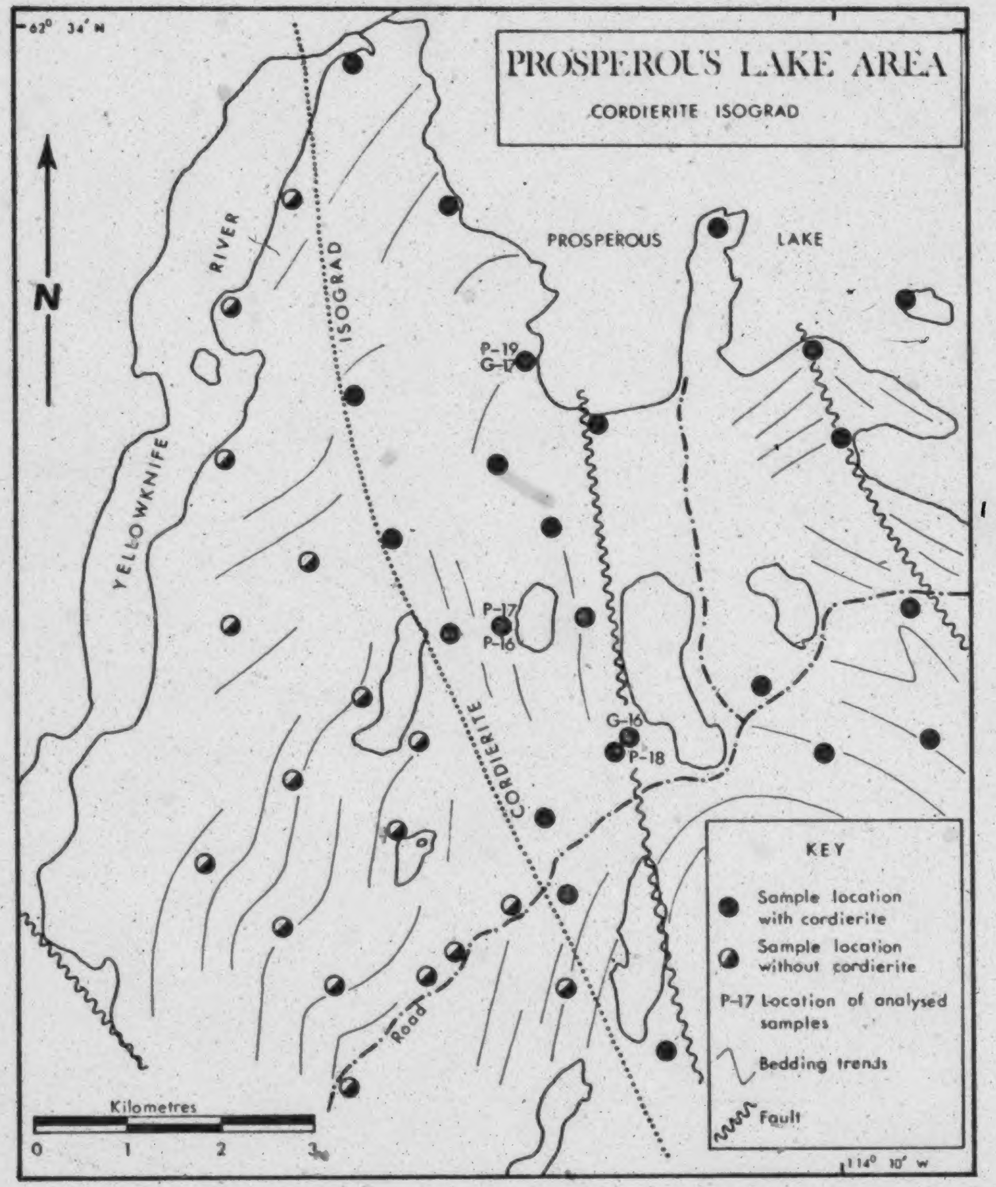
62° 34' N
PROSPEROUS LAKE AREA
CORDIERITE ISOGRAD
N
YELLOWKNIFE
RIVER
ISOGRAD
CORDIERITE
PROSPEROUS
LAKE
P-19
G-17
P-17
P-16
G-16
P-18
Road
Kilometres
0
1
2
3
114° 10' W
KEY
Sample location with cordierite
Sample location without cordierite
P-17 Location of analysed samples
Bedding trends
Fault

FIGURE 30 : Mineral assemblages observed in the vicinity of the cordierite isograd, the resulting definition of that isograd and the locations of samples for analysis.

consequence of these restrictions, the experimentally established reaction (above) is unlikely to represent entirely the isograds of real meta-pelites. In particular, the prior appearance of biotite in the pro-grade zonal sequence is the rule rather than the exception and its effects on the growth of cordierite are not known.

The Prosperous Lake cordierite isograd provides an ideal opportunity to study this problem. Biotite is present in rocks below the isograd, its compositional changes with grade are known (above) and the cordierite isograd itself is sharply defined and well exposed.

The Isograd

The cordierite isograd in the Prosperous Lake area was first mapped by Jolliffe (1942 and 1946) as shown in Fig. 4. It has been slightly modified in the small area where detailed study has been made (Fig. 30).

At the isograd cordierite porphyroblasts (Plate 4A) appear in abundance over a very small interval of grade (Fig. 30). There is no particular rock-type in which the cordierite appears first, though commonly at any one outcrop it is present in some beds and not in others. Within the cordierite zone cordierite is ubiquitous but variable in amount and is absent from many rocks.

Table 13 shows the relative frequency of mineral assemblages above and below the isograd. The following points are significant:

1. While chlorite(A) and muscovite coexist in many rocks below the cordierite isograd, they have not

TABLE 13 : Relative frequency of mineral assemblages in samples from the vicinity of the cordierite isograd in the Prosperous Lake area.

Mineral$^{(2)}$ Assemblage		Percentage of samples		
		Below cordierite isograd	Above cordierite isograd	
Chlorite(A)	Muscovite		Without cordierite	With cordierite
O	O	3	18	41
O	X	3	23	49
X	O	27	49	10
X	X	67	10	0
Total %		100	100	100

Notes:
(1) O = Absent or Trace (i.e. $< 1\%$); X = Present.
(2) All assemblages include biotite, quartz and plagioclase.
(3) Total number of samples = 80.

been observed together in cordierite-bearing rocks and very rarely so in cordierite-free rocks above the isograd. (The only two observed exceptions are from the same locality very close to the isograd.) Minor amounts of chlorite (B-X) do coexist with muscovite above the isograd but its formation apparently post-dated the cordierite-forming reaction.

2. Rocks above the isograd commonly contain either chlorite(A) or muscovite.
3. Absence of both chlorite(A) and muscovite is rare below the isograd but much more common above it, especially in cordierite-bearing rocks.

Table 13 therefore indicates that cordierite formed by reaction of chlorite(A) and muscovite. Both were essential reactants and the appearance of cordierite depended on their coexistence. Thus the cordierite-free rocks above the isograd are those which previously lacked either chlorite(A) or muscovite. In these rocks the chlorite(A) or muscovite persisted above the conditions of their mutual incompatibility (Tables 17 and 18). In most cases the cordierite-forming reaction was terminated by complete consumption of the chlorite, leaving excess muscovite; less commonly muscovite was completely consumed first.

The role of biotite cannot be evaluated by these criteria.

The Role of Biotite -- Petrographic Evidence

The amount of biotite present above the isograd is similar to that below it and there is no distinct difference between the

PLATE 4

Features of the cordierite, cordierite-garnet and sillimanite-staurolite zones.

(KEY : As for Plate 3.)

A. Typical outcrop of cordierite-rich biotitic meta-sediments.

B. Typical diffuse poikiloblast of cordierite with numerous inclusions in a meta-greywacke. Crossed nicols.

C. Margin of a cordierite poikiloblast showing depletion of biotite within it and complete lack of marginal biotite concentration. Plane polarised light.

D. Coarse interleaved muscovite and chlorite included in a cordierite poikiloblast. Note associated ilmenite and anhedral (corroded?) biotite. Plane polarised light.

E. Euhedral garnet with few inclusions in a matrix containing biotite and rutile. Plane polarised light.

F. Embayed garnet with relict euhedral shape. The embayments are filled by quartz and are thought to indicate corrosion. Plane polarised light.

G. Large euhedral andalusite (var. chiastolite) porphyroblasts in biotite semi-schist from the Western shore of Prosperous Lake (Fig. 36).

H. Optically continuous relics of corroded staurolite (location shown in Fig. 36) surrounded by abnormally coarse muscovite. Plane polarised light.

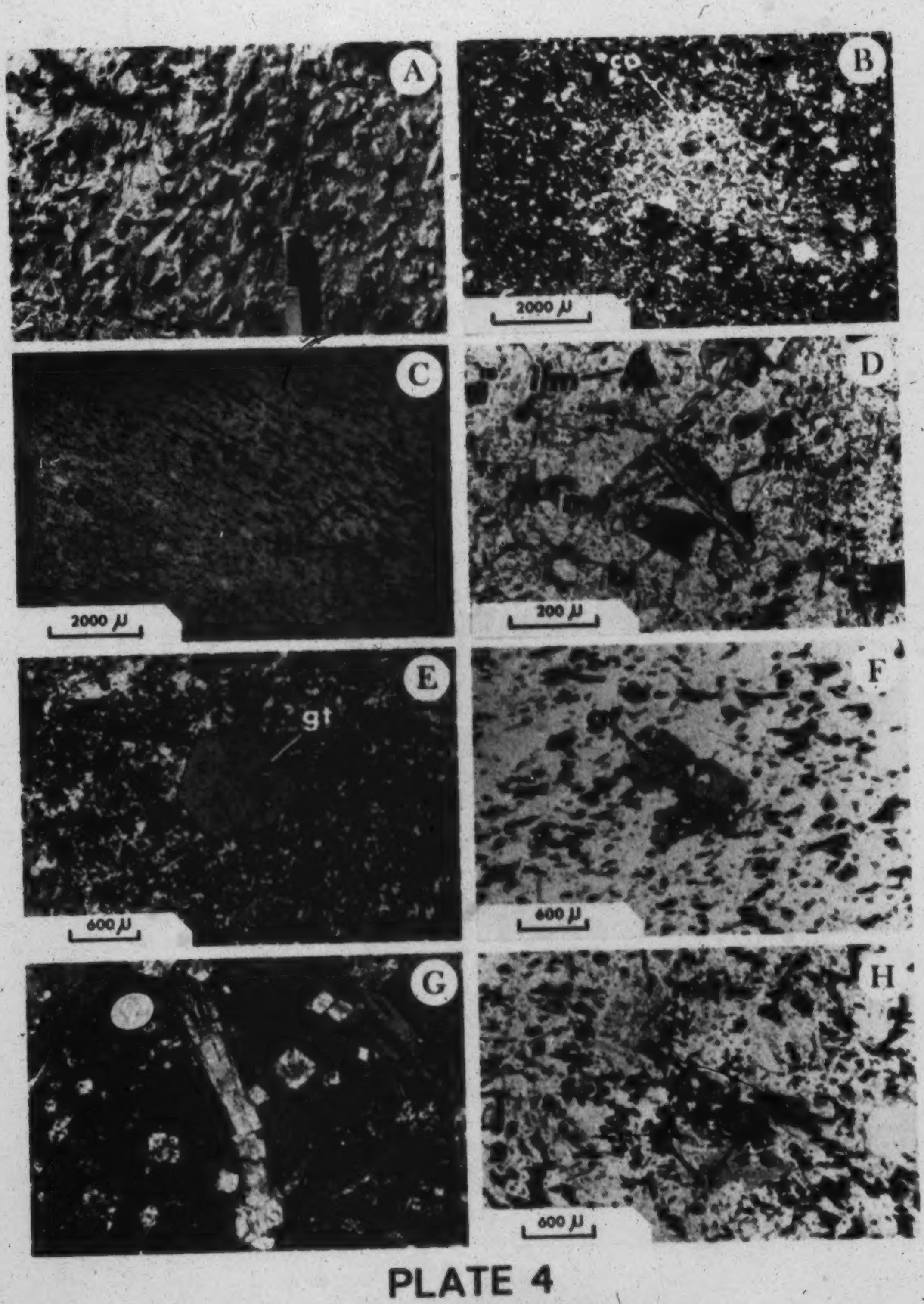
A
B
cp
2000 μ
C
2000 μ
D
hm
200 μ
E
gt
600 μ
F
600 μ
G
H
600 μ

PLATE 4

biotite contents of cordierite-bearing and cordierite-free rocks above the isograd (Fig. 31). This indicates that biotite was not produced co-genetically with cordierite.

A similar conclusion is suggested by consideration of the cordierite poikiloblasts (Plate 4B, C and D). Biotite is definitely depleted in these relative to the amount present outside them (Plate 4C). The included biotite grains are also anhedral and reduced in size compared to those outside. Marginal concentration of biotite in the vicinity of the poikiloblasts is very rare.

Although the above indicates that biotite was not produced with cordierite, there is one possible point of evidence to the contrary. In some thin-sections there is evidence that two biotite generations are present. Kretz (1968, Plate IV) and Kamineni (pers. comm. 1971) have noted the same and it might be argued that the subordinate generation was co-genetic with cordierite. There is no marked compositional distinction between the two generations (Table 14) and no evidence of an association between cordierite and either one. It is suggested below (Fig. 37a) that there was a sporadic early biotite followed by the principal biotite generation, both formed before the cordierite.

The petrographic criteria therefore indicate that no new biotite crystallised with cordierite.

The Cordierite Poikiloblasts

Cordierite forms large (ca. 0.5-2.0 cm.), diffuse poikiloblasts with numerous inclusions and ragged margins (Plate 4B)

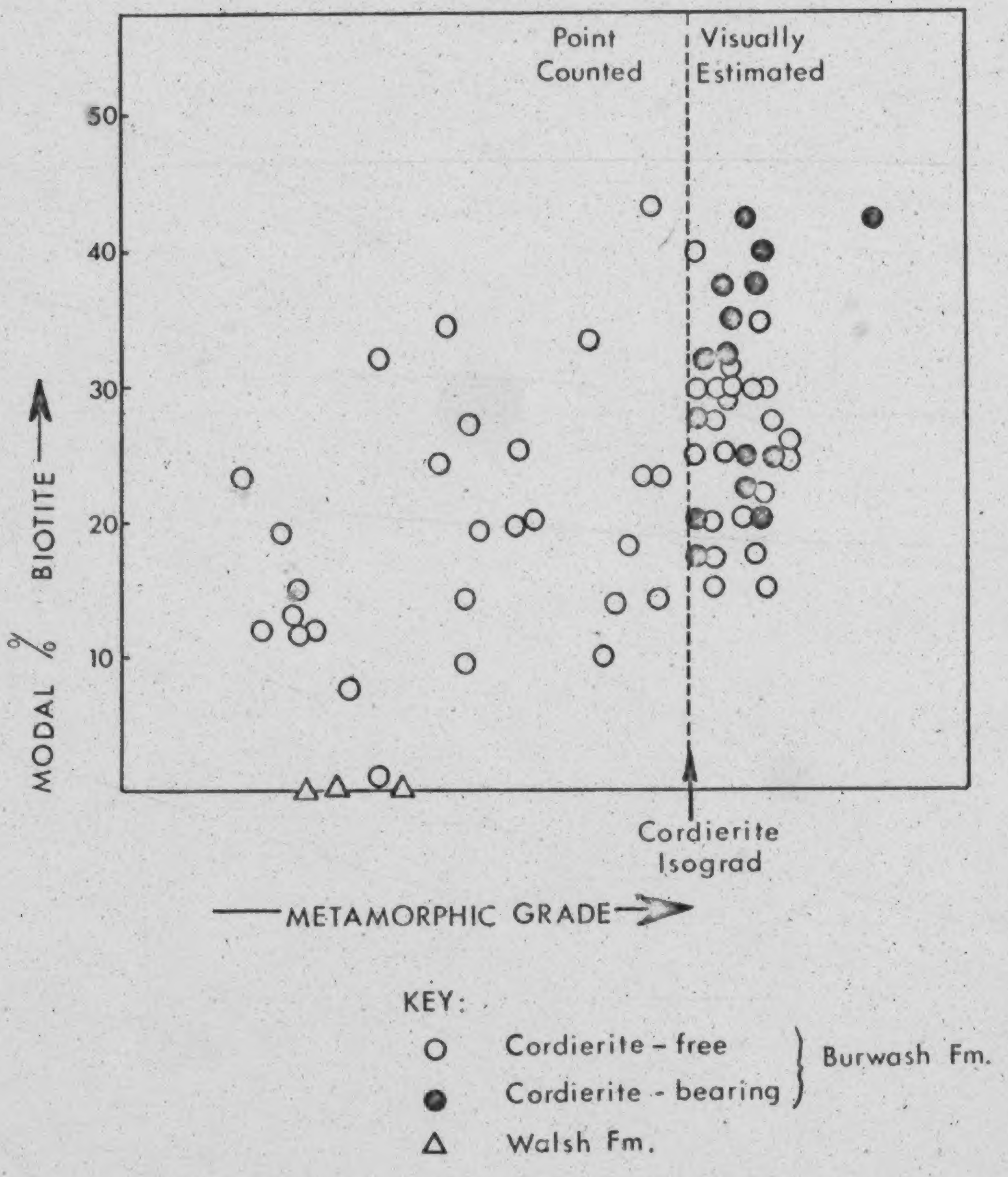

FIGURE 31 : Illustrating the modal percentage of biotite in rocks above and below the cordierite isograd.

TABLE 14 : Micro-probe analyses (weight %) and structural formulae of minerals in cordierite-free rocks and the groundmasses of cordierite-bearing rocks from the vicinity of the cordierite isograd, Prosperous Lake area.

	Biotite						Chlorite(A)		Chlorite(B)
Sample No.	P-16	G-16	P-17**		G-17	P-19	P-16	G-17	P-17
SiO_2	35.64	35.22	35.73	35.14	35.57	34.85	24.72	24.79	24.31
TiO_2	1.69	1.55	1.55	1.70	1.48	1.60	0.08	0.09	0.12
Al_2O_3	19.13	19.70	19.55	19.49	18.00	19.55	23.51	22.38	23.15
ΣFeO***	18.01	18.87	18.85	19.01	18.63	19.27	23.29	23.18	24.37
MnO	0.17	0.22	0.13	0.13	0.21	0.13	0.29	0.37	0.18
MgO	10.44	10.03	9.88	9.77	10.98	9.57	15.45	15.57	14.77
CaO	0.04	0.04	0.03	0.01	0.05	0.00	0.05	0.02	0.03
Na_2O	0.08	0.27	0.23	0.21	0.15	0.18	0.01	0.01	0.17
K_2O	9.76	9.33	9.08	9.10	9.30	8.86	0.07	0.06	0.08
Total	94.96	95.23	95.03	94.56	94.32	94.01	87.48	86.47	87.18
Si	5.404	5.339	5.407	5.359	5.442	5.348	2.583	2.624	2.568
Al^{IV}	2.596	2.661	2.593	2.641	2.558	2.652	1.417	1.376	1.432
Al^{VI}	0.822	0.858	0.895	0.863	0.687	0.884	1.478	1.416	1.450
Ti	0.193	0.177	0.176	0.195	0.170	0.185	0.006	0.007	0.010
Fe***	-	-	-	-	-	-	2.035	2.052	2.153
Fe^{3+}*	0.105	0.110	0.109	0.111	0.109	0.113	-	-	-
Fe^{2+}*	2.179	2.282	2.276	2.314	2.274	2.360	-	-	-
Mn	0.022	0.028	0.017	0.017	0.027	0.017	0.026	0.033	0.016
Mg	2.359	2.266	2.229	2.221	2.504	2.189	2.406	2.457	2.326
Ca	0.006	0.006	0.005	0.002	0.008	0.000	0.006	0.002	0.003
Na	0.024	0.079	0.067	0.062	0.044	0.054	0.002	0.002	0.035
K	1.888	1.804	1.753	1.770	1.815	1.734	0.009	0.008	0.011
ΣX-site	1.918	1.890	1.825	1.834	1.868	1.788	-	-	-
ΣY-site	5.679	5.721	5.702	5.720	5.772	5.748	5.968	5.977	6.004

*Based on the average of two determined FeO : Fe_2O_3 ratios throughout (Table 3).

**May be different biotite generations (see text).

***Total Fe as FeO or Fe^{2+}.

Structural formulae: Biotite - 22 oxygen ions
Chlorite - 14 oxygen ions

which are often pinitised. These poikiloblasts have consistent textural features relevant to their origin:

1. They include medium-grained muscovite flakes which are distinct from those of the exterior groundmasses both in appearance (Plate 4D) and composition (Table 15).
2. Many poikiloblasts also contain large chlorite flakes which are petrographically distinct from chlorites not included by cordierite (Plate 4D).
3. These included chlorite and muscovite flakes are, in some instances, interleaved, a feature never observed outside the poikiloblasts (Plate 4D).
4. Almost all the poikiloblasts contain more ilmenite than is present in the groundmass.
5. Round some cordierites there is marginal concentration of coarse chlorite or muscovite.
6. Biotite in the poikiloblasts is greatly reduced in amount relative to the rest of the rock (Plate 4C). The biotite that is included is fine-grained and anhedral. There is no indication that pre-existing biotite was pushed aside and marginally concentrated during growth of cordierite (Plate 4C).

The nature of the poikiloblasts therefore implies that biotite was consumed in the reaction (at least in small amounts where the poikiloblasts are now situated) and that minor amounts of muscovite, chlorite and ilmenite were produced with cordierite.

TABLE 15 : Micro-probe analyses (weight %) and structural formulae of cordierites, minerals included in cordierite and a pinite from the cordierite isograd, Prosperous Lake area.

	Cordierites			Pinite	Inclusions in cordierite			
					Muscovite		Chlorite	Biotite
Sample No.	G-16	P-17	P-19	G-16	P-17	P-19	P-19	P-19
SiO_2	48.78	48.92	48.34	47.97	45.43	44.93	23.65	33.45
TiO_2	0.00	0.00	0.00	0.01	0.20	0.24	0.08	1.69
Al_2O_3	32.92	32.95	33.17	30.50	36.44	36.61	23.47	20.00
ΣFeO^*	7.56	8.13	8.19	4.27	0.84	0.80	24.42	19.23
MnO	0.66	0.33	0.35	0.03	0.00	0.00	0.18	0.10
MgO	7.89	8.03	7.70	2.47	0.44	0.39	14.35	8.99
CaO	0.00	0.00	0.00	0.14	0.02	0.00	0.04	0.01
Na_2O	0.57	0.27	0.27	0.12	0.88	1.47	0.00	0.22
K_2O	0.05	0.05	0.06	7.36	8.87	9.10	0.07	9.05
Total	98.44	98.68	98.08	92.86	93.12	93.55	86.27	92.74
Si	5.018	5.019	4.994	-	6.104	6.039	2.528	5.229
Al^{IV}	0.982	0.981	1.006	-	1.896	1.961	1.472	2.771
Al^{VI}	3.009	3.004	3.032	-	3.876	3.841	1.485	0.914
Ti	0.000	0.000	0.000	-	0.020	0.024	0.006	0.199
Fe*	0.650	0.698	0.708	-	0.085	0.081	2.183	**
Mn	0.058	0.029	0.031	-	0.000	0.000	0.016	0.013
Mg	1.210	1.228	1.186	-	0.088	0.078	2.286	2.095
Ca	0.000	0.000	0.000	-	0.003	0.000	0.005	0.002
Na	0.114	0.054	0.054	-	0.229	0.383	0.000	0.067
K	0.007	0.007	0.008	-	1.520	1.560	0.010	1.805
ΣX-site	-	-	-	-	1.753	1.944	-	1.873
ΣY-site	5.046	5.018	5.018	-	4.070	4.024	5.991	5.734

*Total Fe as FeO or Fe^{2+}.

**$Fe^{3+} = 0.115$; $Fe^{2+} = 2.399$ (Calculated as in Table 14).

Ilmenites included in cordierite are given in Table 11.

TABLE 16 : Mineral assemblages of rocks from the cordierite isograd in which minerals have been analysed.

Mineral	P-16	G-16	P-17	G-17	P-19
Cordierite	O	XX	XX	O	XX
Biotite	XX	XX	XX	XX	XX
Chlorite(A)	XX	O	O	XX	O
Chlorite(B-X)	O	X	X	O	X
Muscovite	O	O	X	O	O

All assemblages include quartz and plagioclase.

XX = 5%
X = 0-5%
O = Absent or Trace

Mineral Compositions

Tables 14, 15 and 16 give mineral analyses and modal constitution for several rocks from the vicinity of the cordierite isograd (Fig. 30). Analyses of cordierite zone minerals from other areas are given by Folinsbee (1940, 1941, 1942).

Biotite. The compositions of biotites in cordierite-bearing and cordierite-free rocks may only be compared with due reference to the controls exerted by metamorphic grade and rock composition (above). This is done in Fig. 32. The biotites from cordierite-free rocks conform entirely to the established pro-grade trends in mineral composition (above). Those in cordierite-bearing rocks, however, are generally distinctly different (see also Fig. 34), notably in having higher Al^{IV}/Si, Fe/Mg, Na/K and Al^{VI} content. The biotite included in cordierite exhibits even greater deviations (in the same sense) from the trends for cordierite-free rocks.

Figure 32 therefore leads to two important conclusions:

1. The pro-grade compositional changes in biotite established in the biotite zone are further substantiated.
2. The formation of cordierite led to distinct but subtle changes in the composition of biotite. When cordierite was produced the partition equilibria shifted so that biotite effectively supplied Si, Mg and K to the reaction in exchange for Al, Fe and Na.

The two possible biotite generations described above are very similar in composition. The differences in composition between them are not consistently the same as between the biotites of

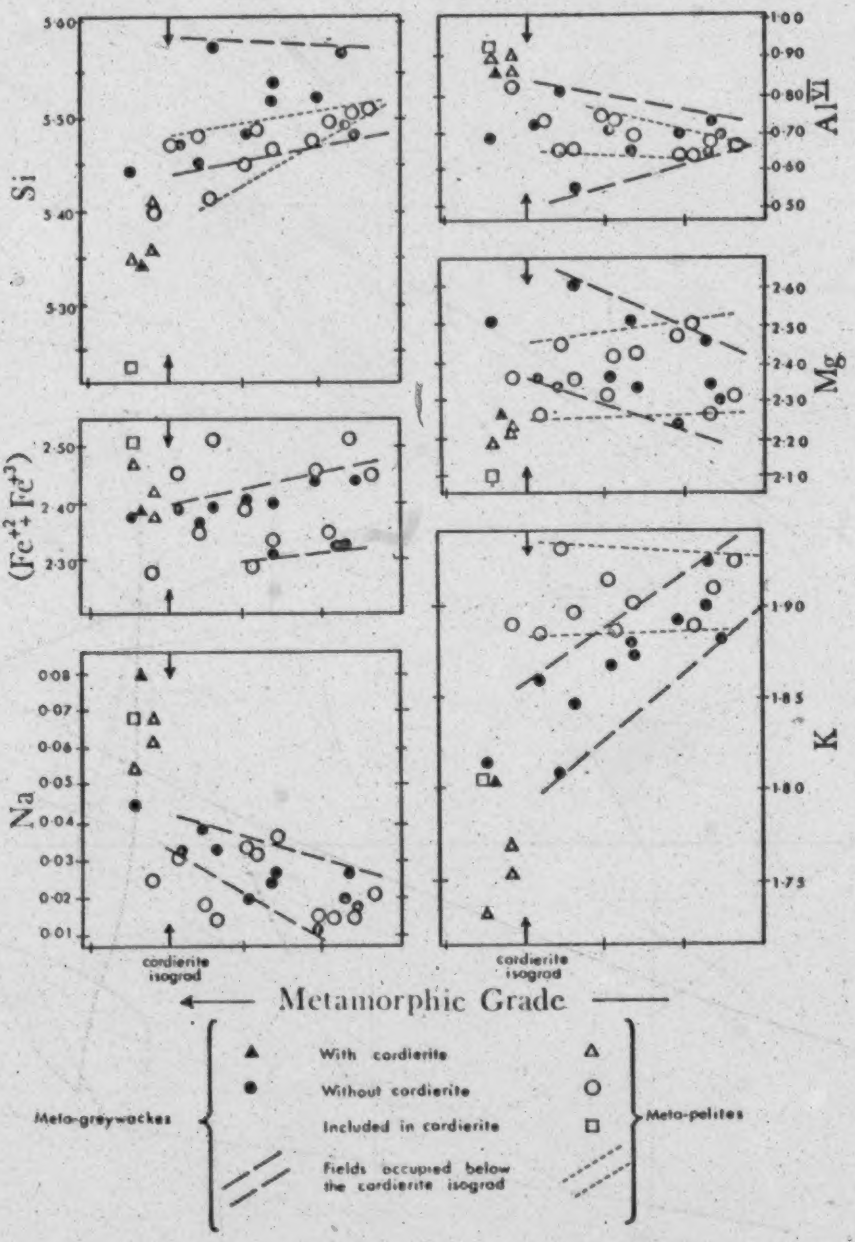

FIGURE 32 : Illustrating the compositions of biotites above the cordierite isograd in relation to the pro-grade compositional trends previously established (Fig.19). Points below the cordierite isograd are transferred from Fig. 19.

cordierite-bearing and cordierite-free rocks, a further indication that the subordinate one was not co-genetic with cordierite.

Muscovite. The muscovites included in cordierite are compositionally more ideal than those outside the poikiloblasts (compare Tables 15 and 3). They also contain markedly more Na than expected from the grade-dependent trends.

Chlorite. All the analysed chlorites (Tables 14 and 15) conform to the established compositional trends with grade. The coarse chlorite enclosed in cordierite is slightly more Al-rich and has higher Fe/Mg than the groundmass chlorite. There is no apparent difference between the chlorites of cordierite-bearing and cordierite-free rocks.

Ilmenite. The ilmenites in the cordierite poikiloblasts are very similar to those of the groundmasses (Table 11).

The Cordierite-forming Reaction

The cordierite isograd in the Prosperous Lake area (and perhaps in much of the Slave Craton) represents the complex reaction

$$\text{Chlorite} + \text{Muscovite(1)} + \text{Quartz} + \text{Biotite(1)} \longrightarrow$$
$$\text{Cordierite} + \text{Biotite(2)} + H_2O + \left[\text{Ilmenite, Chlorite, Muscovite(2)}\right]$$

Chlorite and muscovite were consumed in the reaction but a little muscovite was also produced with the cordierite. There was probably no crystallisation of new biotite but some was consumed and the remainder was modified in composition.

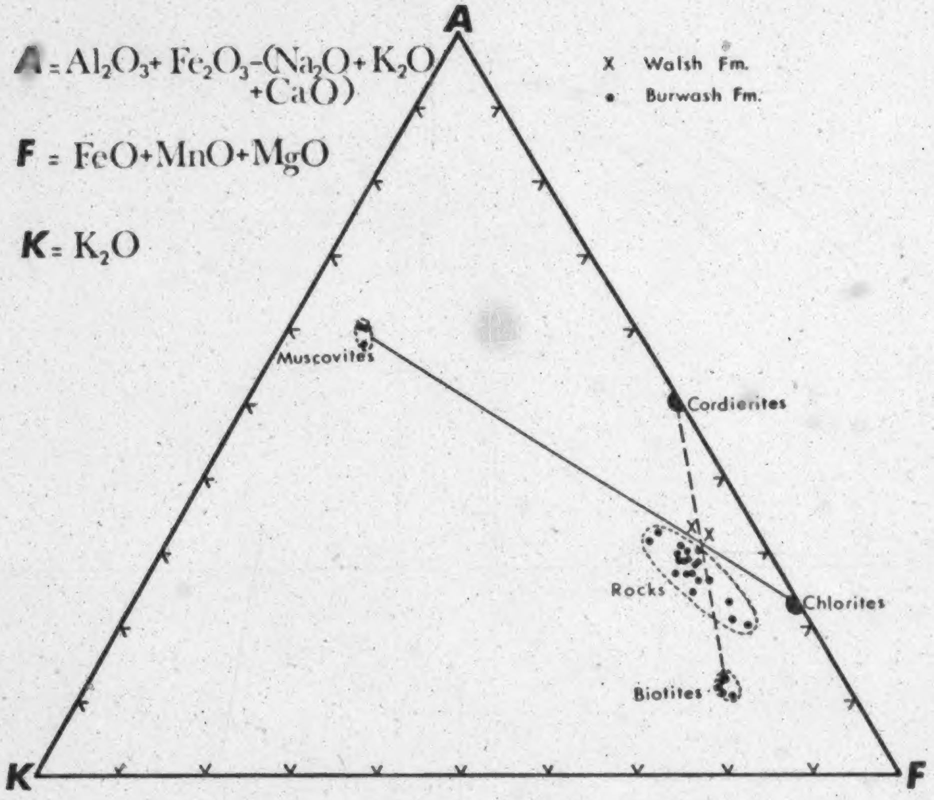

FIGURE 33 : AKF diagram depicting the compositions of minerals from the immediate vicinity of the cordierite isograd and all the available rock analyses for this area. Muscovites : P-1, P-3 and G-1; Chlorites : P-16, G-17; Cordierites and biotites from Tables 14 and 15; Rocks from Table 2, Boyle (1961) and Henderson (1972).

Controls of the Appearance of Cordierite

Mineral assemblage. Cordierite was formed only in those rocks in which chlorite and muscovite coexisted. This in turn was controlled by the biotite-forming process and its termination.

Rock compositions. The work of Seifert (1970) and Hess (1969) suggests that bulk rock composition has important controls on the appearance and production of cordierite. In the Prosperous Lake area there is no indication that cordierite was more readily formed in either meta-greywackes or meta-pelites (e.g. Table 16). This is presumably because of the similar mineralogies and bulk compositions of these two rock types (Fig. 13).

Figure 33 shows the relationships of the rocks and minerals in the AKF diagram and confirms what Seifert (1970) stated about the sequence of appearance of biotite and cordierite. All the Burwash Fm. rocks plot below the muscovite-chlorite join and developed biotite before cordierite. The two Walsh Fm. rocks plot just above that tie-line and lack biotite at grades above the biotite isograd. Presumably at higher grades they would develop cordierite before biotite.

Figure 34 shows the mineral and rock compositions in the Thompson AFM projection which was the basis of Hess's (1969) criteria for the stability field of cordierite. (1) Hess pointed out that most meta-pelites plot on the Fe side of the Al_2SiO_5-chlorite tie-line and therefore must develop garnet rather than cordierite until that tie-line is broken. The compositional field of the Prosperous Lake rocks straddles that tie-line (Fig. 34) but it is impossible, with the available data, to determine which rocks would develop cordierite and which would not. It is therefore uncertain whether or not the

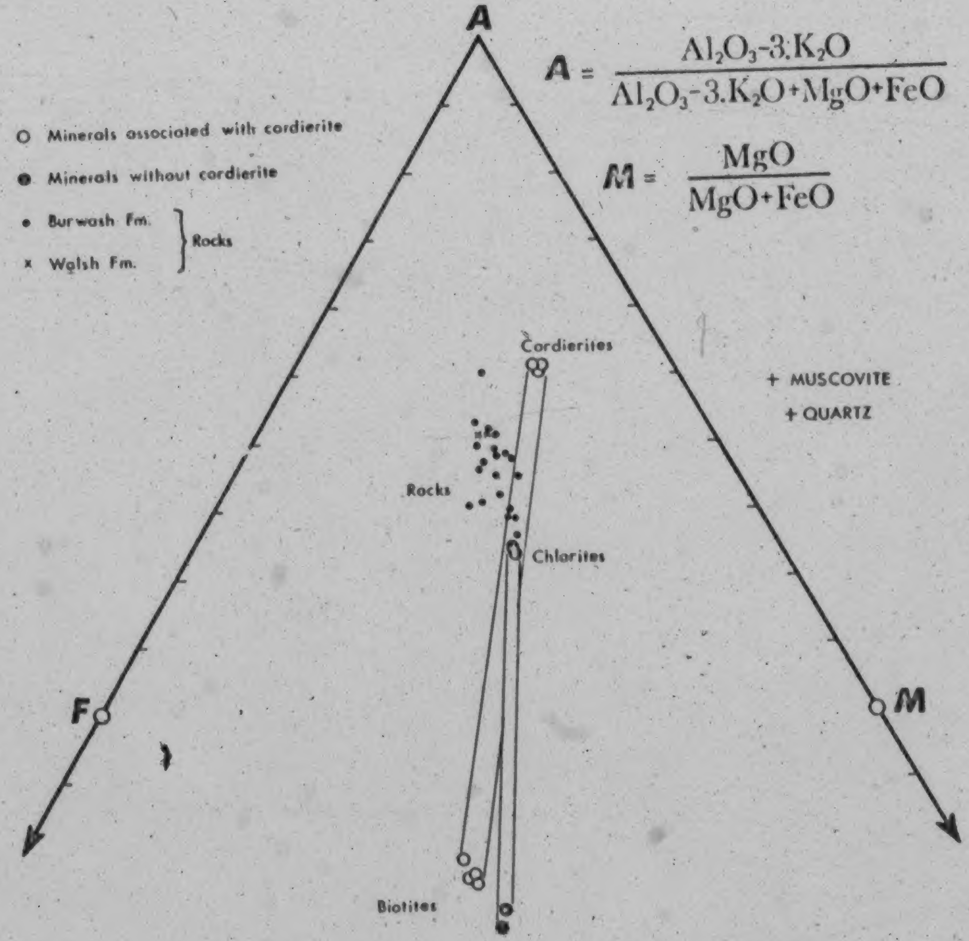
A
$A = \frac{Al_2O_3-3.K_2O}{Al_2O_3-3.K_2O+MgO+FeO}$
$M = \frac{MgO}{MgO+FeO}$
○ Minerals associated with cordierite
● Minerals without cordierite
• Burwash Fm.
× Walsh Fm.
Rocks
Cordierites
+ MUSCOVITE
+ QUARTZ
Rocks
Chlorites
F
M
Biotites

FIGURE 34 : Thompson AFM projection depicting rocks and minerals from the immediate vicinity of the cordierite isograd. Data as in Fig. 33.

Al_2SiO_5-chlorite tie-line was stable at the cordierite isograd. Since the proportion of rocks bearing cordierite is much greater than the proportion of rocks on the Mg side of the tie-line, it seems probable that the tie-line had been broken below the cordierite isograd.

(2) The present results are at variance with Hess's statement that, ". . . if the bulk compositions fall beneath the garnet-chlorite tie-line then the important reaction is

$$\text{Chlorite} + \text{Muscovite} + \text{Quartz} \longrightarrow$$
$$\text{Biotite} + \text{Cordierite} + \text{Garnet} + H_2O\text{"}$$

The Prosperous Lake rocks project well on the Al-rich side of the garnet-chlorite tie-line and yet the operative reaction was very similar to that cited by Hess.

Minor Reaction Products

The reaction deduced above lists ilmenite, chlorite and muscovite as minor products. Ilmenite is always present in the poikiloblasts but the amounts of chlorite and muscovite vary greatly. As an example, a single poikiloblast straddling a bedding plane has different character in the two beds, as shown by Fig. 35. Such evidence suggests a problem similar to that encountered with the minor products of the biotite-forming reaction, i.e. the abundance of the minor products seems to be dependent on the relative abundances of the reacting phases. It is not simply related to the amount of the principal products.

Relation to Experimental Work

The deduced reaction approximates that studied by

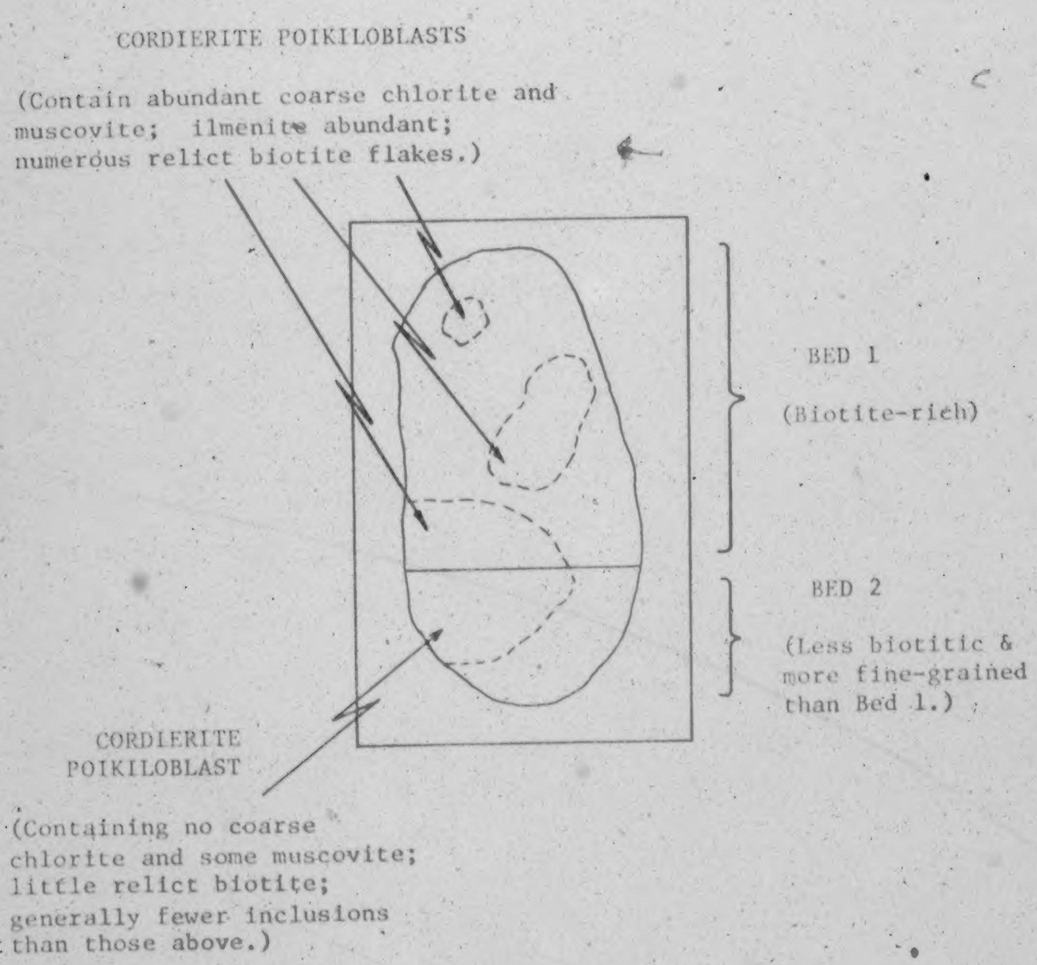
CORDIERITE POIKILOBLASTS
(Contain abundant coarse chlorite and muscovite; ilmenite abundant; numerous relict biotite flakes.)
BED 1
(Biotite-rich)
BED 2
(Less biotitic & more fine-grained than Bed 1.)
CORDIERITE POIKILOBLAST
(Containing no coarse chlorite and some muscovite; little relict biotite; generally fewer inclusions than those above.)

FIGURE 35 : Sketch of a thin-section of a Burwash Fm. rock illustrating the different nature of cordierite poikiloblasts in adjacent beds.

several workers (see above) and experimentally determined by Seifert (1970) and Bird and Fawcett (1971). There is close agreement between these two studies but Seifert's is the more comprehensive and is the definitive work at present. It was made on an Fe-free system with bulk composition deliberately selected to yield cordierite and biotite simultaneously. At 3.0 kb. (the average pressure estimated for the Prosperous Lake facies series) the equilibrium temperature for the reaction is 560° C. Prior to these studies Winkler (1967) reported preliminary results for the same reaction in an Fe-bearing system. As would be expected, the equilibrium temperature is rather lower (530° C.) but Winkler noted that varying the Mg/Fe ratio of the system made little difference to the equilibrium conditions. Detailed studies of more natural systems which followed this (Hirschberg and Winkler, 1968) found aluminium silicate in the reaction products with equilibrium temperature of about 540° C. @ 3.0 kb. Again the similarity of Fe-rich and Mg-rich systems was noted.

The reaction at Prosperous Lake differs from the system studied by Hirschberg and Winkler in that biotite and feldspar were present in the reacting assemblage and ilmenite, muscovite and occasionally chlorite were produced. It differs from that studied by Seifert in that Fe, Mn, Ti, etc. were additional components. As a result, ilmenite was present in the products. It also differs in that biotite was present in the reactant assemblage; a factor which led to the following modifications: (1) Some biotite was consumed during cordierite growth. (2) No new biotite was formed but the existing biotite was compositionally modified. Further, the experimental studies operated with P(water)=P(total), a condition unlikely to have applied to these rocks. Considering these differences between the real and haplopelitic systems, it is impossible to assign accurately a reaction temperature to the cordierite isograd. If the Mg/Fe ratio has little control on the equilibrium temperature (Winkler, 1965, 1967; Hirschberg and Winkler, 1968) then the temperature would be close to the 560° C. (at 3.0 kb) given by Seifert's (1970) curve. The present study and that of Hirschberg and Winkler suggest that an aluminous phase is produced by this reaction in more natural systems. If the aluminium silicate found by Hirschberg and Winkler is taken as equivalent to the coarse muscovite at Prosperous Lake in this respect, then perhaps the 550° C. of their curve is applicable to the reaction at Prosperous Lake. There is, however, no way of estimating the effects of the reactant biotite or the product ilmenite on the equilibrium temperature. The best estimate is, therefore, that the cordierite isograd represents temperatures of 550±20° C. @ ca. 3kb. This is a rather higher temperature than the 530±10° C. given by Davidson (1967) on the basis of Winkler's (1965) data.

THE CORDIERITE ZONE

The cordierite zone comprises the area between the cordierite isograd and the first appearance of garnet. As shown in Fig. 36, the cordierite isograd and the 'garnet line' (see below) are not parallel so the cordierite zone is of irregular shape in this area. Its further extensions are shown in Fig. 15.

The important facet of this zone is the isograd itself (discussed above) and there is little change in the rocks between the cordierite isograd and the garnet line. No detailed petrological work has been attempted and the following merely reports on a preliminary

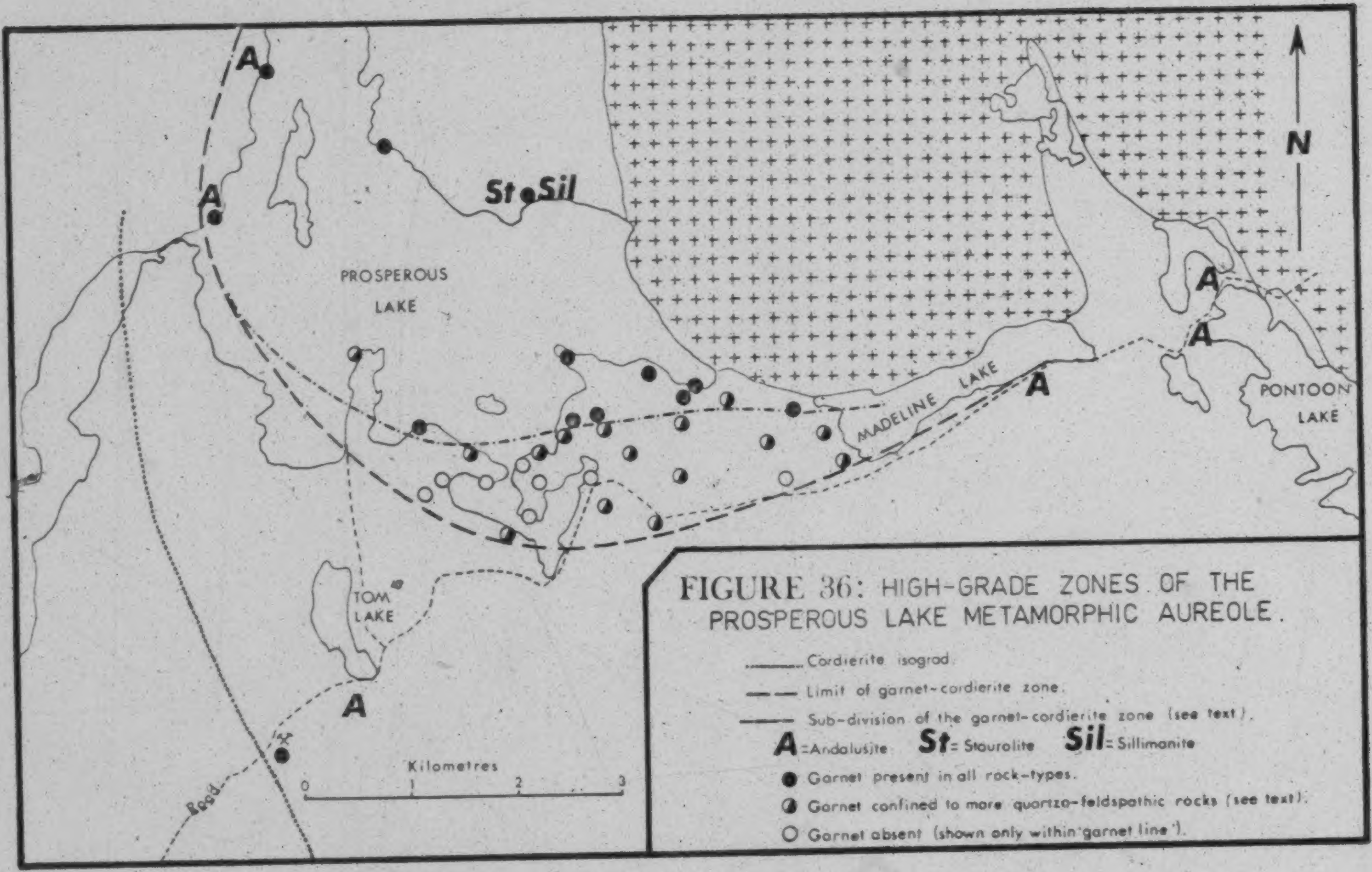
A
A
St Sil
PROSPEROUS LAKE
N
A
A
MADELINE LAKE
A
PONTOON LAKE
TOM LAKE
A
Road
Kilometres
0
1
2
3
Cordierite isograd.
Limit of garnet-cordierite zone.
Sub-division of the garnet-cordierite zone (see text).
A = Andalusite
St = Staurolite
Sil = Sillimanite
● Garnet present in all rock-types.
◑ Garnet confined to more quartzo-feldspathic rocks (see text).
○ Garnet absent (shown only within 'garnet line').

FIGURE 36: HIGH-GRADE ZONES OF THE PROSPEROUS LAKE METAMORPHIC AUREOLE.

petrographic study of some eighty thin-sections from the cordierite zone.

No comprehensive study of equivalent rocks in the Slave Craton has been published but pertinent data have been reported by Folinsbee (1940, 1941, 1942), Henderson (1943), Tremblay (1952), Ross (1966), Davidson (1967), Kretz (1968 and in press), Heywood and Davidson (1969) and Kamineni and Wong (1973). Detailed studies are currently being made on equivalent rocks from the Sparrow Lake area by R. Kretz and D. C. Kamineni (University of Ottawa) but their data are not presently available.

Rocks of the Cordierite Zone

The rocks in this zone are massive to semi-schistose and consist of quartz, plagioclase and biotite with chlorite, muscovite and(or) cordierite. Andalusite occurs sporadically. Rutile is the principal oxide. Hematite is sometimes present but it is uncertain whether it is of primary or secondary origin.

Texturally the rocks are medium-grained semi-schists. The original mudstones have a fine-grained granoblastic matrix of quartz and plagioclase which contains biotite in variably developed lepidoblastic foliation. The original greywackes retain some blasto-psammitic texture but have coarser, more uniform matrix material than at lower grades. They tend to be more massive and display less preferred orientation than the meta-pelites. Meta-pelites and meta-greywackes are not as readily distinguishable as at lower grades but may be recognised in thin-section.

Thin calc-silicate or quartzitic beds and boudins are still recognisable at these grades. They are characterised by calcic and non-calcic amphiboles.

Mineralogy

Cordierite occurs in large porphyroblasts (usually ca. 2-4 cm.; see Plate 4A) in many rocks. There is no noticeable change in these porphyroblasts through the cordierite zone and the description given above applies throughout.

Andalusite appears sporadically in the cordierite and cordierite-garnet zones (Fig. 36), usually as spectacular, euhedral meta-crysts several centimetres in length (Plate 4G). The distribution and origin of these is discussed below.

Biotite occurs in all the meta-sedimentary rocks in the cordierite zone. The problem of the two possible generations (above) persists throughout the zone and no conclusive evidence on this point has been observed.

Muscovite is present in some of the rocks as small flakes in the matrix, commonly with lepidoblastic orientation. This muscovite is texturally similar to that of lower grades and apparently is inherited from those grades (see discussion of the cordierite isograd). There is, in addition, a rare type of muscovite which cross-cuts biotite and therefore is paragenetically later than it (see Plate V of Kretz, 1968).

Chlorite. Both chlorites(A) and (B-X) are present. Chlorite(B) may also occur in a few rocks but it is difficult to distinguish at these grades from coarse chlorite(A) or abundant chlorite(B-X).

Oxides. Rutile is the predominant oxide, presumably as a result of the reaction relationships described above. Some hematite is present but it is impossible to judge whether it is of primary or secondary origin.

The Mineral Assemblages

Table 17 lists the observed assemblages and shows their relation to metamorphic grade.

As noted above the biotite flakes are cut by chlorite (B-X) and muscovite(X) which post-date the formation of biotite and probably cordierite. Thus Table 17 shows that chlorite(B-X) commonly coexists in apparent stability with muscovite although chlorite (A) does so only very rarely because of the mutual incompatibility demonstrated at the cordierite isograd.

Table 17 also suggests that muscovite is a stable member of the assemblage to the highest grades within the cordierite zone. Chlorite(A), however, has not been observed in the upper cordierite zone. The compositionally similar chlorite(B-X) persists further from the cordierite isograd, perhaps as a result of formation during the decline of metamorphic conditions.

There are several noteworthy differences between the mineral assemblages of cordierite-bearing and cordierite-free rocks (Tables 13 and 17): (1) Chlorite(A) is more abundant in cordierite-free rocks. This simply reflects the considerable proportion of rocks below the cordierite isograd which contain chlorite without muscovite and therefore could not produce cordierite. (2) Muscovite is more abundant in cordierite-bearing rocks. This is a result of two factors. Firstly, muscovite was produced together with cordierite. Where

TABLE 17 : Observed mineral assemblages and their relation to metamorphic grade in the cordierite zone of the Prosperous Lake aureole.

METAMORPHIC GRADE →

Rocks without Cordierite			
Chl. A	Musc.	Chl. B-X	Musc. X
○	●●	○	○
○	○	○	○ *
○	○	○	●
○	○	○	●
○	○	○	○**
○	○	●	○
○	○	○	○**
●	○	●	○
●	○	○	○
○	○	○	○**
●	○	Tr	○
○	○	●	○
●	○	○	○
○	●●	●●	○
○	○	●	○
●	○	●	○
●	○	●	○
●●	○	○	○
●●	○	○	○
Tr	●●	●	○
○	○	Tr	○
○	●	●●	○
●●	●●	Tr	○
●●	○	Tr	○
Tr	Tr	●	○
○	Tr	●	○
○	●●	●	○

Rocks with Cordierite			
Chl. A	Musc.	Chl. B-X	Musc. X
○	●●	○	●
○	●●	○	○
○	●●	○	○
○	●	●	○
○	●●	○	○
○	○	●	○
○	○	●	○
○	●●	Tr	○
○	●●	Tr	○
○	○	Tr	○
○	○	●	○
○	Tr	●	Tr
○	○	●	○
Tr	○	●	○
●	○	●	○
○	Tr	●	○
○	●●	●	○
○	●	●	○
Tr	●	●	○
○	○	●	○
○	●●	●	○
○	●●	●	○
○	●●	●	○
●	●●	●	○
○	●●	●	○
●●	○	●	●
○	●●	●	○

(1) All assemblages include quartz and plagioclase.
(2) ○ = not present; Tr = <1%; ● = 1-5%; ●● = >5% modal.
(3) Chlorites (A) and (B-X) are explained in the text. Muscovite(X) cross-cuts biotite. It and chlorite(B-X) probably post-date the growth of cordierite.
(4) The metamorphic grade index is the perpendicular distance from the cordierite isograd.
(5) All cordierite zone samples are listed except for calc-silicate rocks and those showing evidence of pervasive hydrothermal retrogression.

* Contains andalusite. ** Contains cummingtonite.

recognisable, this new muscovite has been closely associated with cordierite, but it might also have crystallised in the matrix. Secondly, some of the rocks contain muscovite left in excess after complete consumption of chlorite in the cordierite-forming reaction. (3) Chlorite (B-X) is more commonly present in cordierite-bearing rocks. Since the origin of this chlorite is not understood, it is impossible to say why this is so. Its origin is clearly not solely due to the formation of cordierite but perhaps some of the chlorite formed with cordierite crystallised in the groundmass, adding to the amounts of coarse chlorite.

The Origin of Andalusite

The andalusite in the cordierite and cordierite-garnet zones is similar and there is nothing to suggest that its origin in the latter is related to the presence of garnet. It is therefore considered here as a sporadic member of the cordierite zone assemblage.

The distribution and origin of andalusite in a similar aureole has been discussed in some detail by Davidson (1967) (see also Heywood and Davidson, 1969, and Folinsbee, 1942). Davidson recognised four modes of occurrence for the andalusite at Benjamin Lake:

1. Large pink crystals associated with vein quartz, sometimes below the cordierite isograd.
2. Thin rims at the edges of cordierite porphyroblasts.
3. Porphyroblasts in cordierite schists.
4. Chiastolite in graphitic biotite schists.

In the Prosperous Lake rocks, type 3 has been observed but not type 2.

Type 1 has also been observed but cannot be distinguished from type 4.

Davidson also demonstrated the existence of an "andalusite line" which was "approximately parallel to and 5 miles east of" the cordierite isograd (Heywood and Davidson, 1969). Below this line andalusite is rare, occurring mainly as chiastolite in graphitic slates; above it, andalusite is increasingly common.

Type 1 or 4. The occurrence just East of the Ptarmigan Mine (Fig. 36) belongs to either type 1 or 4. Deep pink euhedral andalusites occur in black slates near a quartz vein. They clearly transect a schistosity which is axial planar to a typical Hay Lake domain fold. Therefore, andalusite formation post-dated the main phase of deformation and cordierite growth.

On the West shore of Prosperous Lake andalusite is common in biotitic rocks containing garnet and(or) cordierite. It is most spectacularly developed near quartz veins (Plate 4G) and the rocks are very dark-coloured so this occurrence is tentatively equated with Davidson's types 1 or 4.

In these rocks the andalusite is usually present as poikiloblasts with numerous inclusions. These contain more opaque mineral and much less biotite than the matrix. There is no sign of marginal biotite concentration. Muscovite is associated only in trace amounts, if at all. Where garnet or cordierite is present there is no suggestion of genetic relationship between andalusite and these phases. The reaction producing andalusite is therefore of the form

$$\text{Biotite} + \ldots \longrightarrow \text{Andalusite} + \text{Oxide} + \ldots$$

The significance of the association with quartz veins in uncertain.

Perhaps they simply provided a more hydrous medium in which andalusite growth could occur very readily.

Type 3. Andalusite is common in the porphyroblastic schists near Madeline and Pontoon Lakes. This type belongs to Davidson's type 3 in that it occurs in otherwise normal pelitic and semi-pelitic schists. The andalusite is not, however, restricted to cordierite-bearing rocks.

In such rocks the andalusite forms ragged poikiloblasts whose appearance in hand specimen is very similar to the cordierite porphyroblasts. They are usually associated with coarse muscovite flakes and in some cases include opaque minerals. Biotite inside the poikiloblasts is reduced in grain-size and abundance relative to the rest of the rock and there is no sign of marginal biotite concentration. These textures suggest that a reaction of the form

$$\text{Biotite} + \ldots \longrightarrow \text{Andalusite} + \text{Muscovite} + \ldots$$

occurred to form the andalusite. This reaction is very different from that suggested by Davidson (1967) which involved reaction of cordierite and muscovite to andalusite and biotite with increasing pressure. In the suggested reaction considerable Fe is not accounted for in the products. Small amounts of opaque oxide are included in the andalusite poikiloblasts and may account for some of the Fe liberated. There is no textural evidence of another mafic phase being produced and there is therefore an unresolved problem with the disposal of Fe and Mg in the product assemblage.

Conclusion

Cordierite was formed (as described above) at the cordierite isograd but thereafter changed very little within the cordierite zone. Andalusite occurs in two distinct modes as described by Davidson (1967) being derived in both cases by reactions of biotite. At grades near the cordierite isograd it occurs as sporadic porphyroblasts which are particularly well developed near quartz veins. These andalusites demonstrably post-date the main metamorphic maximum. Closer to the granite it is more common and occurs in more typical rocks, apparently as a normal member of the pro-grade paragenetic sequence. Sample distribution is inadequate to test whether Davidson's (1967) 'andalusite line' applies to the Prosperous Lake area but the observed distribution is compatible with his observations even to the approximate separation of the cordierite isograd and the andalusite line.

THE CORDIERITE-GARNET 'ZONE'

It has been known for a long time that garnet occurs in the inner metamorphic zones of the Prosperous Lake pluton (Folinsbee, 1942; Jolliffe, 1942 and 1946). Its occurrence is characteristic of comparable aureoles in the craton (e.g. Kretz, 1968) but it is not always present (e.g. Heywood and Davidson, 1969). Its presence with cordierite in these thermal aureoles presents a problem in terms of the conditions permitting such parageneses (Chinner, 1959 and 1962, and many other authors).

In the Slave Craton the evolution of the mineral assemblages in this zone has never been elucidated. Folinsbee (1942) believed garnet to be present as a result of regional changes in the composition of the meta-sediments, those near Prosperous Lake being more suited to garnet formation than those near Duck Lake. Since Folinsbee's study, however, the meta-sediments have been shown to be turbidites (Ross, 1962; Henderson, 1972) so that compositional variations are unlikely on such a scale. A detailed study of garnet zoning and grain-size distribution at Sparrow Lake has been made by Kretz (in press, 1973) in order to elucidate the kinetics of garnet growth. He suggested various garnet-forming reactions and based the kinetic study on direct derivation of garnet from chlorite and quartz. He concluded that the reaction rate was highly acceleratory and that this could have resulted from a steady increase in temperature. D. C. Kamineni is currently making detailed studies of similar high-grade rocks from Sparrow Lake but only part of his data have so far been published (Kamineni and Wong, 1973).

In this context, 'zone' has only geographic meaning. Since the garnet and cordierite are paragenetically distinct (below) the status of this 'zone' in the pro-grade succession is uncertain. Similarly, the garnet-forming reaction is unknown and the term 'garnet isograd' is avoided.

In the present study no detailed examination of the cordierite-garnet zone rocks has been made. This section merely reports the results of field observations in the immediate vicinity of Prosperous Lake and the petrographic inspection of about fifty thin-sections from that area. It serves to define, rather than solve, the problem.

The Areal Distribution of Garnet

Figure 36 shows the observed distribution of garnet and the limits of the zone which are very similar to those mapped by Jolliffe (1946). The zone is asymmetrically located with respect to both the cordierite isograd and the pluton contact. It may be divided into two gradational sub-zones (Fig. 36). In the lower-grade sub-zone garnet is present only in some rock types. These cannot be completely defined at present but generally garnet is present at lower grades in the more quartzo-feldspathic, biotite-poor meta-sediments. In the upper sub-zone garnet is present in all rock types, including the biotite-rich ones, though not in all rocks. The implication is that garnet was stable further from the pluton contact in rocks with higher Al : (Mg+Fe) ratio.

Of all the samples collected, only one does not conform to this distribution pattern. At the Ptarmigan Mine, near the cordierite isograd and far from the garnet zone (Fig. 36), an apparently normal meta-greywacke contains garnet whose appearance suggests that it has undergone corrosion. The significance of this occurrence is discussed below.

Mineralogy and Textural Relations

Garnet: The garnets are euhedral to subhedral porphyroblasts up to about 2 mm. in diameter (Plate 4E) containing a few small inclusions of quartz and(or) feldspar. They display no particular mineralogical association and are randomly distributed in the rocks. They have been observed included in both cordierite and andalusite, but these instances are no more common than dictated by chance and the included garnet shows no sign of corrosion. Where the relations of the garnets to biotite foliation may be observed, the former cut cleanly across the latter with no sign of rotation or bending of the foliation. This arrangement implies considerable textural equilibration.

There is considerable, though not unequivocal, evidence for corrosion of the garnets. They range in appearance from euhedral grains with sharp margins and few inclusions (Plate 4E), through the most common type which have subhedral, slightly embayed outlines and a moderate number of inclusions, to very embayed or even skeletal crystals with relict euhedral outline (Plate 4F). The interpretation of these textures as evidence of corrosion is subjective and open to dispute as they might also be interpreted as growth textures, the embayments simply being marginal inclusions which could not be consumed or pushed aside. In fact, Kretz (in press, 1973, and pers. comm.) reports the Sparrow Lake garnets to be euhedral and uncorroded, although Kamineni (pers. comm. to Kretz) believes some from the same area to be corroded. The highly embayed garnets at Prosperous Lake are believed to be corroded for the following reasons: (1) Some garnets in similar rocks are euhedral showing that coarse quartz or feldspar did not lead to embayed outlines. (2) Many embayed garnets have relict euhedral shape. (3) The embayments are always occupied by quartz or feldspar. (4) The minerals in the embayments commonly seem a little coarser, and perhaps more abundant, than elsewhere in the rock. (5) The occurrence of embayed garnet in a normal meta-greywacke outside the cordierite-garnet zone suggests that garnet had, at one time, a much wider distribution.

It is therefore suggested that the garnets have suffered variable degrees of corrosion in different rocks. The rocks in which corrosion is considered to have definitely occurred are all meta-greywackes but probable corrosion has also been observed in many meta-pelites. Thus no control of the degree of corrosion has been recognised and the textures indicate no reaction products other than quartz or feldspar.

Cordierite. Cordierite occurs in the same abundance, distribution and style as described for the cordierite zone.

Andalusite. The occurrence and origin of this mineral has also been discussed above.

Cummingtonite and gedrite. Non-calciferous amphiboles are commonly present in the highest-grade portions of this zone. Cummingtonite is a characteristic mineral of the metamorphism in this craton, both in meta-sedimentary and meta-volcanic rocks (e.g. Kretz, 1968; Heywood and Davidson, 1969). It is first formed, in the pro-grade sequence, in the calc-silicate lenses and boudins, but at higher grades is also present in non-calcic, biotitic rocks. Gedrite is more rarely observed and is apparently confined to the immediate vicinity of the contact. Gedrite from equivalent rocks has been studied in detail by Kamineni and Wong (1973).

Biotite is present in all the meta-sedimentary rocks and is apparently stable throughout the zone. It is variably foliated and there is commonly subjective evidence of the two biotite generations discussed above. Muscovite occurs in abundance in a few rocks and in some instances is present in trace amounts cross-cutting biotite grains. Chlorite(A) is abundant in a few rocks, but chlorite(B-X) is ubiquitous.

The Mineral Assemblages

As shown in Table 18, the minerals occur in most possible combinations. The components may be taken to be SiO_2 -- $(Fe, Al)_2O_3$ -- $(Fe, Mn)O$ -- MgO -- Na_2O -- K_2O -- TiO_2 -- H_2O (totalling 8). In some rocks there were nine phases -- quartz, biotite, garnet, cordierite, andalusite, chlorite, Ti-oxide, plagioclase and fluid. If the intensive variables are taken to be T, P and P_{H_2O} the phase rule is $F = C - P + 3$ and the system is divariant. (Since there is evidence that P_{O_2} is important in controlling garnet stability, this pre-supposes that P_{O_2} was not independently variable.) In rocks with less than this maximum number of phases, the variance is greater. In general, therefore, these complex assemblages are compatible with the phase rule and may be in equilibrium even though texturally unequilibrated.

Several other points may be noted from Table 18:

1. Muscovite occurs in garnet-free rocks but only rarely, and then in trace amounts, does it coexist with garnet.
2. Chlorite(A) occurs with garnet but is absent from garnet-free rocks.
3. Chlorite(B-X), andalusite and cummingtonite occur in garnetiferous and garnet-free rocks.

While the complexity of the paragenesis prevents any detailed interpretation of these observations, they are at least compatible with the generation of garnet from chlorite (A), muscovite and quartz as

TABLE 18 : Observed mineral assemblages in rocks from the cordierite-garnet zone of the Prosperous Lake aureole. All assemblages include quartz, plagioclase, biotite and usually rutile.

Garnet	Cordierite	Andalusite	Muscovite	Chlorite	
				(A)	(B-X)
●	●	●	○	○	●
●	●	●	○	○	○
●	●	○	○	●	○
●	●	○	Tr	○	●
●	●	○	○	○	●
●	?	○	○	○	●
●	○	●	Tr	●	○
●	○	●	○	●	○
●	○	○	○	○	●
●	○	○	○	○	○ *
●	○	○	○	○	Tr *
○	●	●	○	○	●
○	●	○	●	○	○
○	●	○	○	○	●
○	●	○	Tr X	○	●
○	●	○	●	○	Tr
○	○	●	Tr X	○	●
○	○	●	●	○	○
○	○	○	●	○	○
○	○	○	○	○	●
○	○	○	○	○	○ *

●	Mineral present
Tr	< 1 % modal
○	Mineral absent
X	Muscovite(X)
?	Retrogressed porphyroblast
*	Cummingtonite or Gedrite

suggested by Hirschberg and Winkler (1968). By this hypothesis garnet did not form in rocks lacking chlorite(A), with the result that muscovite is still present. In the garnet-bearing rocks the reaction was terminated by complete consumption of muscovite, leaving excesses of chlorite(A).

Evolution of the Cordierite-Garnet Zone

The following are the crucial factors in interpreting the paragenesis of this zone:

1. The distribution of garnet bears no simple relationship to either the cordierite isograd or the pluton margin. The zone is, however, directly adjacent to the pluton.
2. Garnet is present in less biotitic rocks further from the contact.
3. Corroded garnet has been found in a normal metagreywacke near the Ptarmigan Mine.
4. The garnet underwent thorough equilibration followed by variable degrees of corrosion. No obvious products are associated with the corroded garnets.
5. Garnet is included in both andalusite and cordierite but the garnet decomposition did not yield the cordierite.
6. The textures suggest a complex paragenesis in which cordierite post-dated garnet.
7. The available data are compatible with the formation

of garnet from chlorite, muscovite and quartz at moderate pressures.

8. Without detailed whole-rock data it is impossible to define exactly the compositional fields in which garnet, garnet + cordierite and cordierite are present. In view of the limited compositional range of the rocks (Fig. 13) it is probable that bulk composition was not the principal control of garnet-cordierite relationships.

Thus an early mineral assemblage including garnet, biotite, chlorite (A) and(or) muscovite was texturally equilibrated before changing conditions added cordierite and andalusite in a renewed series of reactions. The problem of the corroded garnet is not the common one in which an early garnet decomposes in a thermal aureole to give cordierite (Chinner, 1959 and 1962). At Prosperous Lake the origin of cordierite was unrelated to garnet, garnet is present in the innermost parts of the aureole and, if removal of garnet by corrosion actually did occur, it did so from the outside inwards.

The controls of cordierite-garnet parageneses are extremely complex (Eskola, 1914; Chinner, 1959 and 1962; Hsu, 1968; Muller and Schneider, 1971) involving all of the variables P, T, bulk composition and oxygen partial pressure. Without compositional information, one can only speculate on what controls operated at Prosperous Lake. To this author, however, it seems significant that a late chlorite(B-X), which is paragenetically unaccounted for, should exist in rocks which may previously have contained a garnet whose removal left no apparent products. The following model therefore bears closer examination.

The initial phases of metamorphism produced a zone, extending from about the present cordierite isograd to the present pluton, in which sporadic garnet became increasingly abundant North-Eastwards. Later, with intrusion of the Prosperous Lake pluton or during the cooling which followed it, the garnet became unstable in the outermost parts of the aureole and was hydrated to chlorite(B-X). Hsu (1968) showed that the critical factors controlling this reaction are oxygen fugacity and temperature and it seems possible that these should vary across the aureole in such a fashion that chlorite was stable in the outer parts and garnet in the inner parts. The exact conditions of garnet decomposition were apparently modified by bulk composition. Such a model might also account for the asymmetrical garnet distribution if oxygen fugacity was controlled by water migration into or out of the pluton and this was not the same in all directions. The principal objection to this model is that coarse chlorite is also present within the cordierite-garnet zone.

THE SILLIMANITE-STAUROLITE 'ZONE'

(The word 'zone' in this context implies only that staurolite and sillimanite are found in the same area, not that they were paragenetically equivalent.)

Staurolite and incipient sillimanite have been observed at only two locations, both close to the pluton margin. One of these locations is shown in Fig. 36, the other is at the mouth of the Cameron River (sample collected by Dr. R. St. J. Lambert). In additton staurolite is recorded in several localities North-East of River Lake by Jolliffe (1946).

The Assemblages

At the first of these localities (Fig. 36) corroded relics of staurolite surrounded by coarse muscovite (Plate 4H) occur in a rock with biotite, quartz, feldspar and minor chlorite and muscovite. Another rock from the same locality is an ordinary biotite semi-schist except that the incipient breakdown of biotite to sillimanite and oxides is readily apparent.

At the mouth of the Cameron River the remarkable assemblage quartz-plagioclase-biotite-andalusite-staurolite-sillimanite-chlorite(B-X)-muscovite-rutile-opaque oxide-possible (retrogressed) cordierite has been observed. This is patently a disequilibrium assemblage in which relict staurolite is wholly included in andalusite and sillimanite is commonly associated with andalusite and with oxide phases.

Paragenesis

There is little doubt that the staurolite in this zone is the relic of large porphyroblasts whose stability limits were exceeded. An earlier staurolite-bearing assemblage had a later phase of cordierite and sillimanite formation superimposed upon it. This zone therefore constitutes the marginal sillimanite zone of the pluton with staurolite relics.

METAMORPHIC HISTORY

A notable feature of this rock suite is the paragenetic history recorded in the textures of rocks from all zones. Most rocks show evidence of two, and sometimes three, phases of mineral formation. The suggested evolution of these parageneses is schematically represented by Figs. 37a, b and c which are successively more interpretive and hypothetical.

Figure 37a is a conventional paragenesis diagram in which the earlier assemblages in each zone have been called Phase I and the later ones Phase II. Phase IIb is added on a tentative basis to account for the late chlorite(B-X), the late andalusite and (perhaps) the corrosion of garnet. No time connotation is implied between zones in this figure. It simply records that, within each zone, the Phase II assemblages post-dated Phase I assemblages on the basis of textural relations.

Figure 37b is the logical successor to Figure 37a but is based on the further assumption that all the Phase I assemblages were penecontemporaneous and pre-dated all the Phase II assemblages which were also penecontemporaneous. The zonal progression (Fig. 37a) and geographical distribution (Fig. 37b) of Phase I minerals suggests a gradual increase in grade to the North-East, not directly related to the Prosperous Lake pluton which later intruded the Phase I staurolite zone. The Phase II assemblages show a parallel increase of metamorphic grade ranging from chlorite zone near Yellowknife Bay to sillimanite zone near the pluton contact and effectively overprinted on the Phase I assemblages.

The facies series. The assignment of absolute temperatures and pressures to these assemblages depends on reliable recognition of the facies series and the mineral-forming reactions. The reactions yielding the Phase II minerals have been identified above but experimental data are available only for the cordierite-forming

FIGURE 37a Conventional paragenesis diagram illustrating the observed distribution of minerals in the Prosperous Lake aureole and their paragenetic sequence (inferred from textural relations) within each metamorphic zone.

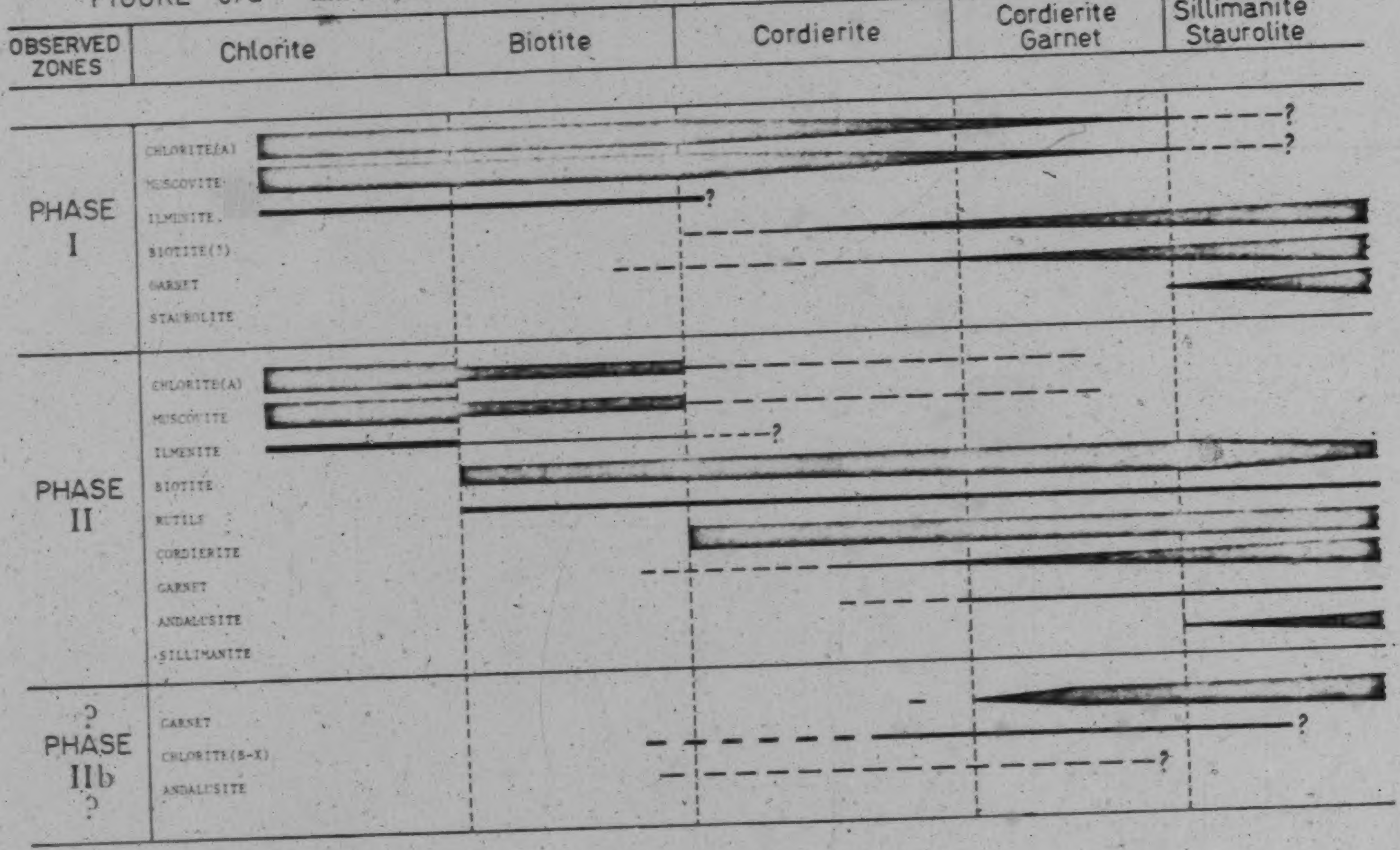
OBSERVED ZONES
Chlorite
Biotite
Cordierite
Cordierite Garnet
Sillimanite Staurolite
PHASE I
CHLORITE(A)
MUSCOVITE
ILMENITE
BIOTITE(?)
GARNET
STAUROLITE
PHASE II
CHLORITE(A)
MUSCOVITE
ILMENITE
BIOTITE
RUTILE
CORDIERITE
GARNET
ANDALUSITE
SILLIMANITE
? PHASE IIb ?
GARNET
CHLORITE(B-X)
ANDALUSITE
?

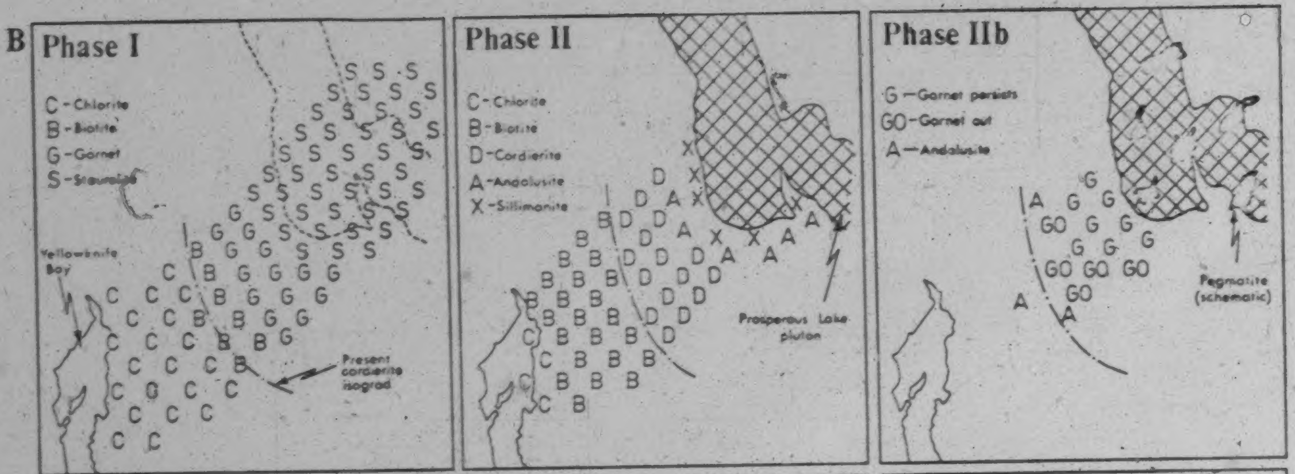
B
Phase I
C - Chlorite
B - Biotite
G - Garnet
S - Staurolite
Yellowknife Bay
Present cordierite isograd
Phase II
C - Chlorite
B - Biotite
D - Cordierite
A - Andalusite
X - Sillimanite
Prosperous Lake pluton
Phase IIb
G — Garnet persists
GO - Garnet out
A — Andalusite
Pegmatite (schematic)

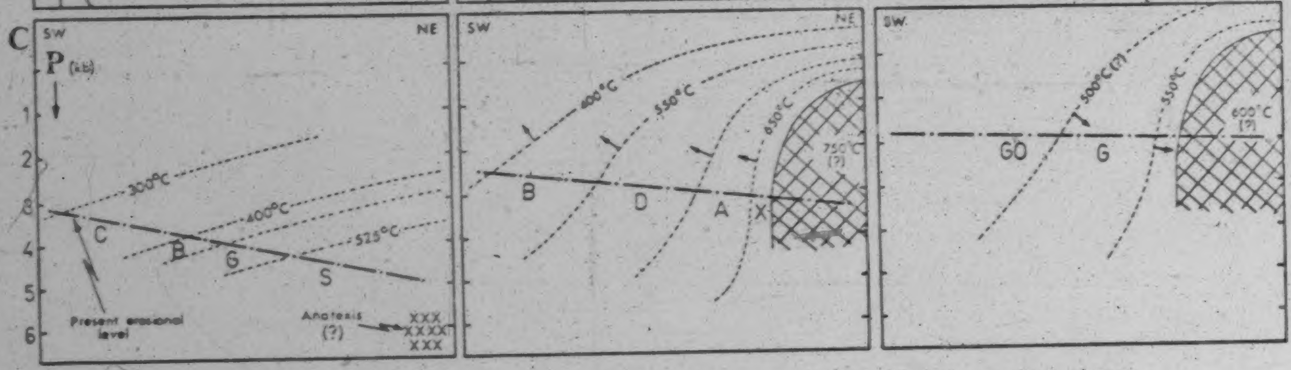
C
SW
NE
P (kb)
1
2
3
4
5
6
300°C
400°C
525°C
C
B
G
S
Present erosional level
Anatexis (?)
XXX
XXXX
XXX
400°C
550°C
650°C
750°C (?)
D
A
X
500°C (?)
550°C
600°C (?)
GO

FIGURE 37B : Suggested areal distribution of index minerals during the various phases of metamorphism (see text and Fig. 37A).

FIGURE 37C : Suggested evolution of metamorphic conditions during the metamorphic cycle (see text and the other parts of Figure 37).

reaction. The reactions in the Phase I assemblages are unknown. The assigned temperatures are therefore approximate. Since chlorite, biotite, garnet, staurolite, andalusite and sillimanite have all been formed at some stage in the paragenesis it may be assumed that there are no compositional restrictions on their presence. Therefore the pro-grade sequence in each phase may be used to deduce the facies series and pressures of metamorphism.

There is, however, considerable uncertainty in the literature about the nomenclature and pressure regimes of the facies series, particularly at pressures below the aluminium silicate triple point, whose uncertainty confuses the issue still further. The following lists the commonly accepted facies series and gives three recent estimates of pressure for them. The less common series are bracketed and only the lower pressure regime is considered:

	Hietanen (1967)	Hess (1969)	Lambert (1972)
Contact	2-2.5 kb.	3-5 kb.	1-3 kb.
(Bosost)	-	-	-
Abukuma	2.5-3.5	3- 4	2-4.5
Buchan	3-4	3.5-4.5	
(Idahoan)	3.5-6	7.3	
Barrovian	3.5-7.0	7	3-9

Other pressure estimates have been made by Den Tex (1971; generally higher pressures than above), Winkler (1967; rather similar to the above) and Turner (1968; generally lower).

The Phase I facies series contained garnet rather than cordierite, implying that pressure exceeded about 3 kb. @ 650° C. (Lambert, 1972; Richardson, 1968; Hietanen, 1967). The complete absence of kyanite indicates that pressures were less than in the Idahoan series (Hess, 1969; Hietanen, 1967). Hietanen has pointed out

(1967, p. 206) that the grade at which andalusite appears is a good indicator of pressure (see also Zwart, 1969). In Phase I staurolite is present at lower grade than andalusite, which presumably would have appeared just beyond the area studied. According to Hietanen this indicates pressures greater than the Buchan facies series. James (1955) described a facies series remarkably similar to that of Phase I and Hietanen called this the 'Michigan Type', concluding that it occurred at slightly lower pressures than the Idahoan series. Thus it seems reasonable to conclude that the Phase I facies series formed at conditions ranging from about 300° C. @ 3 kb. to 700° C. @ 5 kb., though the highest grades have not been observed during this study.

The index succession in Phase II is chlorite-biotite-cordierite-andalusite-sillimanite. Andalusite first appears in the upper cordierite zone, staurolite is unstable and garnet was probably close to its lower pressure limit. The stability of andalusite, cordierite and muscovite in the upper cordierite zone indicates pressures of less than 3 kb. @ 620° C. (Lambert, 1972) but this is not entirely in agreement with the petrogenetic grid of Hess (1969). The assemblage cordierite-biotite-andalusite is a critical assemblage in this grid and indicates pressures of 3-4.5 kb. @ 600° C. The index succession is very similar to that of the Abukuma facies series although andalusite appears at rather higher grades than usual. Because this is an aureole rather than a regional thermal metamorphism, it is probable that there was rather less pressure increase with grade than is typical of the Abukuma series. All these considerations lead to the conclusion that the Phase II assemblages represent conditions from 350° C. @ 2.5 kb. to 700° C. @ 3.0-3.5 kb.

There is no way of determining accurately the conditions of Phase IIb, particularly as oxygen and water pressures were probably critically important. The overall trend of decreasing pressure, the occurrence of andalusite in the lower cordierite zone or even the biotite zone (Davidson, 1967) and the apparent unstability of the garnet suggest that the pressure was lower than in Phase II, perhaps 2.0-2.5 kb.

Metamorphic evolution. All these observations and interpretations are thought to suggest the evolutionary model depicted in Fig. 37c. During Phase I the thermal regime in the area was rather uniform with gently dipping isotherms of regional extent and a broad metamorphic zonation in the low and medium grades of metamorphism. In Phase II the thermal regime became much less uniform with the development and upward migration of an intense thermal dome cored (asymmetrically) by anatectic granitic melt. The up-doming of the isotherms caused them to steepen and migrate outwards, compressing a wide range of grade into a distance which previously covered only a small range and superimposing the Phase II assemblages on Phase I. These changes were accompanied by a decrease of pressure. Phase IIb apparently occurred after the climax of Phase II and is tentatively correlated with a stage in which isotherms migrated inwards as the pluton cooled.

Timing of the phases. Phase II is reliably dated, by the zonation of its mineral assemblages round the late potassic plutons and by the structural information (above), as contemporaneous with the Prosperous Lake pluton. Phase I is known to pre-date Phase II and therefore occurred some time between the emplacement of the early granodiorite batholiths and the intrusion of the Prosperous Lake pluton. The grade in Phase I increases away from any known granodiorite but in the same direction as Phase II. It was therefore probably formed in an early stage of the same thermal dome. In Phase IIb the chlorite(B-X) and the late andalusites are known to post-date Phase II and the garnet corrosion may also have occurred at this stage. It is tentatively correlated with cooling of the pluton and the intrusion of the associated pegmatites.

Conclusion

These rocks evolved in a complex metamorphic cycle involving the development and decay of a single thermal dome accompanied by continuous pressure decrease. The texturally distinct phases do not represent separate metamorphic events but different stages in the evolution of a single metamorphic cycle.

(summarised in 1961). Other important studies are those of Coleman

[illegible] (1958) and [illegible] on the

4. Other irregular quartz stringers, lenses and bodies of limited extent. (The 'irregular veins' discussed below are of this category.)

This classification scheme adequately describes the quartz veins of the Prosperous Lake area, though no deposits related to isoclinal folds are known there.

Mineralogy. These are all massive quartz bodies (e.g. Plat[illegible] containing usually less than 1-2 per cent of other minerals. Pyrite, sphalerite and galena are the principal sulphides but there are sometimes traces of chalcopyrite, arsenopyrite, pyrrhotite, tourmaline, or feldspar present. Native gold is commonly associated with sulphide-bearing quartz and an association with sphalerite in particular has been noted (e.g. Henderson and Fraser, 1948). No detailed study of the mineralogy of the deposits in the meta-sediments has been made but Coleman (1953 and 1957) deduced a complex paragenesis for those in the meta-volcanic rocks. He examined only three samples from deposits in the meta-sediments (Ptarmigan) and gave no details of mineralogy or paragenesis. He noted, however, that sulphosalts appeared to be absent but the sulphides were of the same variety, relative abundance and inter-relationship as observed in the other deposits. In his detailed study of the Giant Yellowknife mine (1957) he made the following identifications:

Ubiquitous	Common	Others
Pyrite	Gold	Antimony
Arsenopyrite	Pyrrhotite	Lead
Sphalerite	Galena	Marcasite
Chalcopyrite	Stibnite	Others
	Aurostibite	
	Sulphosalts	

He concluded that there were three phases of mineralisation by magmatic solutions introduced into dilatant zones during deformation. These phases produced

1. Pyrite, arsenopyrite and most of the gold.
2. Sphalerite, chalcopyrite and minor pyrrhotite.
3. Sulphides and sulphosalts of Pb and Sb.

P-T conditions changed progressively from the first phase (> 500° C. and high P) to the last (< 350° C. and "fairly low" P).

It should be repeated here that there is no certainty that the mineralogy, paragenesis or origin of deposits in the metasediments is the same as that given above. The evidence is, however, that they are rather similar.

Genetic Theories

By the nature of their structural controls, the deposits in the meta-sediments can be more precisely dated with respect to the tectonic history than can the shear zones in the greenstones. Despite this, almost all the recorded theories of genesis apply principally to the latter and only peripherally to the former. Henderson and Jolliffe (1939) thought the gold of the greenstone belts to have originated in a deep-seated igneous body via the major late faults. They made no conclusions on the origin of the meta-sediment gold deposits but noted a change in character from high-temperature veins in the more metamorphosed rocks to lower-temperature veins in the less metamorphosed ones. Despite this, they suggested that the gold was derived from the granites.

Folinsbee (1942) noted that the gold deposits were concentrated just within the 'nodular zone' in the meta-sediments and suggested that this was because that section of the metamorphic aureoles represented the maximum hydrothermal metamorphism.

Boyle's detailed work on the deposits of the greenstones (1955, 1959, 1961) led him to believe that the vein material was derived by lateral secretion during metamorphism and he extended this model to the deposits in the meta-sediments. His theory has, however, provoked much criticism from authors believing in hydrothermal models (e.g. Coleman, 1957; McConnell, 1964; Chary, 1971) including Ames (1962) who re-interpreted Boyle's own data to argue in favour of a hydrothermal origin. Critical in this context are the data of Robertson and Cumming (1968) which have recently been modified (Robertson, pers. comm.) to indicate that the ores are exactly the same age as the enclosing volcanics.

The discussion is, therefore, thoroughly polarised into two traditional schools. It is agreed that the ores were deposited by hot, aqueous fluids but one school would argue an igneous derivation for these while the other favours a lateral secretion of fluids carrying ore elements, probably during metamorphism.

Scope of the Present Investigation

This disagreement might be solved by resolving (1) the exact temporal relation of the deposits and the tectonic events and (2) the nature and temperature of the depositional fluids. The following is a reconnaissance study which attempts to apply these two criteria by discussing the structural setting of deposits in the Prosperous Lake area and presenting the results of a fluid inclusion survey.

THE GOLD DEPOSITS

Four deposits bearing (academically) significant gold mineralisation are known in the Prosperous Lake area. Three of these have been examined and sampled in some detail, the other has been only cursorily examined. Their locations are shown in Fig. 41.

Ptarmigan Mine

This mine was closed in 1942 as a result of war-time conditions and has not been re-opened. The property is owned by Ptarmigan Mines Ltd. of Trail, British Columbia. Its exploration and production history has been described by Lord (1951) and aspects of its geology by Lord (1951) and Boyle (1961).

The geological setting of the main (No. 1) vein is shown in Fig. 38. It is long (ca. 400 m. in all) and approximately straight with a maximum width of about 15 m. and an average of about 4 m. (Lord, 1951). It dips vertically and has been explored underground to a depth of about 275 m. by nearly 1800 m. of drifts on seven levels.

The contacts with the wall-rocks are generally sharp, particularly on the south-west side, but the north-east margin has up to one or two metres of inter-lacing quartz veinlets forming a stockwork. Narrow stockwork zones are occasionally present on the south-west side. The country rocks (typical Burwash Fm. metasediments) are fractured or slightly sheared in places near the contact but there is no indication of a continuous or discrete 'shear zone'. Jolliffe (1936) noted that there were several en echelon quartz bodies rather than a single vein.

Quartz of several types makes up this vein: (1) Sugary,

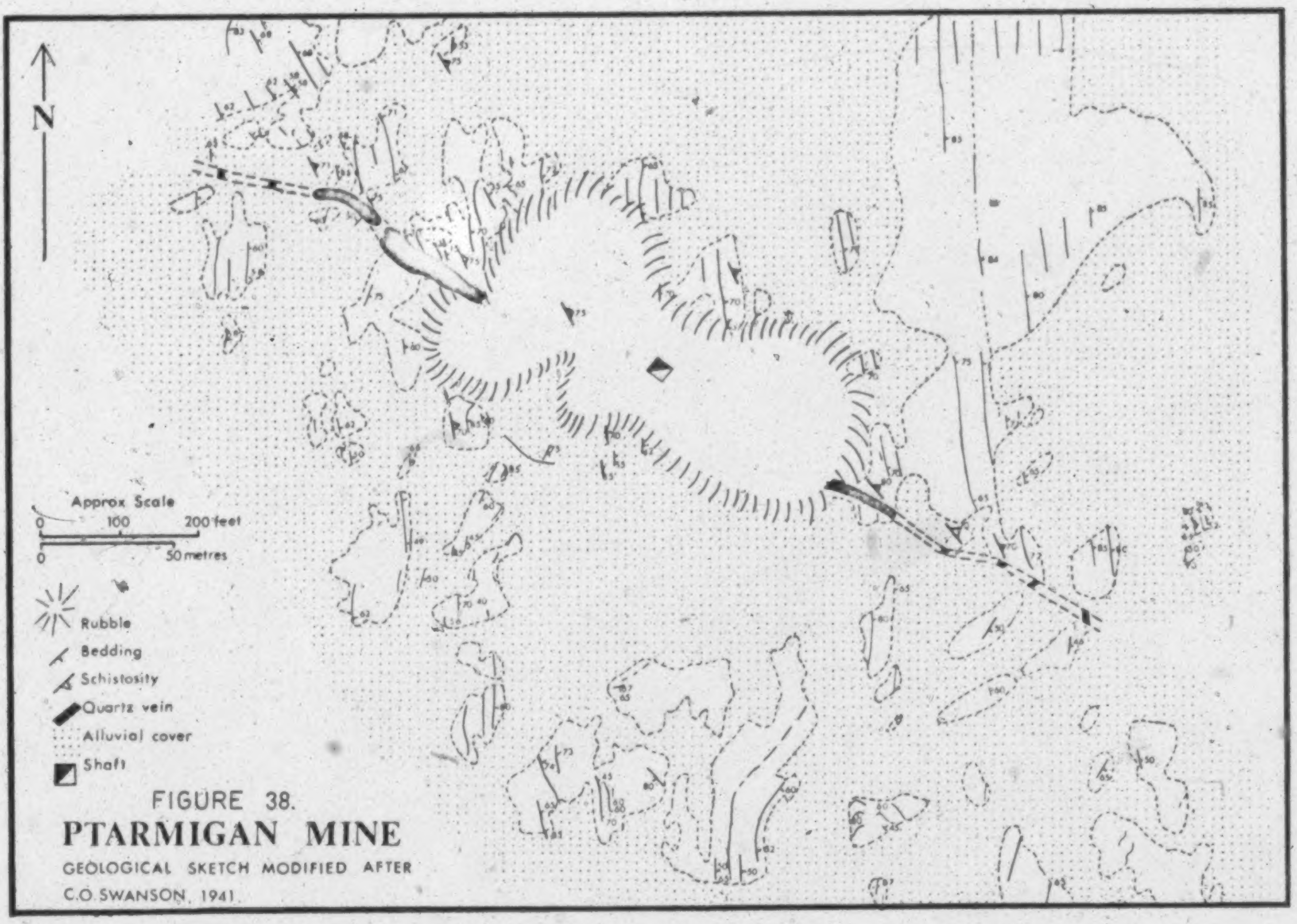
N
Approx Scale
0
100
200 feet
0
50 metres
Rubble
Bedding
Schistosity
Quartz vein
Alluvial cover
Shaft

FIGURE 38.

PTARMIGAN MINE

GEOLOGICAL SKETCH MODIFIED AFTER
C.O. SWANSON, 1941

grey quartz. (2) Massive, milky white quartz. (3) Drusy quartz, often with sulphides and usually on recognisable fractures. (4) Stockworks of narrow quartz veinlets in the adjacent country rocks. Types (1) and (2) are the dominant ones and were thought by Boyle (1961) to be of different ages, the white cross-cutting the grey. Certainly the grey type comprises the bulk of the vein but boundaries with the white type are diffuse and definite cross-cutting relationships are seldom visible. Type (3) is, however, definitely later than the bulk of the veins. Cavities in these fractures commonly contain drusy quartz coated with pyrite, sphalerite or galena. Boyle reported that calcite and ankerite occurred in these fractures and that gold was present in some of the cavities. Lord (1951) noted that where gold content was appreciable, sulphides were usually present. The gold is usually in grey ribboned quartz and the massive white quartz contains little gold. Tourmaline is present in the massive quartz.

The Tom Veins

These veins are due north of the Ptarmigan Mine and are part of the same vein set (Fig. 41). They have not produced gold but the No. 3 vein was thoroughly explored by Cominco Ltd. in 1940-1942 (under option). This included an exploration shaft (about 16 m. deep). Caen Yellowknife Mines Ltd. acquired the property in 1945, changed its name to Cassidy Yellowknife Mines Ltd. and drilled numerous holes.

Six veins are known on the Tom claim, all striking north-west to west. The main (No. 3) vein is visible at the surface for about 400 m., being terminated at the eastern end by the Ptarmigan fault. (A possible eastern extension of the same vein occurs

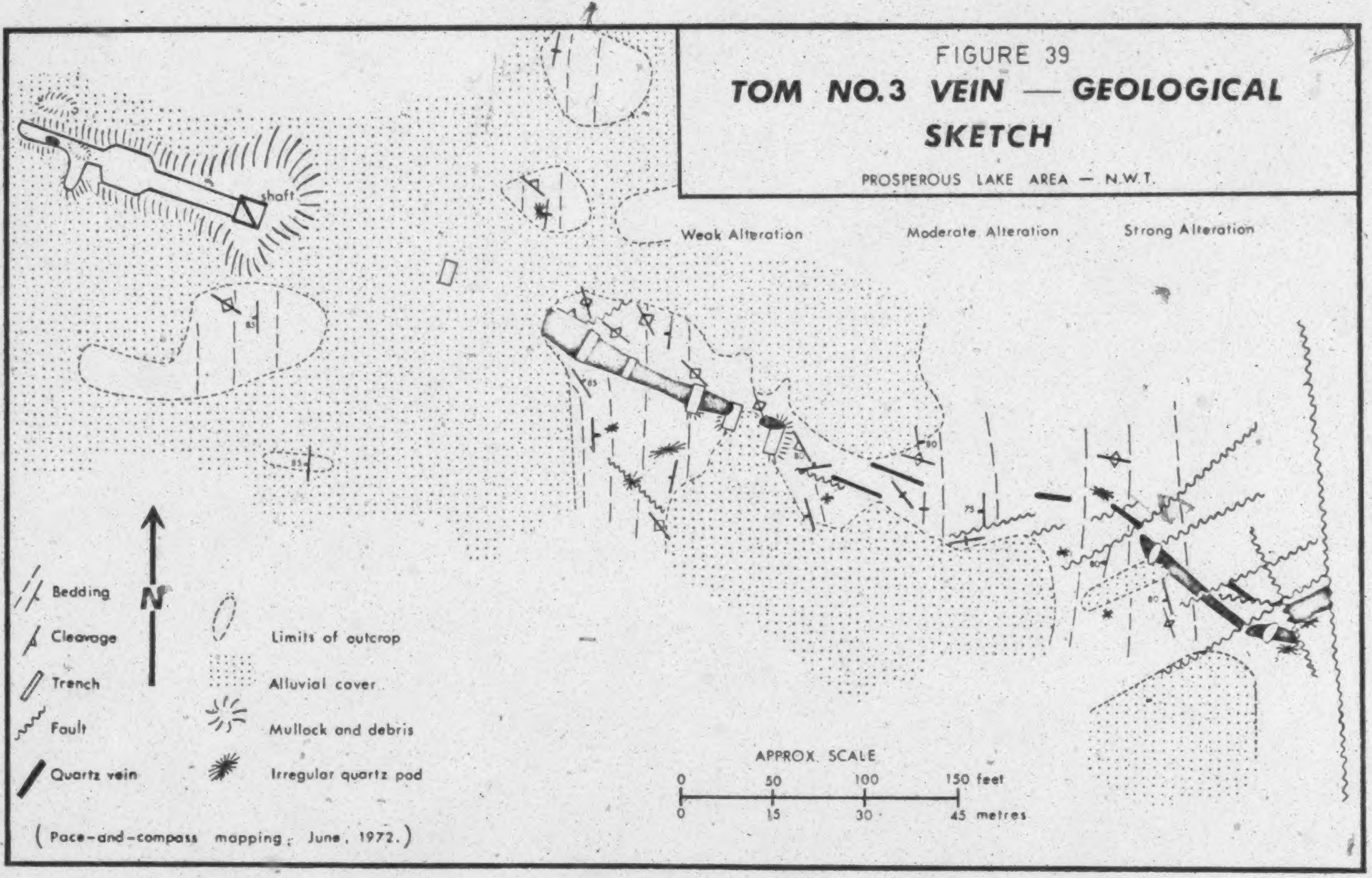

FIGURE 39

TOM NO.3 VEIN — GEOLOGICAL SKETCH

PROSPEROUS LAKE AREA — N.W.T.

Weak Alteration
Moderate Alteration
Strong Alteration
shaft
N
Bedding
Cleavage
Trench
Fault
Quartz vein
Limits of outcrop
Alluvial cover
Mullock and debris
Irregular quartz pod
APPROX. SCALE
0
50
100
150 feet
0
15
30
45 metres

(Pace-and-compass mapping, June, 1972.)

about 300 m. north on the other side of the fault.) The No. 3 vein is essentially long and straight (Fig. 39) and its width in core is reported to vary from 1 m. to about 7 m. It has been tested in depth to a maximum of 106 m. and dips vertically or very steeply northwards (Boldy, 1959). Three of the veins are shown by Jolliffe (1946) but no published account of them is known.

The No. 3 vein is similar to the main Ptarmigan vein (Fig. 39). It apparently consists of en echelon pods connected by just a few small veins. This surface configuration suggests that in three dimensions there is a plane with thick lenses at intervals along it. The vein contacts are generally sharp but are discoloured by a rusty or yellowish stain and have rather more marked schistosity than most of the country rocks. This schistosity is commonly irregular, being parallel to the vein wall adjacent to it and gradually merging outwards (over one or two metres) with the schistosity of the country rocks. The nature of the contacts does not suggest shearing. Some fragments of altered country rock are included in the quartz but there is no sign of marginal quartz stockwork.

Alteration of the wall-rocks at the vein margins is confined to within a few feet of the contact and consists mainly of the yellow discolouration of both wall-rock and quartz. In some instances there is a few centimetres of rusty-coloured boxwork. On some contacts and in some included wall-rock fragments there has been alteration to a biotite-sulphide rock and included and marginal wall-rock is enriched in pyrrhotite. This alteration is markedly distinct from that associated with the Ptarmigan fault at the eastern end of the vein (Fig. 39), which is typical of the pervasive hydrothermal alteration associated with the major faults in the area (see above). This pervasive alteration increases in intensity towards the fault plane.

The vein consists almost entirely of massive quartz with a few included pieces of wall-rock and minor amounts of other minerals. The sulphides usually comprise less than one per cent of the vein but in places they appear to be concentrated along the contacts and samples predominantly of sulphide have been removed from the exploration shaft. Most of the quartz is white and entirely massive with slivers of country rock in places. Most usually the sulphide-rich quartz is grey and massive but there are some vuggy patches of white quartz with associated pyrite. Pyrite is the most common sulphide in the vein but massive galena and sphalerite are present in samples from the shaft. Pyrrhotite is commonly present in the included and adjacent meta-sediments. There are no clear age relationships between the massive white and grey quartz types but the vuggy type associated with pyrite is probably later than the rest.

The Rich Deposit

This deposit (Fig. 40) has been described by Jolliffe (1936 and 1938) and Lord (1951). The property was explored by Burwash Yellowknife Mines Ltd. in 1935 and yielded about sixteen tons of rock which reportedly assayed at 13.6 oz. of gold per ton. An exploration shaft (28 m. deep), considerable drilling and several hundred feet of trenching were completed in the ten years to 1945, but no further gold was produced.

Figure 40 shows the geology of the shaft area. The rocks are sediments of the Burwash Fm., metamorphosed to chlorite

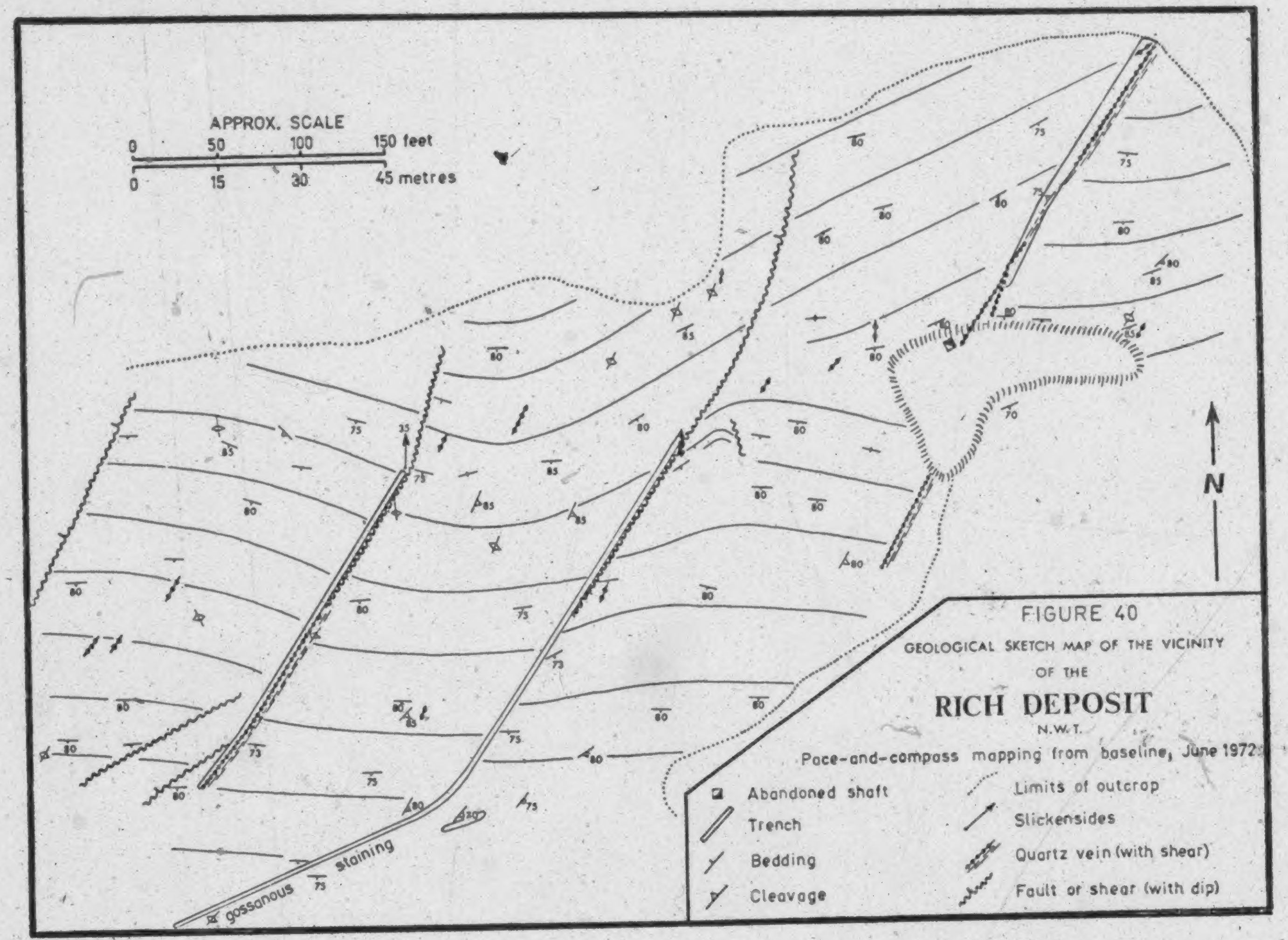

FIGURE 40

GEOLOGICAL SKETCH MAP OF THE VICINITY OF THE

RICH DEPOSIT

N.W.T.

Pace-and-compass mapping from baseline, June 1972

APPROX. SCALE
0
50
100
150 feet
0
15
30
45 metres
N
Abandoned shaft
Trench
Bedding
Cleavage
Limits of outcrop
Slickensides
Quartz vein (with shear)
Fault or shear (with dip)
gossanous
staining

or lowest biotite grade. They have a weak schistosity which strikes east of north in most places and is sub-vertical, suggesting that the area is in the Yellowknife Bridge structural domain (above). The beds are cut by a set of parallel shears or faults which strike N. N. E. and dip steeply to the west, probably at 60-75°. These are narrow shear zones marked by small scarps, slickensides, quartz veining and minor shearing. Horizontal displacement on them is small and the beds on the west have moved up and slightly south (Jolliffe, 1938).

Quartz veins of two distinct types are recognisable in this area:

1. Small lenses, a few feet in length, randomly dispersed in the country rocks but always striking parallel to the schistosity. These are barren.
2. Irregular veins, pods and narrow stockworks located discontinuously along the shears. These are of variable thickness but are seldom thicker than about 60-70 cms. The shaft is located on the main one of these veins.

The quartz in the shears is dark-coloured, often slightly pyritic and has sheared chloritic margins. It contains some carbonate. The gold is primarily in the quartz but there is a little in the carbonate and the chlorite schist (Jolliffe, 1938). Jolliffe gave the principal sulphides, in order of appearance, as arsenopyrite, pyrite, marcasite, chalcopyrite, galena and pyrrhotite.

The Tin Deposit

This deposit has been only cursorily examined during the present survey. It has been mapped and described in more detail in unpublished company reports (e.g. Williams, 1967). There is a small pit on the main outcrop and considerable drilling was carried out on the property by Tarbell Mines Ltd. in 1955.

The country rocks are folded strata of the Burwash Fm., metamorphosed in the cordierite-garnet zone and cut by numerous faults and quartz veins. Williams (1967) concluded that the gold (with massive sphalerite) occurred along a bedding-plane fault in a north-westerly plunging syncline. The dominant feature is a schist zone, stained red and yellow, and about one metre wide as now exposed. The rock in this schist zone is a yellowish sericitic schist containing small and irregular pods, veins and lenses of grey quartz. This schist grades into normal massive meta-sediments in the space of a few centimetres. Within the schist zone the schistosity strikes consistently north-west (320°) and dips steeply southwards, this being the orientation of typical schistosity in the Hay Lake structural domain but inclined to the trend of the schist zone. It seems unlikely, therefore, that the mineralised zone is a simple shear or fault.

The quartz generally contains sphalerite (up to 40 per cent), some pyrite and pyrrhotite. Gold is commonly associated with sphalerite (Williams, 1967).

STRUCTURAL RELATIONS

The main Ptarmigan and Tom veins (as well as the others in the set) display similar relations to the local structures. Both are long and fairly straight and cut across bedding at a high angle. It has been noted that both are approximately parallel to the axes of local folds but in fact they deviate slightly in orientation from the typical joint planes or cleavages in the Hay Lake domain. The sub-parallel nature of this mineralised vein set with the dominant Hay Lake domain structures is, however, unlikely to be coincidental (see below).

According to Williams (1967) mineralisation on the Tin-Lanas is related to a fold whose axial plane strikes north-west. Apparently this deposit too is controlled by Hay Lake domain structures.

The controlling structures of the Rich deposit are shear zones which strike N.N.E. This area has not been structurally mapped or definitely assigned to one of the structural domains, but the fact that cleavage near the shaft strikes east of north suggests that the area belongs to the Yellowknife Bridge domain. In this case it seems more than coincidental that the controlling shears are sub-parallel to the dominant axial plane orientation of this domain.

Several small scattered deposits in the Walsh Lake area have also been briefly examined. In all cases the controlling structures strike north to north-east and dip very steeply. The few cleavage measurements available (Fig. 41) indicate that the Yellowknife Bridge domain can also be extended into this area. In this case the Walsh Lake deposits are also controlled by structures parallel to the characteristic orientation of this structural domain.

In Fig. 41 this argument is extrapolated to all the known gold-bearing structures of the Yellowknife district. Gold deposits are only known in the Hay Lake and Yellowknife Bridge domains. In the Hay Lake domain all the controlling structures strike about north-west and are either dilatant zones or, in one case, probably a fold (Williams, 1967). All the controlling structures in the

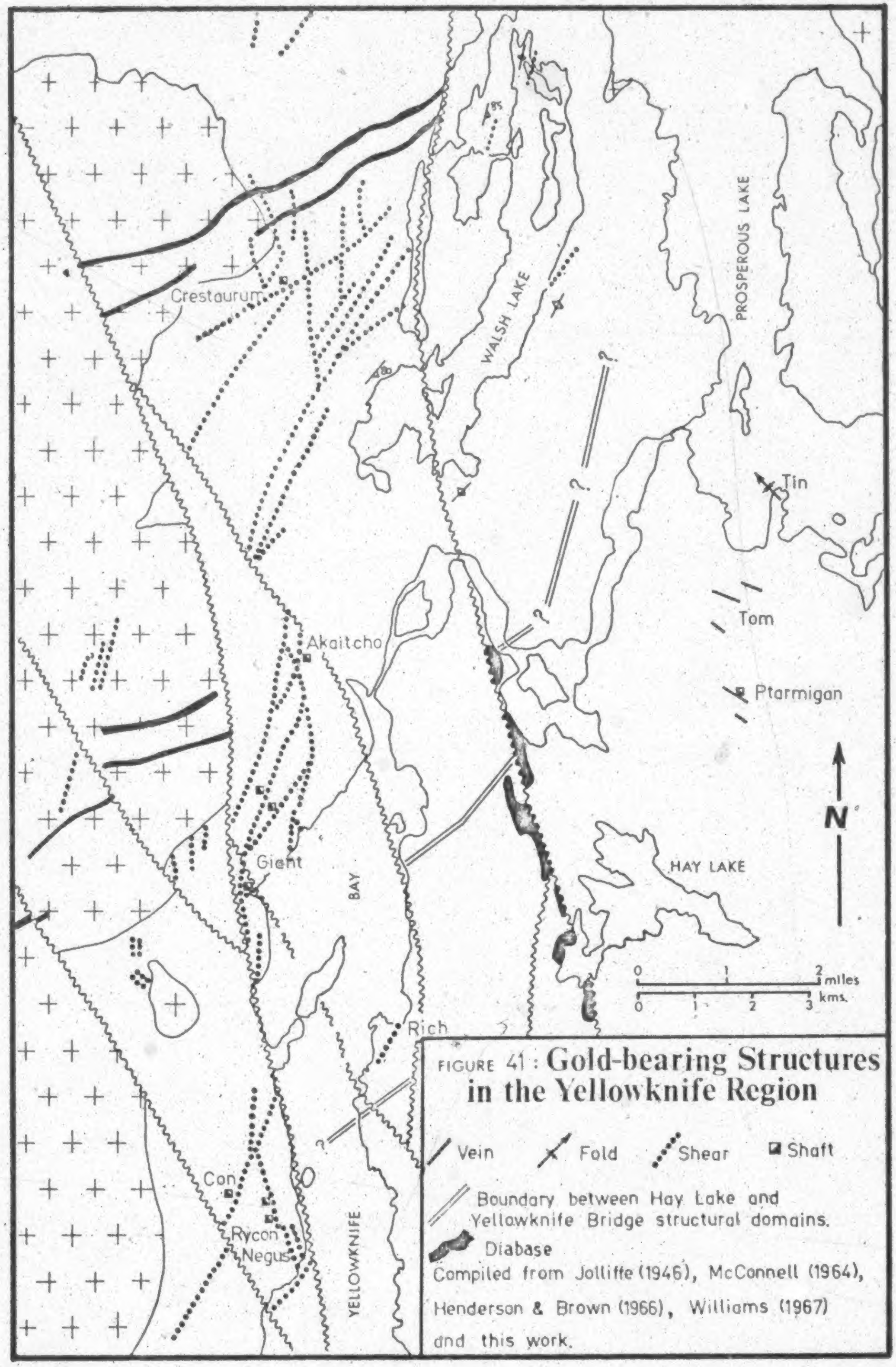
Crestaurum
WALSH LAKE
PROSPEROUS LAKE
85
80
?
Tin
Tom
Ptarmigan
Akaitcho
Giant
BAY
HAY LAKE
N
0 1 2 miles
0 1 2 3 kms.
Rich
Con
Rycon
Negus
YELLOWKNIFE

FIGURE 41 : **Gold-bearing Structures in the Yellowknife Region**

Vein Fold Shear Shaft

Boundary between Hay Lake and Yellowknife Bridge structural domains.

Diabase

Compiled from Jolliffe (1946), McConnell (1964), Henderson & Brown (1966), Williams (1967) and this work.

Yellowknife Bridge domain and its assumed extensions are shear zones predominantly oriented N. N. E. or north-east, regardless of what rock type they occur in.

Thus several important conclusions can be made:

1. The orientation of the controlling structures was determined by the structural domain.
2. The type of controlling structure was not dependent on the country-rock type (cf., for example, Henderson and Jolliffe, 1939) but on the structural environment.
3. It has been suggested above that the structural domains are intimately related to the emplacement of the major plutons. It follows that the gold-controlling structures were contemporaneous with the plutons. Further, those of the Yellowknife Bridge domain probably pre-dated those of the Hay Lake domain (Table 1). Thus the gold mineralisation itself is probably of two similar but distinct ages, the first being penecontemporaneous with the Western Granodiorite, the second with the Prosperous Lake pluton (see also Robertson and Cumming, 1968).

There are several points which permit more exact suggestion of the time of gold deposition in relation to the tectonic history. (1) Fortier (1946) gave evidence for the formation of gold-quartz veins between intrusion of the late potassic granites and their attendant pegmatites. (2) It is generally accepted that the mineralised structures are structures of dilatancy (Coleman, 1953 and 1957; Boyle, 1959; this study) which implies that they formed during relaxation of compression. (3) The dilatant zones are sub-parallel, rather than exactly parallel, to the characteristic orientation in their domains which is compatible with their formation during release of the compression which caused deformation. (4) McConnell (1964) has pointed out that mineralised shears occur in the Western Granodiorite (Fig. 41). The pluton must therefore have been solid at the time of their formation, at least in this locality near the margin. In view of these points a fourth conclusion may be added to the three above:

4. The gold-bearing structures were formed, and probably mineralised, during release of deforming compression, i.e. when batholith inflation ceased and possibly minor contraction occurred.

IRREGULAR QUARTZ BODIES

The ubiquitous presence of these small irregular bodies of vein quartz in the meta-sediments has been previously noted (e.g. Boyle, 1961) but they are not known to contain any gold mineralisation.

These bodies are of massive, milky white quartz occasionally slightly pyritic or gossanous. They are of limited extent (typically 1-5 m. across) and are characterised by complete lack of rational shape or consistent relation to other features (Plate 5B). They are commonly filiamentous with a more massive core area but can take almost any other irregular shape. They are apparently unrelated in distribution to any of the granitic plutons and occur at all grades in the Prosperous Lake aureole.

Only a few geological features indicative of their age have been observed. One irregular vein has been observed cut by a diabase and another by a long straight quartz vein striking 020°. Commonly they warp the schistosity of the surrounding rocks. At one location an irregular vein displayed signs of being deformed by a typical Hay Lake domain fold but at others undeformed equivalents occur on fold closures. They occur in rocks within the Prosperous Lake aureole and in those well removed from its influence.

The mode and exact time of their origin is therefore uncertain. In some areas they are abundant in pelitic units but absent from meta-greywackes. This and their irregular, filiamentous form indicate that they originated by segregation of siliceous, aqueous solutions during metamorphism. The few observed geological relationships and their widespread distribution suggest that this occurred before the development of the thermal dome (Phase II in Fig. 37c), i.e. before intrusion of the Prosperous Lake pluton. It is this mode of origin which is tentatively accepted in the following discussion.

TEMPERATURE RELATIONS : FLUID INCLUSIONS

No previous work has been done on the deposition temperatures of veins in the meta-sediments, but there is some information on those in the meta-volcanic rocks. Boyle (1954) carried out a decrepitation study on the Campbell and Negus-Rycon shear zones. He found that the quartz was very unsuitable for study because it had been extensively crushed and recrystallised but detected a decrease of decrepitation temperature with depth in the Campbell System. Boyle avoided deducing depositional temperatures from his decrepitation data but almost all the decrepitation temperatures were between

150-250° C. Coleman (1957) used his detailed paragenetic study to deduce that depositional conditions varied from about 500° C. in the initial stages to <350° C. in the latter stages, with a parallel pressure decrease. Chary (1971) used sulphur isotope fractionation and some fluid inclusion data to derive a depositional temperature of 300-350° C. for the ores of the Con mine.

Scope of the Fluid Inclusion Study

Understanding the origin of these deposits depends largely on knowing the constitution and depositional conditions of the vein-forming fluids so that their genesis may be discussed with respect to igneous or metamorphic sources. This problem has been approached as follows. Petrographic study of inclusions in various quartz vein generations was carried out to indicate the nature of the fluids. The prevailing conditions in the country rocks were examined through the petrological data (above) and by an homogenisation study of the irregular quartz veins which were apparently syn-metamorphic. The depositional temperatures of the gold-bearing veins have been studied by an homogenisation survey of the Tom and Ptarmigan veins.

The study has been severely restricted by the lack of freezing and crushing stages. Details of methodology are given in the Appendix.

Petrological Constraints

The metamorphic reactions and paragenesis discussed in detail above indicate a progressively increasing temperature across the aureole from about 350° C. at the lowest grades to about 650° C. at the pluton contact in Phase II (Fig. 37). The cordierite isograd, which is almost adjacent to the Ptarmigan deposit and at slightly lower grade than the Tom veins, has been shown to represent 550±20° C. at 3 kb. These temperatures apply only to the climax of the thermal phase of metamorphism and the structural relations (above) indicate that gold vein formation just post-dated the metamorphic maximum. Therefore, the veins were deposited at temperatures of less than about 500° C. and pressures of nearly 3 kb., the exact conditions depending on the period between the metamorphic maximum and vein formation. Insofar as Coleman's (1957) conclusions can be applied to the veins in the meta-sediments, his suggested decline of temperature from about 500° C. is entirely compatible with the metamorphic criteria.

The petrological constraints on the conditions during Phase I metamorphism are less exact. Figure 37c suggests, however, that conditions intensified North-Eastwards from about 250° C. @ 3 kb. near Yellowknife Bay to about 525° C. @ 4.5 kb. on the Eastern shore of Prosperous Lake. It is under this thermal regime that the irregular quartz veins are thought to have formed.

Fluid Inclusions in the Irregular Veins

It has been tentatively concluded above that these quartz bodies formed by silica segregation immediately preceding Phase II of metamorphism, i.e. development of the Prosperous Lake aureole. They are, therefore, rather earlier in the sequence than the gold-bearing veins, but offer the opportunity of studying the thermal regime in the earlier phases of metamorphism.

Accordingly, samples of quartz from irregular veins were collected at all metamorphic grades across the aureole. From these a suite of twenty samples were selected (Fig. 42). All of these were petrographically examined and homogenisation temperatures were determined in eleven of them.

The inclusions. The quartz veins contain an enormous number of inclusions with a maximum size of about 30-40 microns (Plate 5C). Inclusions larger than ten microns are rare and the great majority are smaller than one micron diameter. As a result, heating-stage determinations are only possible on a very small proportion of the inclusions present. Ordinary petrographic examination at high magnification is possible for a rather larger proportion but there is undoubtedly marked sample bias (as in most fluid inclusion studies).

Several types of inclusion are recognisable, most of these categories merging with one another. The principal subdivision is into primary and secondary categories. Most of the criteria for the distinction of primary, secondary and pseudo-secondary inclusions (Roedder, 1967 and 1972) cannot be applied in these veins because the quartz is massive and displays no growth features. The only criteria which can be used to indicate primary origin are an isolated and random distribution unrelated to healed fractures and a compact shape lacking dendritic appearance or indications of necking down. Plate 5F and L exemplify these criteria. It is impossible, therefore, to be absolutely certain that any one particular inclusion is primary and the inclusions have consequently been classified into three categories:

1. Demonstrably secondary, i.e. on healed fractures containing numerous inclusions.
2. Assumed primary, i.e. displaying no indications of being secondary.

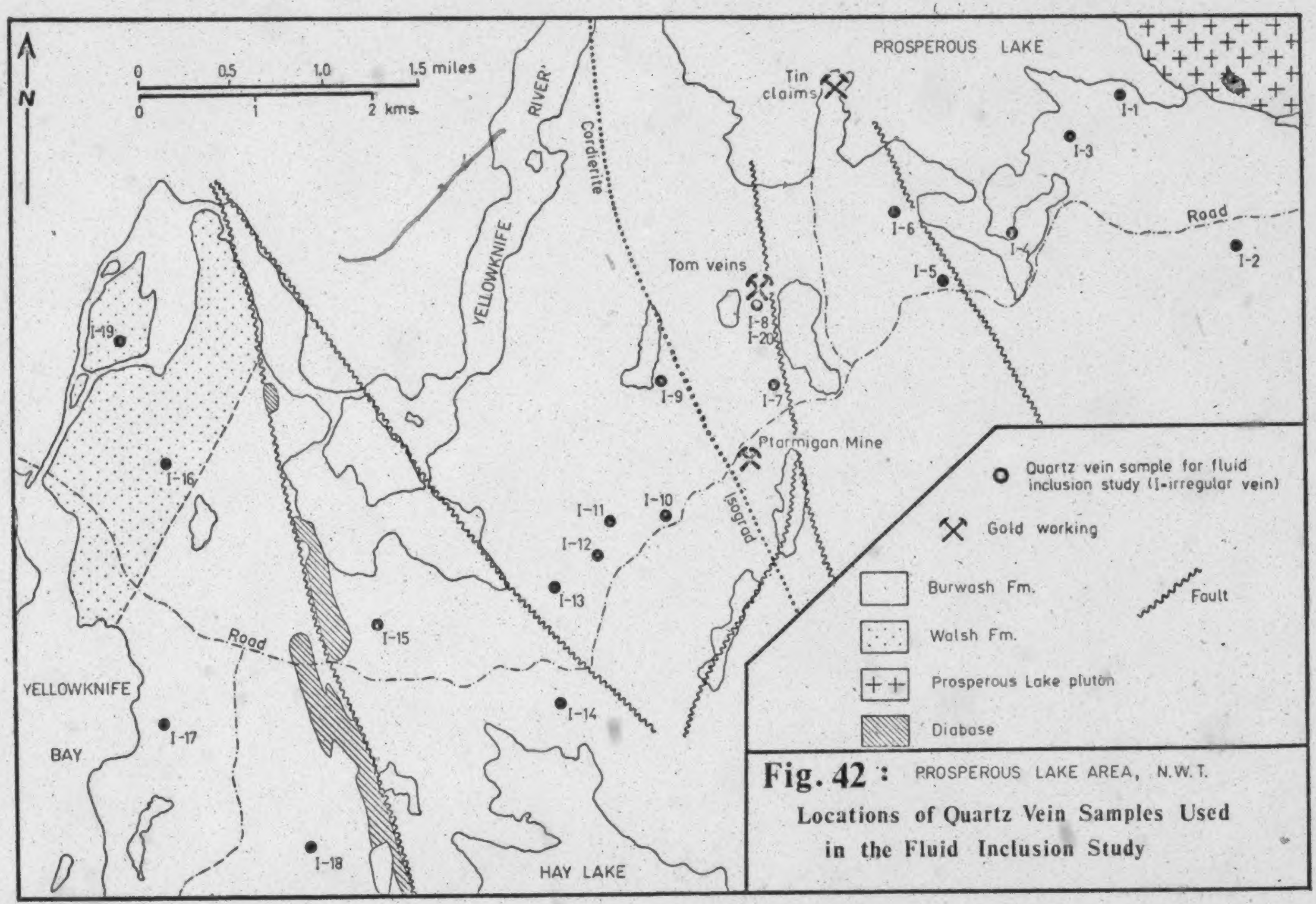
N
0
0.5
1.0
1.5 miles
0
1
2 kms.
PROSPEROUS LAKE
Tin claims
I-1
I-2
I-3
I-4
I-5
I-6
Road
Tom veins
I-8
I-20
I-7
I-9
YELLOWKNIFE RIVER
Cordierite
Isograd
Ptarmigan Mine
I-10
I-11
I-12
I-13
I-14
I-15
I-16
I-17
I-18
I-19
Road
YELLOWKNIFE BAY
HAY LAKE
Quartz vein sample for fluid inclusion study (I-irregular vein)
Gold working
Fault
Burwash Fm.
Walsh Fm.
Prosperous Lake pluton
Diabase

Fig. 42 : PROSPEROUS LAKE AREA, N.W.T.

Locations of Quartz Vein Samples Used in the Fluid Inclusion Study

3. Probably primary. These are inclusions which are thought to be primary but display some hint of the secondary characteristics listed above.

The inclusions can be further subdivided on the bases of the phases[1] present. These inclusion types are gradational with one another but examples are illustrated in Fig. 43 and Plate 5 and described below:

Type I. Liquid-rich. These are the most numerous inclusions in both primary and secondary categories. They consist simply of a colourless liquid phase and a small bubble of vapour (Plate 5D and others; Fig. 43). The sizes of these bubbles are given by the homogenisation temperatures (below) but they are typically about 15-25 per cent by area of the inclusion.

Type II. Liquid-rich with solid daughter(s). Some liquid-rich inclusions contain small colourless daughter minerals occasionally in identifiable cubes (Fig. 43; Plate 5L). A few contain two colourless daughters, the second in some cases being a birefringent prism. Very occasionally a tiny opaque daughter mineral is observed. The identification of these phases is very difficult but the recognisable properties (refractive index, birefringence and sometimes temperature coefficient of solubility) suggest

---

[1] There is much uncertainty in the phase terminology of multi-component, multi-phase fluid systems (Roedder and Coombs, 1967, p. 419), compounded in this case by the uncertainties in phase identification (see text). Herein the following usage is adopted. 'Liquid' is sub-critical. 'Fluid' is super-critical. 'Vapor' should imply low density but the character of bubbles cannot be reliably identified with the available apparatus. Phases described as 'vapour' may therefore include some which are super-critical fluid.

Explanation of Plate 5 continued.

J. Example from a presumed primary array of three-phase (Type V) inclusions containing a liquid aqueous phase, a liquid CO_2-rich phase and a vapour bubble. Sample Irreg-13.

K. As in J above. Note the difference of phase ratios between J and K. Sample Irreg-13.

L. Planar array of irregular, necked-down(?) secondary inclusions many of which contain solid daughter minerals. Sample Irreg-2.

PLATE 5

Quartz veins and fluid inclusions.

(KEY : lw = aqueous liquid; lc = CO_2-rich liquid; v = vapour; s = solid daughter mineral.)

A. Massive quartz vein. Southernmost of the gold-quartz veins in the Tom Lake set (Fig. 41) and typical of them. Note the sharp, unsheared, sub-vertical contact with the meta-sediments.

B. Example of an irregular quartz vein.

C. Typical distribution, concentration, size and appearance of fluid inclusions in these quartz vein samples. Note the difficulty in assigning definite primary or pseudo-secondary origin to any particular inclusion. Sample Ptarm-1.

D. Exceptionally large, isolated, two-phase inclusion (Type I) presumed to be primary. Sample Irreg-1.

E. Array of three different inclusions typical of the types observed. The top one is a simple two-phase inclusion of Type I. It may be secondary as a vague planar array is visible near it. The middle inclusion is presumed to be primary. It is a three-phase (Type V) inclusion with two liquid phases (visible in the photograph) and a small vapour bubble (which was highly mobile and could not be photographed). The lower inclusion is also apparently primary. It is a vapour-filled (Type IV) or possibly vapour-rich (Type III) inclusion. Note that the lower two inclusions and possibly the upper one belong to the same primary array which has variable phase ratios. Sample Irreg-4.

F. Illustrating the main criterion used for the distinction of primary and secondary inclusions. The former are unrelated to healed fractures, the latter aligned in them. Note also that the three large primary inclusions have very variable phase ratios though apparently part of the same primary array. Sample Irreg-1.

G. Three-dimensional array of typical two-phase (Type I) inclusions presumed to be primary. Note, however, that the large inclusion may have a very narrow double meniscus round the vapour bubble. If so it should be classified as a Type V inclusion. Sample Irreg-1.

H. Three-dimensional random array of presumed primary inclusions containing both liquid-rich (Type I) and vapour-filled (Type IV) inclusions. Sample Irreg-2.

I. Planar array of secondary, vapour-filled (Type IV) inclusions in sample Irreg-3.

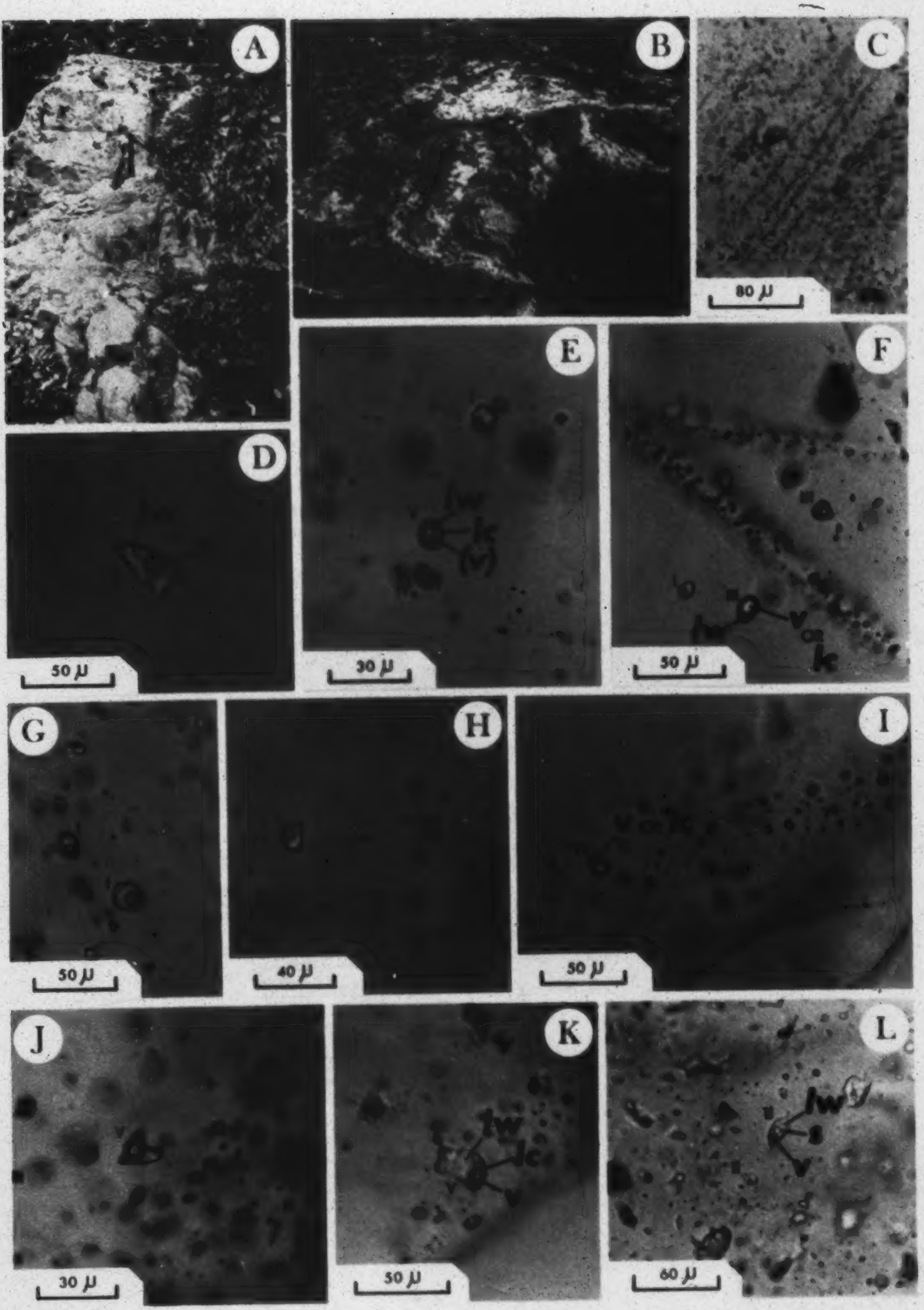
A
B
C
80 μ
D
50 μ
E
lw
lc
(v)
30 μ
F
lw
v or
lc
50 μ
G
50 μ
H
40 μ
I
50 μ
J
v
30 μ
K
lw
lc
v
50 μ
L
lw
s
v
60 μ

PLATE 5

that almost all of the daughter phases are halite. In the rare instances where two solid cubes(?) are present their very different rates of dissolution on heating suggest that the second is sylvite. The birefringent prisms may be anhydrite. There is no way of identifying the very rare opaque daughter. The relative frequency of these solid phases may be judged from Table 19.

Inclusions with solid daughters are present in many of the samples (Table 19) but comprise only a minute proportion of the total number of inclusions. The solid phases are invariably very small, being of the order of 1-2 per cent by volume of the inclusion. Further, almost all of the solid daughters observed are in demonstrably secondary or possibly secondary inclusions.

Type III. Vapour-rich. By arbitrary definition any inclusion in which the bubble constituted more than 50 per cent by area of the inclusion has been called vapour-rich (Fig. 43; Plate 5E and F). The bubble is of variable size and this type probably grades into the vapour-filled category below. Vapour-rich inclusions occur in most of the rocks though in rather smaller numbers than the liquid-rich types. They are most commonly primary but a few indeterminate ones and a few secondary ones have been observed (Table 19). No solid daughter minerals have been observed in vapour-rich inclusions.

FIGURE 43

Types of fluid inclusions observed in irregular veins and gold-quartz veins from the Prosperous Lake area. Open arrows indicate gradation of types. Dotted arrows indicate different types thought to be related by phase changes. KEY : lw = aqueous liquid; lc = CO_2-rich liquid; v = vapour or super-critical CO_2-rich fluid (see footnote above); s = solid daughter mineral, probably halite; x = second solid daughter mineral, either sylvite(?) or anhydrite(?) or an opaque mineral. Roman numerals indicate the Type to which such an inclusion would be assigned (see text).

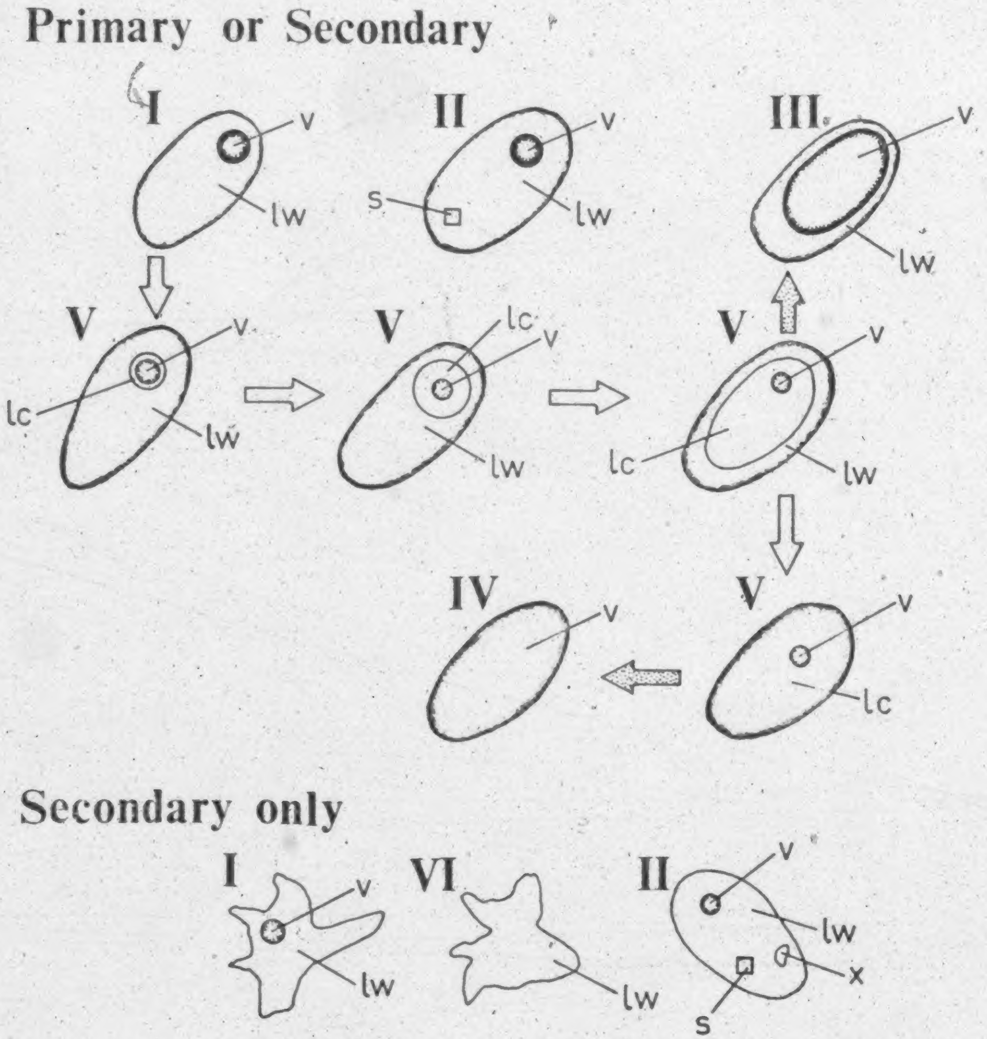
Primary or Secondary
I
v
lw
II
v
s
lw
III
v
lw
V
v
lc
lw
V
lc
v
lw
V
v
lc
lw
IV
v
V
v
lc
Secondary only
I
v
lw
VI
lw
II
v
lw
x
s

The vapour-rich inclusions display two interesting features: (1) In some of them the bubble is of rather lower relief against the liquid phase than is typical of vapour bubbles. Relief can be highly misleading in such instances (Roedder, 1972) but this does suggest that the vapour phase is rather more dense than usual. In a few cases such low-relief bubbles were induced, by cooling to about 10° C., to separate into a liquid phase and a small, highly mobile bubble. This suggests that the large 'vapour' bubble was actually super-critical CO_2-rich fluid and that some of these two-phase vapour-rich inclusions are super-critical equivalents of the CO_2-bearing category below. Because of the unreliability of relief as a diagnostic tool, it is impossible to estimate what proportion of the vapour-rich inclusions are CO_2-rich. (2) Characteristically these inclusions do not homogenise within the observed heating range (to 350° C.). Further, they commonly display little or no change in this temperature range (Fig. 44). In some cases the bubble increased on heating, in others there was no observable change, and in others the bubble appeared to shrink slightly. This behaviour also applies to a few vapour-rich secondary inclusions (Fig. 44) whereas all other secondaries homogenised at low temperatures. The significance of these features is discussed below.

Type IV. Vapour-filled. These are high-relief inclusions which appear empty (Fig. 43; Plate 5H and I) but grade into the vapour-rich category (III above). They are common both as primary (Plate 5H) and secondary (Plate 5I) types, though not in such numbers as the liquid-rich inclusions. It is impossible to see into most of these inclusions so the identification of their contents is difficult and no tests have been performed on them. In a few instances, however, inclusions which appear to be normal vapour-filled inclusions also contain a small, highly mobile bubble with low relief (at room temperature). This suggests that these inclusions are filled with CO_2-rich fluid, usually super-critical but occasionally sub-critical.

Type V. CO_2-bearing. Some inclusions contain two definite liquid phases and a small, mobile, low-relief bubble (Fig. 43; Plate 5J and K). In a few instances the latter can be made to disappear under intense illumination. This fact and the relative refractive indices of the phases indicate that the two liquids are water and liquid CO_2. The phase ratios vary from inclusions in which the liquid CO_2 is more abundant than water (e.g. Type IV above), through those with sub-equal amounts of CO_2 and water, through those in which minor CO_2 forms a definite double meniscus round the bubble (Plate 5J and K), to those in which a thin double meniscus is probably present but it cannot with certainty be distinguished from optical effects

(Plate 5G). Those inclusions which are definitely CO_2-bearing therefore grade to the simple, two-phase, liquid-rich type. In addition, they are very similar in nature to the unknown number of liquid-rich, vapour-rich or vapour-filled inclusions in which the 'vapour phase' is super-critical CO_2-rich fluid.

Inclusions of this category occur in many of the rocks though the amount of liquid CO_2 is usually small enough that the inclusion must be listed as only probably having three phases (Table 19). Inclusions definitely containing liquid CO_2 have been observed in both primary and secondary categories.

Type VI. Liquid-filled. Some highly irregular, dendritic inclusions on healed fractures are single-phase, aqueous inclusions. Many show evidence of having necked down but some do not.

Table 19 summarises the types and approximate abundances of inclusions observed in the twenty samples. Considering the suite as a whole, the liquid-rich inclusions are by far the most common primary and secondary inclusions. Solid daughter minerals are uncommon and small in size and are more abundant in secondary inclusions. Vapour-rich primary inclusions are common but some secondaries are also present. Vapour-filled inclusions are common in both primary and secondary categories. Definite CO_2-bearing inclusions with a wide range of liquid phase ratios occur as both primary and secondary inclusions. A few single-phase secondary inclusions filled with aqueous liquid testify to a recrystallisation history

TABLE 19 : Types and approximate abundances of fluid inclusions observed in the irregular quartz veins. In the Type II column the X's refer to cubes, probably halite, and the other words indicate rare second daughter minerals, if present.

Irreg. vein number	I Liquid-rich		II Daughters		III Vapour-rich		IV Vapour-filled		V Liquid CO_2	
	P	S	P	S	P	S	P	S	P	S
1	XXX	XXX	X opaq		XX			XX	XX	
2	XXX	XXX	X	XX	X	X(?)	XXX	XX	?	?
3	XX	XXX(?)		XX prism	XX	XX	XX	XX	?	?
4	XX	XX	X	X prism	XX		XX		X	X
5	XXX	XXX	X prism		X		XX	XX	?	?
6	XXX	XXX		X prism	XX		XX		?	
7	XXX	XXX		X opaq	XX		XX	X	?	
8	XX	XXX		X(?)	X	XX		XX	?	
9	XXX	XXX			XX	X	XX	XX	?	
10	XX	XXX			XX		XX		XX	?
11	XX	XXX		XX	X		X			
12	XXX	XX		XX	XX		XX	XX	?	
13	XXX						XX		XXX	
14	XXX	XX		X	XX		XX	XX	?	?
15	XXX	XXX	X(?)	XX	XX				?	
16	XX	XXX	X				XX	XX	XX	?
17	(?)	XXX		XX	XX		XX			
18	(?)	XXX					(?)	XX		
19	(?)	XXX			X		XX			
20	XXX	XXX	(?)	XX prism	X	X	XX	XX	XXX	?

KEY: XXX = Abundant; XX = Present; X = Only a few observed.
?–Thin double meniscuses, probably liquid CO_2.
P = Primary, S = Secondary.

which continued to low temperatures.

Homogenisation studies. Temperatures of homogenisation have been determined for 145 selected inclusions in eleven samples of irregular veins. Only determinations which satisfied the following criteria of reliability have been accepted as usable: (1) There must be at least two determinations agreeing within 10° C. on each inclusion. (2) On cooling, the inclusion must appear exactly the same as it did before heating. The only exceptions were in the case of Type II inclusions in which only single determinations were made because the daughter minerals commonly failed to re-appear on cooling.

The results are summarised in Figs. 44 and 45. There is a wide variety of homogenisation temperatures ranging from less than 100° C. to more than 360° C. The statistical maxima for the suite taken as a whole are given by Fig. 45. The secondary inclusions mostly homogenise between 115° C. and 165° C. The majority of the primary inclusions homogenise in the range 210-270° C., possibly with a subordinate maximum at 315-335° C.

Thirty of the inclusions tested did not homogenise in the working temperature range (Fig. 44). Of these, sixteen had bubbles which appeared to shrink as the temperature was increased and therefore would probably have homogenised in the liquid phase at some higher temperature. Another three had vapour bubbles which were apparently growing. The other eleven inclusions displayed no noticeable change between room temperature and 350° C., despite having a wide range of initial phase ratios. Two of these were secondary inclusions which should, according to the other determinations

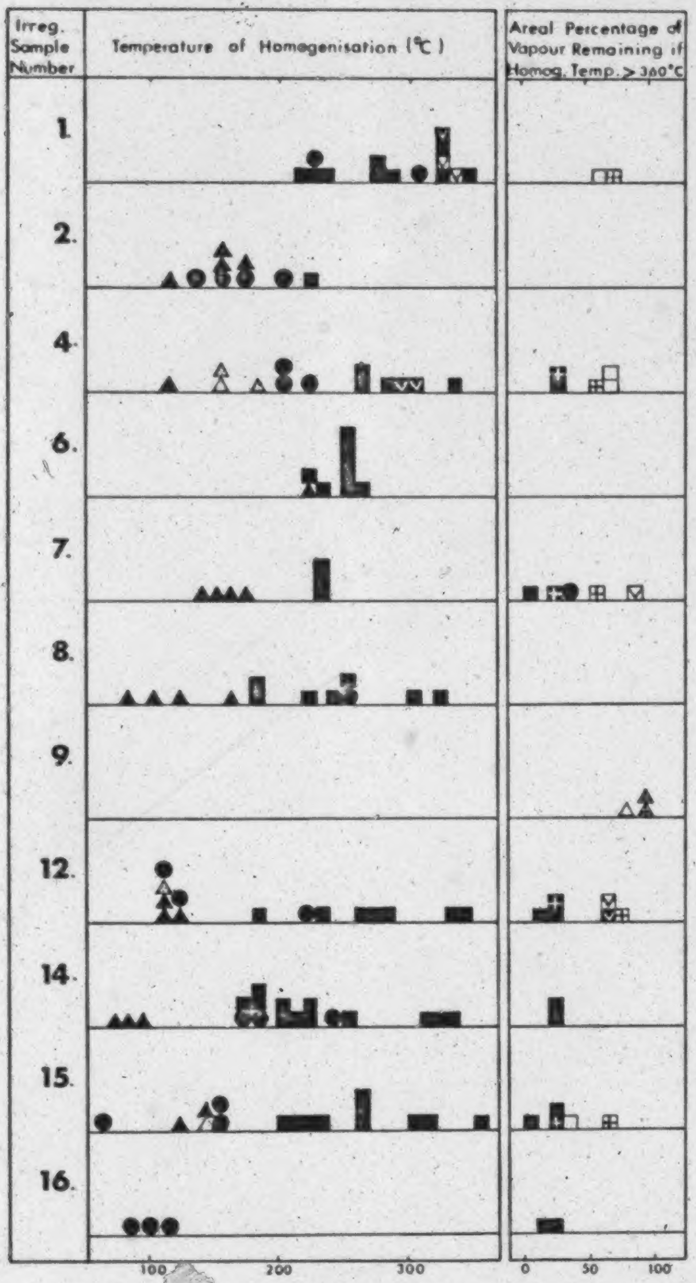

KEY : As in Figure 47

FIGURE 44 : Illustrating the response to heating exhibited by fluid inclusions in the irregular quartz veins.

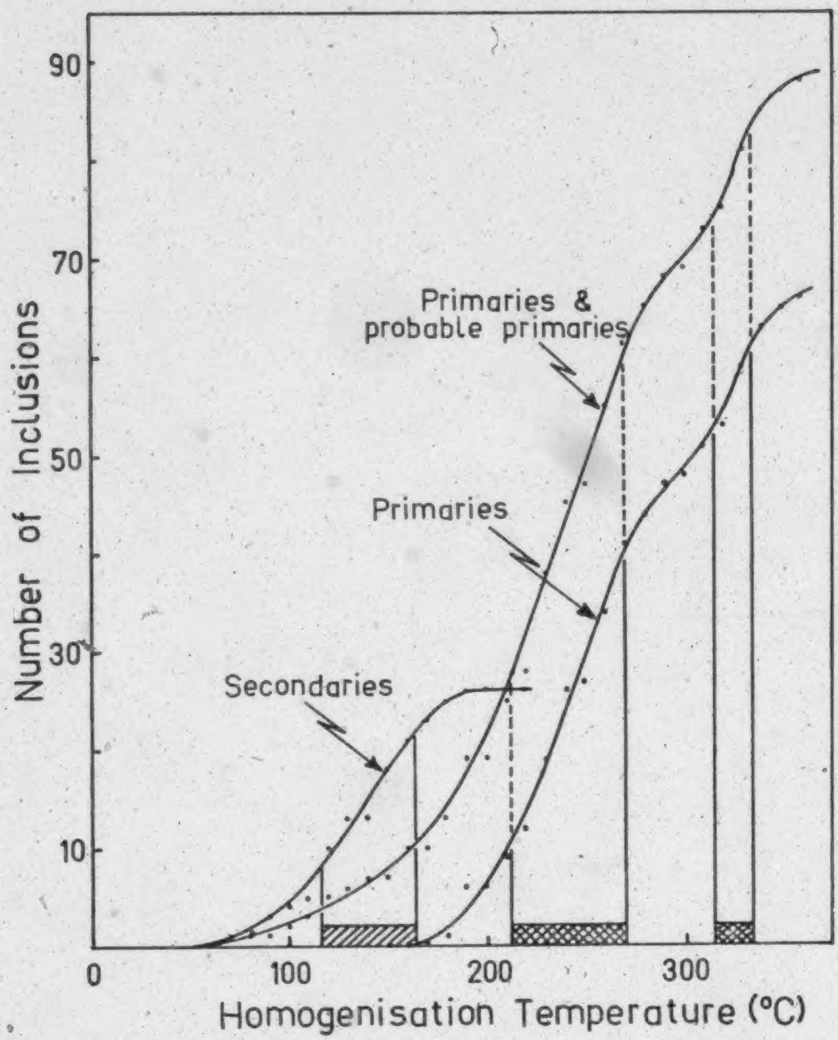

FIGURE 45 : Cumulative frequency plot of homogenisation temperatures of fluid inclusions in irregular quartz veins from the Prosperous Lake area. Only inclusions homogenising below 360°C are shown -- see text.

on secondary inclusions, have homogenised at less than 200° C. The significance of these observations is discussed below.

Salinity. In the absence of freezing point determinations, it is possible to make only crude estimates of salinity. It has already been noted that the primary inclusions are generally undersaturated in salts at room temperature while some, but not all, of the secondary inclusions are saturated. This means only that the primary inclusions contain less than about 26 wt. % equivalent NaCl and the saturated secondaries contain more than this. According to Kelly and Turneaure (1970) those inclusions saturated in both KCl and NaCl contain about 0.126 gms. KCl and 0.258 gms. NaCl per cc. of the solution. A typical saturated secondary inclusion contains about 7-8 per cent by volume of vapour (Fig. 44) and a maximum of 2-3 per cent by volume of solid daughter. These figures give an upper limit of 35 wt. % equivalent NaCl for all the inclusions observed.

Some data on the dissolution temperatures of the solid phases have been collected (Table 20). By using the curves of Keevil (1942) these temperatures can be used to derive approximate salinities. The data apply, of course, only to those inclusions containing solid daughter minerals, i.e. the most saline ones. The results are in agreement with the crude calculations above, indicating that the most saline fluids observed contain about 30 wt. % equivalent NaCl.

Estimates of the actual salinity for the primary inclusions are impossible without freezing data. It must be less than about 26 wt. % equivalent NaCl (above) but the presence of very rare halite cubes suggests that the concentration approaches saturation at room temperature. A salinity of 20 wt. % equivalent NaCl is tentatively

TABLE 20 : Approximate salinity data for (saturated) fluid inclusions in irregular quartz veins.

Sample No.	Primary or Secondary (P or S)	Dissolution Temperature (^{o}C.)	Inferred** Salinity (wt. % equivalent NaCl)
I-1	P	100	28
I-4	S	(1) 150	29
		(2) >240*	?
	S	150	29
	S	186	31
I-7	S	(1) 150-160	30
		(2) >260*	?
	S	(1) 140	29
		(2) >260*	?
	S	130-160	29
I-12	S	103	28
	S	115-120	29
I-15	S	140	29

*Second daughter present. Was not dissolved by slow heating to the specified temperature.

**Curves of Keevil (1942).

accepted for the primary fluids.

The vein-forming fluids. Several of the observations above indicate the nature of this fluid: (1) Water, liquid CO_2 and NaCl are the important phases present in both primary and secondary fluids. (2) The primary fluids were rather less saline (ca. 20 wt. % NaCl) than the secondary fluids (ca. 30 wt. % NaCl). (3) The phase ratios of aqueous and CO_2-rich fluids are very variable, probably from 100 per cent aqueous to 100 per cent CO_2-rich even within the same array of inclusions (Plate 5E, F and H). (4) Some of the inclusions show no sign of change in the phase ratios on heating. (5) Most of the inclusions homogenise in the liquid phase but some homogenise in the vapour phase. Rare inclusions homogenise by fading of the meniscus.

These properties indicate that the veins formed from a two-phase fluid containing immiscible NaCl-water and CO_2-water phases. The existence of such fluids at high temperatures and pressures has been demonstrated by Takenouchi and Kennedy (1965) and their behaviour has been examined in detail by Smith and Little (1959) and Roedder (1965).

Absolute temperatures. Smith and Little (1959) demonstrated that the homogenisation temperature is related to the temperature of formation in one of two ways for such two-phase fluids. Inclusions of either one of the two phases alone have homogenisation temperatures equal to the temperature of formation and requiring no pressure correction. Inclusions which trapped mechanical mixtures of the two phases have homogenisation temperatures greater than the true temperature of formation. Many of the features of Figs. 44 and 45 are immediately explicable. All those inclusions which showed

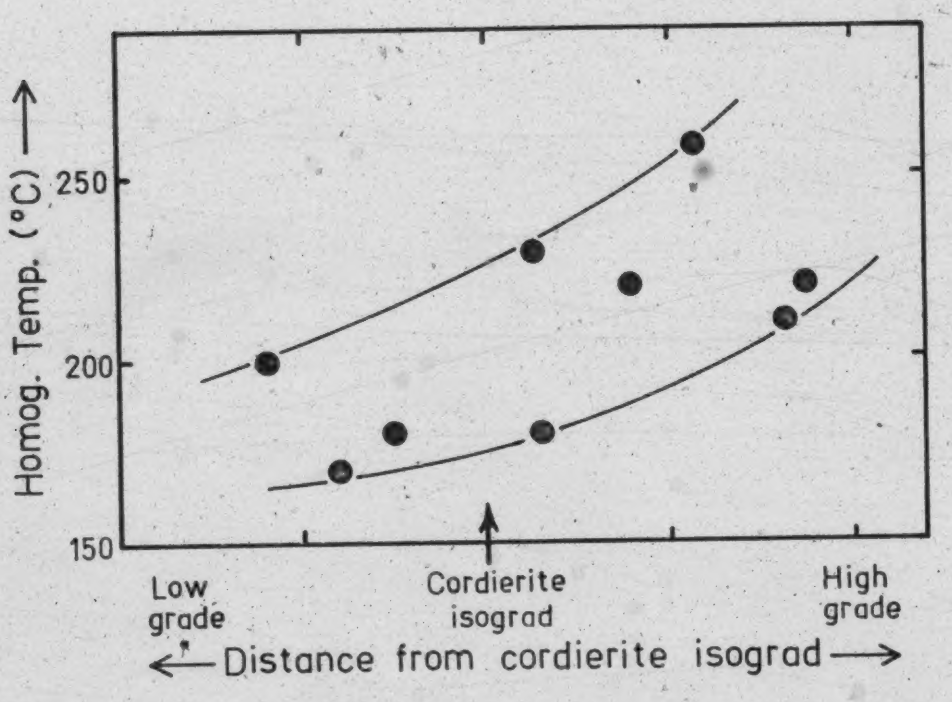

FIGURE 46 : Showing the relationship between the minimum observed temperature of homogenisation of primary inclusions in each irregular quartz vein and their positions in the metamorphic aureole (see text).

little or no change of phase ratios on heating were trapped as mechanical mixtures of the two phases. The pressure corrections (Lemmlein and Klevtsov, 1961), which yield unrealistically high temperatures of 550-650° C. for the majority of the primary inclusions, should not be applied. The homogenisation of some inclusions by expansion of the 'bubble' is due to the entrapment of dominantly the CO_2-rich phase.

These conditions of formation provide an extremely potent tool for the determination of temperatures in high-pressure regimes where pressure and salinity corrections are large, approximate and based on extrapollation of data. Homogenisation temperatures of both H_2O-rich and CO_2-rich inclusions should "approach a minimum, which would be close to the temperature of formation" (Smith and Little, 1959). Further, the inclusions which trapped single-phase fluid are more likely to be aqueous than CO_2-rich. There is no way of distinguishing, in the heating stage or in Fig. 44, inclusions which trapped only aqueous fluid from those which also trapped a small amount of carbonic fluid. The only possible criterion is to take the minimum observed homogenisation temperature for the primary inclusions. Fig. 46 gives the resultant temperatures of formation of the quartz veins in relation to their geographic location (Fig. 42). It shows a general decline from 220-280° C. in the north-east to 160-200° C. in the south-west. The metamorphic temperature during emplacement of these veins (Phase I) is thought to have increased from 250-300° C. in the south-west to 525° C. in the north-east. Figure 46 is compatible with this grade change though the actual temperatures are lower than anticipated from the mineral assemblages. This may be because a salinity correction is,

TABLE 21 : Summary of phases present in fluid inclusions in metamorphic quartz veins studied by previous authors. Data from Roedder (1972, Table I).

Liquid CO_2	Solid NaCl	Solid KCl	Solid Carbonate	Organics	Others
...	...	...	...	...	...
X	X	X	...	...	hem
...	...	...	...	...	H_2S
X	X	...	...	...	...
...	X	...	...	...	...
X	...	...	...	...	...
X	...	...	...	...	...
X	...	...	...	...	...
X	X	X	X	...	...
X	X	X	X	...	...
...	...	...	...	...	X
...	X	...	...	...	...
X	...	...	...	...	...
...	...	...	...	...	...
...	...	...	...	...	...
...	X	...	...	...	...
X	X	X	(?)	...	X
...	...	...	...	...	...
...	...	...	...	...	...
...	...	...	...	...	...
...	...	...	...	...	...
X	X	X	X	...	X, hem
X	X	X	X	...	X, hem, H_2S
...	...	...	...	...	...

X = present; ... = absent; hem = hematite.

required even though a pressure correction is not, or because the veins formed in a slight metamorphic lull between metamorphic Phases I and II (Fig. 37). Another possibility is that the supposed time of their formation is incorrect and they really crystallised in Phase IIb of metamorphism.

Previous work. Table 21 summarises (after Roedder, 1972) previous identifications of phases in inclusions in quartz veins from metamorphic rocks. Carbon dioxide is present in about half the veins listed, solid NaCl in slightly less than half and solid KCl in about a quarter. Clearly the phases identified above are quite commonly present in comparable veins, though their derivation from a two-phase, immiscible fluid mixture may be less common. Examples of immiscibility of aqueous and carbonic phases have been given by Little (1960) and Roedder and Coombs (1967).

Fluid Inclusions in the Gold-Quartz Veins

Inclusions in suites of representative samples from the Ptarmigan No. 1 and Tom No. 3 veins have been studied by petrographic and heating-stage methods. The inclusions in these quartz samples are generally smaller and less suitable for study than those in the irregular quartz veins and homogenisation determinations are accordingly more difficult.

The inclusions. Like the irregular veins, these contain innumerable tiny inclusions (Plate 5C). Rare ones are up 15-25 microns in size, rather more are about 5-10 microns and the vast majority are much less than 5 or even 1-2 microns. Solid inclusions are rather more common than in the irregular veins but the types of

TABLE 22 : Descriptions of gold-quartz vein samples used in the fluid inclusión study.

Location	Sample No.	Description
Ptarmigan	1	Late(?), vuggy quartz with galena and sphalerite.
	2	Barren quartz of dominant vein type.
	3	Barren, milky, massive quartz with surface Fe-staining. Dominant vein quartz.
	4	Milky vein quartz. Massive, but containing a few small vugs filled with sphalerite.
	5	Massive, barren, light grey quartz typifying abundant vein quartz.
	6	Barren, sugary grey quartz. Granular.
Tom	8	Massive, barren, grey quartz.
	9	Massive barren quartz.
	10	Massive, barren, mottled grey and white quartz.
	11	Gossanous, vuggy, pyritic quartz from margin of vein.
	12	Clear grey quartz, slightly vuggy with minor sulphide.

fluid inclusions present are the same. The definition, illustration and description of the inclusion types is therefore exactly the same as given (above) for the irregular veins and no further description is necessary.

Table 22 gives the locations and descriptions of the samples studied. Table 23 is a summary of the types and relative abundances of inclusions observed in these samples. Liquid-rich inclusions are the most abundant in both primary and secondary categories. Solid daughter minerals are rare in primary liquid-rich inclusions but occur in the secondaries in some samples. No daughters have been observed in vapour-rich inclusions which are present in most samples as primary inclusions but much less commonly as secondaries. Vapour-filled primaries are always present and vapour-filled secondaries commonly so. Carbon dioxide has been observed in both primary and secondary inclusions but it is usually present in small amounts and must therefore be listed as being only possibly present. In addition to definite CO_2-bearing inclusions, there are those of Types III and IV which probably contain CO_2. Clearly the types and abundances of inclusions are very similar to those in the irregular quartz veins (compare Tables 19 and 23). Solid daughters are marginally less common and vapour-filled primaries are more ubiquitous in the gold-bearing veins but otherwise the inclusion suites are indistinguishable.

Similarly, the different types of quartz contain very similar suites of fluid inclusions (Table 23). The only noticeable differences are that the late, vuggy, quartz samples contain

TABLE 23 : Types and approximate abundances of fluid inclusions observed in the gold-quartz veins. See notes with Table 19.

Quartz type	Sample number	I Liquid-rich		II Daughters		III Vapour-rich		IV Vapour-filled		V Liquid CO_2		VI Liquid-filled	
		P	S	P	S	P	S	P	S	P	S	P	S
Massive, barren, vein quartz.	Ptarm 2	XXX	XXX		(?)	XX		(?)	XX	XX	?		
	Ptarm 3	XXX	XXX			X		X		X	?		
	Ptarm 5	XXX		XX				XX	XX		?		
	Tom 8	XXX	XXX			X		X		?			
	Tom 9	(?)	XXX	(?)		XX		XX		X			X
	Tom 10	XX	XX			X		X	XX	?			X
Intermediate	Ptarm 6	XXX	XXX					XX	XX		?		X
	Ptarm 4	XXX	XXX	(?)	XX	X		XX	XX	XX	?		X
Late, vuggy, sulphide-rich quartz.	Tom 12	XX	XX	X	XX	X	X	XXX	XX	?			X
	Ptarm 1	XX	XXX			X	X	XX	X	?	XX		
	Tom 11	XXX	XXX				(?)	X	XX		(?)		

KEY: As for Table 19

vapour-rich secondary inclusions while the more massive barren quartz does not.

Homogenisation studies. The gold-quartz veins are highly unsuitable for heating-stage examination. All the inclusions are very small and primary inclusions are both rare and difficult to recognise. In twelve doubly polished quartz plates only 59 useful inclusions have been found (Fig. 47) and homogenised.

The typical, massive, sulphide-free quartz of the veins (probably including sample Ptarm. 4) is particularly free of usable inclusions. Four primary inclusions in quartz of this type (and three probable pseudo-secondaries) homogenised in the range 240-310° C. (Fig. 47) but most showed very little change on heating to 350° C. Two secondaries and one probable secondary inclusion homogenised between 120-150° C.

The two samples of late, vuggy, sulphide-bearing quartz contain rather larger numbers of usable inclusions. (Sample Ptarm. 6, which was classified as 'uncertain' in Table 23, may also belong to this category.) In these two rocks, 17 of the 22 primary inclusions homogenised did so between 140-220° C. Several inclusions, of both liquid-rich and vapour-rich categories, displayed little response to heating.

Thus the limited data available suggest that homogenisation behaviour in the gold-bearing veins is very similar to that established for the irregular veins. For the main vein-forming quartz homogenisation of primary inclusions occurs at rather higher temperatures (ca. 240-310° C.) than in the later, sulphide-bearing quartz (140-220° C.) which is reputed to contain the gold (see above). Most

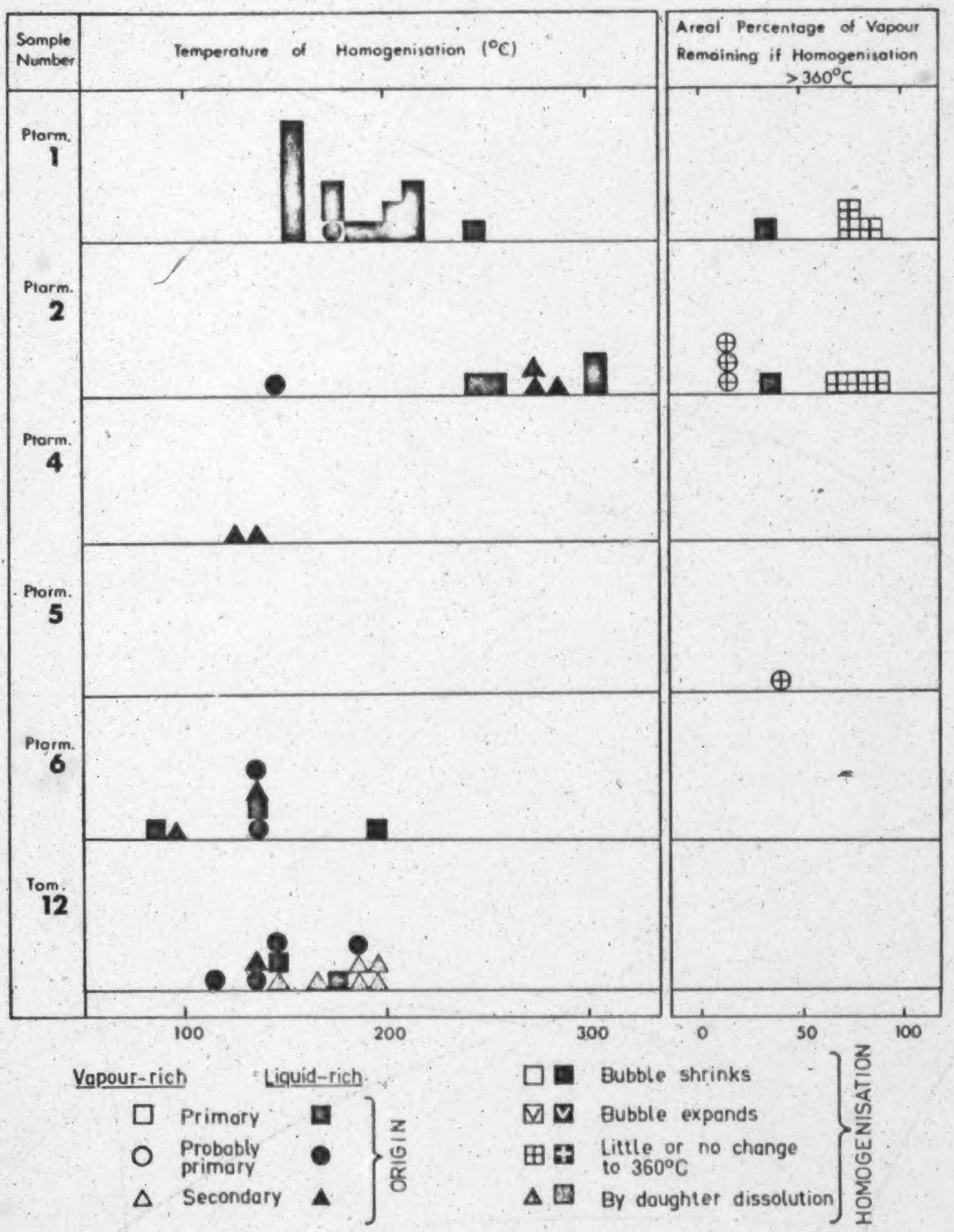

FIGURE 47 : Illustrating the response to heating exhibited by fluid inclusions in the gold-quartz veins.

of the secondary inclusions in both quartz types homogenised in the range (120-200° C.).

Salinity. Table 23 shows that the presence of daughter salts is erratic, even within one quartz type. Only single cubes have been observed and no inclusions contain more than one daughter. All the observed cubes are probably halite but this cannot be proven without freezing apparatus.

The salinity can only be crudely determined with the available data. The primary inclusions in the massive, barren quartz are apparently undersaturated at room temperature but probably are saline, perhaps in the range 15-25 wt. % NaCl. Solid daughters are more common in the secondary inclusions but their presence is still erratic. Of the late, vuggy quartz samples, only one contained abundant solid daughter material and Table 24 gives some crude salinity data for this sample. Apparently the maximum salinity attained by these fluids was about 31 wt. % equivalent NaCl.

The vein-forming fluids. The arguments presented above to show that the irregular veins formed from an immiscible mixture of CO_2-rich and H_2O-rich fluids apply equally to the gold-bearing veins. The salinity of the hydrous phase was generally moderate (perhaps 20 wt. % NaCl) but there were sporadic influxes of more saline fluids (up to about 31 wt. % NaCl). No consistent distinction between the fluids of the massive barren quartz and that of the later, vuggy, sulphide-bearing quartz has been observed.

Absolute temperatures. It follows that the homogenisation data for these veins should be interpreted according to the model of Smith and Little (1959). The data are limited in amount but suggest,

TABLE 24 : Approximate salinity data for (saturated) fluid inclusions in the late(?) sulphide-rich phase of a gold-quartz vein.

Sample No.	Primary or Secondary (P or S)	Dissolution Temperature (^{o}C.)	Inferred* Salinity (wt. % equivalent NaCl)
Tom 12	S	165	30
	S	192	31
	S	140	29
	S	187	31
	(?)S	180	30.5
	(?)S	193	31

*After Keevil (1942).

on this model, that the main portion of the veins were deposited at about 250° C. while the vuggy, sulphide-rich quartz was deposited at about 150° C.

Previous work. Table 25 lists the phases identified in previous studies of gold-quartz veins. Liquid CO_2 is a very common phase, occurring in nearly half of the recorded rocks. Solid daughter minerals are apparently rare. Thus the nature of the fluid identified above is typical of previous descriptions of gold-quartz veins.

Gold deposits apparently very similar to these have been described by Koltun (1965). He found a similar variety of inclusions including three-phase inclusions with CO_2 and noted a "fair variety of phase volumes." These veins were, however, formed at lower pressures than probable for the Yellowknife deposits. Koltun concluded that vein formation began at about 420-370° C. with the formation of quartz-cassiterite-scheelite veins and that temperature declined steadily thereafter. Milky-white quartz with pyrite, tourmaline, ankerite and other minerals (perhaps equivalent to the massive quartz of the Tom and Ptarmigan veins) formed from 310-180° C., followed by quartz with gold and the bulk of the sulphides (including pyrite, galena and sphalerite) at 180-150° C. This last stage seems comparable with the late, vuggy, sulphide-rich phase of the Yellowknife veins. At still lower temperatures (120-70° C.) Koltun observed another phase of quartz-sulphide-gold mineralisation followed by calcite and pyrite at 100-30° C. These two phases have not been observed at Yellowknife, at least in veins in the meta-sediments.

Although the first and last of the phases observed by Koltun have not been observed in the Tom and Ptarmigan veins there

TABLE 25 : Phases previously identified in inclusions in the quartz of gold-quartz veins. (After Roedder, 1972.)

Liquid CO_2	Solid NaCl	Solid KCl	Solid Carbonate	Organics	Others
X	...	...	...	...	...
...	...	...	...	...	...
X	...	...	...	...	...
...	X	...	...	...	...
X	...	...	...	...	...
X	...	...	...	...	...
...	...	...	...	...	...
...	...	...	...	...	...
...	...	...	...	...	...
X	X	X	...	...	...
X	...	...	...	...	...
X	...	...	...	...	...
...	...	...	...	...	...
...	...	...	...	...	...
...	...	...	...	...	...
X	...	...	...	...	...
...	...	...	...	...	...
...	...	...	...	...	...
...	...	...	...	...	...

is a remarkable similarity of mineralogical paragenesis and fluid inclusion types. The absolute temperatures cited by Koltun were corrected by about 34^{o} C. for pressure, which has not been done here. Considering this, the temperature sequence of equivalent mineralisation phases is also very similar.

GOLD IN THE COUNTRY ROCKS

There is little information on the gold contents of unmineralised country rocks at Yellowknife. Some data have been given by Boyle (1961; see Table 26) and these may be supplemented by analyses of rocks from an Archaean greenstone complex in Manitoba (Stephenson and Ehmann, 1971; Table 26). Gold is apparently present in both the greenstones and the meta-sediments but is not enriched in these rocks relative to the others. The noteworthy feature of Table 26 is that the hypabyssal dykes seem commonly to contain much more (x10) gold than the other rocks. Stephenson and Ehmann concluded tentatively that the mafic intrusions were the source of the gold in the Rice Lake area. However there is no known spatial relationship between such intrusions and the ore deposits at Yellowknife.

ORIGIN OF THE GOLD DEPOSITS

The previous theories for the origin of these gold deposits were reviewed in the introduction to Part IV (above). The structural and fluid inclusion evidence presented above leads this author to suggest the following model for the origin and evolution of the deposits. It is derived principally from work on deposits in the meta-sediments but can probably be extrapolated to those in the meta-volcanic rocks.

TABLE 26 : Published data on the gold contents of rocks of Archaean greenstone belts in Canada.

Yellowknife (N. W. T.)		Rice Lake (Manitoba)	
	Au(p. p. m.)		Au(p. p. b.)
Greenstones	0.01, 0.008	Meta-basalts	0.2
Basic dykes	<0.01	Mafic intrusions	18.2
Tuffs	0.01 to 0.07		
Mêta-pelite	0.01		
Meta-greywacke	<0.01		
Quartz-mica schist	0.01		
W. Granodiorite	<0.01	Quartz diorite	1.1, 1.9
Qtz-fsp porphyry	0.10	Qtz-fsp porphyry	6.1, 1.1
Prosperous Lake Granite	0.01	Qtz monzonite	0.3
Pegmatites	<0.01		
Boyle (1961)		Stephenson and Ehmann (1971)	

The gold-bearing structures and their contained minerals were formed in the waning stages of deformation and metamorphism when relaxation of deforming stresses allowed the formation of dilatant zones controlled by the remnant deformational forces. Deformation in each structural domain was related to batholith emplacement and it seems probable that stress relaxation was due to cessation of batholith inflation. The deposits in the meta-volcanic rocks therefore formed immediately following emplacement of the Western Granodiorite (see also Robertson and Cumming, 1968) and those in the metasediments slightly later, following intrusion of the Prosperous Lake pluton (see also Fortier, 1946).

These dilatant zones formed channelways for the upward(?) passage of hot siliceous solutions which deposited quartz, sulphides and gold. There is no systematic spatial relationship between between gold-bearing veins and any batholith and they are randomly widespread in the region. This implies that suitable fluids were present throughout and that deposition of quartz and gold occurred only where essential structural, physical and chemical conditions operated. The ore-forming fluids were metamorphic pore-fluids which migrated into structurally determined zones as soon as relaxation of deforming pressure allowed this to happen. The nature of the fluids themselves is compatible with such a derivation.

The gold-bearing fluid was an immiscible mixture of an aqueous phase of moderate salinity with a CO_2-rich phase saturated in water. Such a fluid would be expected to form during metamorphism of a sedimentary pile of this type. Prolonged dehydration accompanying metamorphism would provide abundant water. Graphite is present in the meta-sediments and French (1966) has shown that fluids in equilibrium with graphite must contain abundant CO_2. Boyle (1961) reports Cl concentrations of 100-400 p.p.m. in the meta-sediments and it seems entirely reasonable that chloride ions should be concentrated in the pore-fluid leading directly to the dissolution of Na and probably K in the fluid phase (e.g. see Burnham, 1967). Pyrrhotite and pyrite are the main sulphides present in the meta-sediments and Seward (1973) has shown that solutions buffered by this assemblage can dissolve appreciable quantities of gold over a wide range of pH. Since most of the gold in the meta-sediments is contained in sulphides (Boyle, 1961) prolonged coexistence of fluids with these sulphides is very likely to have dissolved both sulphide and gold.

There has been extensive discussion in the literature on the hydrothermal transport of gold and the nature of the solutions which carry it. There are two basic schools of thought: (1) That gold is dissolved and transported in acid chloride solutions (Ogryzlo, 1935; Krauskopf, 1951; Helgeson and Garrels, 1968) particularly under oxidising conditions (Barnes and Czamanske, 1967) and (2) That it is carried in alkaline sulphide solutions (Ogryzlo, 1935; Barnes and Czamanske, 1967; Boyle, 1969; Weissberg, 1970). Most recently Seward (1973) has pointed out that most hydrothermal ore fluids are probably close to neutral in pH and has demonstrated that thio-complexes of gold, particularly $Au(HS)_2^-$, are of great importance, especially in neutral solutions. He concluded that gold is probably transported as both thio- and chloro- complexes and is deposited by changes in temperature, pressure, pH, oxidation potential and(or) total sulphur concentration.

In the Burwash Fm. the initial stages of quartz vein formation did not precipitate gold. The later, gold-bearing phases of the quartz mineralisation contain more sulphide than the preceding phases and were probably deposited at about 150° C. from a two-phase fluid whose brine phase contained considerable quantities of base metals, sulphur and gold. The earlier, barren quartz of the gold-bearing veins was deposited from a very similar brine-CO_2 two-phase fluid at about 250° C. but contains much less sulphide and gold. The irregular quartz veins were deposited from similar fluids over a temperature range from about 160-260° C. (Fig. 46) but perhaps at higher pressure than the gold-bearing veins. They contain only traces of sulphide and apparently no gold.

It appears, therefore, that sulphur was the critical factor in the formation of gold mineralisation, either by its absence from the earlier solutions or by its precipitation from the later ones. Gold chloro-complexes may have been present but the gold was apparently not deposited from these because there is no detected difference between the salinities of the barren and gold-bearing quartz. Thus it was the decomposition of gold thio-complexes which led to precipitation of both sulphides and gold. Since the pH of the solutions is unknown, one cannot judge which thio-complex was involved but it seems likely to have been the $Au(HS)_2^-$ suggested by Seward (1973) or the AuS^- of Barnes and Czamanske (1967). The reason for the decomposition of the complex and consequent deposition of the gold is uncertain. Boyle (1969) has argued that the reduction of pressure in dilatant zones was the critical factor but Seward (1973) believed it to have only a minor effect. It seems probable that fluids passing in such channelways are derived from a variety of sources and therefore, when mixed, have different chemical properties from those of any particular supply of metamorphic fluids. Thus gold-bearing fluids equilibrated with reduced meta-sediments might be introduced suddenly into dilatant zones of very different oxidation potential or acidity. Such changes could produce precipitation of both gold and sulphide. Reduction of temperature would have the same effect as there is a marked decline in the solubility of most of the gold-bearing species (Seward, 1973, Fig. 11) below about 200^{o} C., which agrees fairly well with the suggested depositional temperatures of the gold-bearing quartz.

This model calls on the dissolution of gold from the country rocks during metamorphism but does not explain the ultimate origin of the gold. This author has no new data on this subject but is impressed by the anomalously high gold content of the hypabyssal dyke rocks in the area (Table 26). The basic dykes in the meta-volcanic rocks are thought to have been penecontemporaneous with the lavas (e.g. Henderson and Brown, 1966) and therefore were potential source rocks during the metamorphism which produced the gold-bearing veins (see Stephenson and Ehmann, 1971). It was suggested in Part II (above) that the sediments were derived from volcanic and hypabyssal rocks which formed island clusters above the present granodiorite batholiths. If the high gold contents of the quartz-feldspar porphyries and tuffs (Table 26) is representative of many rocks in this phase of plutonism then the sediments derived from them would contain abundant gold.

Thus the gold deposits are thought to have originated by a lateral secretion mechanism of the type suggested by Boyle (1961 and other papers). This conclusion is directly at variance with the various authors (e.g. Henderson and Jolliffe, 1939; Coleman, 1957; McConnell, 1964; Ames, 1962; Chary, 1971) who concluded that the gold was deposited from hydrothermal waters of magmatic origin. It is in agreement with the suggestions of Folinsbee (1942) insofar as the deposits were metamorphically generated in the waning stages of metamorphism but differs from his suggestion that they were formed by retrogressive or hydrothermal metamorphism.

PART V: SUMMARY AND CONCLUSIONS

CONCLUSIONS OF LOCAL APPLICABILITY

Structure

The structural geology of the area has been investigated at a reconnaissance level. The area is structurally inhomogeneous and can be divided, on the basis of orientation and style of folds and cleavage, into five small structural domains whose approximate extents are shown in Fig. 4. Three of these domains are spatially and genetically related to batholith emplacement while the fourth and fifth are considered to be due to the interaction of two others. Superimposition of folding phases is generally apparent in only one of these domains (the Island Lake domain) but there are some suggestions of multiple deformation in the Yellowknife Bridge and Hay Lake Domains. The existence of these domains testifies to the action of deformational forces of very limited extent and a batholith inflation model (Clifford, 1972) accounts for many of the observed features. The structural characteristics of the individual domains may be seen from Figs. 5 to 11 and have been summarised in Part II above.

These structural observations, together with previous geochronology, lead to the tectonic history presented in Table 1 and to the evolutionary model (after Glikson, 1972) represented schematically by Fig. 12. The region evolved from Archaean oceanic crust in a single tectonic cycle in which all events were genetically related. Emplacement of the batholiths was the critical causative factor throughout the cycle being directly related to sedimentation, deformation and metamorphism.

The Prosperous Lake Aureole

The Prosperous Lake pluton is surrounded by a wide (ca. 10 km.) metamorphic aureole with some paragenetic complexities but approximating an Abukuma facies series. The following pro-grade succession occurs in the pelitic and semi-pelitic rocks: (1) *Chlorite Zone*. Rocks of this grade have not been observed in the study area but have been reported by other authors (e.g. Henderson, 1972). They are very fine-grained phyllites and semi-schists characterised by the stable coexistence of chlorite, muscovite and ilmenite and the absence of biotite. (2) *Biotite Zone*. The biotite isograd has not been observed but there is a wide biotite zone in which biotite is present in every rock which contained the essential biotite-forming reactants (see below). This means that all Burwash Fm. rocks which have escaped complete hydrothermal retrogression contain biotite but Walsh Fm. rocks within the biotite zone do not. Biotite and rutile porphyroblasts in a chlorite-muscovite-ilmenite matrix inherited from the chlorite zone (Plate 3) are the characteristics of the biotite zone, which is sharply terminated by the cordierite isograd. (3) *Cordierite Zone*. In a short pro-grade interval (Fig. 30) cordierite porphyroblasts appear in all rocks which contained the essential cordierite-forming reactants chlorite and muscovite. Cordierite is present throughout the rest of the pro-grade sequence. The presence of cordierite and the absence of garnet characterises the zone. Andalusite occurs sporadically, mainly in the upper cordierite zone. (4) *Cordierite-garnet 'Zone'*. In the higher grades near the pluton (Fig. 36) is a large area in which cordierite and garnet coexist. The garnet is, however, paragenetically earlier than the cordierite and in some rocks shows signs of unstability and corrosion. Andalusite occurs sporadically. Cummingtonite and, less commonly, gedrite occur in some rock types. Problems of paragenesis and spatial distribution make the status of garnet in the pro-grade succession uncertain.

(5) Sillimanite-staurolite 'Zone'. Incipient sillimanite occurs at the highest metamorphic grades in rocks adjacent to the pluton (Fig. 36). It is present in complex assemblages associated with corroded staurolite of an earlier paragenesis.

This zonation has been interpreted in terms of a single metamorphic episode of gradually changing character (Fig. 37). Initially a moderate pressure (3-5 kb.) regime of regional extent prevailed, probably with metamorphic grade increasing North-Eastwards from Yellowknife Bay. Pressure gradually decreased and the 'thermal dome' associated with the Prosperous Lake pluton superimposed a more thermal facies series (2.5 to 3.5 kb.) on the existing assemblages. Further pressure reduction and slow cooling led to late metamorphic changes after the metamorphic climax. Hydrothermal retrogression was the last event, being separate from the main metamorphic cycle and related to faulting and diabase intrusion.

Biotite Zone Mineralogy

Rocks of the biotite zone are comprised of the following minerals: biotite -- chlorite -- muscovite -- quartz -- plagioclase with minor amounts of rutile, ilmenite, K-feldspar, pyrrhotite, pyrite and chalcopyrite. The mineral chemistry of the principal phases is summarised in Figs. 16 to 23. There are very restricted ranges of composition within which subtle differences due to metamorphic grade and host-rock chemistry may be discerned.

The biotites are normal aluminous biotites with roughly equal amounts of Mg and Fe in the octahedral site. Those in meta-greywackes display compositional trends with grade but those in meta-pelites do not (Fig. 19). The muscovites are slightly phengitic and approach ideality at higher metamorphic grades (Fig. 20). There is little differentiation between muscovites of meta-pelites and meta-greywackes in the Burwash Fm. but those of the Walsh Fm. are subtly distinct. The chlorites are ripidolites which display little compositional variation with grade (Figs. 21 and 22). The plagioclases of the Walsh Fm. are very sodic. Those in Burwash Fm. meta-greywackes have a wide range of composition at low grades but display progressive equilibration towards intermediate compositions at higher grades (Fig. 23).

Controls of Biotite Zone Mineralogy

The analyses reveal a complex inter-play of factors controlling mineral compositions. The order of dominance of these controls varied for different mineral groups, for different host-rocks and even at different metamorphic grades. The effects of pressure and differing mineral assemblages were minimised by selection of a mineralogically similar suite of rocks from an aureole. Metamorphic temperature controlled biotite composition but only where permitted to do so by the bulk-rock composition, i.e. in meta-greywackes but not in meta-pelites (Fig. 19). In some instances (e.g. K) this means that there is no apparent bulk compositional control at low grades but an obvious one at higher grades. Compositional changes in muscovites were determined almost entirely by metamorphic grade (Fig. 20). The influence of bulk composition was small within the Burwash Fm. but noticeable between the Walsh and Burwash rocks. Metamorphic grade apparently had little influence on chlorite (Fig. 22), its composition being determined by the necessity to take up all Mg in the rock because no other Mg-rich phase was present. The principal control was therefore the Mg/Fe ratio of the host-rock. For the plagioclases an homogenisation process was induced by increased temperature (Fig. 23) but the final composition of the homogenised plagioclase was determined by the Ca content of the rock because no other Ca-rich phase was present.

The Origin of Biotite

The textural features of the biotite-zone rocks (Plate 3) and the mutual variation of the modal percentages (Fig. 25) suggest that biotite grew by a complex reaction approximated by the formula

$$\text{Chlorite} + \text{Muscovite(1)} + \text{Ilmenite} \longrightarrow$$
$$\text{Biotite} + \text{Muscovite(2)} + H_2O + [\text{Rutile, Qtz, K-feldspar}]$$

The reaction occurred by chemical modification of chlorite which was simply consumed in the reaction without any compositional modification of the chlorite which remained. Ilmenite was similarly consumed (Fig. 27). Muscovite, however, was modified in composition while being partially consumed. As more biotite was produced the muscovite became depleted in K and (Mg+Fe+Mn) but enriched in Ti (Fig. 26).

This is interpreted to mean that decomposition of muscovite yielded rather less K and (Mg+Fe+Mn) and rather more Ti than could be accommodated in the biotite so that the excesses and deficiencies were re-distributed in the remaining muscovite. The composition of the biotite produced depended somewhat on the extent of reaction (Fig. 24), implying that there were scarcities of some elements which caused deviations from the optimum biotite composition as more biotite was formed. Rutile was not produced in a fixed ratio to biotite (Fig. 27), apparently being formed only in amounts necessary to fix Ti excesses which could not be accommodated in biotite. Quartz and K-feldspar may similarly have been produced only as necessary to fix excess components rather than in fixed stoichiometric ratios.

The Origin of Cordierite

Textural relations (Plate 4) and micro-probe analyses (Fig. 32) of minerals from the cordierite isograd (Fig. 30) indicate that cordierite was formed by a modification of a well-known reaction:

$$\text{Chlorite} + \text{Muscovite(1)} + \text{Quartz} + \text{Biotite(1)} \longrightarrow \text{Cordierite} + \text{Biotite(2)} + H_2O + \left[\text{Ilmenite, Chlorite, Muscovite(2)}\right]$$

This differs from the commonly reported reaction in that biotite was present before the appearance of cordierite. As a result the existing biotite was compositionally modified rather than a new biotite being formed (Fig. 32). Cordierite appeared at the isograd in all those rocks which contained the essential reactants, notably chlorite and muscovite. The coexistence of these minerals was determined by the previous reaction history of the rock and there was no direct control by bulk composition on the appearance of the cordierite. The cordierite isograd represents temperatures of 550±20° C. @ ca. 3 kb.

Origin of the Gold Deposits

Three of the gold deposits in the Burwash Fm. have been examined (Figs. 38, 39 and 40) and sampled. The relationship of these deposits to the characteristic structures of the structural domains in which they occur (Fig. 41) indicate that they were deposited during the relaxation stage of deformation in each domain. Dilatant zones permitted by this relaxation but still controlled by the remnant deforming forces channelled hot siliceous fluids which deposited quartz and gold. The fluid inclusions are very varied (Fig. 43) and represent a two-phase immiscible mixture of a brine of moderate salinity and a CO_2-rich fluid. The nature of this fluid is entirely compatible with an origin as pore-fluids in the country-rocks during metamorphism. The deposits were formed by lateral secretion of these metamorphic fluids into dilatant zones. The initial stages of quartz vein formation occurred at about 250° C. from two-phase fluids which either contained little gold and sulphide or were not constrained to precipitate them. The later fluids contained or precipitated much more sulphide and gold and deposited them at rather lower temperatures (probably about 150° C.). The common association of gold and sulphides suggests that sulphide was the essential complexing agent for transporting the gold rather than chloride.

CONCLUSIONS OF GENERAL APPLICABILITY

The work reported above has led the author to the following conclusions of more general application.

Evolution of Cratons

This area seems best explained by an evolutionary model of the type suggested by Glikson (1972) and Green and Baadsgaard (1971) in which the craton was formed during a single cycle of vulcanism, plutonism, sedimentation, deformation and metamorphism. A model has been suggested in which extensive elongate 'island clusters' represented the upper levels of the batholiths now exposed, continuously shedding detritus onto oceanic crust in the intervening basins while upward migration of the batholithic masses beneath initiated deformation. It seems, further, that the continued upward movement and lateral inflation of these batholiths were the cause of much of the tectonic history which followed. Such a mechanism appears equally applicable to the extensive sediment-filled basins of the Slave Craton and the narrow synclinal keels of greenstone in the Rhodesian and Transvaal Cratons.

Controls of Mineral Composition

The factors which control the composition of minerals forming in metamorphic rocks are very numerous. They may operate simultaneously or individually, in similar or opposite senses, on some mineral groups or on all. One may modify or even prevent the operation of another in certain circumstances, but this does not mean that the same priorities will apply in other circumstances. The identification of these factors will be a long and complicated process but a suggested scheme of sub-division has been presented in Part III above: In essence it is as follows:

1. Permissive Controls
    - Energetic (stability fields)
    - Crystallographic (required elements available)
2. Modifying Controls
    - Partition Equilibria
    - Electrical Neutrality
    - Temperature
    - Pressure
    - Bulk composition
    - Modal proportions
    - Reaction relationships
    - Others

The Biotite Isograd

Under some circumstances, at least, the titaniferous oxides are essential to the formation of biotite. This may explain the common discrepancy between the Ti contents of suggested reactant assemblages and the biotite produced.

Mather (1970) demonstrated that the celadonite content of muscovite could produce a bulk compositional control of the grade at which biotite was formed. In low-pressure facies series, however, the biotite isograds of different rock compositions will occur at very similar grades provided that the rocks are mineralogically similar.

Stoichiometry of Reactions

In the above studies of both the biotite-forming and the cordierite-forming reactions it became apparent that the minor reaction products were not always formed in the same amounts relative to other products (e.g. Figs. 27 and 35). Rutile, for example, is present in smaller amounts in more biotitic rocks (Fig. 27). One particular reaction in a single rock must be governed by stoichiometry but it seems that such reactions differ in detail from one rock to another. Thus there is, strictly, not one reaction but a set of similar reactions whose exact nature is determined by the relative amounts of reactant phases present. The minor products differ accordingly in relative amounts and the major products can apparently differ slightly in composition (Fig. 24).

Hydrothermal Transport of Gold

This study provides geological evidence that gold was deposited from sulphide complexes rather than chloride complexes.

BIBLIOGRAPHY

AMES, R. L., 1962. The origin of the gold-quartz deposits, Yellowknife, N.W.T. Econ. Geol. 57, 1137-1140.

ANDERSON, A. T., 1968. The oxygen fugacity of alkaline basalt and related magmas, Tristan da Cunha. Am. J. Sci. 266, 704-727.

ANHAEUSSER, C. R., MASON, R., VILJOEN, M. J., & VILJOEN, R. P., 1969. A reappraisal of some aspects of Precambrian shield geology. Bull. geol. Soc. Am. 80, 2175-2200.

ANHAEUSSER, C. R., ROERING, C., VILJOEN, M. J. & VILJOEN, R. P., 1968. The Barberton Mountain Land: a model of the elements and evolution of an Archaean fold belt. Trans. geol. Soc. South Africa 71, 225-254.

BARAGAR, W. R. A., 1966. Geochemistry of the Yellowknife volcanic rocks. Can. J. Earth Sci. 3, 9-30.

BARNES, H. L. & CZAMANSKE, G. K., 1967. Solubilities and transport of ore minerals. Pp. 334-381 in Geochemistry of Hydrothermal Ore Deposits (ed. Barnes, H. L.). New York: Holt, Rinehart and Winston.

BARTH, T. F. W., 1962. Theoretical Petrology (Second Edition). New York and London: John Wiley and Sons.

BIRD, G. W. & FAWCETT, J. J., 1971. Some metamorphic reactions in the system K_2O-MgO-Al_2O_3-SiO_2-H_2O. Trans. Am. geophys. Un. 52, 377.

BOLDY, J., 1959. Unpublished company report on Cassidy Yellowknife Mines Ltd. to Giant Yellowknife Mines Ltd.

BOYLE, R. W., 1954. A decrepitation study of quartz from the Campbell and Negus-Rycon shear zone systems, Yellowknife, Northwest Territories. Bull. geol. Surv. Can. 30.

BOYLE, R. W., 1955. The geochemistry and origin of the gold bearing quartz veins and lenses of the Yellowknife greenstone belt. Econ. Geol. 50, 51-66.

BOYLE, R. W., 1959. The geochemistry, origin, and role of carbon dioxide, water, sulphur, and boron in the Yellowknife gold deposits, Northwest Territories, Canada. *Econ. Geol. 54*, 1506-1524.

BOYLE, R. W., 1961. The geology, geochemistry and origin of the gold deposits of the Yellowknife district. *Mem. geol. Surv. Can. 310*.

BOYLE, R. W., 1969. Hydrothermal transport and deposition of gold. *Econ. Geol. 64*, 112-115.

BROWN, E. H., 1967. The greenschist facies in part of Eastern Otago, New Zealand. *Contr. Miner. Petrol. 14*, 259-292.

BROWN, E. H., 1968. The Si^{+4} content of natural phengites: A discussion. *Contr. Miner. Petrol. 17*, 78-81.

BROWN, E. H., 1971. Phase relations of biotite and stilpnomelane in the greenschist facies. *Contr. Miner. Petrol. 31*, 275-299.

BURNHAM, C. W., 1967. Hydrothermal fluids at the magmatic stage. Pp. 34-76 in *Geochemistry of Hydrothermal Ore Deposits* (ed. Barnes, H. L.). New York: Holt, Rinehart and Winston.

BUTLER, B. C. M., 1965. Compositions of micas in metamorphic rocks. Pp. 291-298 in *Controls of Metamorphism* (ed. Pitcher, W. S. & Flynn, G. W.). Edinburgh: Oliver and Boyd.

BUTLER, B. C. M., 1967. Chemical study of minerals from the Moine Schists of the Ardnamurchan area, Argyllshire, Scotland. *J. Petrology 8*, 233-267.

CALDER, A. B., 1971. Statistics. Pp. 11-51 in *Modern Methods of Geochemical Analysis*. (ed. Wainerdi, R. E. & Uken, E. A.). New York-London: Plenum Press.

CAMPBELL, N., 1947. Regional structural features of the Yellowknife area. *Econ. Geol. 42*, 687-693.

CHARY, K. N., 1971. *An isotopic and geochemical study of gold-quartz veins in the Con-Rycon Mine, Yellowknife, (N.W.T.)*. M.Sc. thesis. University of Alberta.

CHAYES, F., 1971. *Ratio Correlation*. Chicago: University of Chicago Press.

CHINNER, G. A., 1959. Garnet-cordierite parageneses. *Yb. Carnegie Instn Wash. 58*, 112-113.

CHINNER, G. A., 1960. Pelitic gneisses with varying ferrous/ferric ratios from Glen Clova, Angus, Scotland. *J. Petrology 1*, 178-217.

CHINNER, G. A., 1962. Almandine in thermal aureoles. *J. Petrology 3*, 316-341.

CIPRIANI, C., SASSI, F. P., & SCOLARI, A., 1971. Metamorphic white micas: definitions of paragenetic fields. *Schweiz. miner. petrogr. Mitt. 51*, 259-302.

CLIFFORD, P. M., 1972. Behaviour of an Archean granitic batholith. *Can. J. Earth Sci. 9*, 71-77.

COLEMAN, L. C., 1953. Mineralogy of the Yellowknife Bay area, N.W.T. *Am. Miner. 38*, 506-527.

COLEMAN, L. C., 1957. Mineralogy of Giant Yellowknife gold mineralisation, Yellowknife, N.W.T. *Econ. Geol. 52*, 400-425.

COOKE, H. C., 1946. Canadian lode gold areas (summary account). *Geol. Surv. Can. Econ. Geol. Ser. 15*.

COOPER, A. F., 1972. Progressive metamorphism of metabasic rocks from the Haast Schist Group of Southern New Zealand. *J. Petrology 13*, 457-492.

CRAWFORD, M. L., 1966. Composition of plagioclase and associated minerals in some schists from Vermont, U.S.A., and South Westland, New Zealand, with inferences about the peristerite solvus. *Contr. Miner. Petrol. 13*, 269-294.

DAVIDSON, A., 1967. *Metamorphism and intrusion in the Benjamin Lake map-area, Northwest Territories*. Ph.D. thesis, University of British Columbia.

DAVIDSON, A., 1972. Granite studies in the Slave Province. *Pap. geol. Surv. Can. 72-1A*, 109-115.

DEER, W. A., HOWIE, R. A. & ZUSSMAN, J., 1962. *Rock-forming Minerals, Volume 3 (Sheet Silicates)*. London: Longmans, Green and Co. Ltd.

DEER, W. A., HOWIE, R. A. & ZUSSMAN, J., 1966. *An Introduction to the Rock-forming Minerals*. London: Longmans, Green and Co. Ltd.

DEN TEX, E., 1971. The facies groups and facies series of metamorphism, and their relation to physical conditions in the Earth's crust. *Lithos 4*, 23-41.

DENTON, W. E., 1940. The metamorphism of the Gordon Lake sediments, Northwest Territories. M.Sc. thesis, McGill University.

DEPT. OF INDIAN AFFAIRS AND NORTHERN DEVELOPMENT, 1971. Mines and Minerals North of 60. Mining Activity in the Yukon and the Northwest Territories. Annual publication of the Northern Economic Development Branch, D. I. A. N. D., Government of Canada.

DICKIE, G. J., 1972. A quantitative geologic analysis of Cretaceous and Jurassic oil and gas pools in Alberta. Ph.D. thesis, University of Alberta.

ERNST, W. G., 1963. Significance of phengitic micas from low-grade schists. Am. Miner. 48, 1357-73.

ESKOLA, P., 1914. On the petrology of the Orijarvi region in southwestern Finland. Bull. Comm. geol. Finl. 40.

EVANS, B. W. & GUIDOTTI, C. V., 1966. The sillimanite--potash feldspar isograd in Western Maine, U. S. A. Contr. Miner. Petrol. 12, 25-62.

EVERETT, D. H., 1959. An Introduction to the Study of Chemical Thermodynamics. London: Longmans, Green and Co. Ltd.

FLANAGAN, F. J., 1969. U. S. Geological Survey standards - III. First compilation of data for the new U. S. G. S. rocks. Geochim. cosmochim. Acta 33, 81-120.

FLEISCHER, M., 1969. U. S. Geological Survey standards - I. Additional data on rocks G-1 and W-1, 1965-1967. Geochim. cosmochim. Acta 33, 65-79.

FOLINSBEE, R. E., 1940. Gem cordierite from the Great Slave Lake area. Am. Miner. 25, 216.

FOLINSBEE, R. E., 1941. Optic properties of cordierite in relation to alkalis in the cordierite-beryl structure. Am. Miner. 26, 485-500.

FOLINSBEE, R. E., 1942. Zone facies of metamorphism in relation to the ore deposits of the Yellowknife-Beaulieu region. Ph.D. thesis, University of Minnesota.

FOLINSBEE, R. E., BAADSGAARD, H., CUMMING, G. L. & GREEN, D. C., 1968. A very ancient island arc. Geophys. Monogr. Am. geophys. Un. 12, 441-448.

FOLINSBEE, R. E., KIRKLAND, K., NEKOLAICHUK, A. & SMEJKAL, V., 1972. Chinkuashih--a gold-pyrite-enargite-barite hydrothermal deposit in Taiwan. *Mem. geol. Soc. Am. 135*, 323-335.

FORTIER, Y. O., 1946. Notes on the Yellowknife-Beaulieu region, Northwest Territories. *Pap. geol. Surv. Can. 46-23.*

FRENCH, B. M., 1966. Some geological implications of equilibrium between graphite and a C-H-O gas phase at high temperatures and pressures. *Rev. geophys. 4*, 223-253.

FYFE, W. S., TURNER, F. J. & VERHOOGEN, J., 1958. Metamorphic reactions and metamorphic facies. *Mem. geol. Soc. Am. 73.*

GEOLOGICAL SURVEY OF CANADA, 1901. *Ann. Rept. geol. Surv. Can., 1898, Part R*, 32-33.

GLIKSON, A. Y., 1972. Early Precambrian evidence of a primitive ocean crust and island nuclei of sodic granite. *Bull. geol. Soc. Am. 83*, 3323-3344.

GOODWIN, A. M., 1972. The Superior Province. Pp. 527-623 in *Variations in Tectonic Styles in Canada* (eds. Price, R. A. & Douglas, R. J. W.). *Spec. Pap. geol. Assoc. Can. 11.*

GREEN, D. C., 1968. *Precambrian geology and geochronology of the Yellowknife area, N.W.T.* Ph.D. thesis, University of Alberta.

GREEN, D. C., & BAADSGAARD, H., 1971. Temporal evolution and petrogenesis of an Archaean crustal segment at Yellowknife, N.W.T., Canada. *J. Petrology 12*, 177-217.

GUIDOTTI, C. V., 1969. A comment on 'Chemical study of minerals from the Moine Schists of the Ardnamurchan area, Argyllshire, Scotland', by B. C. M. Butler, and its implications for the phengite problem. *J. Petrology 10*, 164-170.

GULSON, B. L., & LOVERING, J. F., 1968. Rock analysis using the electron probe. *Geochim. Cosmochim. Acta 32*, 119-122.

HAMILTON, W., & MYERS, W. B., 1967. The nature of batholiths. *Prof. Pap. U.S. geol. Surv. 554-C.*

HARKER, A., 1939. *Metamorphism. A Study of the Transformation of Rock-Masses.* (Second Edition) London: Methuen and Co. Ltd.

HELGESON, H. C. & GARRELS, R. M., 1968. Hydrothermal transport and deposition of gold. *Econ. Geol. 63*, 622-635.

HENDERSON, J. B., 1970. Stratigraphy of the Archean Yellowknife Supergroup, Yellowknife Bay-Prosperous Lake area, District of Mackenzie. *Pap. geol. Surv. Can. 70-26.*

HENDERSON, J. B., 1971. A contribution to the structural geology at Yellowknife, District of Mackenzie. *Pap. geol. Surv. Can. 71-1B*, 106-109.

HENDERSON, J. B., 1972. Sedimentology of Archean turbidites at Yellowknife, Northwest Territories. *Can. J. Earth Sci. 9*, 882-902.

HENDERSON, J. B., CECILE, M. P. & KAMINENI, D. C., 1972. Yellowknife and Hearne Lake map-areas, District of Mackenzie, with emphasis on the Yellowknife Supergroup (Archean). *Pap. geol. Surv. Can. 72-1A*, 117-119.

HENDERSON, J. F., 1943. Structure and metamorphism of early Precambrian rocks between Gordon and Great Slave Lakes, N. W. T. *Am. J. Sci. 241*, 430-446.

HENDERSON, J. F. & BROWN, I. C., 1966. Geology and structure of the Yellowknife greenstone belt, District of Mackenzie. *Bull. geol. Surv. Can. 141.*

HENDERSON, J. F. & FRASER, N. H. C., 1948. Camlaren Mine. Pp. 269-272 in *Structural Geology of Canadian Ore Deposits--a Symposium.* Ottawa: Can. Inst. Min. Metall.

HENDERSON, J. F. & JOLLIFFE, A. W., 1939. Relation of gold deposits to structure, Yellowknife and Gordon Lake areas, Northwest Territories. *Trans. Can. Inst. Min. Metall. 42*, 314-336.

HENDERSON, J. F. & JOLLIFFE, A. W., 1941. Beaulieu River, District of Mackenzie, Northwest Territories. *Geol. Surv. Can. Map 581A.*

HERMES, O. D., 1973. Paragenetic relationships in an amphibolitic block in the Franciscan terrain, Panoche Pass, California. *J. Petrology 14*, 1-32.

HESS, P. C., 1969. The metamorphic paragenesis of cordierite in pelitic rocks. *Contr. Miner. Petrol. 24*, 191-207.

HEY, M. H., 1954. A new review of the chlorites. *Mineralog. Mag. 30*, 277-292.

HEYWOOD, W. W. & DAVIDSON, A., 1969. Geology of Benjamin Lake map-area, District of Mackenzie. Mem. geol. Surv. Can. 361.

HIETANEN, A., 1967. On the facies series in various types of metamorphism. J. Geol. 75, 187-214.

HIRSCHBERG, A. & WINKLER, H. G. F., 1968. Stabilitatstengiebungen zwischen chlorit, cordierit, und almandin bei der metamorphose. Contr. Miner. Petrol. 18, 17-42.

HOFFMAN, P. F. & HENDERSON, J. B., 1972. Archean and Proterozoic sedimentary and volcanic rocks of the Yellowknife-Great Slave Lake area, Northwest Territories. XXIV Internat. Geol. Congress Guidebook A-28.

HSU, L. C., 1968. Selected phase relationships in the system Al-Mn-Fe-Si-O-H : A model for garnet equilibria. J. Petrology 9, 40-83.

HUTCHINSON, R. W., 1955. Regional zonation of pegmatites near Ross Lake, District of Mackenzie, Northwest Territories. Bull. geol. Surv. Can. 34.

JAMES, H. L., 1955. Zones of regional metamorphism in the Precambrian of Northern Michigan. Bull. geol. Soc. Am. 66, 1455-1488.

JOLLIFFE, A. W., 1936. Yellowknife River area, Northwest Territories. Pap. geol. Surv. Can. 36-5.

JOLLIFFE, A. W., 1937. Mineral possibilities of the Northwest Territories. Trans. Can. Inst. Min. Metall. 40, 663-677.

JOLLIFFE, A. W., 1938. Preliminary report, Yellowknife Bay-Prosperous Lake area, Northwest Territories. Pap. geol. Surv. Can. 38-21.

JOLLIFFE, A. W., 1942. Yellowknife Bay, District of Mackenzie, Northwest Territories. Geol. Surv. Can. Map 709A.

JOLLIFFE, A. W., 1944. Rare-element minerals in pegmatites, Yellowknife-Beaulieu area, Northwest Territories. Pap. geol. Surv. Can. 44-12.

JOLLIFFE, A. W., 1946. Prosperous Lake, District of Mackenzie, Northwest Territories. Geol. Surv. Can. Map 868A.

JOLLIFFE, A. W., 1948. The north-western part of the Canadian Shield. XVIII Internat. Geol. Congress, Part 13, 141-149.

KAMINENI, D. C. & WONG, A. S., 1973. Gedrite from the Yellowknife-Beaulieu region, District of Mackenzie, N.W.T. Can. Miner. 11, 1012-1015.

KANEHIRA, K., BANNO, S., & NISHIDA, K., 1964. Sulfide and oxide minerals in some metamorphic terranes in Japan. Jap. J. Geol. Geogr. 35, 175-191.

KEEVIL, N. B., 1942. Vapour pressures of aqueous solutions at high temperatures. J. Am. Chem. Soc. 64, 841-850.

KELLY, W. C. & TURNEAURE, F. S., 1970. Mineralogy, paragenesis and geothermometry of the tin and tungsten deposits of the Eastern Andes, Bolivia. Econ. Geol. 65, 609-680.

KLEIN, C., 1964. Cummingtonite-grunerite series: a chemical, optical, and X-ray study. Am. Miner. 46, 642-653.

KOLTUN, L. I., 1965. Application of mineralothermometric analysis in studies of the origins of certain gold deposits in Ural. Pp. 426-457 in Research on the Nature of Mineral-forming Solutions (ed. Yermakov, N. P.). New York: Pergamon Press.

KRAUSKOPF, K. B., 1951. The solubility of gold. Econ. Geol. 46, 858-870.

KRETZ, R., 1968. Study of pegmatite bodies and enclosing rocks, Yellowknife-Beaulieu region, District of Mackenzie. Bull. geol. Surv. Can. 159.

KRETZ, R., 1970. Variation in the composition of muscovite and albite in a pegmatite dyke near Yellowknife. Can. J. Earth Sci. 7, 1219-1235.

KRETZ, R., 1973. Kinetics of the crystallisation of garnet at two localities near Yellowknife. Can. Miner. (in press).

LAMBERT, R. St. J., 1959. The mineralogy and metamorphism of the Moine Schists of the Morar and Knoydart Districts of Inverness-shire. Trans. R. Soc. Edinb. 63, 553-588.

LAMBERT, R. St. J. L., 1972. The metamorphic facies concept--continued. XXIV Internat. Geol. Congress, Part 2, 100-108.

LANG, A. H., GOODWIN, A. M., MULLIGAN, R., WHITMORE, D. R. E., GROSS, G. A., BOYLE, R. W., JOHNSTON, A. G., CHAMBERLAIN, J. A., & ROSE, E. R., 1970. Economic minerals of the Canadian Shield. Pp. 151-226 in Geology and Economic Minerals of Canada (ed. Douglas, R. J. W.). Econ. Geol. Rept. geol. Surv. Can. 1.

LEMMLEIN, G. G. & KLEVTSOV, P. V., 1961. Relations among the principal thermodynamic parameters in a part of the system H_2O-NaCl. Geochemistry 2, 148-158.

LITTLE, W. M., 1960. Inclusions in cassiterite and associated minerals. Econ. Geol. 55, 485-509.

LORD, C. S., 1951. Mineral industry of District of Mackenzie, Northwest Territories. Mem. geol. Surv. Can. 261.

MAKANJUOLA, A. A. & HOWIE, R. A., 1972. The mineralogy of the glaucophane schists and associated rocks from Ile de Groix, Brittany, France. Contr. Miner. Petrol. 35, 83-118.

MASON, B., 1968. Kaersutite from San Carlos, Arizona, with comments on the paragenesis of this mineral. Mineralog. Mag. 36, 997-1002.

MATHER, J. D., 1970. The biotite isograd and the lower greenschist facies in the Dalradian rocks of Scotland. J. Petrology 11, 253-275.

McCONNELL, C. W., 1964. Yellowknife gold quartz deposits. Econ. Geol. 59, 328-330.

McGLYNN, J. C. & HENDERSON, J. B., 1970. Archean volcanism and sedimentation in the Slave Structural Province. Pp. 31-44 in Basins and Geosynclines in the Canadian Shield (ed. Baer, A. J.). Pap. geol. Surv. Can. 70-40.

McGLYNN, J. C. & HENDERSON, J. B., 1972. The Slave Province. Pp. 505-526 in Variations in Tectonic Styles in Canada (eds. Price, R. A. & Douglas, R. J. W.). Spec. Pap. geol. Assoc. Can. 11.

McNAMARA, M. J., 1965. The lower greenschist facies in the Scottish Highlands. Geol. För. Stockh. Förh. 87, 347-389.

McNAMARA, M. J., 1966. Chlorite-biotite equilibrium reactions in a carbonate-free system. J. Petrology 7, 404-413.

MULLER, G., 1966. Die autometamorphe retrograde umwandlung von biotiten in chlorite und muskowite in sauren tiefengesteinen. Contr. Miner. Petrol. 13, 295-365.

MULLER, G. & SCHNEIDER, A., 1971. Chemistry and genesis of garnets in metamorphic rocks. Contr. Miner. Petrol. 31, 178-200.

NATIONAL BUREAU OF STANDARDS, 1970. Catalog of standard reference materials. Spec. Publ. Nat. Bur. of Standards, U.S. Dept. of Commerce, 260.

NORRISH, K. & CHAPPELL, B. W., 1967. X-ray fluorescence spectrography. Pp. 161-214 in Physical Methods in Determinative Mineralogy (ed. Zussman, J.). London and New York: Academic Press.

OGRYZLO, S. P., 1935. Hydrothermal experiments with gold. Econ. Geol. 30, 400-424.

PETTIJOHN, F. J., 1957. Sedimentary Rocks. New York: Harper Bros.

PINSENT, R. H., 1971. Precambrian geology along the Fraser River between Mount Robson and Tete Jaune Cache, British Columbia. M.Sc. thesis, University of Alberta.

RAMBERG, H., 1952. The origin of metamorphic and metasomatic rocks. Chicago: University of Chicago Press.

RAMSAY, C. R., 1973. Controls of biotite zone mineral chemistry in Archaean meta-sediments near Yellowknife, Northwest Territories, Canada. J. Petrology (in press).

RAMSDEN, J., 1970. Till fabric studies in the Edmonton area, Alberta, with special emphasis on methodology. M.Sc. thesis, University of Alberta.

REED, S. J. B., 1970. The analysis of rocks in the electron probe. Geochim. Cosmochim. Acta 34, 416-421.

RIBBE, P. H. & SMITH, J. V., 1966. X-ray-emission microanalysis of rock-forming minerals IV. Plagioclase feldspars. J. Geol. 74, 217-233.

RICHARDSON, S. W., 1968. Staurolite stability in a part of the system Fe-Al-Si-O-H. J. Petrology 9, 467-488.

RILEY, C., 1938. Some observations on structure at Gordon Lake, N.W.T. Can. Min. J. 59, 558-560.

ROBERTS, D., 1971. Abnormal cleavage patterns in fold hinge zones from Varanger Peninsula, Northern Norway. Am. J. Sci. 271, 170-180.

ROBERTSON, D. K. & CUMMING, G. L., 1968. Lead and sulphur isotope ratios from the Great Slave Lake area, Canada. Can. J. Earth Sci. 5, 1269-1276.

ROEDDER, E., 1965. Liquid CO_2 inclusions in olivine-bearing nodules and phenocrysts from basalts. Am. Miner. 50, 1746-1782.

ROEDDER, E., 1967. Fluid inclusions as samples of ore fluids. Pp. 515-574 in Geochemistry of Hydrothermal Ore Deposits (ed. Barnes, H. L.). New York: Holt, Rinehart and Winston.

ROEDDER, E., 1972. Composition of fluid inclusions. Data of Geochemistry, Prof. Pap. U. S. geol. Surv. 440JJ.

ROEDDER, E. & COOMBS, D. S., 1967. Immiscibility in granitic melts, indicated by fluid inclusions in ejected granitic blocks from Ascension Island. J. Petrology 8, 417-451.

ROSS, J. V., 1962. Deposition and current direction within the Yellowknife Group at Mesa Lake, N. W. T., Canada. Bull. geol. Soc. Am. 73, 1159-1162.

ROSS, J. V., 1966. The structure and metamorphism of Mesa Lake map-area, District of Mackenzie. Bull. geol. Surv. Can. 124.

ROSS, J. V. & McGLYNN, J. C., 1965. Snare-Yellowknife relations, District of Mackenzie, N. W. T., Canada. Can. J. Earth Sci. 2, 118-130.

ROWE, R. B., 1952. Pegmatitic mineral deposits of the Yellowknife-Beaulieu region, District of Mackenzie, Northwest Territories. Pap. geol. Surv. Can. 52-8.

RUCKLIDGE, J. C., GASPARRINI, E., SMITH, J. V., & KNOWLES, C. R., 1971. X-ray emission microanalysis of rock-forming minerals. VIII. Amphiboles. Can. J. Earth Sci. 8, 1171-1183.

RUMBLE, D., 1971. Fe-Ti oxide minerals and the behaviour of oxygen during regional metamorphism. Yb. Carnegie Instn. Wash. 70, 157-165.

SCHREYER, W. & YODER, H. S., 1961. Petrographic guides to the experimental petrology of cordierite. Yb. Carnegie Instn. Wash. 60, 147-152.

SEIFERT, F., 1970. Low-temperature compatibility relations of cordierite in haplo-pelites of the system K_2O-MgO-Al_2O_3-SiO_2-H_2O. J. Petrology 11, 73-100.

SEWARD, T. M., 1973. Thio complexes of gold and the transport of gold in hydrothermal ore solutions. Geochim. cosmochim. Acta 37, 379-399.

SHAW, D. M., 1956. Geochemistry of pelitic rocks. Part III. Major elements and general geochemistry. Bull. geol. Soc. Am. 67, 919-934.

SMITH, D. G. W. & TOMLINSON, M. C., 1970. An APL language computer program for use in electron microprobe analysis. Kans. Geol. Surv. Comput. Contrib. 45.

SMITH, F. G. & LITTLE, W. M., 1959. Filling temperatures of H_2O-CO_2 fluid inclusions and their significance in geothermometry. *Can. Miner. 6*, 380-388.

SMITH, J. V. & RIBBE, P. H., 1966. X-ray-emission microanalysis of rock-forming minerals III. Alkali feldspars. *J. Geol. 74*, 197-216.

STEPHENSON, J. F. & EHMANN, W. D., 1971. Neutron activation analysis of gold in Archean igneous and metamorphic rocks of the Rice Lake-Beresford Lake area, Southeastern Manitoba. *Econ. Geol. 66*, 933-939.

STOCKWELL, C. H., 1933. Great Slave Lake-Coppermine River area, Northwest Territories. *Ann. Rept. geol. Surv. Can., 1932, Part C*, 37-63.

STOCKWELL, C. H., McGLYNN, J. C., EMSLIE, R. F., SANFORD, B. V., NORRIS, A. W., DONALDSON, J. A., FAHRIG, W. F., & CURRIE, K. L., 1970. Geology of the Canadian Shield. Pp. 43-150 in *Geology and Economic Minerals of Canada* (ed. Douglas, R. J. W.). *Econ. geol. Rept. geol. Surv. Can. 1*.

TAKENOUCHI, S. & KENNEDY, G. C., 1965. The solubility of carbon dioxide in NaCl solutions at high temperatures and pressures. *Am. J. Sci. 263*, 445-454.

THORPE, R. I., 1971. Comments on rock ages in the Yellowknife area, District of Mackenzie. *Pap. geol. Surv. Can. 71-1B*, 76-79.

TILLEY, C. E., 1924. Contact-metamorphism in the Comrie area of the Perthshire Highlands. *Q. J. geol. Soc. Lond. 80*, 22-71.

TILLEY, C. E., 1926. Some mineralogical transformations in crystalline schists. *Mineralog. Mag. 21*, 34-46.

TREMBLAY, L. P., 1952. Giaque Lake, Northwest Territories. *Mem. geol. Surv. Can. 266*.

TURNER, F. J., 1948. Evolution of the metamorphic rocks. *Mem. geol. Soc. Am. 30*.

TURNER, F. J., 1968. *Metamorphic Petrology. Mineralogical and Field Aspects*. New York: McGraw-Hill Book Co.

TURNER, F. J. & VERHOOGEN, J., 1951. *Igneous and Metamorphic Petrology*. New York, Toronto and London: McGraw-Hill Book Co.

TURNER, F. J. & VERHOOGEN, J., 1960. Igneous and Metamorphic Petrology (Second Edition). New York, Toronto and London: McGraw-Hill Book Co.

TURNER, F. J. & WEISS, L. E., 1963. Structural Analysis of Metamorphic Tectonites. New York: McGraw-Hill Book Co.

VELDE, B., 1965. Phengite micas: synthesis, stability and natural occurrence. Am. J. Sci. 263, 886-913.

VELDE, B., 1967. Si^{+4} content of natural phengites. Contr. Miner. Petrol. 14, 250-258.

VELDE, B., 1968. The Si^{+4} content of natural phengites: A reply. Contr. Miner. Petrol. 17, 82-84.

WANLESS, R. K., BOYLE, R. W. & LOWDON, J. A., 1960. Sulphur isotope investigation of the gold-quartz deposits of the Yellowknife district. Econ. Geol. 55, 1591-1621.

WANLESS, R. K. & LOVERIDGE, W. D., 1972. Rubidium-strontium isochron age studies, Report 1. Pap. geol. Surv. Can. 72-23.

WEISSBERG, B. G., 1970. Solubility of gold in hydrothermal alkaline sulfide solutions. Econ. Geol. 65, 551-556.

WESTRA, L., 1970. The role of Fe-Ti-oxides in plurifacial metamorphism of alpine age in the south-eastern Sierra de los Filabres, S. E. Spain. Academisch Proefschrift, Vrije Universiteit te Amsterdam.

WHITE, A. J. R., CHAPPELL, B. W., & JAKES, P., 1972. Coexisting clinopyroxene, garnet and amphibole from an "eclogite", Kakanui, New Zealand. Contr. Miner. Petrol. 84, 185-191.

WILLIAMS, H. K., 1967. Cassidy property. Unpublished company report to Giant Yellowknife Mines Ltd.

WILLIAMS, P. F., 1972. Development of metamorphic layering and cleavage in low grade metamorphic rocks at Bermagui, Australia. Am. J. Sci. 272, 1-47.

WILSON, J. T., 1941. Structural features in the Northwest Territories. Am. J. Sci. 239, 493-502.

WINKLER, H. G. F., 1962. Experimentelle gesteinsmetamorphose --VI: Einfluss von anionen auf metamorphe mineralreaktionen. Geochim. cosmochim. Acta 26, 145-180.

WINKLER, H. G. F., 1965. *Petrogenesis of Metamorphic Rocks.* New York: Springer-Verlag.

WINKLER, H. G. F., 1967. *Petrogenesis of Metamorphic Rocks.* (Revised Second Edition). New York: Springer-Verlag.

WINKLER, H. G. F. & von PLATEN, 1958. Experimentelle gesteinsmetamorphose--II. Bildung von anatektischen granitischen schmelzen bei der metamorphose von NaCl-fuhrenden kalkhaltigen tonen. *Geochim. cosmochim. Acta 15*, 91-112.

WIWCHAR, M. B., 1957. Consolidated Discovery Yellowknife Mine. Pp. 201-209 in *Structural Geology of Canadian Ore Deposits* (6th Commonwealth Min. Metall. Congr.). *Can. Inst. Min. Metall.*

YODER, H. S., 1959. Experimental studies on micas : a synthesis. Pp. 42-60 in *Proc. 6th Nat. Conf. Clays and Clay Minerals.* New York: Pergamon Press.

ZWART, H. J., 1969. Metamorphic facies series in the European orogenic belts and their bearing on the causes of orogeny. *Spec. Pap. geol. Assoc. Can. 5*, 7-16.

APPENDIX : METHODOLOGY

MAPPING AND SAMPLING

Aerial photographs and the published maps of Jolliffe (1942 and 1946) give abundant, highly reliable, data on bedding trends, dips and way-up determinations. Field mapping was therefore designed to check bedding data rather than to trace beds, while giving as much information as possible on minor structures. Mapping was done on overlays on aerial photographs at a scale of about 1 : 20,000 and later transferred to a master sheet on which photograph centres were located by the wing-point method. This yields a partially controlled mosaic.

On the map the outcrop limits of volcanic and plutonic rocks have been taken from Jolliffe's maps, having been checked in many localities and modified in a few. All the faults and bedding trends were deduced from the aerial photographs and checked on the ground. All structural data on the map was derived independently of Jolliffe's maps though there is little disagreement between the two.

Samples. Samples of meta-sediments have been collected from about 170 localities in the aureole of the Prosperous Lake pluton, giving a sample density of approximately two sample localities per sq. km. The locations of all samples on which detailed work has been done are given on diagrams in the text. At each sampling locality a suite of between 2 and 8 samples was collected to represent the mineralogical variability at that location. As far as possible representative samples of meta-pelitic and meta-greywacke compositions were taken at each point. Samples of quartz veins and calc-silicate lenses were also collected at all grades but in rather smaller numbers.

Selection of samples. All collected samples from the biotite zone and the lower cordierite zone were studied in thin-section. Before selection of samples for detailed study all were examined for weathering and secondary alteration. All weathered samples were rejected. Minor localised alteration was unavoidable in some samples (see text) because almost every rock in the area has suffered secondary alteration to some extent. Fortunately this alteration is not pervasive but is commonly localised on fractures and readily recognised and avoided.

Detailed maps. Several geological sketches of small areas are given in the text. These were made by pace-and-compass mapping from one or more compass-surveyed base-lines.

STRUCTURAL METHODS

The plunges of most of the micro-fold axes were measured with an inclinometer and some bedding dips were similarly determined. All cleavage dips, however, have been visually estimated. Further, the schistosity is weak and most outcrops smoothly glaciated. Dips of schistosities are therefore only approximate (±10° estimated).

The fold orientation *rose diagrams* were constructed by marking all fold axial traces on the map, measuring their orientation and counting one fold for each axial trace.

Definition of domains. The boundaries of the structural domains were determined by plotting on a map all the available structural data and then delimiting the areas within which the characteristic features of the domains had been observed.

Structural contour diagrams. Once the limits of the domains had been determined all the structural data from within each domain were plotted on equal area projections and the resultant point densities contoured. This was done by a computer programme developed in the University of Alberta. This is a sophisticated programme described in detail by Ramsden (1970). It determines point density by counting points directly on the reference hemisphere. The computer counts the points within circles at 333 different locations on the reference hemisphere and then prints out the point density values at each of the 333 locations on an equal area projection. These values can then be manually contoured. The radius of the counting circle is variable and can be set to any desired fraction of the total hemisphere. In this study a one per cent counting circle has been used throughout, which tends to emphasise the small-scale density variations in the point distribution (Ramsden, 1970).

Mean vectors. Another programme described by Ramsden (1970, p. 204) has been used to determine the mean vector representing the observed distribution of linear structures or poles to planes.

PETROGRAPHIC METHODS

All samples from the biotite zone and the lower cordierite zone were studied in thin-section. Samples selected for analytical work were also examined in polished section. All the selected

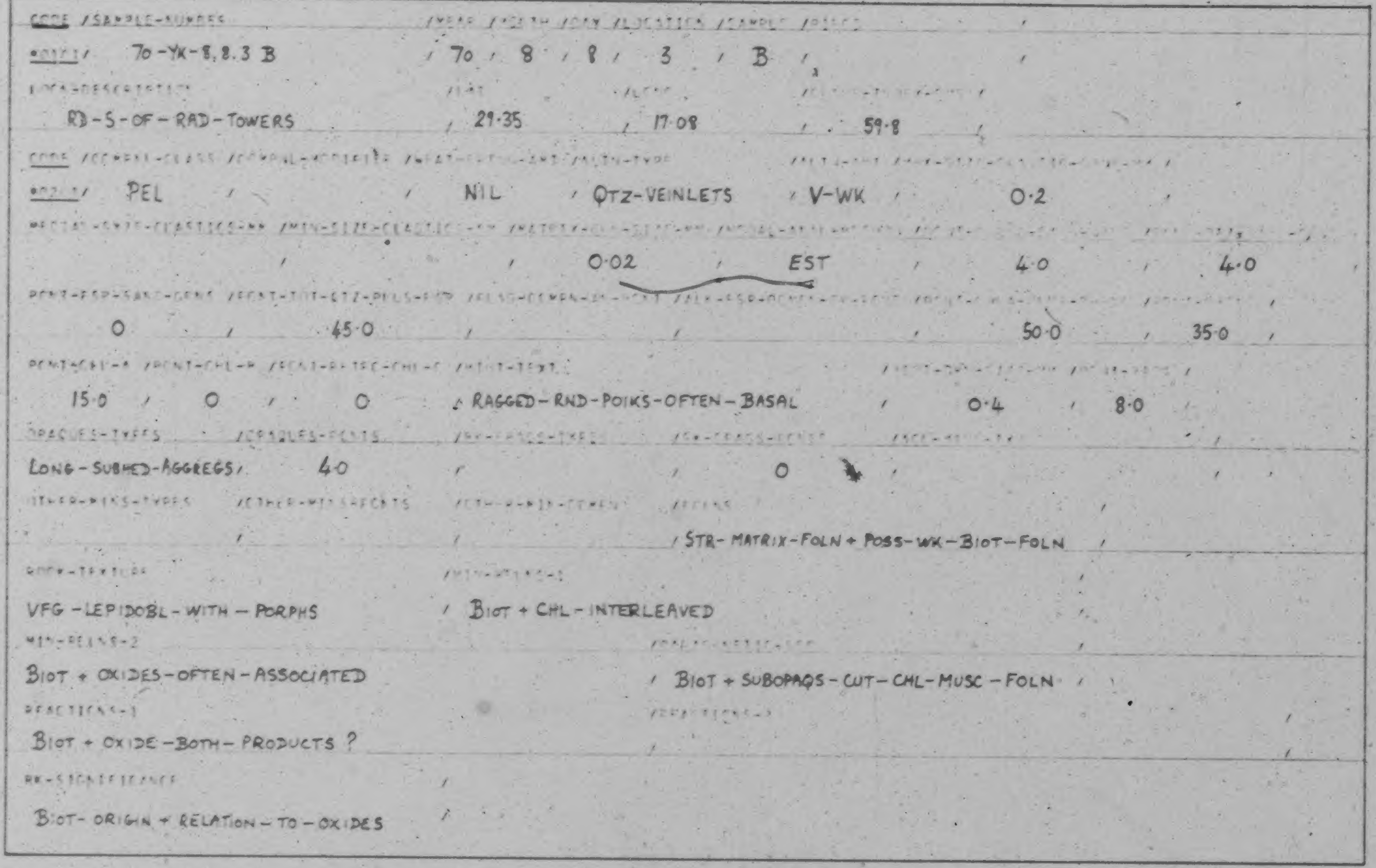

CODE /SAMPLE-NUMBER /YEAR /MONTH /DAY /LOCATION /SAMPLE /PIECE /

/ 70-YK-8,8.3 B / 70 / 8 / 8 / 3 / B / /

RD-S-OF-RAD-TOWERS / 29·35 / 17·08 / 59·8 /

CODE

/ PEL / / NIL / QTZ-VEINLETS / V-WK / 0·2 /

/ / 0·02 / EST / 4·0 / 4·0 /

0 / 45·0 / / / 50·0 / 35·0 /

15·0 / 0 / 0 / RAGGED-RND-POIKS-OFTEN-BASAL / 0·4 / 8·0 /

OPAQUES-TYPES /OPAQUES-PCNTS

LONG-SUBHED-AGGREGS / 4·0 / / 0 / / /

OTHER-MINS-TYPES

/ / / STR-MATRIX-FOLN + POSS-WK-BIOT-FOLN /

ROCK-TEXTURE /MIN-RELNS-1

VFG-LEPIDOBL-WITH-PORPHS / BIOT + CHL-INTERLEAVED /

MIN-RELNS-2

BIOT + OXIDES-OFTEN-ASSOCIATED / BIOT + SUBOPAQS-CUT-CHL-MUSC-FOLN /

REACTIONS-1

BIOT + OXIDE-BOTH-PRODUCTS ? / /

RK-SIGNIFICANCE

BIOT-ORIGIN + RELATION-TO-OXIDES /

FIGURE A-1 : Sample petrographic description sheet for data input to the SAFRAS data storage system. This information is introduced to the system via punched cards.

samples from the biotite zone were stained for K-feldspar by an HF etch followed by immersion in sodium cobaltinitrite.

Manipulation of petrographic data. For all the 170 biotite zone samples petrographic data were systematically recorded and temporarily stored in a computerised data file which permitted selective retrieval and tabulation of the data. The SAFRAS (Self-Adaptive Flexible-Format Retrieval And Storage) system was used for this purpose. It has been described by Dickie (1972) and in references therein.

The SAFRAS system is a complex of programmes which builds a data storage file from a list of data specifications. The system can introduce data into this file, edit it, or selectively retrieve data from it. Once the system is operating the user needs no detailed understanding of its operations and no special skills in computer language or programming. The data specifications may include any item specified by the user and the commands for data retrieval are simple. The data may be retrieved in any combinations and subject to any chosen conditions. For example, the system might be requested to list the sample numbers, metamorphic grade indexes and chlorite percentages of all meta-greywackes in which the maximum clastic grain-size is less than 0.5 mm. and the biotite content is greater than 20 per cent modal.

Figure A1 is a sample petrographic description sheet showing the data items specified for each of the thin-sections studied. Figure A2 is an example of the type of tabulation which may be retrieved from the file. In this case the computer was told to find all rocks which had been called meta-pelites and to print out their sample

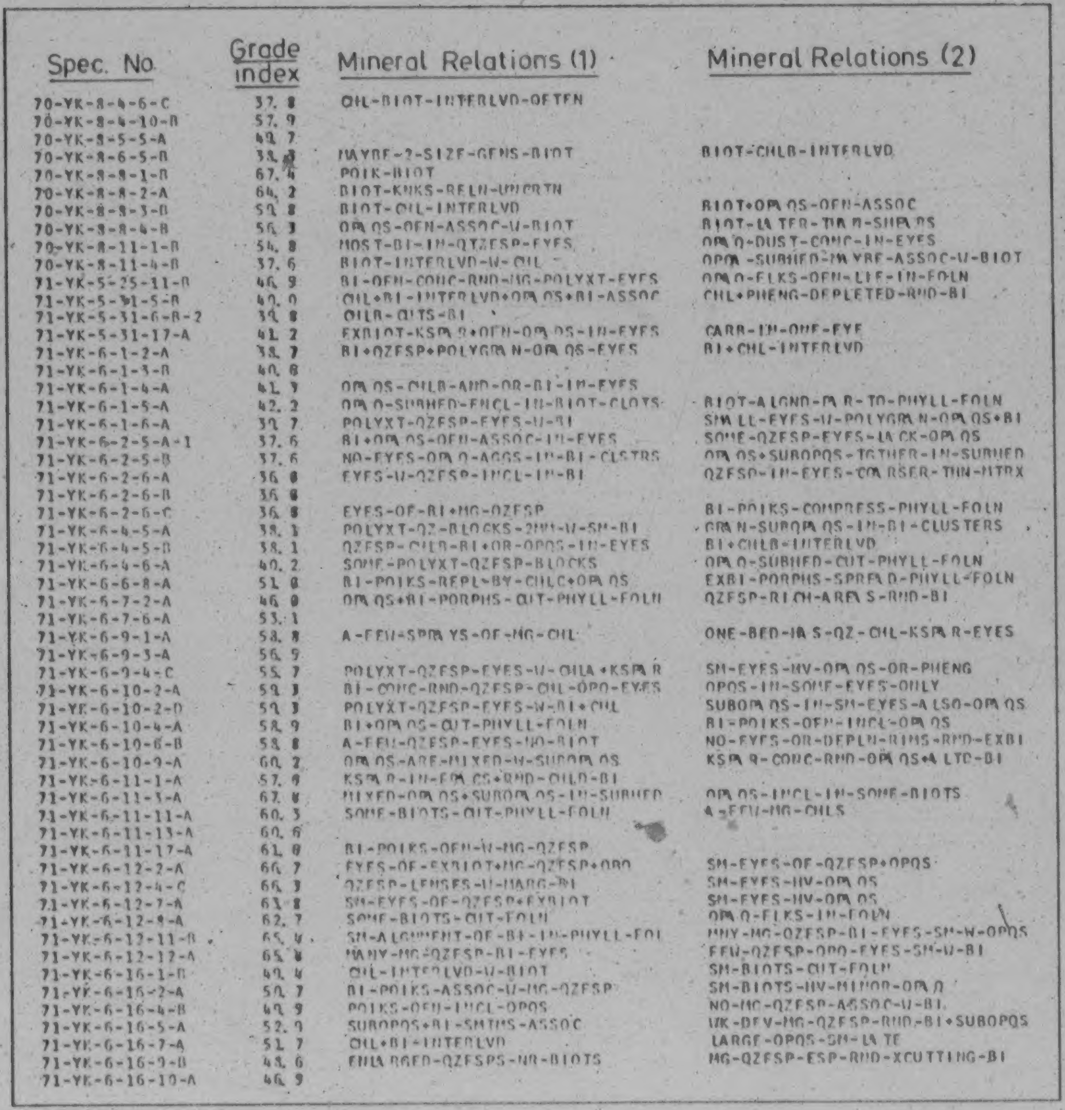

Spec. No	Grade index	Mineral Relations (1)	Mineral Relations (2)
70-YK-8-4-6-C	37.8	CHL-BIOT-INTERLVD-OFTEN	
70-YK-8-4-10-B	57.9		
70-YK-8-5-5-A	49.7		
70-YK-8-6-5-B	38.3	MAYBE-2-SIZE-GENS-BIOT	BIOT-CHLB-INTERLVD
70-YK-8-8-1-B	67.4	POIK-BIOT	
70-YK-8-8-2-A	64.2	BIOT-KNKS-RELN-UNCRTN	
70-YK-8-8-3-B	59.8	BIOT-CHL-INTERLVD	BIOT+OPAQS-OFN-ASSOC
70-YK-8-8-4-B	56.3	OPAQS-OFN-ASSOC-W-BIOT	BIOT-LATER-THAN-SHEARS
70-YK-8-11-1-B	54.8	MOST-BI-IN-QTZFSP-EYES	OPAQ-DUST-CONC-IN-EYES
70-YK-8-11-4-B	37.6	BIOT-INTERLVD-W-CHL	OPQA-SUBHED-MAYBE-ASSOC-W-BIOT
71-YK-5-25-11-B	46.9	BI-OFN-CONC-RND-MG-POLYXT-EYES	OPAQ-FLKS-OFN-LIE-IN-FOLN
71-YK-5-31-5-B	49.0	CHL+BI-INTERLVD+OPAQS+BI-ASSOC	CHL+PHENG-DEPLETED-RND-BI
71-YK-5-31-6-B-2	39.8	CHLB-CUTS-BI	
71-YK-5-31-17-A	41.2	EXBIOT-KSPAR+OFN-OPAQS-IN-EYES	CARB-IN-ONE-EYE
71-YK-6-1-2-A	38.7	BI+QZFSP+POLYGRAN-OPAQS-EYES	BI+CHL-INTERLVD
71-YK-6-1-3-B	40.8		
71-YK-6-1-4-A	41.3	OPAQS-CHLB-AND-OR-BI-IN-EYES	
71-YK-6-1-5-A	42.2	OPAQ-SUBHED-ENCL-IN-BIOT-CLOTS	BIOT-ALGND-PAR-TO-PHYLL-FOLN
71-YK-6-1-6-A	39.7	POLYXT-QZFSP-EYES-W-BI	SMALL-EYES-W-POLYGRAN-OPAQS+BI
71-YK-6-2-5-A-1	37.6	BI+OPAQS-OFN-ASSOC-IN-EYES	SOME-QZFSP-EYES-LACK-OPAQS
71-YK-6-2-5-B	37.6	NO-EYES-OPAQ-AGGS-IN-BI-CLSTRS	OPAQS+SUBOPQS-TGTHER-IN-SUBHED
71-YK-6-2-6-A	36.8	EYES-W-QZFSP-INCL-IN-BI	QZFSP-IN-EYES-COARSER-THN-MTRX
71-YK-6-2-6-B	36.8		
71-YK-6-2-6-C	36.8	EYES-OF-BI+MG-QZFSP	BI-POIKS-COMPRESS-PHYLL-FOLN
71-YK-6-4-5-A	38.1	POLYXT-QZ-BLOCKS-2MM-W-SM-BI	GRAN-SUBOPAQS-IN-BI-CLUSTERS
71-YK-6-4-5-B	38.1	QZFSP-CHLB-BI+OR-OPQS-IN-EYES	BI+CHLB-INTERLVD
71-YK-6-4-6-A	40.2	SOME-POLYXT-QZFSP-BLOCKS	OPAQ-SUBHED-CUT-PHYLL-FOLN
71-YK-6-6-8-A	51.8	BI-POIKS-REPL-BY-CHLC+OPAQS	EXBI-PORPHS-SPREAD-PHYLL-FOLN
71-YK-6-7-2-A	46.8	OPAQS+BI-PORPHS-CUT-PHYLL-FOLN	QZFSP-RICH-AREAS-RND-BI
71-YK-6-7-6-A	53.1		
71-YK-6-9-1-A	58.8	A-FEW-SPRAYS-OF-MG-CHL	ONE-BED-HAS-QZ-CHL-KSPAR-EYES
71-YK-6-9-3-A	56.9		
71-YK-6-9-4-C	55.7	POLYXT-QZFSP-EYES-W-CHLA+KSPAR	SM-EYES-HV-OPAQS-OR-PHENG
71-YK-6-10-2-A	59.3	BI-CONC-RND-QZFSP-CHL-OPQ-EYES	OPQS-IN-SOME-EYES-ONLY
71-YK-6-10-2-D	59.3	POLYXT-QZFSP-EYES-W-BI+CHL	SUBOPAQS-IN-SM-EYES-ALSO-OPAQS
71-YK-6-10-4-A	58.9	BI+OPAQS-CUT-PHYLL-FOLN	BI-POIKS-OFN-INCL-OPAQS
71-YK-6-10-6-B	58.8	A-FEW-QZFSP-EYES-NO-BIOT	NO-EYES-OR-DEPLN-RIMS-RND-EXBI
71-YK-6-10-9-A	60.2	OPAQS-ARE-MIXED-W-SUBOPAQS	KSPAR-CONC-RND-OPAQS+ALTD-BI
71-YK-6-11-1-A	57.9	KSPAR-IN-FRACS+RND-CHLD-BI	
71-YK-6-11-3-A	67.8	MIXED-OPAQS+SUBOPAQS-IN-SUBHED	OPAQS-INCL-IN-SOME-BIOTS
71-YK-6-11-11-A	60.3	SOME-BIOTS-CUT-PHYLL-FOLN	A-FEW-MG-CHLS
71-YK-6-11-13-A	60.6		
71-YK-6-11-17-A	61.8	BI-POIKS-OFN-W-MG-QZFSP	
71-YK-6-12-2-A	66.7	EYES-OF-EXBIOT+MG-QZFSP+OPQ	SM-EYES-OF-QZFSP+OPQS
71-YK-6-12-4-C	66.3	QZFSP-LENSES-W-MARG-BI	SM-EYES-HV-OPAQS
71-YK-6-12-7-A	63.8	SM-EYES-OF-QZFSP+EXBIOT	SM-EYES-HV-OPAQS
71-YK-6-12-9-A	62.7	SOME-BIOTS-CUT-FOLN	OPAQ-FLKS-IN-FOLN
71-YK-6-12-11-B	65.4	SM-ALGNMENT-OF-BI-IN-PHYLL-FOL	MNY-MG-QZFSP-BI-EYES-SM-W-OPQS
71-YK-6-12-12-A	65.8	MANY-MG-QZFSP-BI-EYES	FEW-QZFSP-OPQ-EYES-SM-W-BI
71-YK-6-16-1-B	49.4	CHL-INTERLVD-W-BIOT	SM-BIOTS-CUT-FOLN
71-YK-6-16-2-A	50.7	BI-POIKS-ASSOC-W-MG-QZFSP	SM-BIOTS-HV-MINOR-OPAQ
71-YK-6-16-4-B	49.9	POIKS-OFN-INCL-OPQS	NO-MG-QZFSP-ASSOC-W-BI
71-YK-6-16-5-A	52.9	SUBOPQS+BI-SMTMS-ASSOC	WK-DEV-MG-QZFSP-RND-BI+SUBOPQS
71-YK-6-16-7-A	51.7	CHL+BI-INTERLVD	LARGE-OPQS-SM-LATE
71-YK-6-16-9-B	48.6	ENLARGED-QZFSPS-NR-BIOTS	MG-QZFSP-ESP-RND-XCUTTING-BI
71-YK-6-16-10-A	46.9		

FIGURE A-2 : Sample output table from the SAFRAS data storage system.

numbers, grade indexes and all information recorded on textural relations of the minerals.

Because of the nature of this particular rock suite the data file has not been used to its full potential in this study. For a larger and more varied suite of rocks this approach offers great opportunity for reducing the subjectivity of petrographic surveys and for rapid and accurate manipulation of large amounts of petrographic and analytical information. Although the subjectivity of individual thin-section descriptions is not reduced, that of generalised descriptions and conclusions is improved because the tables of observations are so convenient for surveying features of the rocks.

Modal analyses. The small grain-size, inequigranular texture and variable foliation of these rocks prohibits great accuracy in the modal analyses. Overall accuracy of about ±10 per cent is probably the best that can be claimed for the modal data. Procedure in making the analyses was as follows. A test sequence was first carried out on two rocks. In these, modal percentages were determined successively from 300, 500, 800 and 1,000 counted points. No significant changes occurred beyond 500 points and this number was adopted as standard. Later another 500 points were counted on second thin-sections of the same rocks with the counting grid oriented at right angles (relative to the schistosity) to that of the first determination. There were commonly considerable differences between these two modal determinations. The values given in Table 12 are the averages of the two analyses.

In these analyses all oxide and sulphide phases were counted together as 'opaque minerals'. Relative amounts of the different opaque phases were determined in polished sections as follows. The oxide, and sulphide grains in one field of view were identified and counted. The sample was advanced 1 mm. using a mechanical stage and the procedure repeated on the new field of view. In this way a total of 200 grains were identified and counted in each sample. The relative numbers of each species were expressed as percentages. The modal percentages of each opaque mineral was then determined by multiplying the total 'opaque mineral' mode by the number percentage of each species.

ROCK ANALYSES

The rocks were analysed using an A. R. L. (EMX) micro-probe and a modification of the method of Gulson and Lovering (1968). Rock powders were fused with lithium tetraborate, lithium carbonate, lanthanum oxide and ammonium nitrate as described by Norrish and Chappell (1967). The molten mixtures were poured into a shallow, flat-bottomed Pt-Au dish and allowed to freeze between two asbestos sheets on a hot-plate. This produced a clear glass (fractured into two or three pieces) which could be removed from the dish by gentle tapping. Very brief polishing of this glass on one micron diamond paste produced a large, well polished surface. The polished glass was then attached to the underside of metal washers for mounting in the micro-probe. This technique of casting and mounting the samples avoids the difficulties of casting perfect glass discs and provides a large, perfectly polished surface for analysis without ever bringing the glasses into contact with water.

Homogeneity of the glasses was generally entirely adequate for analysis and the use of a defocussed beam moved rapidly across a large surface served to average out inhomogeneities. Two sources of inhomogeneity were noted. (1) Three of the 24 glasses produced (P-4, P-12 and AGV-1) contained small areas in which a few tiny crystals had formed. These crystals were Al-rich and were possibly sillimanite. They probably resulted from excessively slow cooling of the glass on the hot-plate and it is recommended that this step in the casting procedure be eliminated or minimised. The proportion of these crystals is volumetrically very small and areas containing them were avoided in the analyses. (2) In one sample (P-14) a small area, exactly like the surrounding glass in appearance, was found to be very low in Fe. No reason for this is known.

Oxide concentrations were determined using calibration curves. These were made up from the international geochemical standards W-1, G-2, BCR-1 and AGV-1 (Fleischer, 1969; Flanagan, 1969) and the standard albite NBS-99a (National Bureau of Standards, 1970). As noted above the AGV-1 glass contained some crystals and in several instances it gave points plotting off the curves defined by the other standards. It has therefore been rejected as a standard. Data from these four standards were augmented, where an extension of range or another point was required, by the standard peridotite PCC-1 (Flanagan, 1969) and an analysed Fe-rich biotite. Since this method is not widely used the calibration curves are included here as Fig. A3 to illustrate the linearity attainable. All the curves are linear within the range used but there is some curvature in the FeO calibration plot. This curve indicates a decrease of sensitivity at higher FeO concentrations and the reason for this is not known. Fortunately the curve is linear in the range used.

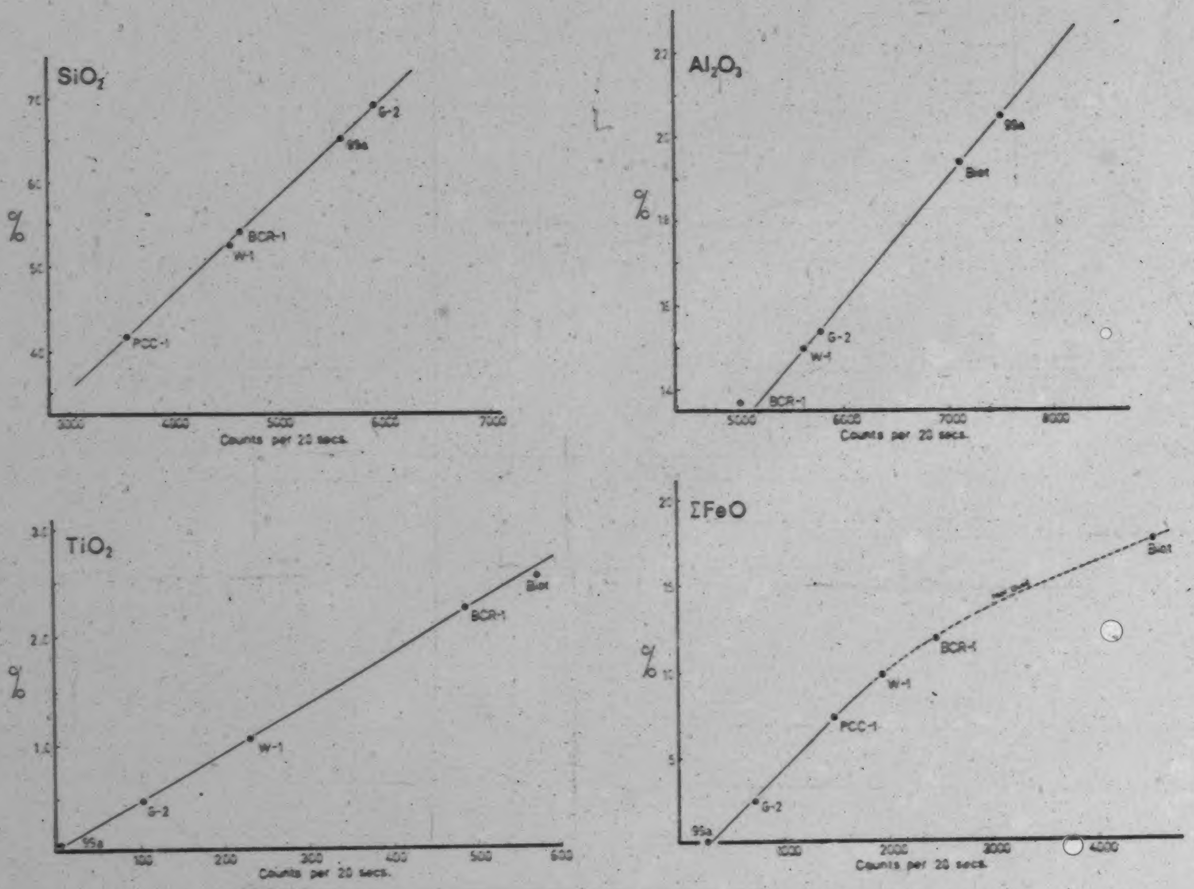

FIGURE A-3 : Calibration curves used in the whole-rock analyses (continued overleaf).

The MnO curve is not shown for reasons of space.

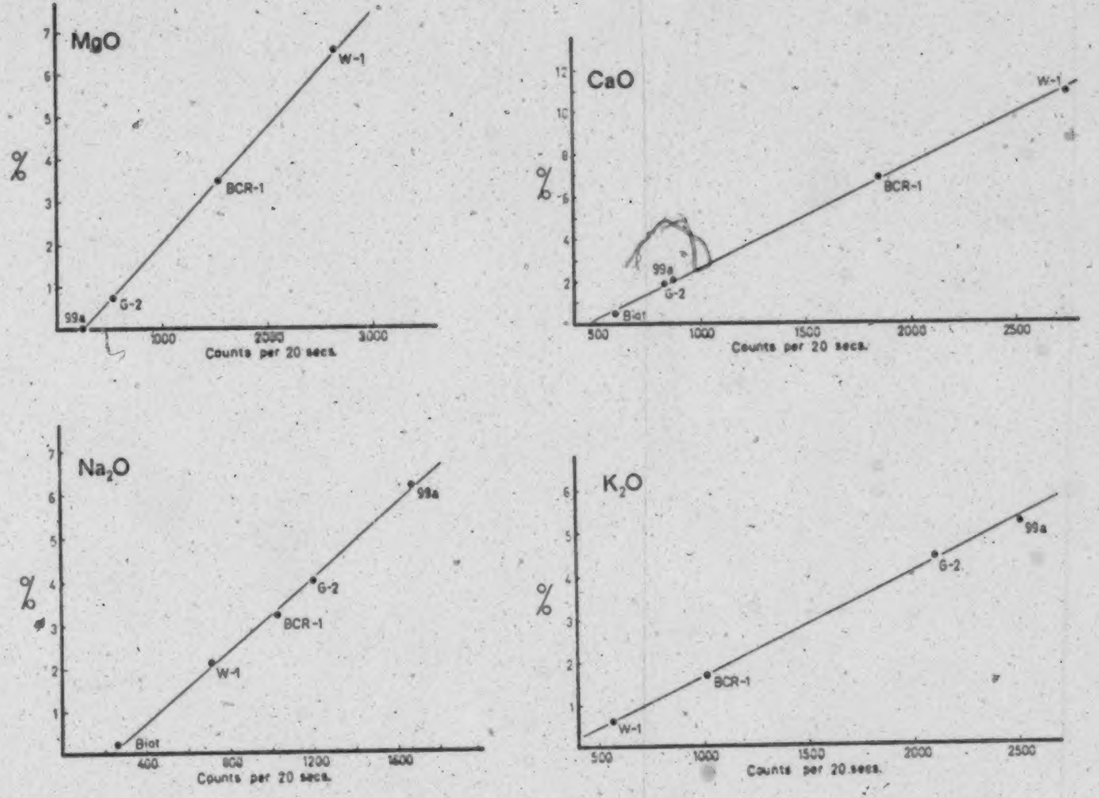

FIGURE A-3 (Continued).

Water and volatile contents of the rocks have been determined roughly in two ways -- by a 'loss on ignition' determination and by calculation from the point-counted modes using assumed water contents for the hydrous minerals. The two sets of results agree sufficiently to indicate that oxidation during ignition was not a major factor and the loss on ignition values have been accepted for Table 2.

FeO concentrations were determined by titration against standard $KMnO_4$ and Fe_2O_3 by subtraction of FeO from the total Fe determined.

Quality of the rock analyses. The resultant analyses (Table 2) are entirely comparable with published analyses of rocks from the same Formation (Boyle, 1961; Henderson, 1972) and the linearity of the calibration curves suggests that the analyses are acceptable. Table A1 gives estimates of precision. Without an accurate water determination the totals are a dubious test of analytical quality but two analyses have been rejected for having unacceptably high totals. One of these (P-4, totalling 102.3 per cent) contained a few crystals in the glass; the other (P-10) totalled 103.9 per cent but there is no known reason for this.

Time. Once the technique has been perfected this is a fairly rapid analytical method. Sample preparation, analysis and computation of 16 analyses using 7 standards and one blank took the author a little over 6 days. This could certainly be improved with practice.

Conclusion. Provided adequate care is taken to ensure the absence of crystals in the glasses this is a fairly rapid and

TABLE A1 : Precision estimates for the whole-rock analyses given in Table 2.

Oxide	*Statistical counting error (99% confidence)		Precision suggested by scatter on calibration curves	Replicate analyses
	% Relative ±	Wt. % ±	(Wt. % oxide)	
SiO_2	1.6	0.9	0.5	
TiO_2	3.8	0.03	0.01	
Al_2O_3	1.5	0.2	0.5	
ΣFeO	3.0	0.2	0.2	
FeO	-	-	-	4.9, 4.9 [4.3, 4.2, 4.2 7.7, 7.7
MnO	7.6	0.01	0.02	
MgO	2.8	0.1	0.1	
CaO	4.6	0.1	0.15	
Na_2O	4.2	0.13	0.1	
K_2O	3.0	0.09	0.1	
l.o.i.	-	-	-	4.5, 4.3

* Doubled to allow for similar error on standards. Calculated for an average rock composition in this suite.

satisfactorily accurate method of making rock analyses (see also Gulson and Lovering, 1968; Reed, 1970). There was apparently no difficulty with loss of alkalis on fusion. The above technique could be improved by more rapid cooling of the glasses followed by regrinding and re-casting and by using standards containing approximately the same amount of water as the samples.

MINERAL ANALYSES

The mineral analyses were performed using the A. R. L. (EMX) micro-probe. Oxide concentrations were determined by comparison with silicate standards after corrections for background, fluorescence, absorption and atomic number effects according to Smith and Tomlinson (1970). For the purpose of these corrections the oxygen concentration was assumed to be equal to the difference between 100 per cent and the sum of the analysed elements. Ferrous : ferric ratios were determined on two biotite separates (by $KMnO_4$ titration) but it proved impossible to isolate either chlorite or muscovite.

The following operating conditions were used during the analyses:

Lines	$K_{alpha}(1, 2)$
Beam size	ca. 1 micron
Operating voltage	15 KV
Beam current	0.1 microamps
Emission current	200 microamps
Take-off angle	52.5°

Standards. A suite of 10 standards was selected and checked for homogeneity and composition (by 'cross-analysis') before

TABLE A-2 : Standards used in the micro-probe analyses.

(1) Biotite Zone : Tables 4, 6, 8, 10 and 11.

Mineral	Name of Standard (U. of A. Number)	Source or Reference	Elements		
			Biotite	Chlorite	Muscovite
Micas and chlorite	Biotite 1 (EPS/12-1)	Crown Point, Adirondacks I.S.E. Carmichael (unpubl.)	Fe, Ti	Fe, Ti, Al	Fe, Ti
	Biotite 3 (EPS/12-2)	Univ. of California (Berkley) No. 15724a	Si, Mg, Al, K	Si, Mg, Mn	Si, Al, K, Na
	Kakanui Kaersutite	Mason (1968) White *et al.* (1972)	Na, Ca	Na, Ca, K	-
	Garnet 12442	Gore Mountain (Adirondacks). Loomis (unpubl.)	Mn	-	-
	E Mn-cummingtonite 4	Klein (1964) Rucklidge *et al.*, (1971)	-	-	Mg, Mn, Ca
Feldspars	Anorthoclase 5748	Smith & Ribbe (1966)	Na, K		
	An_{60} glass	Ribbe & Smith (1966)	Ca		
Oxides	L4-175 Magnetite	Anderson (1968)	Fe, Al		
	E Mn-cummingtonite 4	As above	Si, Mn, Mg		
	Odegaarden Ilmenite (EPM/92)	U. of A. files	Ti		

(2) Cordierite Zone : Tables 11, 14 and 15.

All Silicates	Biotite 1 (EPS/12-1)	As above	Ti, Fe
	Biotite 3 (EPS/12-2)	As above	Si, Mg, Mn, K
	Kakanui Kaersutite	As above	Ca, Na
	Hohenfels Sanidine (EPM/82 and 83)	U. of A. files	Al
Oxides	L4-175 Magnetite	As above	Fe, Mg, Si
	Odegaarden Ilmenite (EPM/92)	As above	Ti
	E Mn-cummingtonite 4	As above	Mn
	K13-131.8 Ilmenite	Anderson (1968)	Al

use. Thereafter standards were only used for those elements for which they displayed acceptable homogeneity and agreement in cross-analysis. Many were found to be inhomogeneous and to cross-check only within broad limits.

Table A2 lists the standards used. The great majority of the analyses, including all those where precision is critical, have been based on the standards EPS/12-1, EPS/12-2 and Kakanui Kaersutite. These three were selected from the initial standard suite and cross-analysed (Table A3). Their homogeneity was numerically tested (Notes with Table A3). With those three analyses and the homogeneity data it was possible to select 'reliable elements' by the following criteria: (1) The three analyses gave effectively the same values for that element. (2) No significant inhomogeneity was detected for that element. (3) When used as ~~a~~ standard in analysis of the other two minerals, that element gave values close to the known concentrations. These selection criteria are thought to have supplied a reliable standard suite.

Of the other standards (Table A2) the Odegaarden Ilmenite and the Hohenfels Sanidine have been carefully checked in the U. of A. micro-probe laboratory and their analyses were accepted. Garnet 12442 was checked and Mn found satisfactory. The Anderson Ilmenite and Magnetite, the Anorthoclase and the An(60) glass were accepted on recommendation of Dr. T. O. Frisch. The Mn-cummingtonite is inhomogeneous but has only been used for elements with much lower concentrations than in the standard.

Sample damage. The biotites, muscovites and chlorites were checked for sample damage in the electron beam by taking

Notes to Accompany Table A3

(1) Pairs or triplets of counts were taken at each of several locations on the grain(s). Each set was averaged. The detected inhomogeneity is the range of these sets expressed as a percentage deviation [illegible] the overall mean. The allowed inhomogeneity is the statistical counting error (at 99 per cent confidence) for the number of counts in each set. If the detected inhomogeneity is greater than the allowed, the standard is inhomogeneous with respect to that element.

(2) 'Reliable elements' are those which may be reliably used as standards. See text for selection criteria.

(3) The suggested optimum analysis is only different from the original determination if the two new determinations differ consistently and significantly from the original.

(4) Similar results were obtained in an independent check by Dr. T. O. Frisch.

TABLE A3 : Data on the three principal standards used in the micro-probe analyses (in wt. % of each element).

(1) Biotite No. 1 (EPS/12-1)

Element	Original Analysis	Cross-Analysis		Homogeneity(1)		Reliable(2) Elements	Suggested(3) Optimum
		vs. EPS/12-2	vs. KK*	Detected(%)	Allowed(%)		
Si	16.08	16.22	16.27	1.4	1.6	Si	16.2
Ti	1.83	1.90	(1.64)	1.7	3.5	Ti	1.83
Al	7.04	7.12	(7.60)	1.2	1.0	?Al	7.04
Fe	23.43	(24.20)	23.37	1.2	0.9	Fe	23.43
Mn	0.29	0.32	0.33	4.6	ca. 8		0.29
Mg	(2.77)	2.70	2.70	2.6	1.7		2.70
Ca	0.01	0.01	0.01	6.2	ca. 10		0.01
Na	(0.12)	0.07	0.06	3.5	ca. 10		0.07
K	7.64	7.72	(7.39)	0.8	1.1	K	7.64
F	0.65	0.54	-	-	-	?F	0.65

(2) Biotite No. 3 (EPS/12-2) (Single grain)

	Original	vs. EPS/12-1	vs. KK*				
Si	18.05	17.95	18.12	0.8	1.5	Si	18.05
Ti	1.37	1.32	(1.18)	4.5	4.1	Ti	1.37
Al	5.67	5.62	(6.06)	0.9	1.0	Al	5.67
Fe	(14.09)	13.61	13.59	1.8	1.2		13.60
Mn	0.74	0.68	0.77	3.5	ca. 5	Mn	0.74
Mg	8.45	(8.66)	8.42	1.0	0.9	Mg	8.45
Ca	0.01	0.00	0.00	4.7	ca. 10		0.00
Na	0.51	(0.91)	0.46	4.1	5.0	?Na	0.51
K	7.64	7.57	(7.33)	0.5	1.1	K	7.64

(3) Kakanui Kaersutite

	Original	vs. EPS/12-1	vs. EPS/12-2				
Si	18.87	18.68	18.82	1.6	1.5	Si	18.87
Ti	(2.62)	2.92	3.04	1.0	2.8		3.00 (4)
Al	(7.88)	7.30	7.37	0.7	0.9		7.3 (4)
Fe	8.49	8.29	8.58	1.6	1.7	Fe	8.49
Mn	0.07	0.06	0.07	6.8	ca. 10		0.07
Mg	7.72	(7.92)	7.72	1.5	0.9	Mg	7.72
Ca	7.36	-	-	0.7	1.6	Ca	7.36
Na	1.93	-	-	0.8	2.4	Na	1.93
K	(1.70)	1.77	1.77	2.1	2.4		1.77
F	-	-	0.11	-	-		0.11

(1)-(4) See accompanying notes.

Bracketed values appear distinctly different from the other determinations and are therefore suspect.

*Kakanui Kaersutite.

ten successive 20-second counts on the same spot. The biotites and chlorites were unaffected but the muscovites displayed marked K losses.

Precision. The principal errors in the biotite and most chlorite analyses probably derive from uncertainties in the standard composition (eliminated as much as possible above) and the statistical counting error. The muscovites (and some chlorites), however, are very fine-grained, leading to some difficulty in performing the analyses and introducing the possibility of random errors. Further, the muscovite analyses were problematical because of a marked tendency to lose K under the electron beam. Therefore some empirical test of precision is required and replicate analyses have been performed for this purpose (Table A4). This table also attempts to evaluate accuracy by presenting some determinations against different standards.

The precision of the analyses may therefore be judged from Table A4, but a graphical approximation of the uncertainties involved is given in the form of average error bars in Figs. 19, 20 and 22, derived as follows. For small numbers of determinations the standard deviation is approximated by the range. Thus for each replicate set the coefficient of variability was calculated according to the formula

$$\text{Coeff. of variation (V)\%} = \frac{100 \times \text{Range}}{\text{Mean}}$$

(Calder, 1971). The average coefficient of variation for each element was used as a measure of the uncertainty for that element. For Si and

TABLE A4 : Replicate analyses of minerals (in weight %).

	Muscovites			
	P-1	PW-11	P-13	G-5
SiO_2	45.99, (44.87)	47.29, (46.52)	46.05, (45.64)	46.18, (46.45)
TiO_2	0.34, (0.35)	0.23, 0.27	0.38, 0.35	0.36, (0.37)
Al_2O_3	34.00, (35.59)	34.29, (34.25)	34.39, (33.81)	33.45, (33.84)
Fe_2O_3**	1.07, 1.20, (1.03)	1.38, 1.21, (1.11)	1.43, 1.77, (1.45)	1.22, 1.13, (1.09)
MgO	0.64, 0.70, (0.69)	0.86, 0.73, (0.74)	1.14, 0.83, (1.13)	1.36, 0.84, (1.14)
Na_2O	0.50, 0.59, (0.49)	0.46, 0.59, (0.49)	0.26, 0.30, (0.23)	0.33, 0.45, (0.33)
K_2O	10.34, (9.98)	10.28, (10.26)	10.65, (10.67)	10.70, 10.74, (10.33)
	P-3	P-6	G-1	G-15
SiO_2	-	-	-	47.02, (48.62)
TiO_2	0.42, 0.44	0.44, 0.45	-	0.33, (0.23)
Al_2O_3	-	-	-	32.31, (32.23)
Fe_2O_3**	0.99, 1.21	1.21, 1.23	1.02, 1.12	1.45, 1.70, (1.46)
MgO	0.94, 0.83	0.71, 0.82	0.58, 0.59	1.28, 1.46, (1.49)
Na_2O	0.36, 0.39	0.45, 0.50	0.68, 0.60	0.28, 0.27, (0.21)
K_2O	10.70, 10.52	-	10.51, 10.42	10.88, 10.96, (10.72)
	G-7	G-11	GW-12	G-14
Fe_2O_3**	1.18, 1.18	1.92, 2.07	1.07, 1.33	1.32, 1.42
MgO	1.02, 0.80	1.22, 1.00	0.79, 0.72	0.93, 0.89
Na_2O	0.49, 0.46	0.36, 0.43	0.69, 0.93	0.29, 0.43
K_2O	10.46, 10.67	10.99, 10.88	10.11, 10.09	10.55, 10.80

Table A4 continued overleaf.

TABLE A4 (Continued)

	P-8	P-9	P-10	P-12
TiO_2	0.43, 0.35	0.44, 0.43	-	0.31, 0.27
Fe_2O_3**	1.24, 1.34	1.20, 1.26	1.36, 1.38	1.41, 1.45
MgO	1.19, 1.41	1.01, 0.93	1.00, 1.00	0.78, 1.07
Na_2O	0.29, 0.35	0.36, 0.41	0.31, 0.38	0.36, 0.33

	P-4	P-5	P-7	P-14
SiO_2	-	-	46.21, (47.26)	-
TiO_2	-	-	0.48, (0.47)	-
Al_2O_3	-	-	33.47, (33.83)	-
Fe_2O_3**	1.07, 1.35	1.15, 1.22	1.29, (1.07)	1.63, 1.71
MgO	0.85, 0.75	0.95, 0.77	0.65, 0.81, (0.85)	1.22, 1.13
Na_2O	0.44, 0.59	0.40, 0.59	0.61, (0.52)	0.28, 0.38
K_2O	10.59, 10.52	-	-	-
BaO	-	-	0.74, (0.84)	-

	Biotites		Chlorites		
	P-1	P-13	P-7	G-5	P-13
SiO_2	35.65, (35.00)	35.89, (35.58)	24.62, (23.83)	24.45, (25.04)	24.22, 24.22
Al_2O_3	18.03, (18.48)	17.48, (17.82)	22.54, (22.96)	21.09, (21.63)	22.33, 22.07
FeO*	19.15, 19.37	19.57, 19.91	23.30, 23.75	23.78, 24.10	25.79, 25.54
MgO	9.88, 9.88, 10.02	9.95, 9.98, 10.02	15.22, 15.47	14.93, 15.50	13.91, 13.80
Na_2O	0.11, 0.08	0.05, 0.06	n.p., 0.01	n.p., n.p.	-
K_2O	9.63, 9.69, 9.76	9.74, 9.79, 9.73	0.09, 0.06	0.03, 0.06	-

*Total Fe as FeO **Total Fe as Fe_2O_3

Bracketed values were determined against different standards from the others.

Also: FeO in biotite G-3 = 17.82, 18.10

Al, which were not replicated, the coefficient of variability was taken as the statistical counting error at 99 per cent confidence. These coefficients of variability were propagated through the structural formulae calculations of average minerals to derive the average error bars shown in the figures. The error bars are large for the Al^{VI} values because they are the sum of the uncertainties in both Si and Al determinations.

FLUID INCLUSIONS

Petrographic examination. The inclusions were first examined in grain mounts at high magnification with a good microscope.

Homogenisation studies. Heating determinations were carried out on doubly polished slabs of quartz about 1.0-1.5 mm. in thickness. They were heated in a Leitz 350 heating stage capable of attaining about 350° C.

Initially temperature determinations were attempted using a Pt-resistance thermometer calibrated to great accuracy. It transpired, however, that the resistance probe was the wrong shape for the receptacle in the stage and this led to excessive thermal lags (approaching 20° C. at 270° C.). The method was therefore discarded but it is to be recommended for accuracy and convenience if the correct probe is available.

Temperature measurements were therefore made using mercury-in-glass thermometers. Calibration by melting sodium nitrite indicated that the lag is only about 2° C. at 270° C. (see also Folinsbee et al., 1972). The lower-range thermometers were not exactly the correct shape for the receptacle and were found to read between 5-10° C. low at their upper limit of 230° C despite various attempts to remedy this lag. The temperature measurements are not therefore particularly accurate and an uncertainty of ±7-10° C. is estimated.

The heating stage was mounted on a Leitz SM Pol microscope with long focal-length objectives. The maximum magnification of this system is sufficient only for viewing the largest inclusions present and the illumination is poor. This adds to the inaccuracy of the determinations.

The rate of temperature increase was determined at different heating currents. It was then possible to maintain a steady temperature increase of about 10-12° C./minute by adjusting the rheostat as temperature increased.

1 of

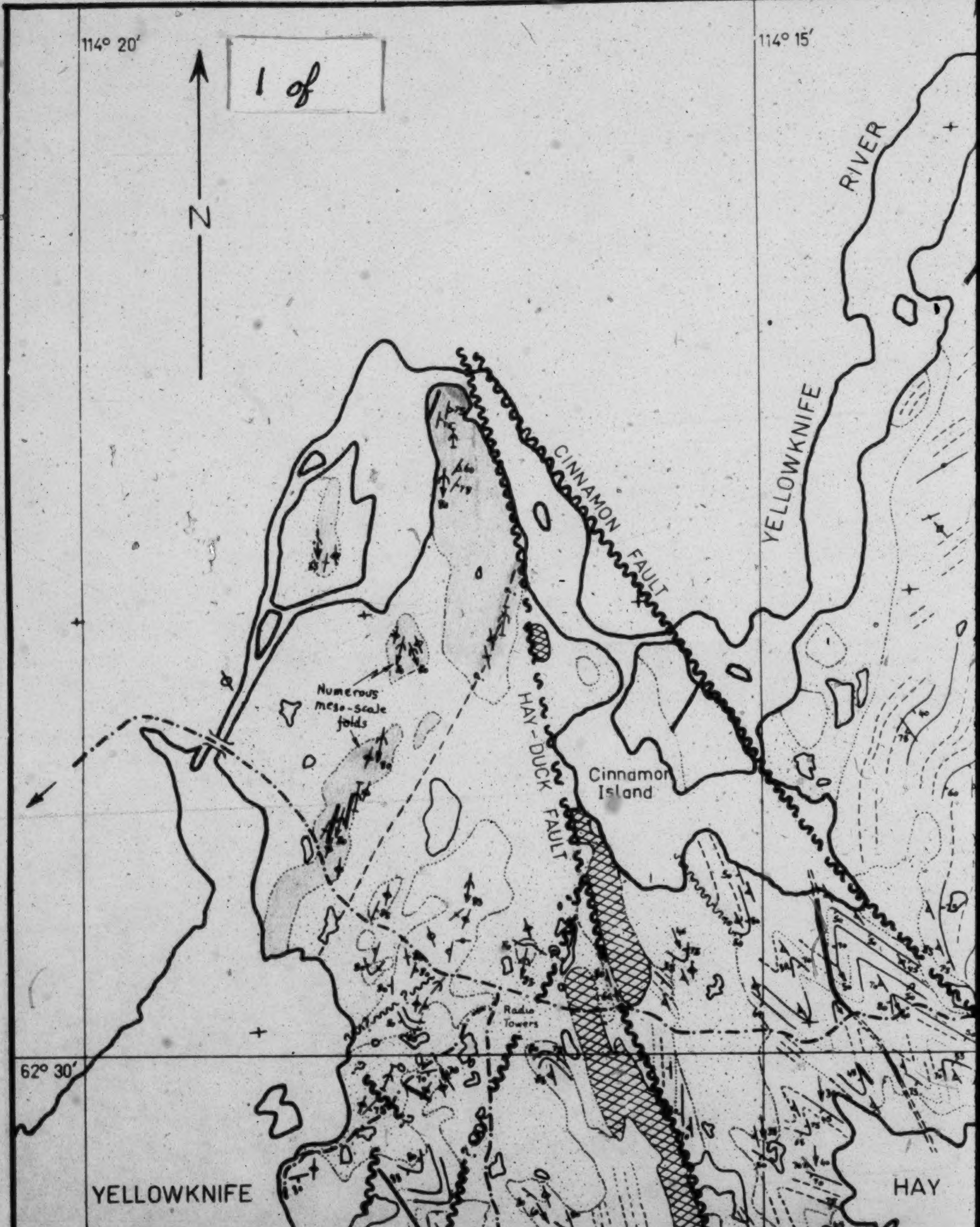
114° 20′
114° 15′
N
RIVER
YELLOWKNIFE
CINNAMON
FAULT
HAY-DUCK
FAULT
Cinnamon Island
Numerous meso-scale folds
Radio Towers
62° 30′
YELLOWKNIFE
HAY

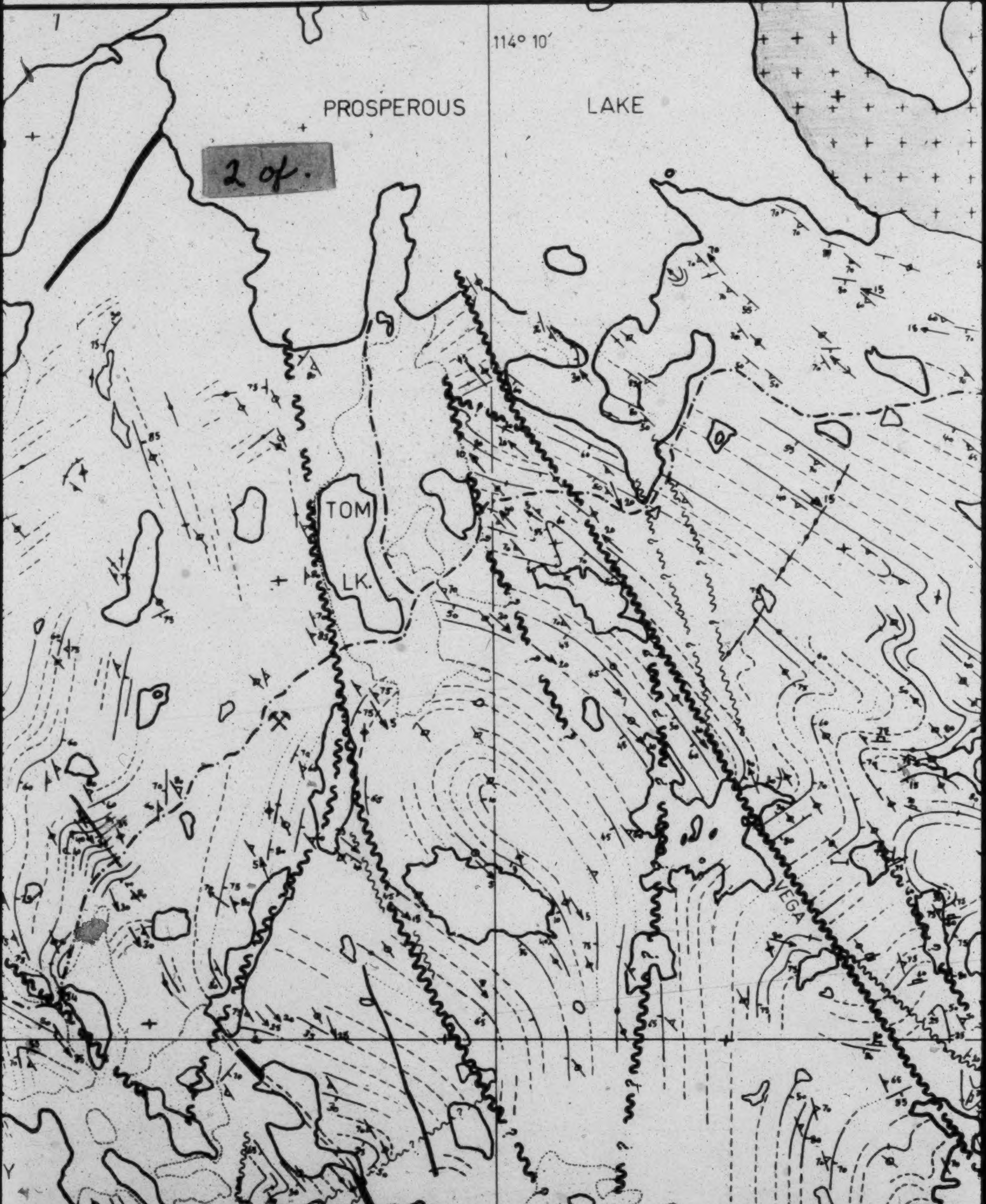
1
114° 10′
PROSPEROUS
LAKE
TOM
LK.
VEGA
Y

2 of.

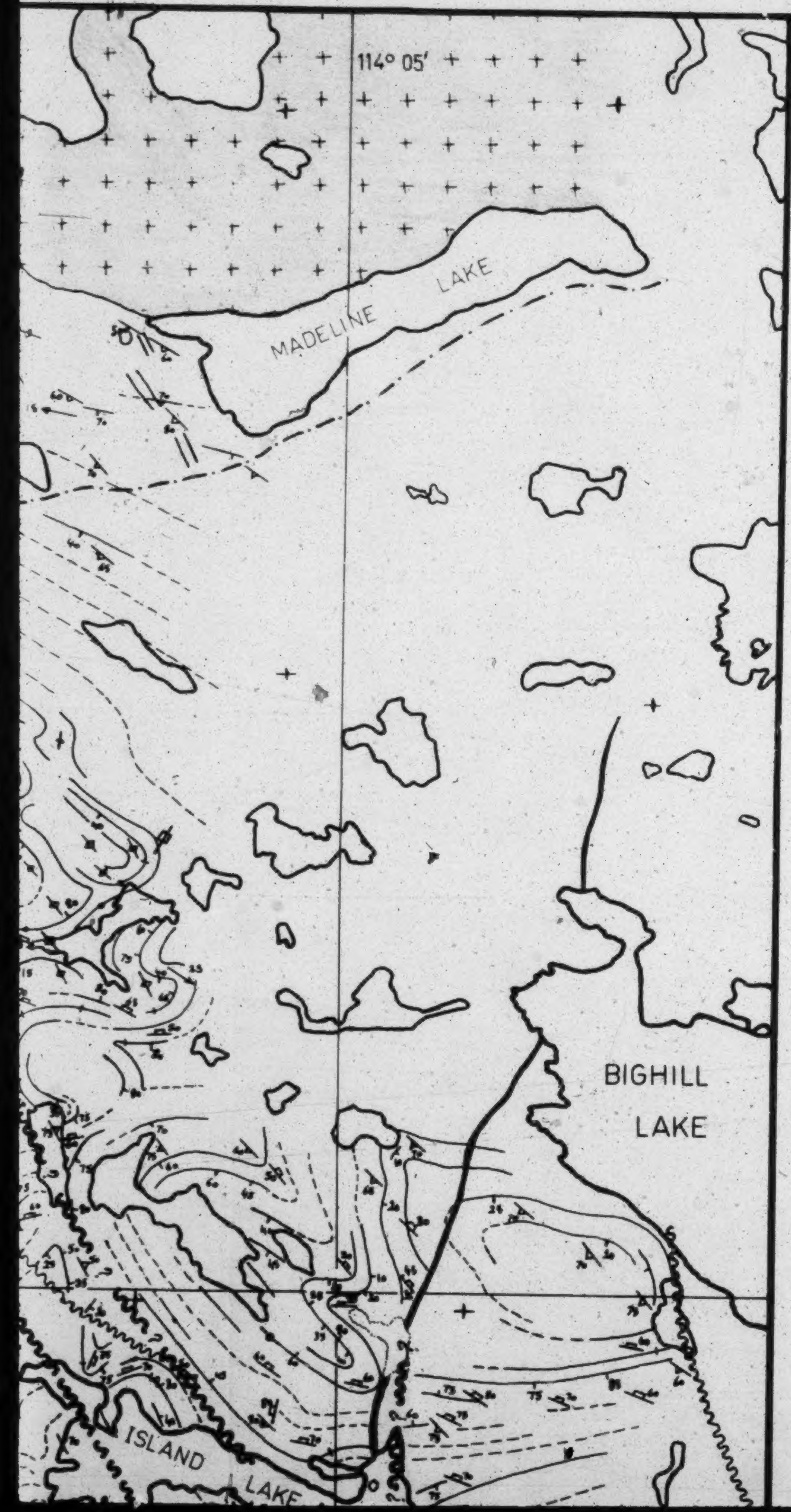
114° 05'
MADELINE LAKE
BIGHILL LAKE
ISLAND LAKE

3 of

124°W
Arctic
GREAT BEAR LAKE
Yellowk
Mackenzie R.
Highway

LEGE

☐ Alluvial cover – little or no outcrop.

▨ Diabase & gabbro.

+ Granitic plutonic rocks.

▨ Mixed rocks of various types (observed, inferred).

———— - - - -?-?- LITHOLOGICAL BOU concealed or inferr

+ Aerial photograph cen

-·-·- Road

BEDDING

Inclined, vertical, dip unknown, overturned, warped.

BIGHILL
LAKE

4 of

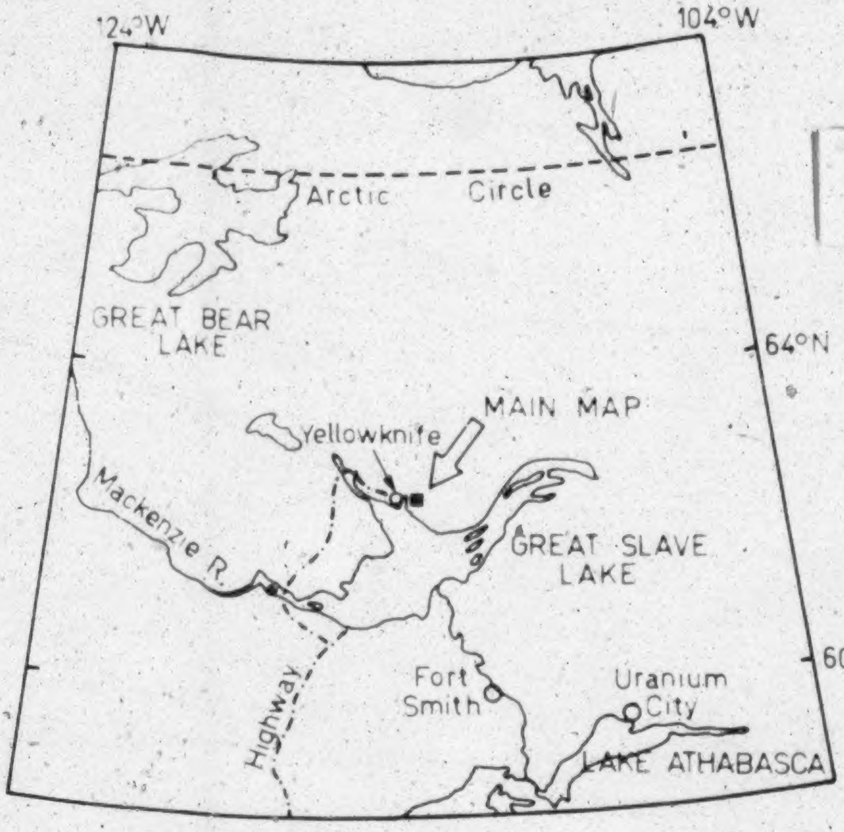
124°W
104°W
Arctic Circle
GREAT BEAR LAKE
64°N
MAIN MAP
Yellowknife
Mackenzie R.
GREAT SLAVE LAKE
60°N
Highway
Fort Smith
Uranium City
LAKE ATHABASCA

LEGEND

☐	Alluvial cover – little or no outcrop.	▨	Walsh Fm. (Thinly bedded metamorphosed mudstones & greywackes.
▩	Diabase & gabbro.	☐	Burwash Fm. (Metamorphosed mudstones and greywackes.
+	Granitic plutonic rocks.	▤	Duck Fm. (Metamorphosed intermediate volcanic rocks.
▨	Mixed rocks of various types (observed, inferred).	●	Acid or intermediate dyke or major pegmatite (with dip).

——— - - - - -?-?- LITHOLOGICAL BOUNDARY Established, approximate, concealed or inferred.

+ Aerial photograph centre.

-·-·- Road

BEDDING

Inclined, vertical, dip unknown, overturned, warped.

BEDDING TRENDS

———	Mapped on the ground.
- - - - - -	From aerial photos.
··········	Speculative.

5 of

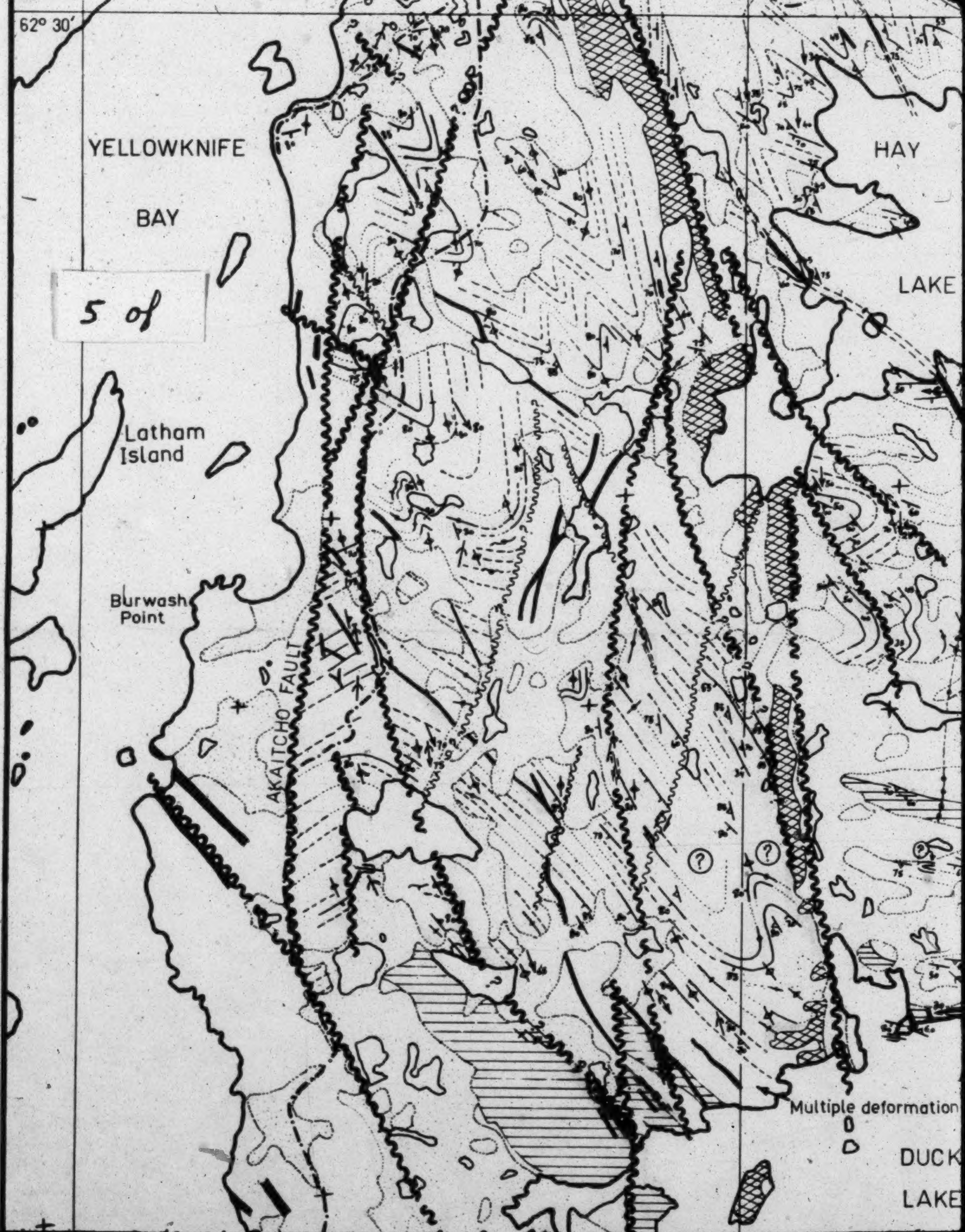

62° 30′
YELLOWKNIFE
BAY
HAY
LAKE
Latham
Island
Burwash
Point
AKAITCHO FAULT
?
?
?
Multiple deformation
DUCK
LAKE

6 of

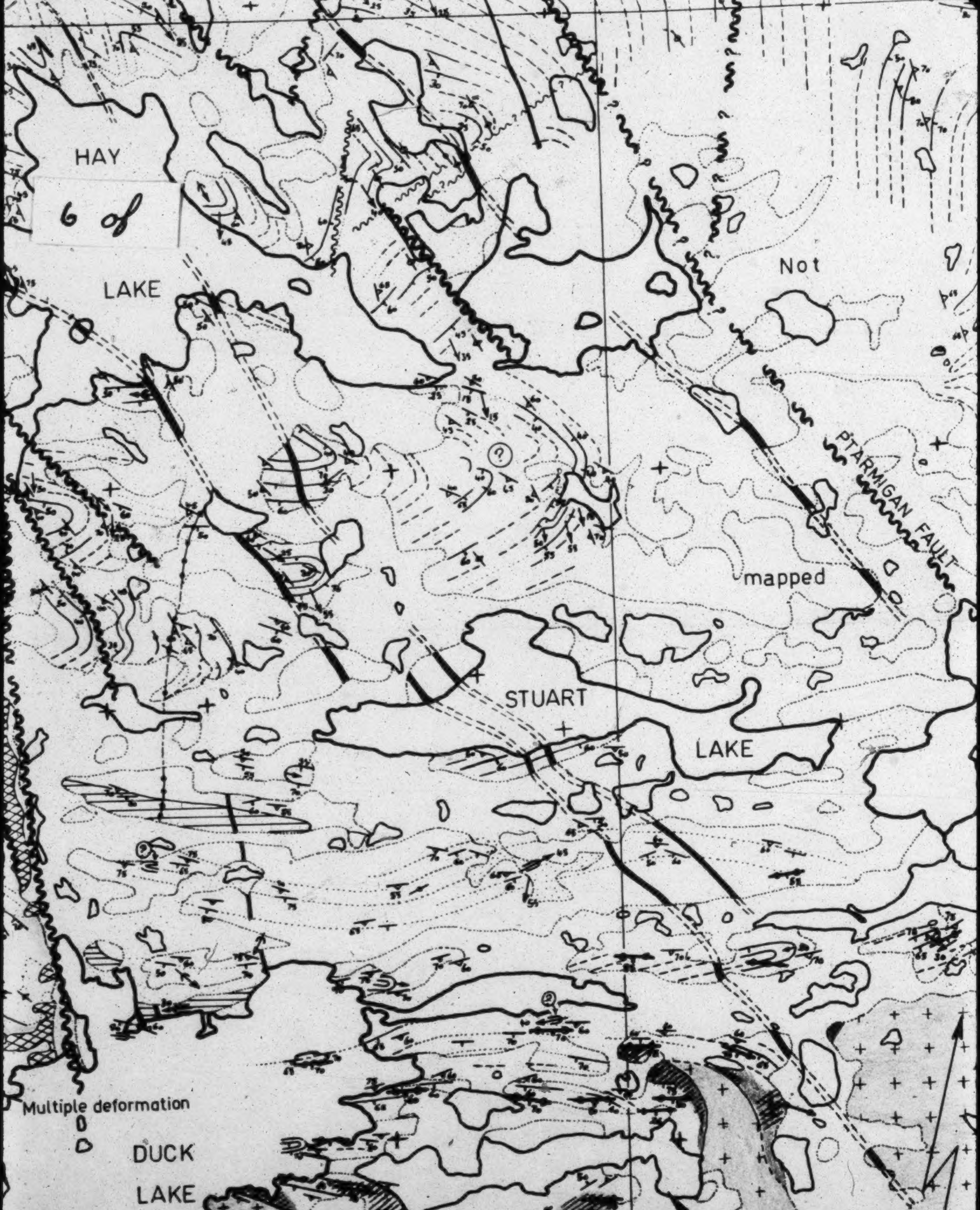
HAY
LAKE
Not
mapped
PTARMIGAN FAULT
STUART
LAKE
Multiple deformation
DUCK
LAKE

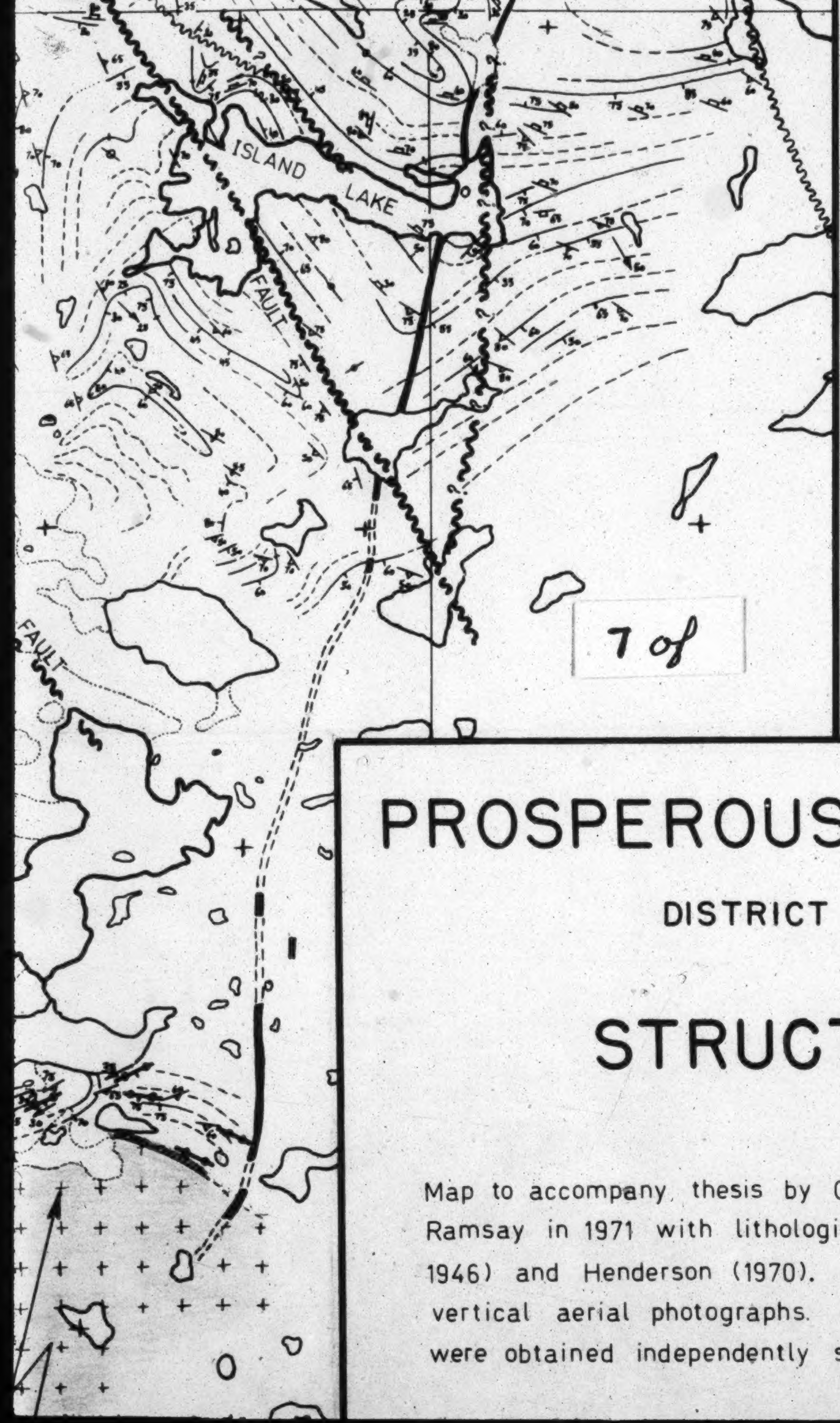
ISLAND
LAKE
FAULT
FAULT
Road
BEDDING
Inclined, ve
unknown, ov
warped.
CLEAVAGE : Type 'A'
Inclined, v
dip unknow
: Type 'B'
Inclined, v
dip unkno
LINEATIONS
Micro-folds
Multiple m
Minor fold
plunge & c
Minor isoc
Minor fold
Plunge of

7 of

PROSPEROUS LAKE – D

DISTRICT OF MACKENZIE

STRUCTURAL G

Map to accompany thesis by C.R.Ramsay, University
Ramsay in 1971 with lithological boundaries slightly
1946) and Henderson (1970). Cartography based o
vertical aerial photographs. Declination : 32° East.
were obtained independently so that this and Jolli

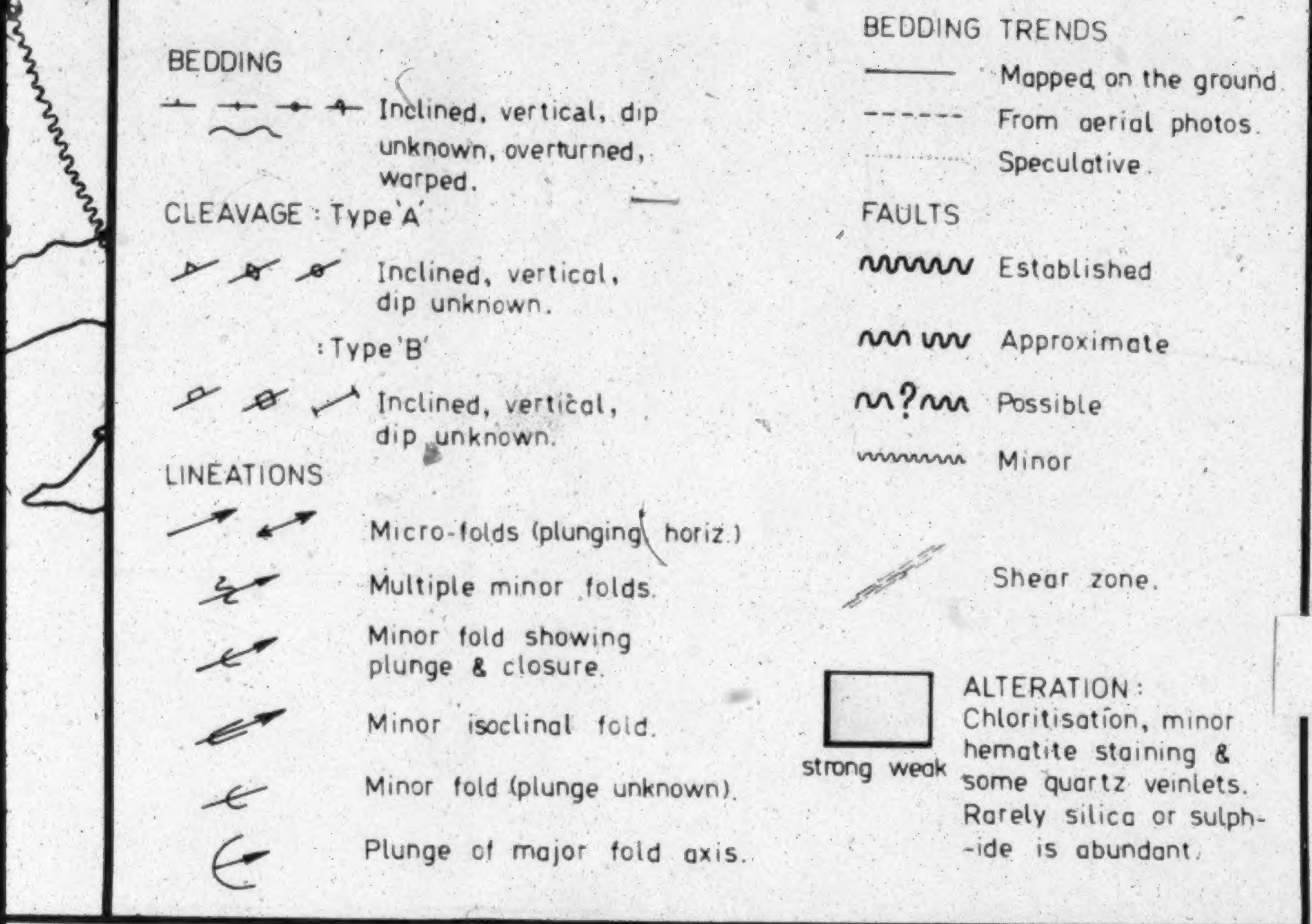

BEDDING

Inclined, vertical, dip unknown, overturned, warped.

CLEAVAGE : Type 'A'

Inclined, vertical, dip unknown.

: Type 'B'

Inclined, vertical, dip unknown.

LINEATIONS

Micro-folds (plunging, horiz.)

Multiple minor folds.

Minor fold showing plunge & closure.

Minor isoclinal fold.

Minor fold (plunge unknown).

Plunge of major fold axis.

BEDDING TRENDS

Mapped on the ground

From aerial photos.

Speculative.

FAULTS

Established

Approximate

Possible

Minor

Shear zone.

ALTERATION : Chloritisation, minor hematite staining & some quartz veinlets. Rarely silica or sulphide is abundant.

strong weak

8 of

US LAKE—DUCK LAKE AREA

RICT OF MACKENZIE, N.W.T.

UCTURAL GEOLOGY

by C.R.Ramsay, University of Alberta, 1973. Mapping by
hological boundaries slightly modified after Jolliffe (1942 and
70). Cartography based on a partially controlled mosaic of
phs. Declination : 32° East. All the structural data shown
ntly so that this and Jolliffe's maps are complementary.

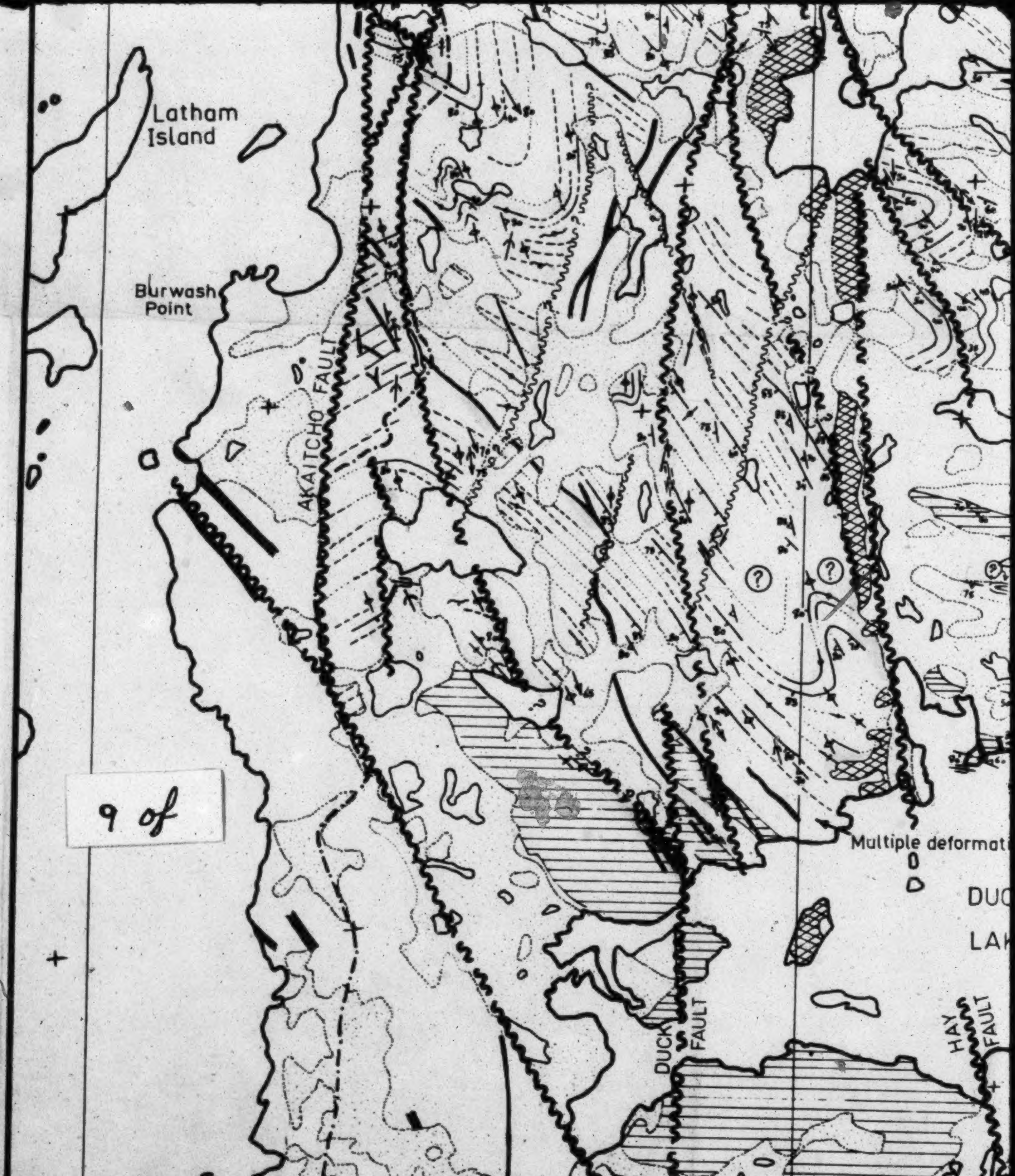
Latham Island
Burwash Point
AKAITCHO FAULT
Multiple deformati
DUC
LAK
DUCK FAULT
HAY FAULT
62° 25′

9 of

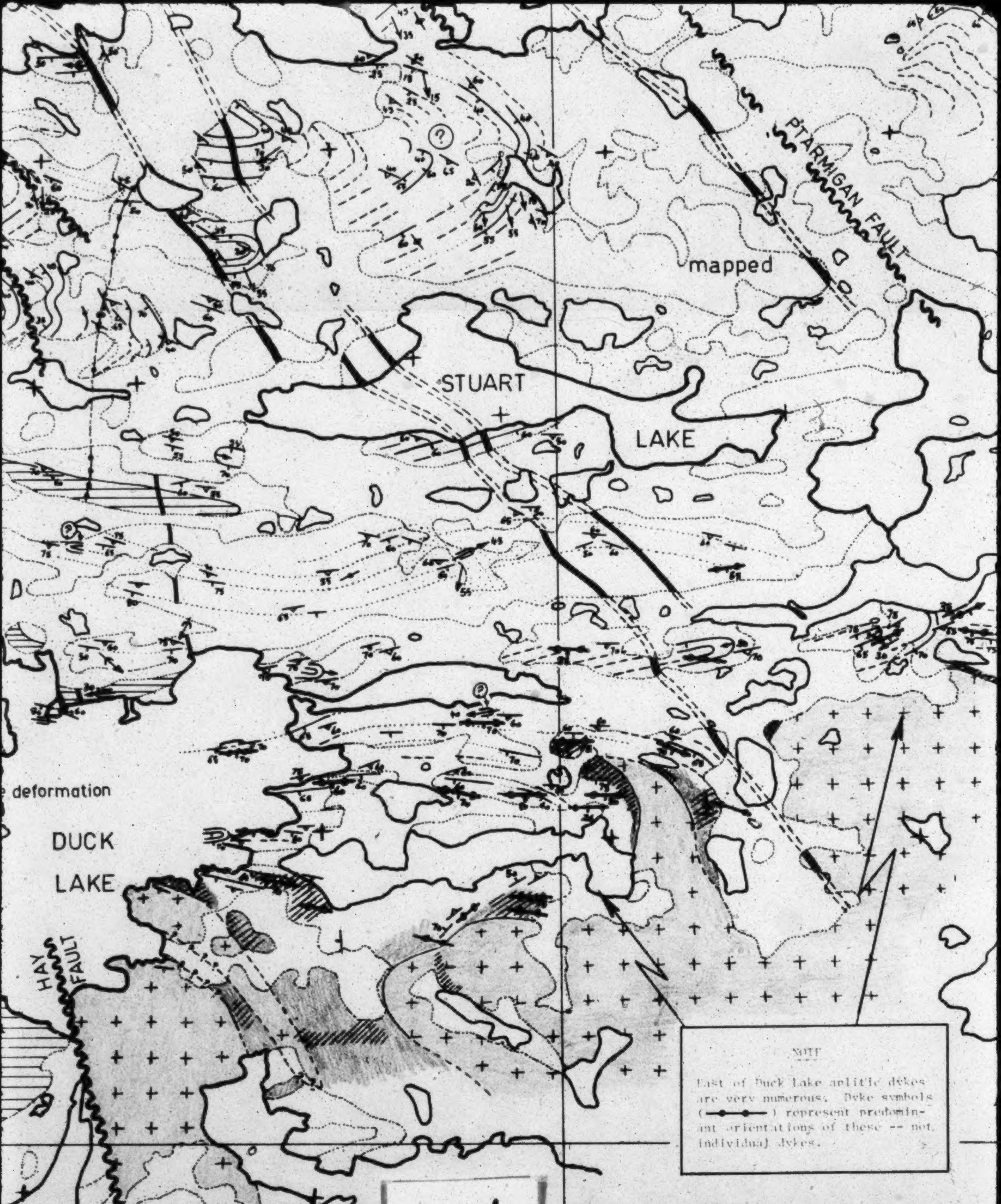
PTARMIGAN FAULT
mapped
STUART
LAKE
e deformation
DUCK
LAKE
HAY
FAULT

NOTE

East of Duck Lake aplitic dykes are very numerous. Dyke symbols (—●—●—) represent predominant orientations of these -- not individual dykes.

10 of

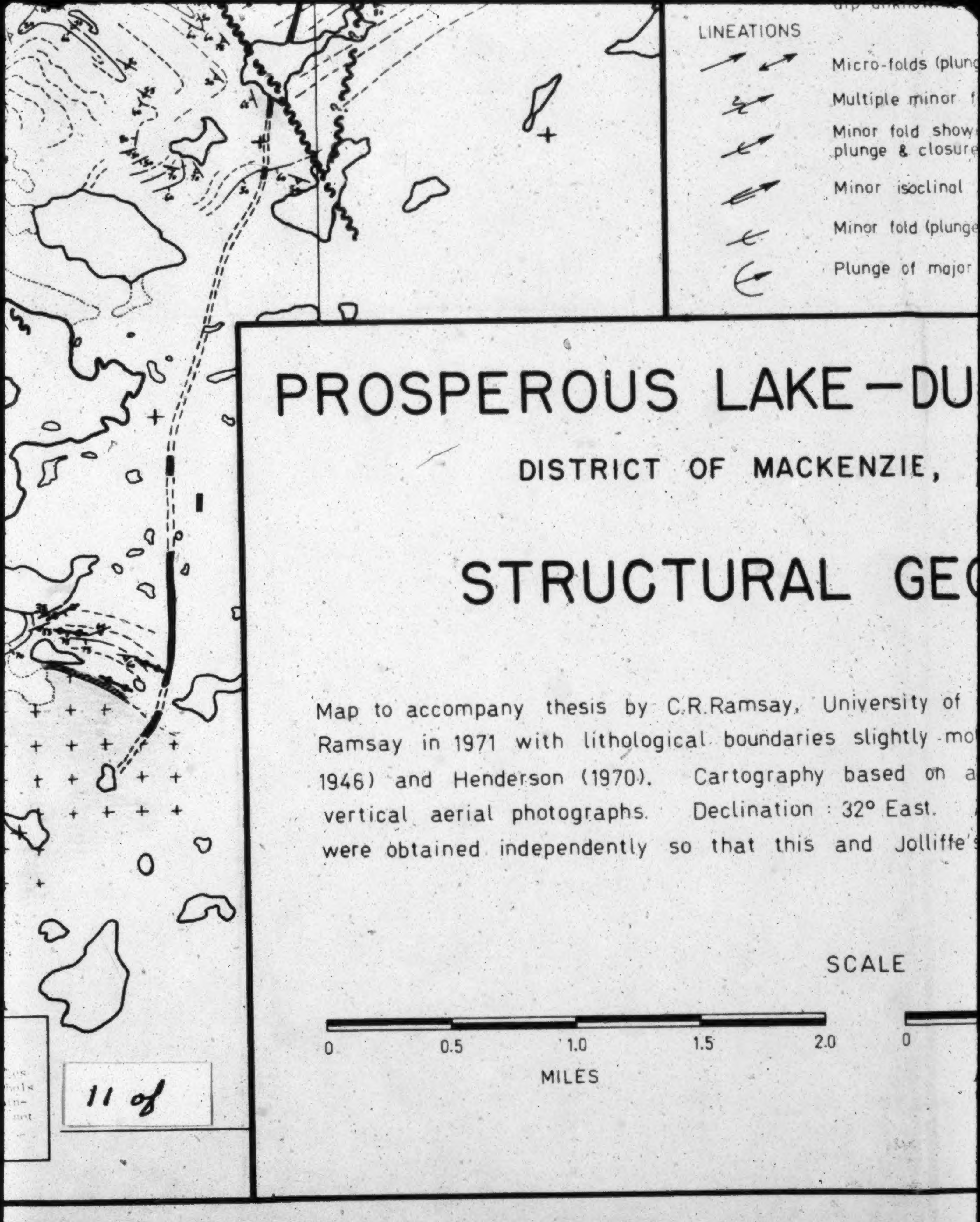
LINEATIONS
Micro-folds (plunc
Multiple minor f
Minor fold show
plunge & closure
Minor isoclinal
Minor fold (plunge
Plunge of major

PROSPEROUS LAKE – DU

DISTRICT OF MACKENZIE,

STRUCTURAL GE

Map to accompany thesis by C.R.Ramsay, University of
Ramsay in 1971 with lithological boundaries slightly mo
1946) and Henderson (1970). Cartography based on a
vertical aerial photographs. Declination : 32° East.
were obtained independently so that this and Jolliffe's

SCALE

0
0.5
1.0
1.5
2.0
MILES
0

11 of

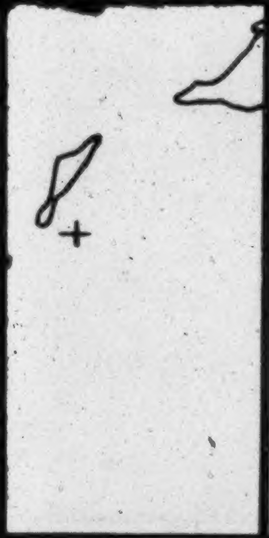

dip unknown.

Minor

LINEATIONS

Micro-folds (plunging, horiz.)

Multiple minor folds.

Minor fold showing plunge & closure.

Minor isoclinal fold.

Minor fold (plunge unknown).

Plunge of major fold axis.

Shear zone.

strong weak

ALTERATION: Chloritisation, minor hematite staining & some quartz veinlets. Rarely silica or sulphide is abundant.

ROUS LAKE – DUCK LAKE AREA

DISTRICT OF MACKENZIE, N.W.T.

TRUCTURAL GEOLOGY

y thesis by C.R.Ramsay, University of Alberta, 1973. Mapping by
with lithological boundaries slightly modified after Jolliffe (1942 and
rson (1970). Cartography based on a partially controlled mosaic of
photographs. Declination : 32° East. All the structural data shown
dependently so that this and Jolliffe's maps are complementary.

12 of 12

SCALE

1.0 1.5 2.0

MILES

0 1 2 3

KILOMETRES